Glucocorticoid signature in a neuronal genomic context
Polman, J.A.E.

Citation
Polman, J. A. E. (2016, May 10). *Glucocorticoid signature in a neuronal genomic context*. Retrieved from https://hdl.handle.net/1887/39295

Version:	Not Applicable (or Unknown)
License:	[Licence agreement concerning inclusion of doctoral thesis in the Institutional Repository of the University of Leiden](https://hdl.handle.net/1887/39295)
Downloaded from:	https://hdl.handle.net/1887/39295

Note: To cite this publication please use the final published version (if applicable).

Cover Page

The handle http://hdl.handle.net/1887/39295 holds various files of this Leiden University dissertation

Author: Polman, J.A.E.
Title: Glucocorticoid signature in a neuronal genomic context
Issue Date: 2016-05-10

Glucocorticoid Signature
in a
Neuronal Genomic Context

Japke Anne Elisabeth Polman

Glucocorticoid Signature
in a
Neuronal Genomic Context

Proefschrift

ter verkrijging van
de graad van Doctor aan de Universiteit Leiden,
op gezag van Rector Magnificus prof. mr. C.J.J.M. Stolker,
volgens besluit van het College voor Promoties
te verdedigen op dinsdag 10 mei 2016
klokke 16:15 uur

door

Japke Anne Elisabeth Polman
Geboren te Gouda in 1980

Promotor	Prof. dr. E.R. de Kloet
Co-promotor	Dr. N.A. Datson
Leden promotiecommissie	Prof. dr. S.M. van der Maarel
	Prof. dr. P.J. Lucassen (University of Amsterdam)
	Prof. dr. G.J. Martens (Radboud University, Nijmegen)
	Prof. dr. O.C. Meijer
	Prof. dr. P.E. Slagboom
	Dr. E. Vreugdenhil

Voor Erik,
mijn onvoorwaardelijke steun

List of Abbreviations

AF	Activation Function
CA	Cornu Ammonis
ChIP	Chromatin Immunoprecipitation
ChIP-seq	ChIP-sequencing
CORT	Cortisol or Corticosterone
DBD	DNA-Binding Domain
DG	Dentate Gyrus
GBS	Glucocorticoid Receptor Binding Site
GCs	Glucocorticoids
GR	Glucocorticoid Receptor
GRE	Glucocorticoid Response Element
HPA-axis	Hypothalamic-Pituitary-Adrenal axis
LBD	Ligand Binding Domain
MR	Mineralocorticoid Receptor
mTOR	mammalian Target of Rapamycin
nGRE	negative GRE
NTD	N-terminal Transactivation Domain
RT-qPCR	Real-time Quantitative Polymerase Chain Reaction

Contents

Chapter One

General introduction

1.1   Corticosteroids and the brain

The Hypothalamus-Pituitary Adrenal (HPA) axis

During daily life, the human body is faced with internal and external stimuli (also referred to as stressors) that challenge homeostasis. The body responds to these stimuli by turning on the "stress response" (Karatsoreos and McEwen, 2013), that enables the body to adapt and cope with the situation until the challenge has passed. The stress response in our body is among others regulated by the sympathetic nervous system and the hypothalamo-pituitary-adrenal (HPA-axis). The onset of the HPA-axis is mediated by the limbic brain structures, i.e. prefrontal cortex, amygdala and the hippocampus, which together form the interface between the incoming sensory information and the appraisal process (de Kloet et al., 2005). When homeostasis is threatened, this results in a release of catecholamines from sympathetic nerves and the adrenal medulla and the secretion of Corticotropin-Releasing Hormone (CRH) from the hypothalamus. CRH stimulates the synthesis and release of Adrenocorticotropic Hormone (ACTH) from the pituitary which in turn promotes the secretion of glucocorticoids (GC), being cortisol (man) or corticosterone (rodent) from the adrenal cortex (reviewed by McEwen (McEwen, 2000)) (Figure 1.1). GC feed back in an inhibitory manner on the pituitary and on the limbic brain structures that have led to the initial activation of the HPA axis (de Kloet et al., 2005).

The hippocampus is one of the limbic brain regions where GC are able to exert a negative feedback action, due to the high concentrations of GC receptors that are expressed there (Chao et al., 1989; Reul and de Kloet, 1985; van Steensel B. et al., 1996). The hippocampus plays an important role in learning, memory consolidation, mood and regulation of the stress response. The hippocampus contains the cell fields Cornu Ammonis (regions CA1 through CA4) and Dentate Gyrus (DG) which together form an internal trisynaptic circuit intended for hippocampal information processing. Hippocampal neurons display a high degree of structural and functional plasticity during exposure to acute and chronic stressors, which is in part modulated by GC via binding to their receptors.

Acute and Chronic stress

A single challenge of the body's homeostasis, such as the acute stressor of a thesis defense, results in secretion of cortisol (CORT) from the adrenal cortex in the blood circulation. This surge of CORT reaches all tissues including the brain and is aimed to restrain the initial stress reaction. CORT promotes adaptation to the stressful situation and restores homeostasis. This process of adaptation to change to restore homeostasis is called allostasis. In case of prolonged exposure to the stressor, a state of "chronic stress" may develop in which patterns of secretion change and exposure
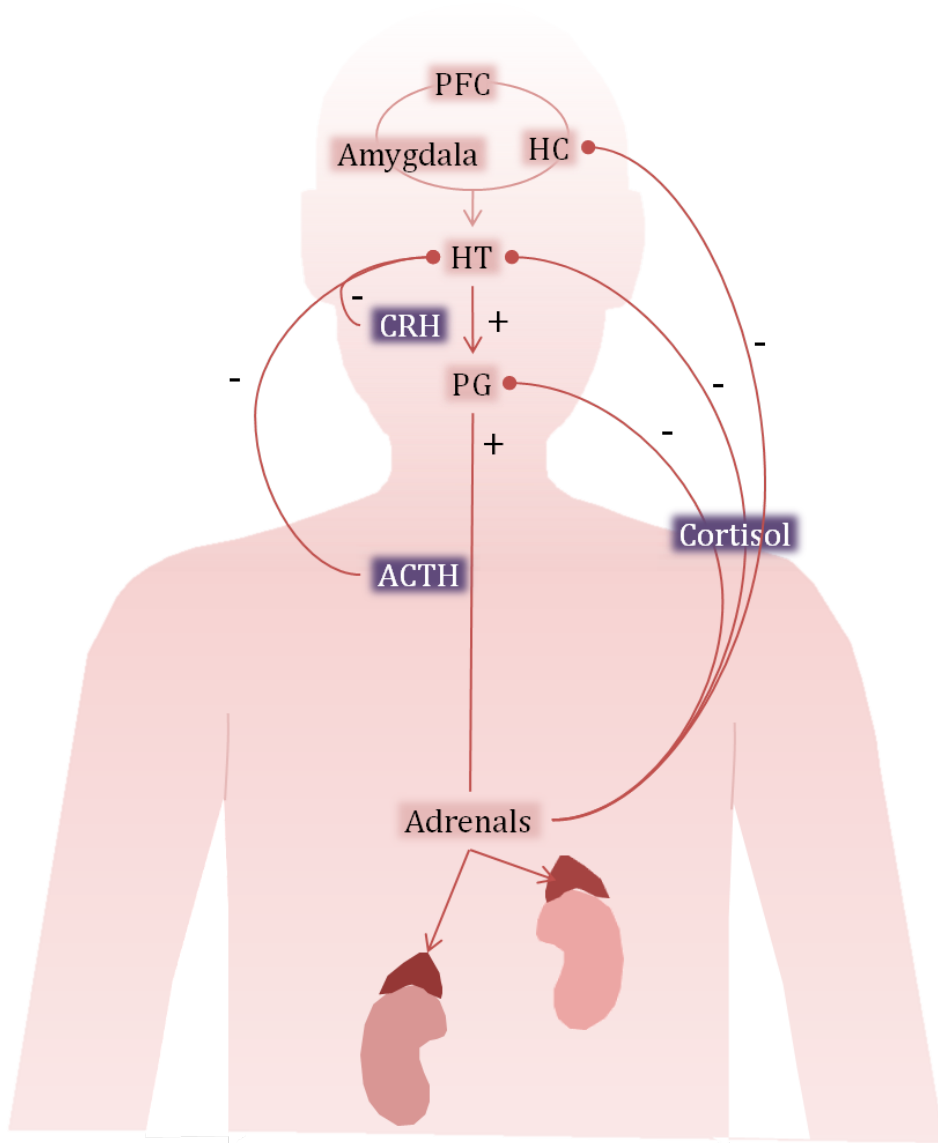
Figure 1.1: The HPA-axis.
Graphic illustration of the Hypothalamus-pituitary-adrenal (HPA) axis. PFC: Prefrontal Cortex, HC: Hippocampus, HT: Hypothalamus, PG: Pituitary Gland

of brain and body to high CORT becomes prolonged. Since CORT also generates energy substrates to cope with a stressor, chronic stress has an increasing cost, also called allostatic load. If such a condition lasts, adaptation is compromised and the organism becomes more vulnerable to develop *e.g.* cardiovascular, metabolic disease and stress-related neuropsychiatric disorders such as major depressive disor-

der or post traumatic stress syndrome. The circumstances during which this shift to impaired adaptation occurs depends among others on the genetic background of the organism and acquired strategies to maximize efficient energy expenditure and adaptation to limit overdrive of the stress reaction (Herman, 2013). The ability of an organism "to cope with environmental tumult by bending and not by breaking" is also referred to by the term "resilience" (Karatsoreos and McEwen, 2013).

Chronic stress affects brain regions at the cellular level as for instance is the case with the hippocampus that is affected structurally and functionally by chronic stress. This is among others reflected in suppression of neurogenesis in the subgranular zone of the dentate gyrus (Heine et al., 2004; Magarinos et al., 1996; Gould et al., 1997). Besides causing structural changes, CORT affects electrical properties of hippocampal neurons. Chronic stress or chronic CORT exposure suppresses hippocampal long term potentiation (LTP), a lasting synaptic strengthening that likely underlies learning and memory formation (Alfarez et al., 2003; Bodnoff et al., 1995; Krugers et al., 2006).

A dual receptor system modulates glucocorticoid action

CORT circulates in the blood where $95\,\%$ is bound to corticosteroid binding globulin (CBG) or albumin which prevents CORT from entering the brain (Pardridge and Mietus, 1979; Moisan et al., 2014). The remaining $5\,\%$ unbound CORT passes the blood-brain barrier and binds to two types of receptors in the brain: the mineralocorticoid receptor (MR) and glucocorticoid receptor (GR) (Reul and de Kloet, 1985). These receptors belong to the superfamily of ligand-activated nuclear receptors and have a distinct localization in the brain. MR is predominantly localized in neurons of limbic structures, while GR is expressed in every cell, albeit at different levels. Stress centers in the brain, such as hippocampus, amygdala and hypothalamus express high amounts of GR (Morimoto et al., 1996). The balanced activation of MR and GR is an important determinant of neuronal excitability, neuronal health and stress responsiveness (de Kloet et al., 1998; de Kloet et al., 2005).

MR is abundantly expressed in the limbic brain structures amygdala and hippocampus (Reul and de Kloet, 1985). This implies that the receptor plays a role in the functionality of these brain areas. Amygdala circuits are important for emotional expressions such as fear and anxiety, while the hippocampal structure provides a context to these emotional reactions in time and place. MR has a high affinity for CORT ($K_d = 0.5\,\text{nM}$), ~10 fold higher than GR ($K_d = 2.5$–$5\,\text{nM}$), and as a result MR is activated during lower, basal concentrations of circulating CORT (Figure 1.2) (Reul and de Kloet, 1985). Activated MR is considered to be important for the tone of the HPA axis, also described as the threshold or sensitivity of the stress response system (de Kloet et al., 1998).

Via MR, CORT exerts both genomic and non-genomic actions. Whereas the non-genomic actions occurring with a delay of seconds to minutes are considered to be responsible for fast CORT effects, the genomic effect is slower and long-lasting.
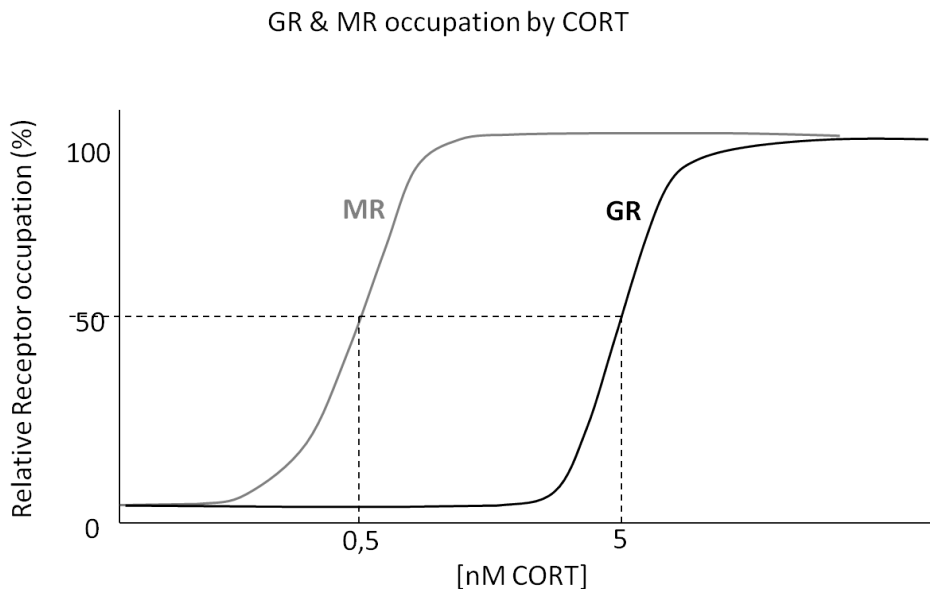
GR & MR occupation by CORT

Figure 1.2: Nuclear Corticosteroid Receptor occupancy by CORT.
Simplified graph representing the relative nuclear MR and GR occupation by CORT. MR has a higher affinity for CORT and becomes occupied at lower concentrations of CORT in comparison to GR (Reul and de Kloet, 1985).

Genomic CORT effects can be detected at 15 – 60 minutes after stress exposure and may last for several hours. Knowledge regarding the actions of genomic MR on the cell has been available for decades, although knowledge on the target genes of MR remains sparse. The features of non-genomic MR-mediated effects of CORT have only recently been uncovered (de Kloet et al., 1998; de Kloet et al., 2005). GR has a lower affinity for CORT in comparison with MR and consequently GR only becomes occupied during elevated concentrations of circulating CORT (Figure 1.2).

Elevated CORT is triggered during the stress reaction and is also observed at the circadian and ultradian peaks (Stavreva et al., 2009). Similar to MR, GR can mediate genomic effects of CORT that modulate the transcription of CORT-responsive genes (Oakley and Cidlowski, 2013). In addition, GR was found to mediate non-genomic actions in the lateral amygdala and medial prefrontal cortex (mPFC), where it is indicated to play a role in memory consolidation (Barsegyan et al., 2010; Johnson et al., 2005).

GR and MR mediate complementary and different, sometimes opposing, actions of CORT. While MR is involved in maintenance of neuronal excitability and basal activity of the stress system and onset of the stress reaction, GR activation results in subsequent suppression of excitability transiently raised by excitatory stimuli, recovery from stress and behavioral adaptation. Their balanced activation is an important determinant of neuronal excitability, neuronal health and stress respon-

siveness (de Kloet et al., 1998; de Kloet et al., 2005) In the current thesis, we aim at gaining more understanding of the interaction of MR and GR with the genome. Because of its role in the normalization of the stress response and how this might be impaired in coping with chronic stress, the GR has received the most attention in the research described in this thesis.

1.2 Glucocorticoid Receptor

The GR protein is composed of three major domains, namely an N-terminal trans-activation domain (NTD), a DNA-binding domain (DBD) and a C-terminal ligand binding domain (LBD) (Figure 1.3) (Reviewed in (Oakley and Cidlowski, 2013)). Whereas the DBD contains motifs that recognize and bind target DNA sequences, the LBD interacts with the ligand and contains an Activation Function (AF2) that interacts with coregulators in a ligand-dependent manner. In addition, the LBD aids in dimerization of GR, a topic which will be described in the following sections (Bledsoe et al., 2002). The NTD contains a second transcriptional activation function (AF1) that is able to interact with coregulators and the basal transcription machinery. The NTD is the primary site for post-translational modifications such as phosphorylation (P), sumoylation (S), ubiquitination (U) and acetylation (A) (Figure 1.3).

The human GR gene is composed of 9 exons, which due to alternative splicing and alternative translation initiation mechanisms can result in various GR-subtypes, namely GRα, GRβ, GRγ, GR-P and GR-A (Figure 1.4) (Reviewed in (Oakley and Cidlowski, 2013)). GRα is the most abundant variant and is known as the classical GR-protein which is able to mediate the genomic actions of glucocorticoids. The second GR-variant, GRβ, has a disrupted LBD and functions independent of ligand as a dominant negative inhibitor of GRα on many glucocorticoid-responsive target genes (Yudt et al., 2003; Oakley et al., 1996; Charmandari et al., 2005). However, the expression of GRβ is low in the human hippocampus (De Rijk et al., 2003). The third variant, GRγ, is widely expressed, albeit at low levels, and binds glucocorticoids and DNA in a manner similar as GRα (Thomas-Chollier et al., 2013). However, GRγ is impaired in its ability to regulate glucocorticoid-responsive reporter genes due to a disrupted DBD and therefore has different DNA-targets in comparison to GRα. Both GR-A and GR-P isoforms miss large regions of the LBD and are not able to bind CORT. The functional role of GR-A and GR-P is less clear, but there are indications that GR-P modulates the transcriptional activity of GRα in a cell-type specific manner (de Lange P. et al., 2001).

The GR-transcripts can be alternatively translated into a subset of GR-protein isoforms. GRα mRNA, the GR-subtype which is known to interact with the genome after being activated by GC, can be translated into 8 protein isoforms: GRα-A, GRα-B, GRα-C1, GRα-C2, GRα-C3, GRα-D1, GRα-D2, and GRα-D3 (Lu and Cidlowski,
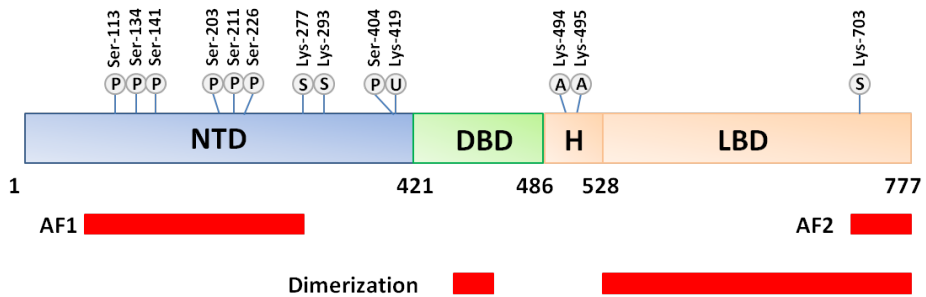
Figure 1.3: GR structure and post-translational modification.
Shown are the N-terminal transactivation domain (NTD), a DNA-binding domain (DBD), a C-terminal ligand binding domain (LBD), transcriptional activation function (AF1) and Activation Function (AF2). H (Hinge region). *Adapted from: Oakley et al, J Allergy Clin Immunol. 2013 Nov; 132(5): 1033–1044.*
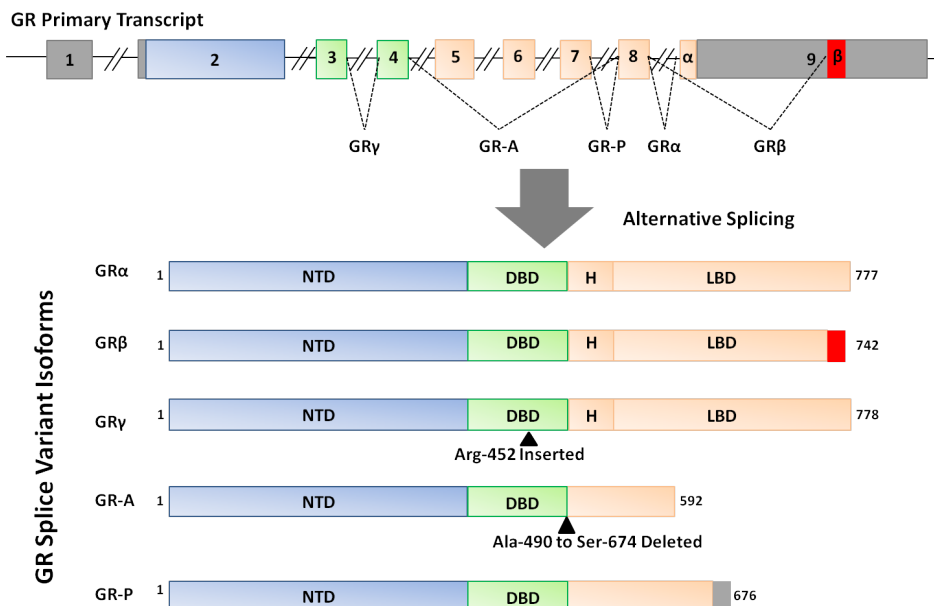
Figure 1.4: GR splice variants.
Alternative splicing events result in the expression of GRβ, GRγ, GR-A, and GR-P. *Adapted from: Oakley et al, J Allergy Clin Immunol. 2013 Nov; 132(5): 1033–1044.*

2005)(Reviewed in (Oakley and Cidlowski, 2013; Yudt and Cidlowski, 2002). These isoforms differ in their NTD-length, which is attributed to 8 AUG codons that are present in exon 2. Since the mRNA transcripts corresponding with GRβ, GRγ, GR-P and GR-A contain exon 2 as well, it is expected that these proteins will have isoforms that are comparable to GRα. The 8 GRα isoforms are conserved through species including rat, are all sensitive to GC and are able to bind GRE's. However, they differ in their intracellular localization when the hormone is absent, are expressed in a

celltype-dependent manner and they have distinct gene transcriptional profiles (Lu and Cidlowski, 2005). What the mechanism behind the isoform translation exactly is and how this differs per celltype, is not yet understood. The antibody used in the current thesis involves H300 (Santa Cruz), which recognizes amino acids 121–420 of human GR and will recognize the GRα-A, GRα-B and the GRα-C isoforms. These isoforms are localized in the cytoplasm of cells in the absence of hormone and translocate to the nucleus on glucocorticoid binding. In the remaining text of this thesis, GR is synonomous for these 3 types of isoforms, unless stated otherwise.

Inactive GR resides in the cytoplasm where it is part of a Heat Shock Protein 90 (HSP90) chaperone complex that prevents GR from being degraded (Pratt and Toft, 1997; Vandevyver et al., 2012). These chaperones include FK506 binding protein 51 (FKBP51) which operates in an ultrashort feedback loop in the control of GR activity (Vermeer et al., 2003). When CORT is present in the circulation, it can diffuse freely through the cell membrane into the cytoplasm where it is able to interact with a variety of proteins. When the concentration of CORT is high enough, GR will bind CORT at its ligand-binding domain (LBD) (Reul and de Kloet, 1985; Spiga and Lightman, 2009). In this activated state, GR can be phosphorylated by several kinases including cyclin-dependent kinases (CDKs), c-Jun N-terminal kinase (JNK) and mitogen-activated kinases (MAPKs). The phosphorylation of GR can either inhibit or facilitate the attraction of cofactors to GR that can modulate its transcriptional activity (Chrousos and Kino, 2009; Galliher-Beckley and Cidlowski, 2009).

After CORT-binding, activated GR translocates to the nucleus using the cytoskeleton facilitated by HSP90 that has a fundamental role in promoting GR nuclear mobility (Reviewed in (Vandevyver et al., 2012).) In addition, there are two nuclear localization signals (NLS) present in the GR protein: NLS1 and NLS2, which are located near the DBD-hinge boundary and within the LBD respectively. These signals are recognized by importins which mediate the nuclear transport of GR as well. Within the nucleus, GR can interact with the genome and other proteins to regulate the transcription of genes. These interactions can be subdivided into two main processes: transactivation and transrepression (Figure 1.5). These two modes of genomic interaction by GR appear to be context-dependen and proceed directly with DNA (transactivation) or indirectly via protein-protein interaction .

Transactivation: Glucocorticoid Response Elements (GRE)

During the process of transactivation, GR binds as a homodimer directly to fifteen-nucleotide-long sequences known as Glucocorticoid Response Elements (GREs). Here, the GR undergoes conformational changes that result in the recruitment of coregulators and chromatin-remodeling complexes that mediate gene transcription. Well-known coactivators include steroid receptor coactivators (SRC 1–3) and histone acetyltransferases CBP/p300 (Zalachoras et al., 2013). This interaction is considered to induce the transcription of the gene that is associated with the GRE. In this thesis we consider the genes that have their transcription start site nearest to
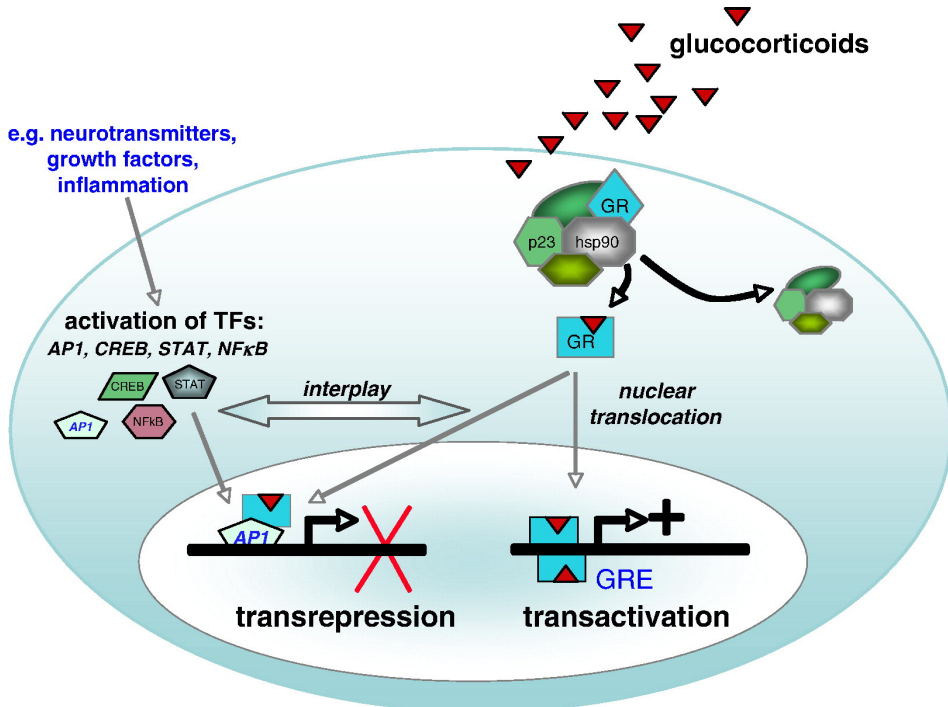
Figure 1.5: Genomic interactions of MR and GR.
The two main interactions that GR can have with the genome: transactivation and transrepression. GR can interact as a dimer with specific 15 nucleotide sequences (GREs or nGRE) as is shown on the right and is called transactivation. The left side represents an indirect protein-protein interaction of GR with the genome via interaction with other transcription factors, called in the literature transrepression. The result of this interaction is that the transcriptional activity of the bound transcription factor is impaired, which is the mechanistic underpinning of the physiological role of glucocorticoids in dampening the initial reaction to stressors. (Reprinted with permission from N.A. Datson.)

the GRE to be GRE-associated and therefore potentially transcriptionally regulated by GR binding to the GRE. However this is not always the case. GREs are known to be localized within promoter-regions of GR-target genes, but recent evidence, including the research described in this thesis, has shown that GREs can be located within introns, exons and intergenic regions at long distances from the nearest gene as well. In the end, whether binding of GR to a GRE is functional has to be demonstrated by differential expression of the associated genes.

A GRE consists of two inverted hexameric half-site motifs separated by three base pairs (Strahle et al., 1987). In 1989, Beato et al published the consensus-sequence for a GRE being 5′-GGTACAnnnTGTTCT-3′, but later research has shown that this GRE-sequence is not as static as presented here (Beato et al., 1989). *In vitro* experiments have shown that GRE composition can differentially affect GR conformation and regulatory activity, indicating that the GRE itself tailors the activity of the receptor towards target genes (Meijsing et al., 2009). How exactly this is achieved *in vivo* remains to be elucidated. Since MR is very similar to GR, it is be-

9

lieved that it is likely to bind to similar sequences at the DNA. However, this needs more investigation.

There are a number of well-known GR-targets that have been linked to a described functional GRE. An example is Period 1 (Per1) which is a protein that is important for the maintenance of circadian rhythms in the brain and is expressed in the rat hippocampus (Conway-Campbell et al., 2010). In the hippocampus, ultradian pulses of injected CORT in adrenalectomized rats have shown to be consecutively followed by 1) nuclear localization of GR in the hippocampus, 2) GR cycling on the GRE-containing Per1 promoter, 3) pulses of heteronuclear RNA (hnRNA) expression of Per1 and 4) accumulation of Per1 mRNA during several hours of treatment reaching a plateau that is maintained by the hourly pulses (Conway-Campbell et al., 2010). When the hourly pulses of CORT decline, Per1 regulation responds accordingly.

Kruppel-like factor 9 (KLF9) is another example of a GRE-containing gene. Klf9 is a transcription factor implicated in neuronal development and plasticity and its mRNA expression is increased in the mouse hippocampus after CORT injection (Bagamasbad et al., 2012). Two GR/MR response elements have been identified upstream of the Klf9 gene and both were shown to be functional. Other genes with documented GREs are CORT-responsive genes Metallothionein 2A (MT2a) (Kelly et al., 1997), Glucocorticoid-Induced Leucine Zipper (GILZ) (Cannarile et al., 2001) and DNA-damage-inducible Transcript 4 (Ddit4) (Datson et al., 2011; So et al., 2007) which will receive more attention in the current thesis.

Identification of functional GREs in the genome is complicated by several factors. In essence, the chromatin should be accessible in order for GR to bind to its targets, which is highly context dependent (Reddy et al., 2012). Factors such as GRE-accessibility and expressed coregulators differ between cell types and therefore provide a different cellular context that determines the cell type-specific stress response (John et al., 2011; Reddy et al., 2009; Yu et al., 2010). Furthermore, GR-GRE interactions are dynamic, with GR hopping on and off the genome to influence gene transcription (Stavreva et al., 2009). This illustrates the challenges that exist in genomic GR-target identification and the difficulties that lie in proper interpretation of new data.

Negative GREs (nGRE)

Besides activating transcription of target genes, direct binding of GR to GREs can also result in a negative regulation of the corresponding gene. However, there is a slightly different composition of the sequence necessary to achieve this and therefore this sequence is referred to as negative GRE (nGRE). A consensus sequence for nGRE that has been published is $CTCC(n)_{0-2}GGAGA$ where the number of nucleotides located between the two main sequences can vary, ranging from $0-2$ nucleotides (Surjit et al., 2011). However this sequence is, similar to the GRE-consensus sequence, not static and the composition differs depending on the nGRE investi-

gated. There are several mechanisms that can explain the inhibitory effect of GR-nGRE interaction. First, it was found that binding of GR to an nGRE promotes the assembly of *cis*-acting GR-SMRT/NCoR repressing complexes (Surjit et al., 2011). Second, evidence was identified *in vitro* that two GR monomers bind nGREs in a reversed repeat orientation with strong negative cooperativity which will result in the presence of monomeric GR at nGREs (Hudson et al., 2013; Surjit et al., 2011). Examples of nGRE-containing genes are POMC (Drouin et al., 1993), Glucose-6-phophatase catalytic subunit gene (G6Pase) (Kooi van der et al., 2005) and Prolactin (Sakai et al., 1988).

Transrepression

GR is able to bind indirectly to the genome via protein-protein interaction with other transcription factors. These sites known as "tethering" GR-binding sites do not contain actual DNA-binding sites for GR itself, but instead contain binding sites for other transcription factors that are bound by GR (Kassel and Herrlich, 2007; Pearce et al., 1998). Since this interaction often results in downregulation of the functional effects of the other transcription factors, these binding sites are also referred to as transrepressive sites. This crosstalk of GR with other transcription factors (TFs) vastly expands the range of GR-control over physiological processes as compared to the classical GRE-driven transcriptional control in simple GREs and it is likely that it underlies the highly context-dependent action of CORT.

Classical transcription factors that interact with GR are Activator Protein 1 (AP-1), cAMP response element-binding protein (CREB) and nuclear factor kappa-b (NFκB) (Figure 1.5) (Pearce et al., 1998; Alboni et al., 2011; Rao et al., 2011; Jonat et al., 1990; De Bosscher K. et al., 2008). NFκB and AP-1 are both well-known for their fundamental role in pro-immunological and pro-inflammatory responses and as such are important pharmacological targets for treating inflammatory disorders. In the brain the capability of NFκB to bind DNA has been described (Unlap and Jope, 1995). NFκB expression is increased in the mouse hippocampus after acute and chronic stress (Djordjevic et al., 2015). DNA-binding by AP-1 has shown to be increased after restraint stress in the hippocampus and CREB is associated with long-term memory formation (Bourtchuladze et al., 1994; Miller et al., 2007). Other examples of transcription factors include Oct1 and Ets1 at composite GREs and Oct-1/2, STAT3 (Langlais et al., 2012), STAT6, SMAD3, 4 and PU.1/Spi-1 at tethering sites (Biola et al., 2000; De Bosscher K. et al., 2006; Gauthier et al., 1993; Imai et al., 1993; Jonat et al., 1990; Kassel and Herrlich, 2007; Schule et al., 1990; Song et al., 1999; Stocklin et al., 1996; Wieland et al., 1991). However, the interaction of GR with these regulators is mainly based on studies describing the immunosuppressive and the tumor suppressor properties of GR (Chebotaev et al., 2007; De Bosscher K. et al., 2008; Glass and Saijo, 2010), while very little is known about crosstalk partners in a neuronal context.

In an attempt to gain understanding of the impact of GR on the entire organism, GR-deficient mice have been developed in the past (Cole et al., 1995). However, these mice die shortly after birth and consequently, other models were developed. For instance, GR$^{dim/dim}$ mutant mice that lack the potential to dimerize and as a consequence cannot modulate gene transcription via GREs but retain the capacity for GR-mediated transrepression were created (Reichardt et al., 1998). Interestingly, these mice are viable and it was concluded that transactivation via GREs does not seem to be essential for viability in mice. Later on this conclusion was nuanced by stating that *in vitro* GR dimer mutants (assumed to be GR monomers) are able to bind specifically to a class of more complex GREs and stimulate transcription. It was postulated that GRs can form concerted multimers in a manner that is independent of the DBD-dimer interface (Adams et al., 2003).

1.3   *De novo* identification of GR-targets

Since GR is involved in many essential processes within the body including immunological- and stress-related processes (Chinenov et al., 2012; de Kloet et al., 2005; Harris et al., 2012; Silverman and Sternberg, 2012; Simoes et al., 2012), research aimed at gaining more insight in GR-functioning has received a lot of focus. A lot of insight in GR function in different contexts or cell types can be obtained by understanding the genes and pathways regulated by GR. While various research groups have been active in this area, it has proven to be a challenge to answer the question "what are the primary GR-targets in the genome?" Below we discuss a variety of methodological approaches that can be used to tackle this question.

Expression profiling

Activation of GR results in GR-binding, either directly or indirectly, to the DNA, thus affecting the expression of associated genes. The altered gene expression can be measured by Real-time Quantitative Polymerase Chain Reaction (RT-qPCR), which is a low to medium throughput methodology especially suitable for analysis of specific genes of interest. However, when research involves the detection of genes that are differentially expressed in a genome-wide manner without prior knowledge or preference, other techniques are available such as RNA microarrays, RNA-sequencing (RNA-Seq) and Serial Analysis of Gene Expression (SAGE) (Datson et al., 2012; Datson et al., 2001b; Reddy et al., 2009).

RNA expression profiling enables the analysis of the cell's transcriptome. This approach has been applied to characterize GR-mediated gene expression in the hippocampus and has increased our understanding of genomic pathways regulated by GR (Datson et al., 2001b). These pathways involve general cellular processes such as energy metabolism, cell cycle and response to oxidative stress, but also genes that are important for neuronal structure and plasticity (Datson et al., 2001b; Datson et

al., 2001a; Datson et al., 2012). However, RNA expression profiling in the brain is challenging due to among others its cellular heterogeneity and small and thus difficult to detect changes in gene expression which are mostly in the range of 10–30 % (Datson et al., 2008). This makes identification of differentially expressed genes as a response to a stressful situation or CORT-injection in brain more difficult.

When characterizing GR-dependent changes in gene expression it is important to bear in mind that not all genes that change their expression in response to GR-activation will represent primary GR-targets. For instance, the time point of gene expression measurement after a stress response or administration of CORT is an important factor. The longer the duration between activation of GR and measuring the transcriptional changes, the less likely it is that these transcriptional changes are primary GR-regulated events but rather secondary or even further downstream events. By using the protein synthesis inhibitor cycloheximide it is possible to rule out all differential expression occurring secondary to the initial GR-binding and thus requiring translation of the primary target (Morsink et al., 2006a). Despite the fact that these approaches have provided enormous insight in GR-function, mRNA analysis remains an indirect measurement to determine the primary genomic GR-targets.

In silico modeling

As mentioned earlier, GR is known to bind to GRE sequences and screening the genome for this sequence is another approach to identify potential primary GR-binding sites in the genome. A genome-wide search for the exact consensus hormone response element (AGAACAnnnTGTTCT) revealed the presence of 565 hits in the entire human genome (Horie-Inoue et al., 2006). When comparing this number with expression profiling data of the rat hippocampus where 203 putative CORT-responsive genes were revealed, a discrepancy is evident (Datson et al., 2001b). Apparently, identifying a GRE sequence that is functional at a given genomic location will not guarantee that GR can bind at that same GRE in all cell types or at all CORT concentrations nor at identical sequences present elsewhere in the genome.

Essentially, the chromatin has to be accessible for GR to allow binding to its genomic target. This accessibility differs per experimental setting, timing and cell type, and also depends on the type and amount of ligand. Furthermore, the sequence surrounding a GRE is of importance for guiding cofactors to assist in the GR-DNA interaction, while the cocktail of expressed and therefore available cofactors may vary per cell-type. Therefore the binding potential of GR to specific DNA binding sites will differ between cell-types. Knowledge that has been acquired in the liver, where GR is abundantly expressed, can by no means be extrapolated to the brain and vice versa. DNA binding sites that are predicted *in silico* or have been identified in other tissues have to be verified in every experimental setting.

Combining expression profiling data with predicted GR-binding sequences gives an extra dimension to the likelihood that *in silico* predicted sites are functional. In

addition, evolutionary conservation appears to be a major predictor of functionality of a subset of transcription factor binding sites (Kunarso et al., 2010). Combining this knowledge, evolutionary conserved GREs can be predicted *in silico* by using a Position Specific Scoring Matrix (PSSM) constructed from known GREs. This PSSM can scan genomic regions surrounding CORT-responsive genes and calculates the likelihood that a given 15 bp-long sequence, the length of a GRE, is in fact a functional GRE. This is considered to be more sensitive and precise than screening the genome for consensus sequences (Stormo, 2000). It has to be noted that *in silico* prediction is based on known GR binding sites and does not consider the fact that other yet undiscovered GR-binding sequences that are distinct from the canonical GR consensus motif might exist as well.

Chromatin Immunoprecipitation (ChIP)

To identify the genomic targets to which GR primarily binds, the most proximal readout is to analyze the actual GR-DNA interaction rather than the altered transcriptome. In the past, binding-assays such as electromobility shift assays, reporter assays and DNase footprinting assays have provided invaluable information regarding transcription factor binding to the DNA and enabled elucidation of DNA recognition sequences to many receptors (Payvar et al., 1983; Hellman and Fried, 2007). Their main drawback however, is that it is difficult to apply them to *in vivo* experimental settings and that they have a low throughput (Vinckevicius and Chakravarti, 2012). The rise of Chromatin Immunoprecipitation (ChIP) has enabled isolation of specific protein-DNA complexes from cells and tissues that can subsequently be used to study interactions of transcription factors and other proteins to the whole genome (Nelson et al., 2006). Briefly, the DNA-protein interactions are fixed using formaldehyde, after which the chromatin is sheared and protein-specific antibodies are used to isolate DNA-fragments to which the protein of interest is bound. Sepharose A-beads will bind the antibody-protein-DNA complexes after which they are reverse crosslinked to release the DNA fragments. The DNA-fragments are purified and can be further analyzed (Figure 1.6). Commonly used downstream methods for further analysis of ChIP DNA fragments are described below.

ChIP-on-chip

The DNA fragments obtained in ChIP can be labeled (with a fluorescent tag) and hybridized to complementary probes that are present on a microarray, a technique also known as ChIP-on-chip (Lemetre and Zhang, 2013; Pillai and Chellappan, 2009). Subsequently, the signals of the labeled fragments are measured and since the signal depends on the amount of target sample that binds to the probes, quantitative calculations can be made when comparisons are made between different samples. The probes with ChIP signals can be mapped back to the genome and as a result, genome-wide protein binding sites can be identified.
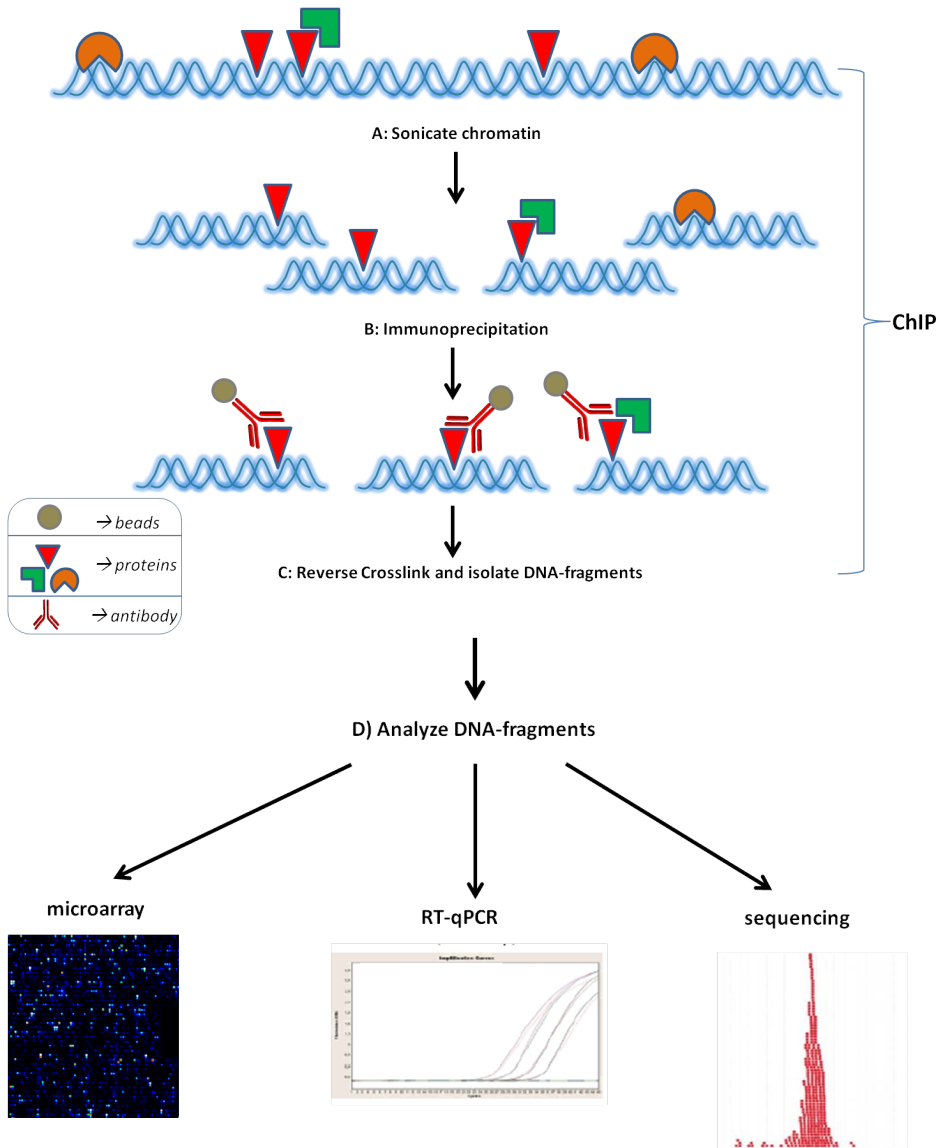
Figure 1.6: Chromatin Immunoprecipitation (ChIP) method.
Graphic illustration representing the basic steps of Chromatin Immunoprecipitation (ChIP). Proteins visualized represent proteins that bind to the DNA, such as transcription factors. A) After crosslinking the DNA-protein complexes, the DNA is sheared by usage of electromagnetic waves, resulting in DNA-fragments. B) By using an antibody specific for the protein of interest, the DNA-fragments to which this protein is bound to, can be selected for isolation. Sepharose-A beads subsequently bind to the antibody-protein-DNA complexes. C) Finally, the complexes are reverse crosslinked and the DNA-fragments are purified. D) The DNA-fragments are now ready for further analysis by Microarray, RT-qPCR and/or sequencing. Here, one sequenced fragment is represented by a red dot. When there is a location highly bound by for instance GR, than it is expected that this region is isolated in a higher amount in comparison to background signals resulting in an overlap of the sequenced fragments (or red dots) visualized by peaks.

15

The DNA fragments that are present on a microarray are variable and it depends on the research questions that one has which microarray composition is preferred. It is possible for instance to focus on promoter regions (affymetrix_ 900775 _ human) or CpG islands (Weinmann et al., 2002). In addition, there is a possibility to screen only elements that are known to be functional in the human genome, also known as ENCODE regions (agilent_ G4495A-014792_human).

Advantages of using a microarray is that it is easy to use, quantitative, relatively fast and flexible with respect to the genetic components one wishes to analyze. A downside is that it does not allow for identification of ChIP-fragments mapping outside the regions represented on the microarray and to analyze a whole genome of human, rat or mouse, a lot of ChIP-material needs to be available, which is unfortunately often not the case, especially when specific animal tissue, such as hippocampus, is concerned.

ChIP-sequencing

Alternatively, the DNA fragments obtained by ChIP can be analyzed by next-generation sequencing, also known as ChIP-sequencing (ChIP-seq), which allows sequencing of low concentrations of short DNA-fragments in an unbiased manner (Mardis, 2007). Briefly, the DNA-fragments are blunted and ligated to sequencing adapters after which the DNA is amplified using PCR. Subsequently, the DNA-fragments are size-separated on an agarose-gel after which fragments containing an average of 300 base pairs (bp) in length are selected for sequencing. Single-end sequencing of the first $35\,\mathrm{bp}$ of all the fragments results in small sequences, also known as reads, which can be mapped back to the genome to define where they originate from. ChIP-sequencing generates millions of reads and it goes without saying that bioinformatics is essential in data analysis. The amount of generated reads depends on the protein investigated, the experimental model used and the read length. However, according to the guidelines that recently have been established by the ENCODE consortium, the goal is to obtain ≥ 10 million reads for mammalian genomes (Landt et al., 2012).

Compared to ChIP-on-chip, ChIP-seq achieves higher sensitivity and sharper resolution of protein-DNA binding sites, while generating less noise (Euskirchen et al., 2007; Ji et al., 2008; Robertson et al., 2007). There are several high-throughput sequencing platforms available. The Solexa Genome Analyzer was one of the first commercial sequencers and after being purchased by Illumina, the next generation sequencing machines such as the Illumina Genome Analyser were among the most frequently used sequencing platforms. There is various peak calling software available that is used to identify regions of ChIP enrichment, including CisGenome (Ji et al., 2008) and the CLC Genomics Workbench (CLC bio). Researchers who have access to bioinformatics support might choose to use home-made algorithms.. In general, successful experiments identify thousands to tens of thousands of peaks for most transcription factors in mammalian genomes (Landt et al., 2012). In the end,

the choice for specific analysis software is subjective and there is not a standard tool for ChIP-seq analysis.

The options that one has with ChIP-seq seem to be endless. Due to the unbiased approach, binding sites in the whole genome can be identified including intronic, exonic and intergenic regions. This means that one does not need to make a decision at forehand on whether to focus only on promoter-regions, which is the more classic location to focus on in the search for TF-binding sites. Furthermore, there are possibilities to analyze one sample and look at binding sites of multiple proteins to see whether they potentially form protein-complexes on the DNA. Binding peaks can be visualized through means of the UCSC Genome Browser(Kent et al., 2002).

ChIP-seq has been applied in the context of *de novo* primary GR-target identification in several studies. However, these studies were performed in non-neuronal cell cultures, including human lung carcinoma cells (A549), mouse adipocytes (3T3-L1), premalignant breast epithelial cells (MCF10A-Myc), murine mammary epithelial cells (3134) and pituitary (AtT-20) cells (John et al., 2011; Pan et al., 2011; Yu et al., 2010). These studies have contributed to an increased insight in the genome-wide repertoire of GR and the involved molecular mechanisms. Perhaps one of the most striking findings is the low degree of overlap in GR binding sites when comparing different cell types, indicating that GR occupancy of genomic binding sites is highly cell type specific (John et al., 2011). This illustrates the importance of cautiousness when extrapolating data from similar experiments performed in different experimental models and underscores the complex nature of GR signaling.

1.4 Hippocampal plasticity and the mTOR pathway

In the current thesis we have investigated whether the candidate pathway mammalian target of Rapamycin (mTOR) is directly regulated by GR. This pathway is fundamental in regulating neuronal plasticity, which is the structural and functional change in response to a given situation, either physiological or psychological. This is fundamental to hippocampus-dependent learning and memory. The mTOR pathway has been studied extensively in relation to cancer (Akhavan et al., 2010), but knowledge in relation to the hippocampus and to stress is a topic that has gained interest more recently (Liu et al., 2014; Lu et al., 2015; Orlovsky et al., 2014).

The mTOR-pathway is activated by a wide variety of extracellular stimuli such as hormones, growth factors and neurotransmitters (Figure 1.7) and plays an important role in conveying extracellular information to the intracellular environment. The mTOR-pathway exists of two different multiprotein complexes within the cells, mTORC1 and mTORC2, whose activity is initially influenced by neuronal surface receptors and channels such as *N*-methyl-D-aspartate receptors (NMDA-R), brain-derived neurotrophic factor (BDNF) and dopaminergic and metabotropic glutamate receptors (mGluRs) which are fundamental to maintaining long-term potenti-
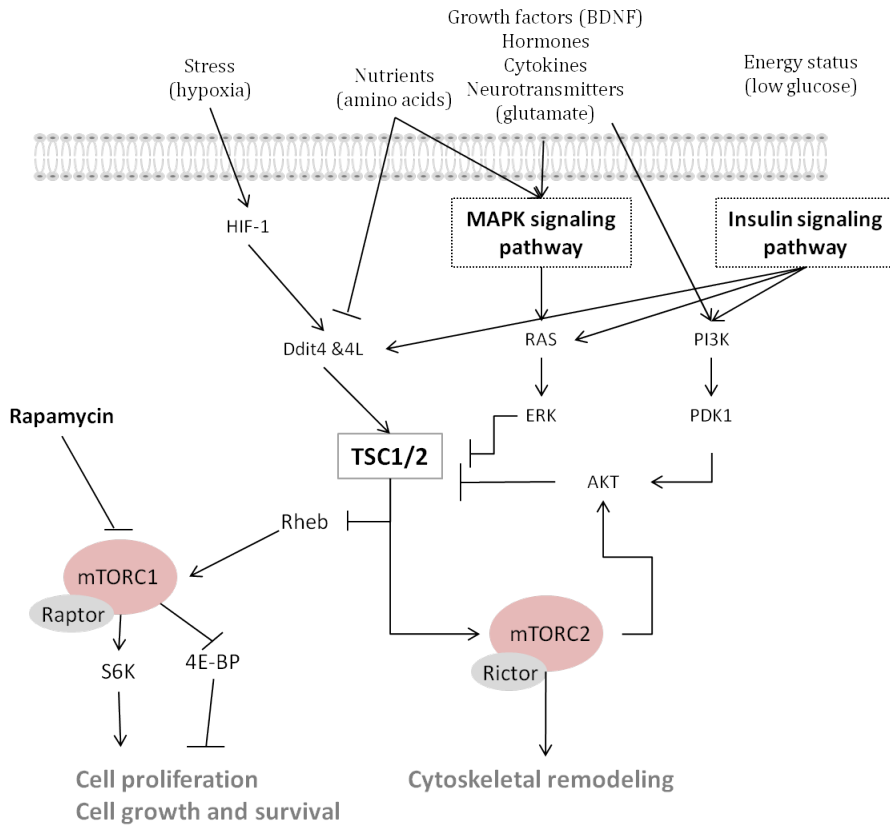
Figure 1.7: The mTOR pathway and its regulators.
Extracellular stimuli such as stress, nutrients, energy status, neurotransmitters and hormones activate intracellular pathways such as the MAPK signaling pathway and the Insulin pathway. Ultimately, this affects mTOR pathway functioning and the processes it is associated with. This includes cytoskeletal remodeling, cell proliferation and cell growth and survival.

ation (LTP) and long-term depression (LTD) (Hou and Klann, 2004; Leal et al., 2014; Ru et al., 2012). As a consequence intracellular pathways, such as the insulin signaling pathway and MAPK signaling pathway are activated, mediating the effect of the extracellular information. Hereby the expression and activity of pathway proteins are affected such as phosphoinositide dependent kinase-1 (PDK1), phosphatidylinositol 3-kinase (PI3K), v-akt thymoma viral proto-oncogene 1 (AKT) and Tuberous sclerosis protein *1* (TSC1) and *2* (TSC2) (Fang et al., 2013; Moghbelinejad et al., 2014; Komatsuzaki et al., 2012) (Figure 1.7).

The two protein complexes mTORC 1 and mTORC2 differ based on their protein-composition as well as on their substrates and their final functional implications within the neuronal cell. Whereas mTORC2 is mainly associated with cytoskeletal remodeling and regulation of cell survival, mTORC1 is involved in mRNA transcription, mRNA processing and protein translation influencing processes like cell prolif-

eration, energy regulation and cell growth and survival (Figure 1.7). The processes are affected in response to environmental/physiological changes such as hypoxia, nutrients, energy status and presence/fluctuations of growth factors, hormones and cytokines (Lipton and Sahin, 2014).

Within the CNS, the mTOR pathway has been associated with synaptic plasticity, memory retention, neuroendocrine regulation associated with food intake and modulation of neuronal repair following injury (Pilar-Cuellar et al., 2013). Malfunctioning of the mTOR pathway has been related to a number of neurological diseases such as autism and tuberous sclerosis, as well as neurodegenerative diseases as Alzheimer's, Parkinson's and Huntington's disease (Bourgeron, 2009; Chong et al., 2012; Malagelada et al., 2008; Mozaffari et al., 2009; Pei and Hugon, 2008; Williams et al., 2008) More recently, the mTOR signaling pathway has been found to be compromised in Major Depressive Disorder (MDD) (Jernigan et al., 2011) and modulation of mTOR is suggested to be a novel approach to develop strategies for the treatment of affective disorders (Dwyer et al., 2012).

The mTOR pathway and glucocorticoids

As discussed above, it is clear that both the mTOR pathway and CORT play a role in neuronal plasticity. While it is known that the mTOR pathway is subject to regulation by CORT in the periphery (Shah et al., 2000a; Wang et al., 2006a), this has been studied less well in the context of the brain. There are studies that have described an inhibitory effect of CORT on mTOR signalling in neuronal cell cultures, in rat hypothalamic organotypic cultures and mouse cortical primary cultures (Howell and Manning, 2011; Shimizu et al., 2010). More recently it has been shown that chronic stress resulted in an increase in GR and mTOR mRNA expression in the rat hippocampus (Orlovsky et al., 2014). This mRNA increase was accompanied by a significant reduction in the number of neuronal and astroglial cells. It is becoming more and more apparent that there is a connection between CORT, mTOR and neuronal plasticity, but the underlying mechanism remains to be elucidated.

In this thesis we used ChIP-Seq to investigate whether any of the mTOR proteins could be identified as primary GR-targets, which may shed light on the crosstalk between CORT, mTOR and neuronal plasticity.

1.5   Scope and outline of the thesis

In the last few years, the knowledge regarding the action of CORT within the brain has expanded enormously. Fundamental for this progress was the discovery that the central action exerted by CORT is mediated by MR and GR, which are abundantly expressed in the limbic system (hippocampus, septum, amygdala), brain regions with a crucial function in emotional expressions such as fear and aggression, learning and memory processes, and stress regulation. At the start of the research described

in this thesis, which was March 2007, the genome-wide inventory of CORT-target genes (Datson et al., 2001b) was not yet complete because of technical limitations. Due to the rapid evolution of innovative technologies, resulting in the first ChIP-seq studies, it became possible to perform genome-wide identification of transcription factor binding sites (Barski et al., 2007; Johnson et al., 2007; Mikkelsen et al., 2007; Reddy et al., 2009; So et al., 2007; Yu et al., 2010).

The aim of this thesis was to apply ChiP-seq combined with *in silico* methodology for identification of whole genome CORT-target genes in a neuronal setting. For this purpose we used a neuronal cell culture and also the rat hippocampus, of which we made an inventory of all genomic DNA binding sites for GR and validated several of these using RT-qPCR. In addition, we investigated the potential of MR to bind to a selection of GR-binding sites in the rat hippocampus. The thesis concludes with a study in rats aimed to investigate the genomic effect of an acute CORT challenge in the context of prior exposure to chronic restraint stress using microarray and ChIP-seq analysis. The results revealed the hippocampal mTOR pathway as a novel direct validated CORT target and showed that this pathway became particularly responsive to CORT following prior exposure to chronic stress.

Objective

The objective of this thesis is to identify all primary genomic targets for GR in a neuronal context by combining *in silico*, ChIP-seq and microarray analysis and then to apply this knowledge in a more detailed analysis of the mTOR pathway in discrete hippocampal regions: the CA3 pyramidal cell field and the dentate gyrus.

Specific aims

The common denominator in all chapters is the identification of primary genomic targets of GR within neuronal tissue. Specific aims of this thesis are:

- To use an *in silico* approach with the goal to predict neuronal-specific GREs in the genome followed by their experimental validation. For this purpose we have developed the Position Specific Scoring Matrix (PSSM) GenSig.

- To identify genome-wide GR-binding sites (GBS) *in vitro* in neuronal PC12 cells and *in vivo* in rat hippocampus using ChIP-seq and to identify genes located in the vicinity of these GBS that are activated/repressed by GR in a neuronal-specific context.

- To investigate whether MR binds to the same GBS as GR in the hippocampus and to measure binding of both receptors to these DNA sites in response to different concentrations of ligand.

- To translate the genome-wide knowledge regarding GBS into a functional application by investigating how chronic stress affects GR-mediated action of acute glucocorticoid exposure to the mTOR pathway as a novel mechanism involved in the regulation of brain plasticity.

Outline

In **Chapter 2** we show that a position-specific scoring matrix can be used to predict the presence of GREs near hippocampal target genes. Furthermore, we analyze the presence of motifs that flank the GRE-sequence which might determine cell-specific transcriptional regulation by CORT within hippocampal neurons.

In **Chapter 3** the identification of genome-wide GBS by ChIP-sequencing in neuronal PC12 cells after continuous stimulation with DEX is reported. We analyze the GBS for the presence of GREs and other known protein-binding motifs. To understand the possible functional implication of GR-binding, we identify the genes nearest to the GBS and perform gene ontology analysis. Finally we compare the GBS that are identified in this neuronal context with known GBS identified in other ChIP-seq studies.

In **Chapter 4** the analysis of genome-wide GBS using ChIP-sequencing is extended to the *in vivo* rat hippocampus after the administration of CORT. An extensive validation of a selection of GBS is presented at varying concentrations of CORT, allowing GR-GBS interaction to be studied in more detail. Furthermore, we measure concentration-dependent MR-binding to this selection of GBS to investigate whether MR and GR bind to the same genomic sequences and to get more insight into the implications of the MR/GR balance under different ligand-conditions.

In **Chapter 5**, the effect of CORT-treatment on the mTOR pathway, a major pathway in cell survival and plasticity, in discrete regions of the rat hippocampus is reported. We compare the effect of acute CORT treatment in the absence or presence of a history of chronic stress experience on the expression of mTOR pathway regulators using microarray analysis. We also investigate with ChIP-seq the capability of GR to bind near these regulators. Furthermore, we measure mTOR protein to see whether CORT and chronic stress can actually influence the mTOR pathway within the rat hippocampus.

In **Chapter 6**, the findings are evaluated and placed in context where their relevance for the stress response is discussed.

Chapter Two

Specific regulatory motifs predict glucorticorticoid responsiveness of hippocampal gene expression

N.A. Datson[1], J.A.E. Polman[1], R.T. de Jonge[1], P.T.M. Van Boheemen[1],
E.M.T. Van Maanen[1], Jennifer Welten[1], B. McEwen[2], H.C. Meiland[3],
O.C. Meijer[1]

[1] Division of Medical Pharmacology, Leiden/Amsterdam Center for Drug Research &
    Leiden University Medical Center, Leiden, the Netherlands
[2] Laboratory of Neuroendocrinology, the Rockefeller University,
    1230 York Avenue, New York, NY 10065, USA
[3] ICT shared service center, Leiden University, Leiden, The Netherlands

THE glucocorticoid receptor (GR) is an ubiquitously expressed ligand-activated transcription factor that mediates effects of cortisol in relation to adaptation to stress. In the brain, GR affects the hippocampus to modulate memory processes through direct binding to glucocorticoid response elements (GREs) in theDNA. However, its effects are to a high degree cell specific, and its target genes in different cell types as well as the mechanisms conferring this specificity are largely unknown. To gain insight in hippocampal GR signaling, we characterized to which GRE GR binds in the rat hippocampus. Using a position-specific scoring matrix, we identified evolutionary-conserved putative GREs from a microarray based set of hippocampal target genes. Using chromatin immunoprecipitation, we were able to confirm GR binding to 15 out of a selection of 32 predicted sites (47 %). The majority of these 15 GREs are previously undescribed and thus represent novel GREs that bind GR and therefore may be functional in the rat hippocampus. GRE nucleotide composition was not predictive for binding of GR to a GRE. A search for conserved flanking sequences that may predict GR-GRE interaction resulted in the identification of GC-box associated motifs, such as Myc-associated zinc finger protein 1, within 2 kb of GREs with GR binding in the hippocampus. This enrichment was not present around nonbinding GRE sequences nor around proven GR-binding sites from a mesenchymal stem-like cell dataset that we analyzed. GC-binding transcription factors therefore may be unique partners for DNA-bound GR and may in part explain cell-specific transcriptional regulation by glucocorticoids in the context of the hippocampus.

2.1 Introduction

Glucocorticoid hormones, i.e. cortisol in humans and corticosterone in rodents (both abbreviated as CORT), released by the adrenal gland in response to stress, are important mediators of the stress response throughout the body and the brain. Cellular adaptation to stress is highly tissue dependent, but mechanisms responsible for the high degree of cell specificity of CORT target genes are largely unknown. The brain is a major target of CORT, which readily passes the blood-brain barrier to affect a wide variety of processes, both in neurons and glia cells. CORT has profound effects on neuronal plasticity and neuronal survival, with consequences for behavior, learning, and memory. These effects are mediated by the coordinate action of high-affinity mineralocorticoid (MR) and low-affinity glucocorticoid receptors (GR), colocalized in neurons of the limbic brain, in particular the hippocampus, and in control of gene expression networks (Datson et al., 2008).

Part of the CORT effects on neuronal function and viability depends on genomic mechanisms involving binding of GR and/or MR to glucocorticoid response elements (GREs) regulating expression of target genes. GRE-dependent processes are important in the brain, because modulation of hippocampal excitability and spatial memory were impaired in $GR^{dim/dim}$ mutant mice, in which the mutation prevented GR homodimerization and therefore binding to most GREs, whereas protein-protein interactions of the receptor with other transcription factors remained undisturbed (Karst et al., 2000; Oitzl et al., 2001).

Several studies have focused on identifying GREs in peripheral tissues (Phuc Le P. et al., 2005) and cell lines, including the A549 human lung epithelial carcinoma cell line and mouse mesenchymal stem-like cells (Reddy et al., 2009; So et al., 2007; So et al., 2008; Wang et al., 2004). However, the GREs responsible for action of GR in vivo in the brain are largely unknown. It is likely that there are brain-specific GREs that selectively function in a neuronal context, given the large diversity of CORT-regulated genes when comparing CORT responses in different tissues. Taking this even a step further, within the brain there are likely to be sequence motifs that determine why CORT induces expression of a particular gene in the dentate gyrus (DG) subregion of the hippocampus, whereas having no effect in cornu ammonis 1, despite the fact that both subregions express GR (Gemert Van et al., 2009; Lee et al., 2003; Schaaf et al., 1998). Understanding the molecular context in which GREs function is necessary for a better understanding of the way in which CORT, via GR, affects the function and morphology of different brain regions and adaptation to stress.

Although in many cases chromatin accessibility is a prerequisite for binding of transcription factors, evolutionary conservation appears to be a major predictor of functionality of a subset of transcription factor-binding sites (Kunarso et

al., 2010), including the GRE (So et al., 2008). We took advantage of this to predict evolutionary-conserved GREs *in silico* using a position-specific scoring matrix from 44 GREs described in literature. Using this matrix, we scanned large genomic regions surrounding CORT-responsive genes in two different expression datasets enriched for CORT-responsive genes: 1) an expression dataset derived from *in vivo* CORT responses in rat hippocampus (Datson, N. A. and B. S. McEwen, unpublished data), and 2) a published expression dataset consisting of genes up-regulated by CORT in mouse C3H10T1/2 mesenchymal stem-like cells (So et al., 2008). Our goals were to 1) identify GREs in the vicinity of GR-induced genes in the hippocampus, 2) analyze how true GREs in the hippocampus differ from nonbinding sequences, and 3) elucidate how primary GR targets in hippocampus differ from those in mesenchymal stem-like cells.

2.2   Materials and Methods

Microarray datasets

Two microarray datasets enriched for CORT-responsive genes were used in this study.

CORT-responsive genes in the rat hippocampus

This *in vivo* dataset was derived from the hippocampal DG subregion of rats injected sc with $5 \, \text{mg/kg/ml}$ CORT dissolved in propylene glycol and killed $3 \, \text{h}$ after injection. The DG was isolated using laser microdisection and used for microarray analysis on Affymetrix Rat Genome 230 2.0 GeneChips. The microarray experiment lead to the identification of 538 CORT-responsive genes, comprising 183 up-regulated and 118 down-regulated genes that could be linked to a gene symbol. We continued with the 183 up-regulated genes for GRE predictions (Table 2.3).

CORT-responsive genes in mouse C3H10T1/2 mesenchymal stem-like cells (So et al., 2008)

This *in vitro* dataset was derived from C3H10T1/2 mesenchymal stem-like cells treated with $1 \, \mu\text{M}$ dexamethasone, a synthetic glucocorticoid, for $90 \, \text{min}$. Sixty-nine genes were found to be up-regulated after treatment, and 17 genes were down-regulated. In this set, 50 GRE sites were shown to bind GR, whereas 119 "predicted GR-binding sequences" did not bind GR. The GR-binding and GR-nonbinding GREs in this study (as in ours) did not differ in nucleotide content (So et al., 2007).
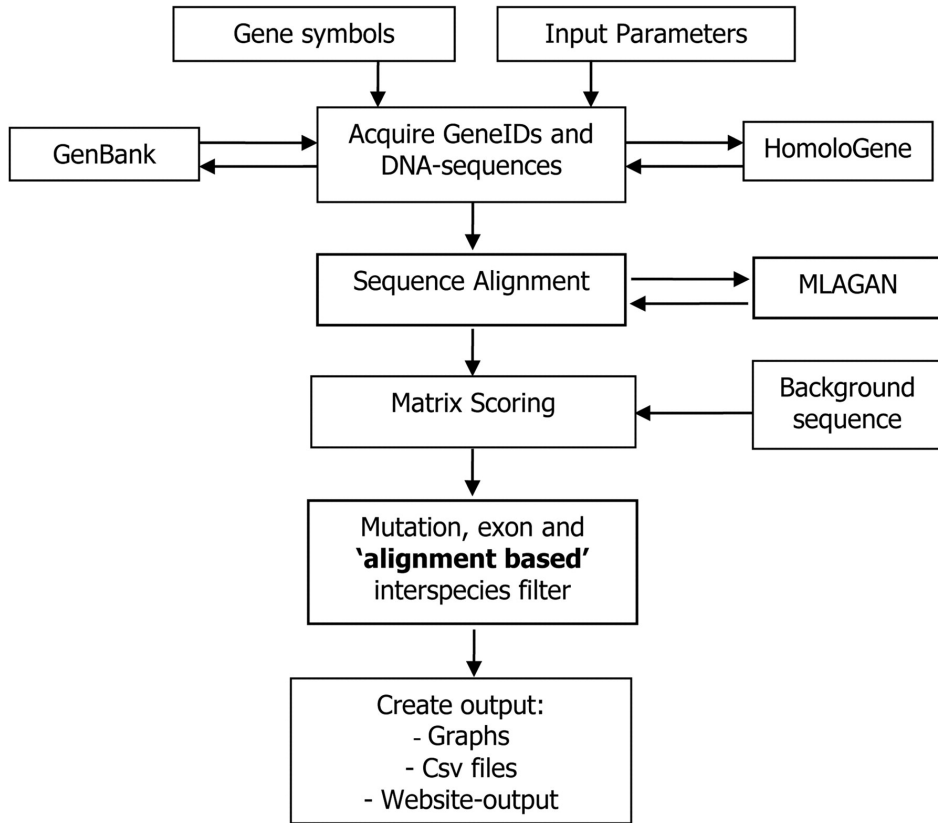
Figure 2.1: Outline of the *in silico* GRE-screening procedure.
Please see text for details.

In silico GRE prediction

For the current study, we constructed a GRE matrix, which is based on 44 GREs described in literature called matrix-44 (Table 2.4). A list of gene symbols representing CORT-responsive genes from the rat hippocampal microarray data was used to score for GRE-like sequences using matrix-44. Only upregulated genes were selected, because these depend on binding to classical GREs. Homologous sequences for multiple species (human, cow, mouse) were retrieved from the homologene database. Mouse and human were chosen for completeness of genomic annotation and supplemented with one additional species that is phylogenetically in between rodent and human (i.e. cow). A genomic region of 50 kb up- and downstream was retrieved per gene per species from the National Center for Biotechnology Information GenBank website. Exonic sequences were excluded. To facilitate identification of positionally and evolutionary-conserved GREs, the sequences of the different species were aligned before scoring using the BioPerl module dedicated to the LAGAN Toolkit, based on the multiple alignment algorithm MLAGAN (Brudno et al., 2003).

After alignment, the sequences of the different species were individually scored, and an interspecies filter was applied, which matches and selects for predicted GREs based on their position in the alignment between multiple species. A maximum of four mismatches between the different species was tolerated. More differences than this resulted in discarding the GRE from further analysis. For each position on the DNA-sequence, a score was computed for the full length of the matrix using a sliding window of 14 nucleotides. Please note that the classical canonical GRE sequence is 15 nucleotides. However, the first position in our matrix-44 did not show any base pair preference and as such did not contribute to the score. Therefore, we decided to omit the first base. Subsequently, a threshold of 0.8 (out of a maximum score of 1) was set, based on a frequency of less than 0.1 % of scores of 0.8 or higher in random DNA sequences (data not shown). The criteria for considering a sequence to be a putative GRE were: 1) location within a region spanning 50 kb upstream and 50 kb downstream of a gene upregulated by CORT in our microarray dataset, 2) a GRE score of at least 0.8 in four different species (rat, mouse, cow, and human), and 3) a maximum of four mismatches between the different species. An outline of the approach is depicted in Figure 2.1.

Animals and treatment

Male Sprague Dawley rats (Harlan, Leiden, The Netherlands) weighing approximately 250 g on the day of surgery were group housed on a 12 h light, 12 h dark cycle (lights on at 0700h) in a temperature-controlled facility. Animals were handled daily for a week before the start of the experiment. Food and water were provided *ad libitum*. All experimental manipulations were done in the morning. Experiments were approved by the Local Committee for Animal Health, Ethics, and Research of the University of Leiden (Dierexperimentencommissie no. 07166). Animal care was conducted in accordance with the European Commission Council Directive of November 1986 (86/609/EEC).

To study GR dynamics, animals were challenged with a high dose of CORT (3 mg/kg ip CORT-hydroxypropyl-cyclodextrin; Sigma-Aldrich, St. Louis, MO). Tail blood samples were taken before and during the challenge to monitor CORT levels in blood. Animals were decapitated ($n = 8$ per time point per treatment group) 0, 60, and 180 min after injection. Brain tissue was collected, snap frozen in isopentane on dry ice, and stored at $-80\,°C$ until further processing. Of each animal, one hippocampus was isolated for chromatin immunoprecipitation (ChIP).

Chromatin immunoprecipitation

ChIP to study binding of GR to predicted GREs was performed as published ChIP to study binding of GR to predicted GREs was performed as published (Sarabdjitsingh et al., 2010a). Briefly, fixed chromatin derived from the hippocampi of three animals was pooled and sheared, yielding fragments of 100–500 bp (20 pulses of 30 sec;

Bioruptor; Diagenode, Liege, Belgium). Immunoprecipitation was performed with either $6\,\mu g$ of GR-specific H300 or normal rabbit IgG (Santa Cruz Biotechnology, Inc., Santa Cruz, CA) overnight at $4\,°C$. Immunoprecipitation with a nonspecific antibody (normal IgG) did not result in increased DNA recovery after treatment and was used to correct the GR immunoprecipitated samples for nonspecific binding. The criterion for binding was a more than 2-fold increase in the yield of the real-time quantitative PCR (RT-qPCR) reaction, compared with the no-hormone condition, and a total recovery of more than $0.1\,\%$ of input material.

Selection of GREs for validation

Out of 183 up-regulated genes, 156 were annotated in all four species that we used for alignment (human, mouse, rat, and cow). GRE predictions were made for these genes, including $50\,kb$ of up- and downstream sequence. Thirty-two predicted GREs from up-regulated genes were selected for validation using RT-qPCR on ChIP material, of which all fitted the criteria of a score above 0.8 in all four species except for two (Adra1d_2 and Slc15a13_3), which were taken along to test how stringent these criteria are. Binding to the metallothionein and myoglobin locus was used as positive and negative control, respectively.

Primer design and RT-qPCR

After DNA recovery (Nucleospin; Macherey-Nagel, Düren, Germany), RT-qPCR was performed *in duplo* to study enrichment of GR-immunoprecipitated DNA fragments harboring the predicted GREs in the different treatment groups. Primers were designed around the *in silico*-predicted GREs using National Center for Biotechnology Information's PrimerBlast and were tested for absence of hairpin formation using Oligo 7. A list of all primers is available in the Table 2.5. RT-qPCR was performed using the LightCycler FastStart DNA Master PLUS SYBR Green I kit (Roche, Indianapolis, IN), according to the manufacturer's instructions.

Motif finding

The flanking sequences of the experimentally tested GREs were screened for additional transcription factor binding motifs. These analyses were done using the motif finding tools MEME (Bailey et al., 2006),MDScan (Liu et al., 2004), and F-Match (Kel et al., 2003). After motif identification, TOMTOM v4.3.0 was used to find corresponding transcription factors in the TRANSFAC database. For MDScan, default settings were used with the following changes: motif width 12 and 5000 nucleotides of mouse intronic sequence (available on the website) was used as background. For both MEME and MDScan, 250 nucleotides left and right of the predicted GRE were used for motif finding. F-Match was used on the BioBase website and is part of the eXPlain v3.0 package. Validation of motif overrepresentation was then determined using 500 nucleotides left and right of predicted GREs.

2.3 Results

Matrix derived from 44 GREs in literature

We used a position-specific scoring matrix based on 44 known GREs from literature (Table 2.4). The resulting sequence logo of these 44 GREs is shown in Figure 2.2.

Prediction of GREs is improved by aligning genomic sequences of multiple species

Because conservation analysis has been shown to predict *in vivo* occupancy of GR-binding sequences at CORT-induced genes (So et al., 2008), we applied an inter-species filter to identify evolutionary-conserved high-scoring GREs in rat, mouse, human, and cow (Figure 2.3). However, the success of this approach is highly dependent on a positionally conserved gene structure, in which conserved GREs are present at exactly the same location and not shifted. Because this is often not the case when comparing multiple species, we applied a multiple sequence alignment before scanning for GREs. The effect of this alignment and interspecies filter is evident from the α-1D-adrenergic receptor (*Adra1d*) gene, which shows large interspecies genomic insertions/deletions. Before alignment, the two high-scoring GREs in the different species are highly dispersed, with distances between species differing up to over 20 kb (Table 2.1 and Figure 2.3). However, after alignment, the predicted GREs are located at exactly the same position, thus facilitating their recognition as conserved sites (Table 2.1 and Figure 2.3).

A

B *Relative frequency matrix*

	1	2	3	4	5	6	7	8	9	10	11	12	13	14
A	0.09	0.54	0.63	0.02	0.70	0.20	0.27	0.31	0.06	0.00	0.06	0.11	0.02	0.13
C	0.20	0.18	0.15	0.70	0.11	0.27	0.27	0.34	0.02	0.02	0.02	0.25	0.90	0.25
G	0.65	0.09	0.09	0.18	0.02	0.31	0.18	0.15	0.04	0.86	0.11	0.13	0.02	0.02
T	0.04	0.18	0.11	0.09	0.15	0.20	0.27	0.18	0.86	0.11	0.79	0.50	0.04	0.59

C *Log likelihood matrix*

	1	2	3	4	5	6	7	8	9	10	11	12	13	14
A	-1.2630	1.0588	1.2730	-2.5849	1.4150	-0.2630	0.1154	0.3219	-1.5849	-3.5849	-1.5849	-1	-2.5849	-0.7776
C	-0.2630	-0.4150	-0.5849	1.4150	-1	0.1154	0.1154	0.4150	-2.5849	-2.5849	-2.5849	0.0000	1.7725	0.0000
G	1.3219	-1.2630	-1.2630	-0.4150	-2.5849	0.3219	-0.4150	-0.5849	-2	1.7004	-1	-0.7776	-2.5849	-2.5849
T	-2	-0.4150	-1	-1.2630	-0.5849	-0.2630	0.1154	-0.4150	1.7004	-1	1.5849	0.9385	-2	1.1699

Figure 2.2: Graphical representation of the GRE matrix based on 44 proven GREs from literature.
A, Logo representation, in which *letter size* corresponds to the frequency of occurrence of nucleotides at each position (`http://weblogo.berkeley.edu/`). B, The frequency matrix. C, The log-transformed likelihood matrix that was used in the scoring procedure, in which scores were expressed relative to the maximal outcome of the matrix, which was set at the value of 1.

	GRE sequence	Position of GRE before alignment	Position of GRE after alignment	GRE score
Adra1d_1				
Homo Sapiens	gaacaccctgtact	77,873	170,141	0.93
Mus musculus	gaacgccctgtact	53,496	170,141	0.83
Rattus norvegicus	gaacggcctgtacc	58,681	170,141	0.81
Bos taurus	gaacaccctgtact	56,374	170,141	0.93
Adra1d_2				
Homo Sapiens	gaacaggacgtcct	−31,585	−25,038	0.84
Mus musculus	ggacaggatgtcct	−37,462	−25,038	0.89
Rattus norvegicus	ggacaggacgtcct	−43,891	−25,038	0.78
Bos taurus	gaacaagatgcctt	−46,743	−25,038	0.74

Table 2.1: Location of GREs before and after alignment in vicinity of *Adra1d* gene.
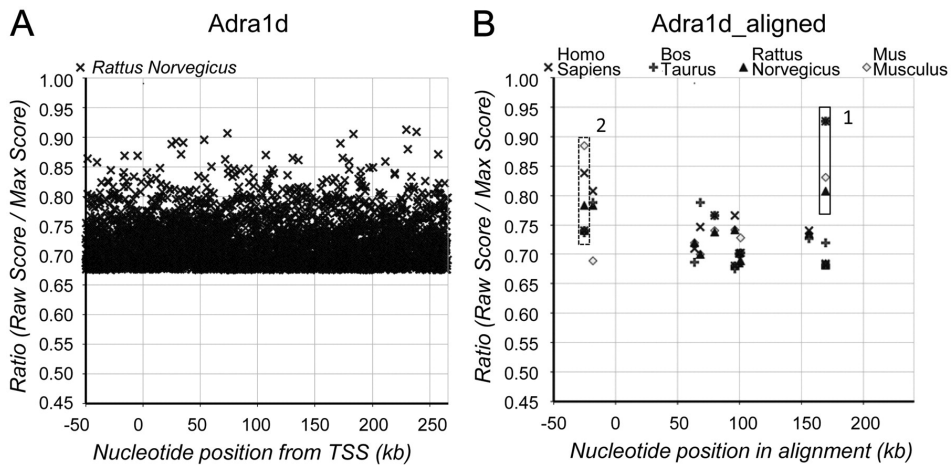
Figure 2.3: Predicted GREs with and without applying an interspecies filter to select for evolutionary-conserved GREs in the *Adra1d* gene.
Boxed scores are the ones aligned to each other. A, GRE matrix scores with a value over 0.65 in rat, plotted relative to the transcription start site of the gene. There are many GREs with a score above 0.8. B, After alignment of the sequences of multiple species and selection for evolutionary-conserved GREs, most of the predicted sites in the rat are lost, leaving two conserved GREs.

Prediction of evolutionary-conserved GREs in CORT-responsive genes in the hippocampus

The 20 selected genes up-regulated by CORT in the hippocampus contained a total of 1614 GREs with a matrix score above 0.8. Adding the demand of conservation of the score being more than 0.8 in all four species strongly reduced the amount of predictions to 32 (Table 2.2). The number of predicted GREs also decreased dramatically if the threshold was raised to 0.85 or 0.9. The 32 evolutionary-conserved GREs with a score above 0.8 were validated experimentally for GR binding. The GRE sequences for the different species are listed in Table 2.6.

Highest score	No. of predicted GREs			No. of conserved GREs		
	>0.9	>0.85	>0.8	>0.9	>0.85	>0.8
Abhd14a	4	15	56	0	1	1
Akap7	3	20	120	0	0	1
Arhgef3	3	15	93	1	1	1
Daam1	2	25	135	0	0	1
Ddit4	2	18	74	1	1	2
Dgat2	5	14	87	0	0	1
Errfi1	0	11	53	0	0	1
Fam55c	1	10	66	0	1	1
Fkbp5	6	19	122	1	1	2
Kcnj11	1	15	63	0	0	2
Klf9	1	16	70	0	1	2
Lyve1	1	8	49	0	0	1
Mfsd2	1	7	63	0	2	2
Msx1	1	9	60	1	1	1
Slc25a13	3	20	143	0	1	1
Srxn1	3	10	58	0	1	3
Tiparp	1	17	62	0	1	4
Tle3	2	12	82	0	0	4
Zfyve28	1	17	111	0	0	1
Znf592	1	9	47	0	1	2
Total	**42**	**287**	**1,614**	**4**	**13**	**34**
Average per gene	2.1	14.4	80.7	0.2	0.7	1.7

Table 2.2: Number of predicted GREs in 20 selected genes before and after selection for evolutionary conserved sequences.

In vivo GR occupancy of predicted GREs in hippocampus

RT-qPCR analysis on ChIP material enriched for GR binding allowed confirmation which of the predicted GREs were bound by GR *in vivo* in the rat hippocampus. Of the 32 tested GREs, GR binding could be shown for 15. Interestingly, the two GREs that did not fully fit the criteria could not be validated. For example, of the two predicted GREs in *Adra1d*, only Adra1d_1, which fitted the criteria, showed GR binding in the tissue and under the conditions we tested in this study (Figure 2.4). Validation of the predicted GREs using ChIP/RT-qPCR *in vivo* in hippocampal rat neurons resulted in a success rate of nearly 50 %. In other words, by applying specific criteria (up-regulation of the gene, evolutionary conservation, and score at least 0.80 in four different species) we can predict with 50 % accuracy GR-binding sites in the hippocampus (Figure 2.5).

Analyzing GRE-flanking regions for conserved motifs

We next compared the sequences and flanking regions of the *bona fide* hippocampal GREs with the predictions that could not be validated. The actual sequence, score, or the extent of conservation was not different. Although the highest fold
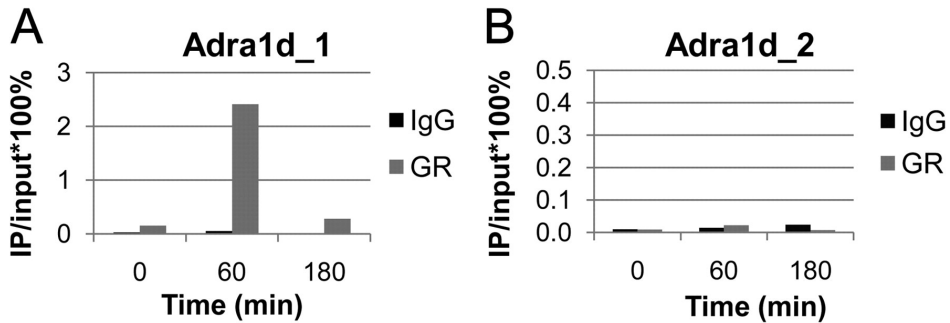
Figure 2.4: ChIP analysis of two predicted GREs indicated in Figure 2.3.
A, Strong enrichment of sequence Adra1d_1 after immune precipitation with a GR antibody of hippocampus material $60\,\mathrm{min}$ after glucocorticoid treatment, compared with $t = 0$ and $t = 180\,\mathrm{min}$ and compared with control IgG. B, Lack of binding to the Adra1d_2 sequence in the same material.
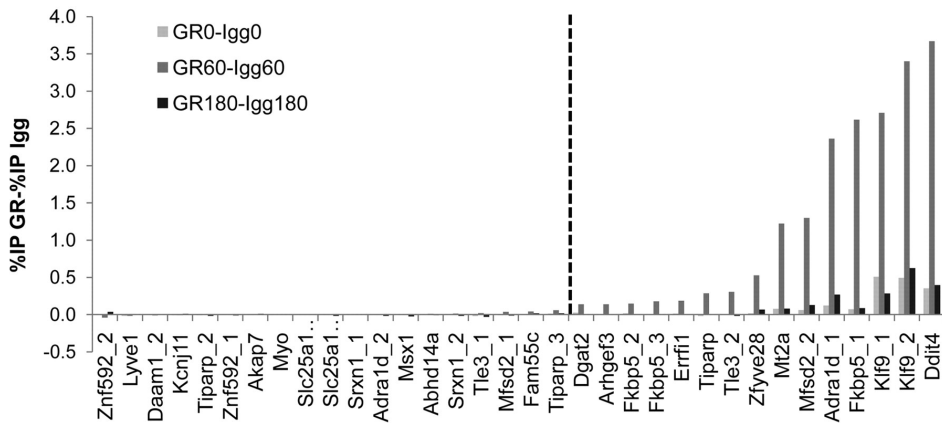
Figure 2.5: Binding profiles for GR on 32 predicted and two control sequences at three time points after CORT injection, expressed as percentage of input material.
Cut-off for enrichment was set at $0.1\,\%$ of input material and enrichment of a factor 2 relative to the time point $0\,\mathrm{min}$. The predicted GREs are ordered by magnitude of GR binding at timepoint $(t) = 60$ (*red bars*), after correction for IgG binding. At $t = 180\,\mathrm{min}$, GR-binding levels are comparable with those before GR activation. Seventeen sequences (*right from dashed line*) were found to be enriched for GR binding at $t = 60$ Myoglobin (Myo) functioned as negative control, the GRE controlling the metallothionein gene (Mt2a) as the positive control.

enrichment tended to be on GREs that were completely conserved (five out of six highest enrichment values), there were also three fully conserved predicted GREs with high scores that showed no enrichment at all. Closer inspection of the flanking sequence of GR-binding and GR-nonbinding GREs showed that they differed strikingly. Scanning 250 nucleotides up- and downstream of the GR-binding GREs showed specific enrichment of a number of predicted binding sites for enriched for the nucleotides cytosine (C) and guanine (G), such as Myc-associated zinc finger protein 1 (MAZ1), Specificity Protein 1 (SP1), Wilms' tumor 1, and zinc finger protein (Znf) 219 (Figure 2.6, A–F). More complete scanning of the sequences around the

GRE showed a higher presence of predicted MAZ1 and SP1 sites up to a distance of about $2,000\,\text{bp}$, with a bias at the $5'$ end. These binding sites correspond with a general increase in GC-motifs in these areas. The sequence motifs to which SP1 and MAZ1 bind are shown in Figure 2.7. As a second control for specificity, we checked for general increase in transcription factor-binding sites by scoring nuclear factor κB sites, which were not different between GR-binding and GR-nonbinding GRE sequences (Figure 2.6, G and H). The enrichment was not related to distance to the transcription start site or extent of conservation (data not shown). Most interestingly, the signature was not detected around the bound GREs from the So dataset derived from mesenchymal stem-like cells (Figure 2.8).

2.4   Discussion

The aim of this study was to identify genes regulated by direct GR-GRE binding in the brain based on *in silico* GRE screening of CORT-responsive genes. By doing so, we revealed that GR-binding sequences differ from nonbinding sequences by the nearby presence of predicted GC-rich binding sites for transcription factors such as MAZ1 and SP1. This characteristic of binding was found to be absent in another dataset with GR-binding and GR-nonbinding sites, suggesting a mechanism for tissue-specific CORT signaling that may determine GRE usage in the hippocampus.

Importance and validity of alignment and matrix

Because there are substantial differences in genomic organization of genes and their flanking regions between species, proper alignment facilitates screening for evolutionary conservation of GREs. Although in most cases alignment works well, we cannot exclude that some conserved sequences were missed due to suboptimal alignment by the available algorithms.

Previous papers strongly suggested that evolutionary conservation (up to $11/15$ nucleotides) is an important predictor of GRE functionality (Reddy et al., 2009; So et al., 2007). The strength of conservation analysis for this sequence is demonstrated by the striking difference in numbers of predicted GREs with and without screening for evolutionary conservation. In the 20 genes listed in Table 2.2, there is a total of 1614 predicted GREs with a score in rat above 0.8. This number drops dramatically to only 32 GREs that survive the evolutionary filter, which is much more in a realistic range. Almost half of these conserved GREs can be validated, confirming that evolutionary conservation has an important predictive value for GR binding.

The matrix that was used for identifying GREs was based on 44 GREs from literature, with proven GR binding in either EMSA or deoxyribonuclease footprint assays. These GREs represent different species, different responsive tissues, and have a bias for sequences proximal to the transcription start sites. There are minor differences
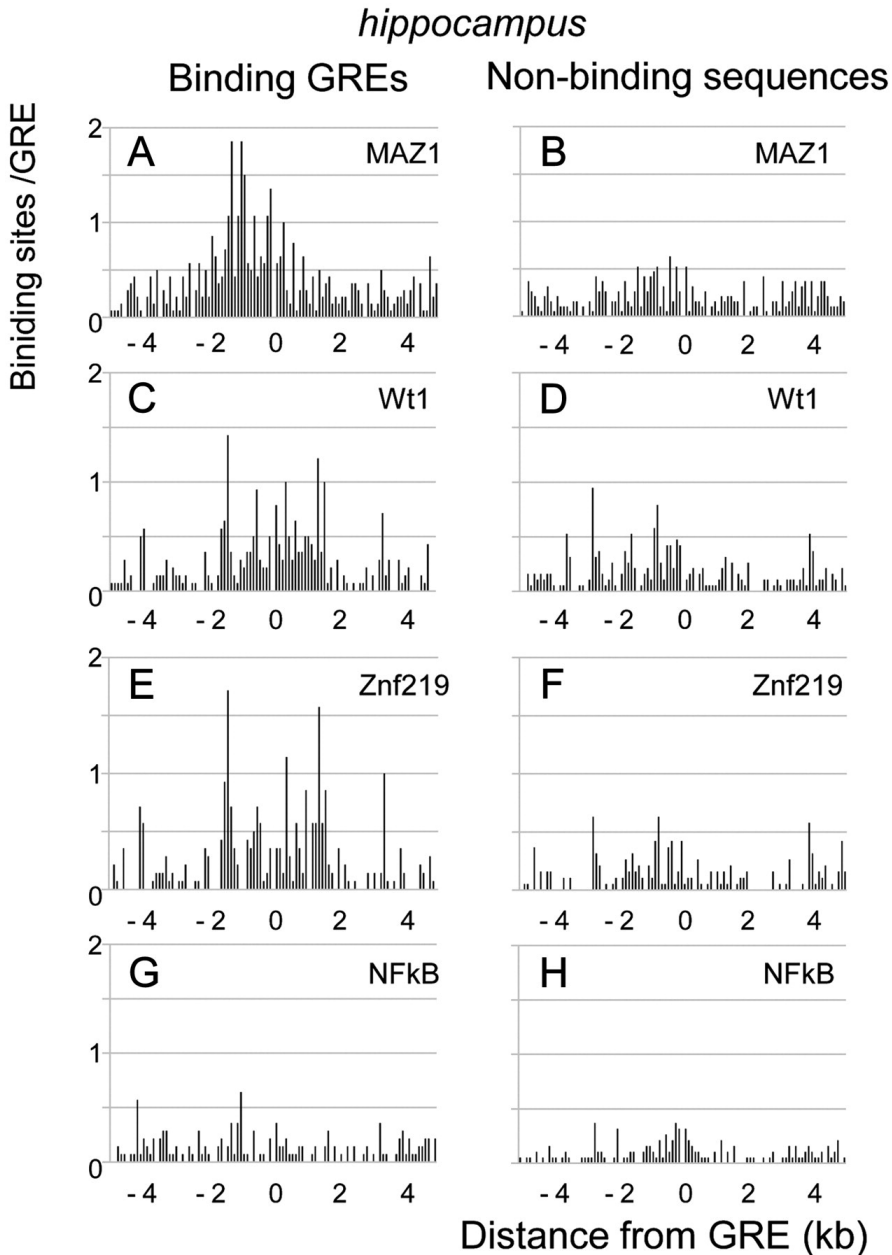
Figure 2.6: Presence of predicted transcription factor-binding sites surrounding true GREs and nonvalidated GREs from rat hippocampus.

Expressed is the occurrence of sites per GRE sequence at particular distances from the GRE sequence. The comparison per transcription factor is between validated GREs (A, C, E, and G) and nonbinding GRE sequences (B, D, F, and H). Binding sites for GC binders, such as MAZ1 (A and B), Wilms' tumor 1 (C and D), and Znf219 (E and F), are enriched up to 2 kb from the GRE, with a tendency for skew on the 5′ site. Nuclear factor κB (NFκB) response element consensus frequency (G and H) did not differ between GR-binding and GR-nonbinding GREs.
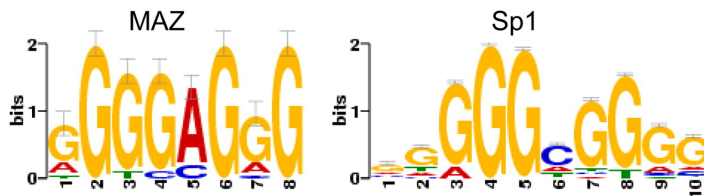
Figure 2.7: Sequence motif of MAZ1 and SP1 transcription factor-binding sites.
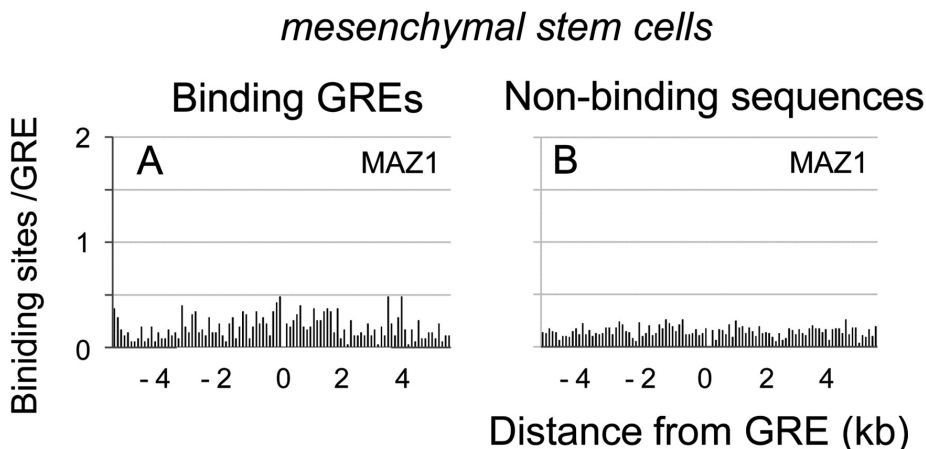
Figure 2.8: MAZ1 sites are not enriched around GR-binding GREs in mesenchymal stem cells. No differences are found for MAZ1 site occurrence between GR-binding (A) and GR-nonbinding (B) GRE sequences.

with matrices derived from large-scale chromatin occupation studies in cell lines (Reddy et al., 2009), which may be due to cell type-specific characteristics of GR binding. However, despite these points, our matrix clearly is suited to predict a substantial number of GREs in the brain, located at considerable distances from the transcription start site of CORT-responsive genes, as demonstrated by the successful validation of 15 GREs consisting of at least 10 novel previously described GREs.

False negatives

There is undoubtedly a number of false negative findings in our GRE scoring. First, the score threshold that we used, requiring a score above 0.8, may be too stringent, thus missing some *bona fide* GREs. Conversely, lowering the threshold below 0.8 results in a number of GRE predictions that likely includes many false positives. Similarly, the requirement for a GRE to be conserved in four different species may also result in missing some GREs, because evolutionary conservation may not be a good predictor for all transcription factor-binding sites (Schmidt et al., 2010). Furthermore, the matrix that we used is not particularly suited for identifying nontypical GREs that deviate from the consensus, despite evidence for direct GR binding

(Costeas and Chinsky, 2000; Kooi van der et al., 2005). Although we included a number of these nontypical GREs in our matrix, their contribution to the matrix is too small to adequately identify such sequences in the scoring procedure. In addition, for those responsive genes in which no GRE could be identified, we simply may have not scanned the relevant DNA region. GREs have been shown to occur at distances up- and downstream of transcription start sites that are even further than the $50\,\mathrm{kb}$ that we used here (Reddy et al., 2009; So et al., 2007).

False positives

Overall, $47\,\%$ (15 out of 32) of the predicted and selected GREs showed GR binding in the hippocampus of rats after administering CORT. Because the GR-GRE interaction and consequently GR-driven gene expression occurs in a cell type-specific way, it is likely that several of the 17 GREs for which we did not observe any GR binding could very well bind GR in other tissues (*e.g.* the perfectly conserved predicted GRE in the *msx* gene, which has an almost maximal matrix score). Chromatin organization controls GRE availability in a number of ways (Biddie et al., 2010), and work on the estrogen receptor and GR has indeed shown considerable cell-specific variation in response to element use (Krum et al., 2008). Future work should elucidate whether nonbinding sequences lack the necessary accessory sites or whether those GRE sequences are inaccessible due to epigenetic regulation. An additional issue is that some of the GREs that we selected for validation may not functionally be associated with the responsive genes in the hippocampus but rather to another gene.

In addition to cell specificity, the kinetics of glucocorticoid signaling may be a basis for elements that came up as false positive, because responses range from immediate early responses (Gemert van et al., 2006) to slower continuous induction (John et al., 2009). Lastly, there may also be "true false positives": sequences that we assign as GREs but that may not bind GR in any tissue or circumstance but rather related nuclear receptors, such as MR, androgen, and progesterone receptors (Nelson et al., 1999), or that have different reasons for evolutionary conservation.

Analyzing GRE-flanking regions

Although the GRE sequence itself may contain information relevant to epigenetic mechanisms (Biddie et al., 2010), we found no relation with responsiveness. Because the exact sequence of the GRE did not distinguish binding from nonbinding, the context of the surrounding sequence may be of relevance (So et al., 2008). Indeed, the binding of GREs could be linked to the presence of MAZ1 and SP1-binding sites. The presence of additional motifs in the flanking sequences of hormone response elements has been reported before (Carroll et al., 2006; Phuc Le P. et al., 2005), but its tissue specificity is less commonly reported. In the current study, we identified an overrepresentation of consensus sites for several GC-box binders, indicating the

presence of a GC-rich area in the flanking region of a substantial part of the GR-binding GREs. The presence of SP1-binding sites surrounding GREs was previously also reported in human A549 lung carcinoma cells (Reddy et al., 2009). Because we did not find an overrepresentation of GC-box transcription factor motifs in the non-validated genes in this study or in the vicinity of the GR-binding GREs identified by So *et al.* (So et al., 2008) in mesenchymal stem cells, we suggest that GC-boxes may play a role in determining tissue specificity of GR binding to a defined group of GREs. Interestingly, a screen on GR-binding sites in mouse liver pointed to enrichment of CCAAT-enhancer-binding protein (C/EBP), rather than GC binders (Phuc Le P. et al., 2005). A recent screen in two mouse cell lines found different motifs associated with GR binding, which were however partly exclusive rather than accessory to GRE (John et al., 2011). Whether such transcription factors determine binding site availability, or the nature of transcriptional responses once GR has bound, remains to be determined. Although both GR- and GC-binding transcription factors are ubiquitously expressed, the combined action in particular target genes may be part of a combinatorial code for specific responses to stress. Irrespective of the exact binding factors, the GC-rich area could be used as an extra criterion in predicting to which GRE GR binds in specific tissues, such as for example the hippocampus.

As a start to further investigate candidate binding factors to the recognized motifs, we queried expression data from the Allen Mouse Brain Atlas (Lein et al., 2007). *MAZ1* had the highest hippocampal expression level compared with the other identified motif-associated proteins. Other factors were expressed at lower levels (*e.g.* SP1 and Znf219) or nondetectable in the brain [Zic family member 3 (Zic3) and zinc finger and BTB domain containing 7B (Zbtb7b)]. MAZ protein is a broadly expressed Cys2His2 zinc finger protein that can interact with SP1 at the same GC-rich binding sites (Song et al., 2001; Song et al., 2003). Among their common target genes are the *N*-methyl-D-aspartic acid (*NMDA*) (Okamoto et al., 2002) and the adrenal medulla glucocorticoid responsive phenylethanolamine *N*-methyltransferase (*PNMT*) gene (Her et al., 2003). Interestingly, the SP family of proteins has been implicated as integratory factors in gene regulation associated with other hormonal signaling pathways (Solomon et al., 2008).

2.5   Conclusion

Using a matrix of 44 published GREs, we have successfully identified 15 GREs that are bound by GR in the rat hippocampus, of which at least 10 are novel. Furthermore, we have identified a signature that distinguishes GR-binding from GR-nonbinding GRE sites in the hippocampus but not in mesenchymal stem cells. This signature is a GC-box, to which transcription factors such as SP1 and MAZ1 can bind. Analysis of additional datasets is essential to further elucidate whether this motif plays a role in determining tissue specificity of GR-responsive transactivated genes. In addition, ChIP analysis with antibodies directed at members of the SP1 family and MAZ proteins could help to further identify exactly which cross talk partners are active in conjunction with GR. We view our current finding as a first step toward understanding the direct downstream pathways of GR signaling in the brain.

Table 2.3: List of 183 genes upregulated by CORT in the dentate gyrus region of the hippocampus.

Please note: some genes are represented by multiple probe sets.

Probe set	Gene Symbol	Gene Title	Parametric p-value	Direction of regulation by CORT
1396113_at	Abhd14a	abhydrolase domain containing 14A	0.0051565	up
1368534_at	Adra1d	adrenergic receptor, alpha 1d	0.0001817	up
1382272_at	Agtrap	angiotensin II, type I receptor-associated protein	2E−006	up
1373078_at	Ahcyl2	S-adenosylhomocysteine hydrolase-like 2	0.0043009	up
1389496_at	Akap7	A kinase (PRKA) anchor protein 7	0.0008697	up
1368365_at	Aldh3a2	aldehyde dehydrogenase family 3, subfamily A2	2.2E−006	up
1373250_at	Anln	anillin, actin binding protein (scraps homolog, Drosophila)	3E−007	up
1391673_at	Arhgap20	Rho GTPase activating protein 20	0.00243	up
1377750_at	Arhgef3_predicted	Rho guanine nucleotide exchange factor (GEF) 3 (predicted)	5.36E−005	up
1368563_at	Aspa	aspartoacylase	2.29E−005	up
1374539_at	Atp10d	ATPase, class V, type 10D	0.0037805	up
1375030_at	B3galt5_predicted	UDP-Gal:betaGlcNAc beta 1,3-galactosyltransferase, polypeptide 5 (predicted)	< 1E−07	up
1374323_at	Bccip_predicted	BRCA2 and CDKN1A interacting protein (predicted)	0.0065831	up
1379368_at	Bcl6_predicted	B-cell leukemia/lymphoma 6 (predicted)	1.1E−006	up
1394375_x_at	Bcl6b	B-cell CLL/lymphoma 6, member B	0.0007852	up
1381804_at	Bcl6b	B-cell CLL/lymphoma 6, member B	1.3E−006	up
1386833_at	Bcl6b	B-cell CLL/lymphoma 6, member B	3.3E−006	up
1373733_at	Bok	Bcl-2-related ovarian killer protein	0.0092297	up
1372855_at	Brd4	Bromodomain containing 4	0.0084915	up
1367657_at	Btg1	B-cell translocation gene 1, anti-proliferative	0.001966	up
1368393_at	C1qr1	complement component 1, q subcomponent, receptor 1	0.0012737	up
1375353_at	Cables1_predicted	Cdk5 and Abl enzyme substrate 1 (predicted)	0.0086606	up
1381637_at	Camk2a	Calcium/calmodulin-dependent protein kinase II, alpha	0.0071659	up
1388736_at	Ccdc43	coiled-coil domain containing 43	0.0031497	up
1384192_at	Chst1	carbohydrate (keratan sulfate Gal-6) sulfotransferase 1	0.0052078	up
1396150_at	Cldn1	claudin 1	0.003693	up
1372774_a t	Coq6	Coenzyme Q6 homolog (yeast)	0.0011843	up
1372629_at	Coro2b	coronin, actin binding protein, 2B	4.93E−005	up
1384454_at	Cpa6_predicted	carboxypeptidase A6 (predicted)	0.0025525	up
1398611_at	Cul4b_predicted	cullin 4B (predicted)	0.0073757	up
1367940_at	Cxcr7	chemokine (C-X-C motif) receptor 7	3.3E−005	up
1386904_a_at	Cyb5	cytochrome b-5	0.0004326	up
1389294_at	Cyfip1_predicted	cytoplasmic FMR1 interacting protein 1 (predicted)	0.0027769	up
1389318_at	Daam1_predicted	dishevelled associated activator of morphogenesis 1 (predicted)	0.0002217	up
1374480_at	Daam1_predicted	dishevelled associated activator of morphogenesis 1 (predicted)	0.0017818	up
1384788_at	Daglb	diacylglycerol lipase, beta	0.0010505	up
1368025_at	Ddit4	DNA-damage-inducible transcript 4	2.21E−005	up
1380817_at	Depdc2_predicted	DEP domain containing 2 (predicted)	8.56E−005	up
1389615_at	Derl1	Der1-like domain family, member 1	0.0033244	up

Probe set	Gene Symbol	Gene Title	p-value	Direction
1371615_at	Dgat2	diacylglycerol O-acyltransferase 2	3.86E−005	up
1368189_at	Dhcr7	7-dehydrocholesterol reductase	0.0010634	up
1367516_at	Dtnbp1	distrobrevin binding protein 1	0.0020268	up
1370830_at	Egfr	epidermal growth factor receptor	0.0005467	up
1391442_at	Ehd3	EH-domain containing 3	0.0033817	up
1373093_at	Errfi1	ERBB receptor feedback inhibitor 1	1.27E−005	up
1389146_at	Fam107b	family with sequence similarity 107, member B	0.0004397	up
1398425_at	Fam110b	family with sequence similarity 110, member B	0.0008749	up
1385046_at	Fam55c /// LOC682630	family with sequence similarity 55, member C /// hypothetical protein LOC682630	0.0012999	up
1374255_at	Farsla	Phenylalanine-tRNA synthetase-like, alpha subunit	0.0073605	up
1387351_at	Fbn1	fibrillin 1	0.000529	up
1368829_at	Fbn1	fibrillin 1	0.0035091	up
1387606_at	Fgf2	fibroblast growth factor 2	0.0007805	up
1388901_at	Fkbp5	FK506 binding protein 5	2E−007	up
1380611_at	Fkbp5	FK506 binding protein 5	7.51E−005	up
1372016_at	Gadd45b	growth arrest and DNA-damage-inducible 45 beta	0.0040849	up
1368577_at	Gjb6	gap junction membrane channel protein beta 6	0.0013882	up
1371363_at	Gpd1	glycerol-3-phosphate dehydrogenase 1 (soluble)	2.03E−005	up
1374648_at	Gpr155_predicted	G protein-coupled receptor 155 (predicted)	0.0003912	up
1388243_at	Gpr176	G protein-coupled receptor 176	0.0004745	up
1374043_at	Gramd3	GRAM domain containing 3	0.0027761	up
1367900_at	Gyg1	glycogenin 1	0.0047381	up
1370491_a_at	Hdc	histidine decarboxylase	0.0001866	up
1373963_at	Hdhd3	haloacid dehalogenase-like hydrolase domain containing 3	0.0073321	up
1374440_at	Hsd17b11	hydroxysteroid (17-beta) dehydrogenase 11	0.0004592	up
1370912_at	Hspa1b	heat shock 70kD protein 1B (mapped)	0.0053864	up
1382220_at	Igf2bp2	insulin-like growth factor 2 mRNA binding protein 2	0.0045324	up
1376895_at	Il16	interleukin 16	0.0048023	up
1373970_at	Il33	interleukin 33	0.0002442	up
1386987_at	Il6ra	interleukin 6 receptor, alpha	1E−006	up
1371091_at	Irs2	insulin receptor substrate 2	0.0039053	up
1383082_at	Jarid1b	jumonji, AT rich interactive domain 1B (Rbp2 like)	0.0029768	up
1390473_at	Kcng2	potassium voltage-gated channel, subfamily G, member 2	0.0007367	up
1387698_at	Kcnj11	potassium inwardly rectifying channel, subfamily J, member 11	0.0013338	up
1391007_s_at	Kcnj11	potassium inwardly rectifying channel, subfamily J, member 11	0.0052578	up
1370209_at	Klf9	Kruppel-like factor 9	0.0003826	up
1373210_at	Lamb1	laminin, beta 1	0.0025957	up
1368006_at	Laptm5	lysosomal-associated protein transmembrane 5	0.0005548	up
1383863_at	Lmo2	LIM domain only 2	7.91E−005	up
1397439_at	LOC497978	similar to diacylglycerol kinase epsilon	0.0035734	up
1372973_at	Lss	Lanosterol synthase	0.0074712	up
1367832_at	Lypla1	lysophospholipase 1	0.0068274	up
1382192_at	Lyve1	lymphatic vessel endothelial hyaluronan receptor 1	0.0004275	up
1371875_at	Manba	mannosidase, beta A, lysosomal	0.0073347	up
1390905_at	Mast4	microtubule associated serine/threonine kinase family member 4	0.0005155	up
1388774_at	Mbd2	methyl-CpG binding domain protein 2	8.17E−005	up

Probe set	Gene Symbol	Gene Title	p-value	Direction
1372966_at	Mfsd2	major facilitator superfamily domain containing 2	0.0009973	up
1372599_at	Mgst2_predicted	microsomal glutathione S-transferase 2 (predicted)	0.0085716	up
1383952_at	Mical1_predicted	microtubule associated monoxygenase, calponin and LIM domain containing 1 (predicted)	3.89E−005	up
1389433_at	Mkks	McKusick-Kaufman syndrome protein	0.0090644	up
1373189_at	Mkl1	megakaryoblastic leukemia (translocation) 1	0.0013132	up
1376410_at	Mmp17_predicted	matrix metallopeptidase 17 (predicted)	4.56E−005	up
1382363_at	Mpp5_predicted	membrane protein, palmitoylated 5 (MAGUK p55 subfamily member 5) (predicted)	0.0065158	up
1368302_at	Msx1	homeo box, msh-like 1	0.0044827	up
1371237_a_at	Mt1a	metallothionein 1a	0.0040924	up
1397644_at	Mtap_predicted	Methylthioadenosine phosphorylase (predicted)	0.00275	up
1371543_at	Mtmr2_predicted	myotubularin related protein 2 (predicted)	0.0020394	up
1394182_at	Mtmr4_predicted	myotubularin related protein 4 (predicted)	0.0065778	up
1372093_at	Mxi1	Max interacting protein 1	0.001482	up
1388139_at	Myh2	myosin, heavy polypeptide 2, skeletal muscle, adult	0.0034219	up
1387004_at	Nbl1	neuroblastoma, suppression of tumorigenicity 1	0.0002314	up
1389507_at	Nedd4l	neural precursor cell expressed, developmentally down-regulated gene 4-like	1.73E−005	up
1370408_at	Nid67	putative small membrane protein NID67	0.0080132	up
1395408_at	Nostrin	nitric oxide synthase trafficker	0.0027857	up
1390828_at	Npy1r	neuropeptide Y receptor Y1	0.0002798	up
1387497_at	Npy5r	neuropeptide Y receptor Y5	0.0053514	up
1373577_at	Nrp1	Neuropilin 1	0.0064527	up
1384112_at	Nt5e	5′ nucleotidase, ecto	0.0007823	up
1369969_at	Parp1	poly (ADP-ribose) polymerase family, member 1	0.0023734	up
1393454_at	Pcdh17_predicted	protocadherin 17 (predicted)	0.0028394	up
1384509_s_at	Pcdh17_predicted	protocadherin 17 (predicted)	0.0028995	up
1368262_at	Phlpp	PH domain and leucine rich repeat protein phosphatase	3.2E−006	up
1368119_at	Pib5pa	phosphatidylinositol (4,5) bisphosphate 5-phosphatase, A	0.0010451	up
1384741_at	Pla2g3_predicted	phospholipase A2, group III (predicted)	0.0002752	up
1368700_at	Plcl1	phospholipase C-like 1	0.0052902	up
1380661_at	Pld3	phospholipase D family, member 3	0.0040563	up
1384355_at	Plxna2_predicted	plexin A2 (predicted)	0.0021167	up
1392157_at	Plxna2_predicted	plexin A2 (predicted)	0.0061316	up
1382604_at	Polr3g	polymerase (RNA) III (DNA directed) polypeptide G	0.0046518	up
1381386_at	Pop5_predicted	Processing of precursor 5, ribonuclease P/MRP family (S. cerevisiae) (predicted)	0.000567	up
1391187_at	Ppl_predicted	periplakin (predicted)	0.002245	up
1373465_at	Pqlc1	PQ loop repeat containing 1	7.7E−006	up
1372135_at	Ptk9l_predicted /// LOC684352	protein tyrosine kinase 9-like (A6-related protein) (predicted) /// similar to twinfilin-like protein	0.0033	up
1378541_at	Pus7l_predicted	pseudouridylate synthase 7 homolog (S. cerevisiae) like (predicted)	0.0013239	up
1383232_at	Rab33b_predicted	RAB33B, member of RAS oncogene family (predicted)	0.0012736	up
1395326_at	Rbm9_predicted	RNA binding motif protein 9 (predicted)	0.0007839	up
1393502_at	RGD1306153	similar to predicted CDS, putative protein of bilaterial origin (4J193)	0.0006468	up
1391239_at	RGD1306926 _predicted	similar to hypothetical protein FLJ22175 (predicted)	0.0015965	up

Probe set	Gene Symbol	Gene Title	p-value	Direction
1377524_at	RGD1307155	similar to CG18661-PA	0.0096282	up
1374176_at	RGD1308059	similar to DNA segment, Chr 4, Brigham & Womens Genetics 0951 expressed	0.0053442	up
1372420_at	RGD1308064_predicted	similar to FKSG24 (predicted)	0.0006842	up
1372843_at	RGD1309410_predicted	LOC363020 (predicted)	0.0032345	up
1374596_at	RGD1309594	similar to RIKEN cDNA 1810043G02; DNA segment, Chr 10, Johns Hopkins University 13, expressed	0.0096133	up
1372805_at	RGD1310444_predicted	LOC363015 (predicted)	0.0011833	up
1382097_at	RGD1310754_predicted	similar to G2 (predicted)	0.0006971	up
1388945_at	RGD1311307	similar to 1300014I06Rik protein	1E−007	up
1383874_at	RGD1560812_predicted	RGD1560812 (predicted)	0.0024907	up
1373075_at	RGD1560888_predicted	similar to Cell division protein kinase 8 (Protein kinase K35) (predicted)	0.0019401	up
1390964_at	RGD1561115_predicted	similar to Gene model 1568 (predicted)	0.0088555	up
1381924_at	RGD1561507_predicted	similar to hypothetical protein FLJ31606 (predicted)	0.0052705	up
1378310_at	RGD1562710_predicted	similar to neuromedin B precursor - rat (predicted)	4.29E−005	up
1379816_at	RGD1563342_predicted	similar to RIKEN cDNA 2410025L10 (predicted)	0.000553	up
1376809_at	RGD1563342_predicted	similar to RIKEN cDNA 2410025L10 (predicted)	0.0016411	up
1379077_at	RGD1564695_predicted	similar to A830059I20Rik protein (predicted)	0.0041516	up
1375151_at	RGD1565168_predicted	Similar to RAP2A, member of RAS oncogene family (predicted)	0.0047119	up
1390942_at	RGD1565884_predicted	Similar to Pellino protein homolog 2 (Pellino 2) (predicted)	1.03E−005	up
1391075_at	Rgs17_predicted	regulator of G-protein signaling 17 (predicted)	0.0065764	up
1388937_at	Rnf19a	ring finger protein 19A	0.0001664	up
1378524_at	Rnf19a	ring finger protein 19A	3.35E−005	up
1368662_at	Rnf39	ring finger protein 39	0.0032395	up
1389202_at	Rpe	ribulose-5-phosphate-3-epimerase	0.003193	up
1371774_at	Sat1	spermidine/spermine N1-acetyl transferase 1	0.0064071	up
1389367_at	Schip1	schwannomin interacting protein 1	0.0010009	up
1388334_a t	Sec14l1	SEC14-like 1 (S. cerevisiae)	0.0001474	up
1373610_at	Sec24d_predicted	SEC24 related gene family, member D (S. cerevisiae) (predicted)	0.0042078	up
1387294_at	Sh3bp5	SH3-domain binding protein 5 (BTK-associated)	0.0015789	up
1376040_at	Sipa1l2	signal-induced proliferation-associated 1 like 2	0.0010188	up
1378356_at	Slc24a4_predicted	solute carrier family 24 (sodium/potassium/calcium exchanger), member 4 (predicted)	0.0056586	up
1389622_at	Slc25a13	solute carrier family 25 (mitochondrial carrier, adenine nucleotide translocator), member 13	0.0001236	up
1392978_at	Slc25a28	solute carrier family 25, member 28	0.0050879	up
1370848_at	Slc2a1	solute carrier family 2 (facilitated glucose transporter), member 1	0.008105	up
1382136_at	Slc2a9	solute carrier family 2 (facilitated glucose transporter), member 9	0.001057	up

Probe set	Gene Symbol	Gene Title	p-value	Direction
1373565_at	Smarca4	SWI/SNF related, matrix associated, actin dependent regulator of chromatin, subfamily a, member 4	0.0021364	up
1370159_at	Smarcd2	SWI/SNF related, matrix associated, actin dependent regulator of chromatin, subfamily d, member 2	0.0006773	up
1370049_at	Smpd2	sphingomyelin phosphodiesterase 2, neutral	0.00024	up
1376649_at	Snf1lk2_predicted	SNF1-like kinase 2 (predicted)	0.0001025	up
1394627_at	Snx19_predicted	sorting nexin 19 (predicted)	0.0097343	up
1372633_at	Spg20	spastic paraplegia 20, spartin (Troyer syndrome) homolog (human)	0.0006206	up
1383839_at	Spg20	spastic paraplegia 20, spartin (Troyer syndrome) homolog (human)	0.0079955	up
1372510_at	Srxn1	sulfiredoxin 1 homolog (S. cerevisiae)	2.88E−005	up
1387705_at	Sstr4	somatostatin receptor 4	0.0016267	up
1376572_a_at	Svil_predicted	supervillin (predicted)	0.002046	up
1388679_at	Tbc1d14	TBC1 domain family, member 14	3.8E−006	up
1375074_at	Tbkbp1	TBK1 binding protein 1	0.0078674	up
1367859_at	Tgfb3	transforming growth factor, beta 3	7.96E−005	up
1374446_at	Tiparp_predicted	TCDD-inducible poly(ADP-ribose) polymerase (predicted)	0.0022931	up
1385407_at	Tiparp_predicted	TCDD-inducible poly(ADP-ribose) polymerase (predicted)	0.0086341	up
1387169_at	Tle3	transducin-like enhancer of split 3, homolog of Drosophila E(spl)	0.0039518	up
1368136_at	Tmpo	thymopoietin	5.79E−005	up
1372664_at	Traf2_predicted	Tnf receptor-associated factor 2 (predicted)	0.0054778	up
1397596_at	Trim2	tripartite motif protein 2	0.0012484	up
1375278_a t	Trim2	tripartite motif protein 2	0.0013462	up
1373578_at	Trim2	tripartite motif protein 2	7.47E−005	up
1392972_at	Trio	triple functional domain (PTPRF interacting)	0.0005398	up
1390709_at	Trio	triple functional domain (PTPRF interacting)	7.56E−005	up
1369164_a_at	Trpc4	transient receptor potential cation channel, subfamily C, member 4	0.0082294	up
1376262_at	Uxs1	UDP-glucuronate decarboxylase 1	1.03E−005	up
1370648_a_at	Wipf3	WAS/WASL interacting protein family, member 3	0.0024273	up
1385275_at	Wnt16	wingless-related MMTV integration site 16	0.003533	up
1368641_at	Wnt4	wingless-related MMTV integration site 4	0.0044844	up
1370537_at	Xrcc6	X-ray repair complementing defective repair in Chinese hamster cells 6	0.0081922	up
1372989_at	Zdhhc14	zinc finger, DHHC domain containing 14	0.0001701	up
1376628_at	Zfp189_predicted	zinc finger protein 189 (predicted)	5E−007	up
1391216_at	Zfp509_predicted	zinc finger protein 509 (predicted)	0.0068222	up
1393572_at	Zfp592_predicted	zinc finger protein 592 (predicted)	0.0040185	up
1393556_at	Zfyve28_predicted	zinc finger, FYVE domain containing 28 (predicted)	0.0030633	up
1391478_at	Znf532_predicted	zinc finger protein 532 (predicted)	0.0033106	up

Table 2.4: Proven GREs from literature used to construct a GRE position weight matrix.

#	ID	GRE sequence	Aligned sequence	BP pos.	Symbol	Gene
1	1_1	AGAACAGA-GTGTCCTC	gaacagagtgtcct	−525	pnmt	Phenylethanolamine N-Methyl-transferase PNMT [1]
2	1_2	GGAACATC-CTGAACTA	gaacatcctgaact	−714	pnmt	Phenylethanolamine N-Methyl-transferase PNMT [1]
3	1_4	AGCACATT-ATGTGCCA	gcacattatgtgcc	−950	pnmt	Phenylethanolamine N-Methyl-transferase PNMT [1]
4	2_1	GAACCCA-ATGTTCT	gaacccaatgttct	−2609	gilz	GILZ Human [2]
5	2_2	TTAACAG-AATGTCCT	taacagaatgtcct	−3070	gilz	GILZ Human [2]
6	3_2	GGACTTG-TTTGTTCT	gacttgtttgttct	−2452	tat	Rat Tyrosine aminotransferase (TAT) [3]
7	4	AGAAGAA-ATTGTCCT	gaagaaattgtcct	−660	trhr	Human TRHR Thyrotropin-releasing hormone receptor gene [4]
8	5	GGCACAG-TGTGGTCT	gcacagtgtggtct	−2421	th	Mouse TH Tyrosine hydroxylase gene [5]
9	6	TTATTTTGA-ACACGGGG-ATCCTA	gaacacggggatcc	−75	igfb1	Rat IGFBP-1 Insulin like growth factor binding protein-1 [6]
10	7_1	CGATCAG-GCTGTTTT	gatcaggctgtttt	−183	g6pc	Glucose-6-phosphatase [7]
11	7_2	TGTGCCT-GTTTTGCT	gtgcctgttttgct	−166	g6pc	Glucose-6-phosphatase [7]
12	7_3	AAATCAC-CCTGAACA	aatcaccctgaaca	−142	g6pc	Glucose-6-phosphatase [7]
13	8_1	CACACAA-AATGTGCA	acacaaaatgtgca	−374	pepck	Rat PEPCK Phosphoenolpyru-vate carboxykinase [8]
14	8_2	AGCATATG-AAGTCCA	gcatatgaagtcca	−353	pepck	Rat PEPCK Phosphoenolpyru-vate carboxykinase [8]
15	9	TGTTCAC-TTTGTTAT	gttcactttgttat	−1102	fgg	Human gamma chain fibrio-gen [9]
16	10_1	CTTCCAT-GCTGTTCC	ttccatgctgttcc	−1432	eln	Human elastin gene [10]
17	10_2	ACCCTCC-CCTGTTCC	ccctcccctgttcc	−1310	eln	Human elastin gene [10]
18	10_3	CCACCTC-CCTGTTCC	cacctccctgttcc	−1018	eln	Human elastin gene [10]
19	11	GGAACAA-TGTGTACC	gaacaatgtgtacc	∼2.3 kb dstr. of poly(A)	dexras1	Human dexras1 gene [11]
20	12_1	AGGACAG-CCTGTCCT	ggacagcctgtcct	∼1 kb ustr. of MT II	mt2	Mouse metallothionein [12]
21	12_2	GAAACAC-CATGTACC	aaacaccatgtacc	∼7 kb ustr. of MT-I	mt1	Mouse metallothionein [12]
22	13	GGACATG-ATGTTCC	ggacatgatgttcc	−229	il6	Interleukin-6 Responsive Ele-ment Type2 [13]
23	14_1	CCAAATCA-CTGGACCT	caaatcactggacc	+191	gr	Human glucocorticoid receptor (hGR) protein [14]
24	15	GGAACAA-CAAGGGCA	gaacaacaagggca	−4432	hcar	Human constitutive androstane receptor [15]
25	16	AGAACAG-CCTGTCCT	gaacagcctgtcct	−5042	cdkn1c	Human cyclin dependent ki-nase inhibitor p57Kip2 [16]
26	17	GGGTGAG-CTTGTTCT	ggtgagcttgttct	−365	adrbk2	Rat Beta2-adrenergic receptor gene [17]

#	ID	GRE sequence	Aligned sequence	BP pos.	Symbol	Gene
27	18_1	GTACCAAG-AATGTGTT-CTGCA	caagaatgtgttct	−759	pnmt	Rat Phenyl ethanolamine N-Methyltransferase (PNMT) gene [18]
28	18_2	TTCTGCAC-TCTCTGTT-CTTAC	gcactctctgttct	−773	pnmt	Rat Phenyl ethanolamine N-Methyltransferase (PNMT) gene
29	19	CCCTGGCAC-ATTTCGTGC	ctggcacatttcgt	−150	alpha 1I3	Rat Liver alpha inhibitor III gene [19]
30	20	CGGACAA-ATGTTCT	ggacaaaatgttct	−1159	sgk1	Human sgk1 gene [20]
31	21	TGAACTG-AATGTTTT	gaactgaatgtttt	−1662	cyp2c9	Cytochrome P450 2C9 [21]
32	22	CTGTACAG-GATGTTCT	gtacaggatgttct	−2590	tat	Rat Tyrosine aminotransferase (TAT) [22]
33	23	ACATGAG-TGTGTCCT	catgagtgtgtcct	−583	chga	Rat chromogranin A [23]
34	24	AGCACAC-ACTGTTCT	gcacacactgttct	−1212	serpine1	Rat type1 plasminogen activator [24]
35	25_1	GACACCA-CCCCTCCC	acaccacccctccc	−139	dbt	Alpha-ketoacid dehydrogenase E2 subunit [25]
36	25_2	GCTCGTT-CCTTCTCT	ctcgttccttctct	−110	dbt	Alpha-ketoacid dehydrogenase E2 subunit
37	26	AGAGCAG-TTTGTTCT	gagcagtttgttct	−6300	cps1	Carbamoylphosphate synthetase [26]
38	27	AGAACTA-TCTGTTCC	gaactatctgttcc	1st intron	pfkfb3	6-phosphofructo-2 kinase [27]
39	28	GGAACAT-TTTGTGCA	gaacattttgtgca	−104	agp	Rat Alpha 1-acid glycoprotein [28]
40	29	TGGGACTAC-AGTGTCCTG	gactacagtgtcct	−1193	sult1a3	Human Sulfotransferase 1a3 (SULT1A3) [29]
41	30	TGTCCTGC-TCGAGGTG-GTTCA	ctcgaggtggttca	−630	atp1b1	Human Na/K-ATPase beta1 gene [30]
42	31	AGAACAG-AATGTCCT	gaacagaatgtcct	−1306	scnn1a	alpha-subunit epithelial Na$^+$ channel alpha-ENaC gene [31]
43	32	CAGGGTAC-ATGGCGTA-TGTGTG	cagggtacatggcg	−447	myc	Murine c-myc [32]
44	33	TGTACAC-TATTGTCT	gtacactattgtct	−756	agtr1a	Rat Angiotensin II Type 1A receptor gene [33]

1. Adams, M., Meijer, O. C., Wang, J., Bhargava, A. & Pearce, D. Homodimerization of the glucocorticoid receptor is not essential for response element binding: activation of the phenylethanolamine N-methyltransferase gene by dimerization-defective mutants. Mol Endocrinol 17, 2583–2592 (2003).
2. Wang, J. C., Derynck, M. K., Nonaka, D. F., Khodabakhsh, D. B., Haqq, C. & Yamamoto, K. R. Chromatin immunoprecipitation (ChIP) scanning identifies primary glucocorticoid receptor target genes. Proc Natl Acad Sci U S A 101, 15603–15608 (2004).
3. Jantzen, H. M., Strähle, U., Gloss, B., Stewart, F., Schmid, W., Boshart, M., Miksicek, R. & Schütz, G. Cooperativity of glucocorticoid response elements located far upstream of the tyrosine aminotransferase gene. Cell 49, 29–38 (1987).
4. Høvring, P. I., Matre, V., Fjeldheim, A. K., Loseth, O. P. & Gautvik, K. M. Transcription of the human thyrotropin-releasing hormone receptor gene-analysis of basal promoter elements and glucocorticoid response elements. Biochem Biophys Res Commun 257, 829–834 (1999).

5. Hagerty, T., Morgan, W. W., Elango, N. & Strong, R. Identification of a glucocorticoid-responsive element in the promoter region of the mouse tyrosine hydroxylase gene. J Neurochem 76, 825–834 (2001).

6. Goswami, R., Lacson, R., Yang, E., Sam, R. & Unterman, T. Functional analysis of glucocorticoid and insulin response sequences in the rat insulin-like growth factor-binding protein-1 promoter. Endocrinology 134, 736–743 (1994).

7. Vander Kooi, B. T., Onuma, H., Oeser, J. K., Svitek, C. A., Allen, S. R., Vander Kooi, C. W., Chazin, W. J. & O'Brien, R. M. The glucose-6-phosphatase catalytic subunit gene promoter contains both positive and negative glucocorticoid response elements. Mol Endocrinol 19, 3001–3022 (2005).

8. Imai, E., Stromstedt, P. E., Quinn, P. G., Carlstedt-Duke, J., Gustafsson, J. A. & Granner, D. K. Characterization of a complex glucocorticoid response unit in the phosphoenolpyruvate carboxykinase gene. Mol Cell Biol 10, 4712–4719 (1990).

9. Asselta, R., Duga, S., Modugno, M., Malcovati, M. & Tenchini, M. L. Identification of a glucocorticoid response element in the human gamma chain fibrinogen promoter. Thromb Haemost 79, 1144–1150 (1998).

10. Del Monaco, M., Covello, S. P., Kennedy, S. H., Gilinger, G., Litwack, G. & Uitto, J. Identification of novel glucocorticoid-response elements in human elastin promoter and demonstration of nucleotide sequence specificity of the receptor binding. J Invest Dermatol 108, 938–942 (1997).

11. Kemppainen, R. J., Cox, E., Behrend, E. N., Brogan, M. D. & Ammons, J. M. Identification of a glucocorticoid response element in the 3'-flanking region of the human Dexras1 gene. Biochim Biophys Acta 1627, 85–89 (2003).

12. Kelly, E. J., Sandgren, E. P., Brinster, R. L. & Palmiter, R. D. A pair of adjacent glucocorticoid response elements regulate expression of two mouse metallothionein genes. Proc Natl Acad Sci U S A 94, 10045–10050 (1997).

13. Kasutani, K., Itoh, N., Kanekiyo, M., Muto, N. & Tanaka, K. Requirement for cooperative interaction of interleukin-6 responsive element type 2 and glucocorticoid responsive element in the synergistic activation of mouse metallothionein-I gene by interleukin-6 and glucocorticoid. Toxicol Appl Pharmacol 151, 143–151 (1998).

14. Geng, C. D. & Vedeckis, W. V. Steroid-responsive sequences in the human glucocorticoid receptor gene 1A promoter. Mol Endocrinol 18, 912–924 (2004).

15. Pascussi, J. M., Busson-Le Coniat, M., Maurel, P. & Vilarem, M. J. Transcriptional analysis of the orphan nuclear receptor constitutive androstane receptor (NR1I3) gene promoter: identification of a distal glucocorticoid response element. Mol Endocrinol 17, 42–55 (2003).

16. Alheim, K., Corness, J., Samuelsson, M. K., Bladh, L. G., Murata, T., Nilsson, T. & Okret, S. Identification of a functional glucocorticoid response element in the promoter of the cyclin-dependent kinase inhibitor p57Kip2. J Mol Endocrinol 30, 359–368 (2003).

17. Cornett, L. E., Hiller, F. C., Jacobi, S. E., Cao, W. & McGraw, D. W. Identification of a glucocorticoid response element in the rat beta2-adrenergic receptor gene. Mol Pharmacol 54, 1016–1023 (1998).

18. Tai, T. C., Claycomb, R., Her, S., Bloom, A. K. & Wong, D. L. Glucocorticoid responsiveness of the rat phenylethanolamine N-methyltransferase gene. Mol Pharmacol 61, 1385–1392 (2002).

19. Abraham, L. J., Bradshaw, A. D., Northemann, W. & Fey, G. H. Identification of a glucocorticoid response element contributing to the constitutive expression of the rat liver alpha 1-inhibitor III gene. J Biol Chem 266, 18268–18275 (1991).

20. Itani, O. A., Liu, K. Z., Cornish, K. L., Campbell, J. R. & Thomas, C. P. Glucocorticoids stimulate human sgk1 gene expression by activation of a GRE in its 5'-flanking region. Am J Physiol Endocrinol Metab 283, E971-E979 (2002).

21. Gerbal-Chaloin, S., Daujat, M., Pascussi, J. M., Pichard-Garcia, L., Vilarem, M. J. & Maurel, P. Transcriptional regulation of CYP2C9 gene. Role of glucocorticoid receptor and constitutive androstane receptor. J Biol Chem 277, 209–217 (2002).

22. Grange, T., Roux, J., Rigaud, G. & Pictet, R. Cell-type specific activity of two glucocorticoid responsive units of rat tyrosine aminotransferase gene is associated with multiple binding sites for C/EBP and a novel liver-specific nuclear factor. Nucleic Acids Res 19, 131–139 (1991).

Chapter 2

23. Rozansky, D. J., Wu, H., Tang, K., Parmer, R. J. & O'Connor, D. T. Glucocorticoid activation of chromogranin A gene expression. Identification and characterization of a novel glucocorticoid response element. J Clin Invest 94, 2357–2368 (1994).

24. Bruzdzinski, C. J., Johnson, M. R., Goble, C. A., Winograd, S. S. & Gelehrter, T. D. Mechanism of glucocorticoid induction of the rat plasminogen activator inhibitor-1 gene in HTC rat hepatoma cells: identification of cis-acting regulatory elements. Mol Endocrinol 7, 1169–1177 (1993).

25. Costeas, P. A. & Chinsky, J. M. Glucocorticoid regulation of branched-chain alpha-ketoacid dehydrogenase E2 subunit gene expression. Biochem J 347, 449–457 (2000).

26. Christoffels, V. M., Grange, T., Kaestner, K. H., Cole, T. J., Darlington, G. J., Croniger, C. M. & Lamers, W. H. Glucocorticoid receptor, C/EBP, HNF3, and protein kinase A coordinately activate the glucocorticoid response unit of the carbamoylphosphate synthetase I gene. Mol Cell Biol 18, 6305–6315 (1998).

27. Pierreux, C. E., Ursø, B., De Meyts, P., Rousseau, G. G. & Lemaigre, F. P. Inhibition by insulin of glucocorticoid-induced gene transcription: involvement of the ligand-binding domain of the glucocorticoid receptor and independence from the phosphatidylinositol 3-kinase and mitogen-activated protein kinase pathways. Mol Endocrinol 12, 1343–1354 (1998).

28. Ratajczak, T., Williams, P. M., DiLorenzo, D. & Ringold, G. M. Multiple elements within the glucocorticoid regulatory unit of the rat alpha 1-acid glycoprotein gene are recognition sites for C/EBP. J Biol Chem 267, 11111–11119 (1992).

29. Bian, H. S., Ngo, S. Y., Tan, W., Wong, C. H., Boelsterli, U. A. & Tan, T. M. Induction of human sulfotransferase 1A3 (SULT1A3) by glucocorticoids. Life Sci 81, 1659–1667 (2007).

30. Derfoul, A., Robertson, N. M., Lingrel, J. B., Hall, D. J. & Litwack, G. Regulation of the human Na/K-ATPase beta1 gene promoter by mineralocorticoid and glucocorticoid receptors. J Biol Chem 273, 20702–20711 (1998).

31. Wang, H. C., Zentner, M. D., Deng, H. T., Kim, K. J., Wu, R., Yang, P. C. & Ann, D. K. Oxidative stress disrupts glucocorticoid hormone-dependent transcription of the amiloride-sensitive epithelial sodium channel alpha-subunit in lung epithelial cells through ERK-dependent and thioredoxin-sensitive pathways. J Biol Chem 275, 8600–8609 (2000).

32. Ma, T., Copland, J. A., Brasier, A. R. & Thompson, E. A. A novel glucocorticoid receptor binding element within the murine c-myc promoter. Mol Endocrinol 14, 1377–1386 (2000).

33. Guo, D. F., Uno, S., Ishihata, A., Nakamura, N. & Inagami, T. Identification of a cis-acting glucocorticoid responsive element in the rat angiotensin II type 1A promoter. Circ Res 77, 249–257 (1995).

Table 2.5: Primers created based on *in silico* predictions.

Gene	GRE pos from TSS	Primer pos from TSS	Fw/Rev	Sequence	Tm	GC	Loop, T, degrees	Length amplicon
Abhd14a	35067	35043	F	CCAGCTCAGGTTACCGTCTT	59.35	55.00	16	88
		35131	R	TGAACTAAGATGGCCAACACC	59.99	47.62		
Adra1d_1	58681	58618	F	TTAAACGGTCCTTGGTGCAT	60.37	45.00		94
		58712	R	TCCTTTATCTGTGGGCTGGTA	59.58	47.62		
Adra1d_2	−43891	−44001	F	TCTGAACCGTGACCAAGGAA	61.64	50.00	17.2	93
		−43908	R	TGACTGAACTGGAAGTGACT	53.03	45.00		
Akap7	154398	154315	F	CATGGGAGATTCTTACAGGCTT	59.61	45.45	19.6	140
		154455	R	GGTGAGGACATGACATTAGCAA	60.00	45.45		
Arhgef3	243344	243319	F	TCCGTCAACATCCTGGATTC	60.87	50.00		90
		243409	R	GAGGTGAAAAGAGGCAGGTG	59.84	55.00		
Daam1	−40707	−40761	F	GAGCAATGGGTTTGTTGGAG	60.50	50.00	2.9	101
		−40660	R	AATCCTCTCTCCATGATGCAC	59.11	47.62		
Ddit4	−20879	−20894	F	CTGTGGGTGAGCTGAGAACA	60.02	55.00		99
		−20866	R	GGCCTGTAGGTCCAGCACTA	60.28	60.00	11.2	
Dgat2	41675	41655	F	CCTGTTTTGTCTGCCTCTCTG	60.04	52.38		116
		41771	R	CACTGAGTCATTTCGCAGGA	59.98	50.00		
Errfi1	−29643	−29723	F	CCTGCATTTCTGGTTTTGAAG	59.73	42.86		105
		−29618	R	TCCTCTCCAGGGGTACACTC	59.10	60.00	23.8	
Fam55c	64366	64283	F	AAATCTTTCACCGGCTCAGA	59.81	45.00		116
		64399	R	CTCACAGCTCCAAACGGAA	59.97	52.63		
Fkbp5_1	62946	62912	F	TCAGCACACCGAGTTCATGT	60.32	50.00		133
		63045	R	CTGGTCACTGCAAAACATCATT	60.04	40.91		
Fkbp5_2	58773	58712	F	GGATGGAGACTGCGTTCTGT	60.27	55.00		99
		58811	R	CTGGAGTTCTGCCTGCACTT	60.59	55.00	30.4	
Fkbp5_3	1097	1026	F	GAACGCGTTGGAAGAAGGTA	60.25	50.00		120
		1146	R	CCGCATGCAGAATTTACTGA	59.83	45.00	7.5	
Kcnj11	−23686	−23707	F	ACCCCTGTCCTTACTCTCCA	53.15	55.00	46.3	79
		−23628	R	ATGGGGCAGGATGTCTATGT	52.16	50.00		
Klf9_1	−6345	−6376	F	ATGATGAAACGTGAGCGCTAT	59.75	42.86	6.8	93
		−6283	R	TTTCCTGTGGTTGTTGTGGA	59.98	45.00	10	
Klf9_2	−5522	−5554	F	ATCTAGGGCAGTTTGTTCAA	54.96	40.00		96
		−5458	R	GGCAGGTTCATCTGAGGACA	61.23	55.00		
Lyve1	−19879	−19951	F	CACCCAGAAAGAAGGCACA	59.81	52.63		104
		−19847	R	CTCTGTAAATGAGGGCCGAG	59.83	55.00	5.1	
Mfsd2_1	−17609	−17675	F	GAGGCATCATACCGGAACTC	59.51	55.00	13	102
		−17573	R	AGAAGATGGGAGATTGGCCT	60.04	50.00		
Mfsd2_2	2297	2215	F	GACCCGTTAGTGACGCTGTT	60.18	55.00	28.9	123
		2338	R	ACAGTGCTCCCATCAGCCTA	60.82	55.00	21.6	
Msx1	30573	30562	F	TGCAAACTCCTGAACAGCCT	60.98	50.00		84
		30646	R	GAGAAGGTGACGCCTGGTTA	60.25	55.00	13.2	
Slc25a13_2	−5588	−5635	F	GGAAAGTCTGCGTCCGTATC	59.7	55.00	9	93
		−5542	R	AGGCAGAAAGCATGAAAGCA	61.05	45.00		
Slc25a13_3	−17970	−18047	F	CTTACCCAGGACCACAAGGA	59.96	55.00		120
		−17927	R	AACAGCCATTAATTTGTGTGGTT	59.7	34.78	7.1	
Srxn1_1	−28091	−28164	F	GATGCTTTTGTGGCCACTCT	60.26	50.00	11.6	100
		−28064	R	GTTGAATGGGAAAGGGACAA	59.77	45.00		
Srxn1_2	−21486	−21509	F	GAATTTCTCATGCACAGCCA	59.81	45.00	16.5	85
		−21424	R	CTCTTTGGACGGGATTCAAG	59.66	50.00		
Tiparp_1	20215	20164	F	GCTAGGATTTCACTCGCACA	59.03	50.00	30.6	107

Gene	GRE pos from TSS	Primer pos Fw/ from TSS	Rev	Sequence	Tm	GC	Loop, T, degrees	Length amplicon
		20271	R	CAAGCTGCTGGTCTCGGTA	60.14	57.89		
Tiparp_2	13493	13481	F	GACCTCCCACATGAACTGC	59.04	57.89		112
		13593	R	CATGTGAACTTAGTTACCAGACCA	58.25	41.67	13.1	
Tiparp_3	1312	1229	F	TTGCCTGGATTGGTGTGATA	59.92	45.00		107
		1336	R	AGGCTCAGTTGGCACAGATT	59.87	50.00		
Tle3_1	70362	70355	F	GTCAAAACAACACCCAGTCC	57.87	50.00	13	116
		70471	R	ATTTGGTGGAGCTGAGCACT	59.87	50.00		
Tle3_2	−725	−782	F	TCGCCGCCTCTGCAGAATCAA	58.85	57.14		119
		−663	R	TGGCGGGAGGGGAGAAAGAGA	58.66	61.90		
Zfyve28	99395	99350	F	CCGGGATTCAGGACTCTAGTT	59.58	52.38		93
		99443	R	CATACAAGCCACTGCAGGAA	59.86	50.00		
Znf592_1	92248	92152	F	CAGCATAGCCCGACTGTGT	59.87	57.89	7.8	102
		92254	R	ATCCCTCTTCCTCCTTCCAG	59.63	55.00		
Znf592_2	90506	90487	F	CCCAGTCTAATCCCTCTTGG	58.59	55.00	8.3	121
		90608	R	ATCCAAGTCCTGCCCTACCT	59.96	55.00		

Table 2.6: Predicted GREs that were selected for validation using ChIP.

Gene	GRE sequence	BP in Aln	BP from TSS	Score
Adra1d_1				
Homo sapiens	gaacaccctgtact	170141	77873	0.93
Mus musculus	gaacgccctgtact	170141	53496	0.83
Rattus norvegicus	*gaacggcctgtacc*	*170141*	*58681*	*0.81*
Bos taurus	gaacaccctgtact	170141	56374	0.93
Adra1d_2				
Homo sapiens	gaacaggacgtcct	−25038	−31585	0.84
Bos taurus	gaacaagatgcctt	−25038	−46743	0.74
Rattus norvegicus	*ggacaggacgtcct*	*−25038*	*−43891*	*0.78*
Mus musculus	ggacaggatgtcct	−25038	−37462	0.88
Abhd14a				
Homo sapiens	gaacagcctgtact	86304	37769	0.93
Bos taurus	gaacattatgtacc	86304	30132	0.90
Rattus norvegicus	*gaacagcctgtacc*	*86304*	*35067*	*0.90*
Mus musculus	gaacagcctgtacc	86304	33829	0.89
Akap7				
Homo sapiens	gcagactttttct	360179	167897	0.81
Bos taurus	gcacattttgtcct	360179	134767	0.89
Rattus norvegicus	*gcagatcctgttct*	*360179*	*154398*	*0.88*
Mus musculus	gcagaccctgttct	360179	150888	0.89
Arhgef3				
Homo sapiens	gaacagtctgtcct	302939	16194	0.95
Bos taurus	gaacacactgtgct	302939	14141	0.93
Rattus norvegicus	*gaacaatctgtcct*	*302939*	*243344*	*0.94*
Mus musculus	gaacactctgtcct	302939	112042	0.95
Ddit4				
Homo sapiens	gaacattgtgttct	8595	−24936	0.94
Bos taurus	gaacattgtgttct	8595	−15283	0.94
Rattus norvegicus	*gaacattgtgttct*	*8595*	*−20879*	*0.94*
Mus musculus	gaacactgtgttct	8595	−22516	0.94
Dgat2				
Homo sapiens	aaacactatgttct	110257	44912	0.91
Bos taurus	aaatactctgttct	110257	49855	0.85
Rattus norvegicus	*gaacactgtgttct*	*110257*	*41675*	*0.95*
Mus musculus	gaacactgtgttct	110257	40233	0.95
Lyve1				
Homo sapiens	gcacaggctgtgct	596	−18228	0.89
Bos taurus	gcacaggctgtgct	596	−18833	0.89
Rattus norvegicus	*tcacagattgtgct*	*596*	*−19879*	*0.80*
Mus musculus	gcacagactgtgct	596	−18909	0.90
Mfsd2_1				
Homo sapiens	gaactccatgtcct	4961	−27297	0.90
Bos taurus	gaactccatgtccc	4961	−27984	0.87
Rattus norvegicus	*gaactccatgtccc*	*4961*	*−17609*	*0.87*
Mus musculus	gaactccatgtccc	4961	−18781	0.87
Mfsd2_2				
Homo sapiens	gcacactgtgttcc	60613	2402	0.88
Bos taurus	gcacaccatgtccc	60613	2165	0.88
Rattus norvegicus	*gcacaccatgtccc*	*60613*	*2297*	*0.88*
Mus musculus	gcacaccatgtccc	60613	2214	0.88
Msx1				
Homo sapiens	gaacagcctgttct	117908	53528	0.98
Bos taurus	gaacagcctgttcc	117908	40500	0.98
Rattus norvegicus	*gaacagcctgttct*	*117908*	*30573*	*0.98*
Mus musculus	gaacagcctgttct	117908	26934	0.98
Slc25a13_2				
Homo sapiens	taatagtttgttct	38873	−8228	0.81
Bos taurus	taacagattgttct	38873	−12309	0.88
Rattus norvegicus	*taacaggctgttct*	*38873*	*−5588*	*0.88*
Mus musculus	taacaggctgttct	38873	−5705	0.88
Slc25a13_3				
Bos taurus	ccataaaattatct	18803	−21180	0.68
Homo sapiens	gcataacattagct	18803	−21125	0.68
Rattus norvegicus	*ccataaaattttct*	*18803*	*−17970*	*0.76*
Mus musculus	ccataaaattttct	18803	−19022	0.76
Srxn1_1				
Homo sapiens	gaccatcttgtccc	−14268	−28256	0.85
Bos taurus	gaccaacttgtccc	−14268	−31089	0.85
Rattus norvegicus	*gaccatcttgtccc*	*−14268*	*−28091*	*0.85*
Mus musculus	gaccatcttgtccc	−14268	−28603	0.85
Srxn1_2				
Homo sapiens	ctgcaggctgttcc	−3941	−20498	0.80
Bos taurus	ctgcagactgttcc	−3941	−23256	0.82
Rattus norvegicus	*ctgcaggctgttcc*	*−3941*	*−21486*	*0.80*
Mus musculus	ctgcaggctgttcc	−3941	−22059	0.80

Gene	GRE sequence	BP in Aln	BP from TSS	Score	Gene	GRE sequence	BP in Aln	BP from TSS	Score
Errfi1					**Tiparp_1**				
Homo sapiens	gaacgaaatgtact	−16545	−44820	0.82	Homo sapiens	gaatatattgtcct	71852	22639	0.86
Bos taurus	gaacaagatgtact	−16545	−34910	0.90	Bos taurus	gaacatgctgtcct	71852	19024	0.93
Rattus norvegicus	*gaacagagtgtacc*	*−16545*	*−29643*	*0.88*	*Rattus norvegicus*	*gaacatactgtcct*	*71852*	*20215*	*0.94*
Mus musculus	ggacagagtgtgcc	−16545	−29939	0.83	Mus musculus	gaacatgctgtcct	71852	20078	0.93
Fam55c					**Tiparp_2**				
Homo sapiens	gcactttctgttcc	202292	50884	0.85	Homo sapiens	gaactgggtgtgcc	62183	15135	0.82
Bos taurus	gcacttcctgttcc	202292	61589	0.85	Bos taurus	gaactgcatgtgct	62183	12005	0.89
Rattus norvegicus	*gcactttctgttcc*	*202292*	*64366*	*0.85*	*Rattus norvegicus*	*gaactgcatgtgct*	*62183*	*13493*	*0.89*
Mus musculus	gcactttctgttcc	202292	59350	0.85	Mus musculus	gaactgcatgtgct	62183	13312	0.89
Fkbp5_1					**Tiparp_3**				
Homo sapiens	gaacagggtgttct	201653	86842	0.94	Homo sapiens	ccacaatctgtgcc	45867	1537	0.82
Bos taurus	gaacagggtgttct	201653	99485	0.94	Bos taurus	ccacaatctgtgcc	45867	−535	0.82
Rattus norvegicus	*gaacagggtgttct*	*201653*	*62946*	*0.94*	*Rattus norvegicus*	*ccacaatctgtgcc*	*45867*	*1312*	*0.82*
Mus musculus	gaacagggtgttct	201653	20724	0.94	Mus musculus	ccacaatctgtgcc	45867	1308	0.82
Fkbp5_2					**Tle3_1**				
Homo sapiens	gtacacactgttct	187860	77853	0.94	Homo sapiens	caacacccagtccc	130075	73749	0.81
Bos taurus	ctacatactgttct	187860	91074	0.89	Bos taurus	caacacccagtccc	130075	76757	0.81
Rattus norvegicus	*gtacacgctgttct*	*187860*	*58773*	*0.92*	*Rattus norvegicus*	*caacacccagtccc*	*130075*	*70362*	*0.81*
Mus musculus	gtacataccgttct	187860	16445	0.83	Mus musculus	caacacccagtccc	130075	67838	0.81
Fkbp5_3					**Tle3_2**				
Homo sapiens	ggacagtgtgttca	39281	1167	0.85	Homo sapiens	gtacagcttgtctt	26890	−387	0.81
Bos taurus	ggacagagtgtaca	39281	−4322	0.80	Bos taurus	gtacagcttgtctt	26890	−1506	0.81
Rattus norvegicus	*ggacagtgtgtaca*	*39281*	*1097*	*0.80*	*Rattus norvegicus*	*gtacagcttgtcct*	*26890*	*−725*	*0.90*
Mus musculus	ggacagggtgtaca	39281	−43907	0.79	Mus musculus	gtacagcttgtcct	26890	−1692	0.90
Kcnj11					**Zfyve28**				
Homo sapiens	gtacaagatggtca	−11257	−24819	0.80	Homo sapiens	gaacgcagtgttcc	248785	161563	0.85
Bos taurus	gtacaagatggtca	−11257	−24012	0.80	Bos taurus	ggacgccgtgttct	248785	64876	0.80
Rattus norvegicus	*gtacaagatggtca*	*−11257*	*−23686*	*0.80*	*Rattus norvegicus*	*gaacaccatgttcc*	*248785*	*99395*	*0.94*
Mus musculus	gtacaagatggtca	−11257	−22705	0.80	Mus musculus	gaacaccatgttcc	248785	105004	0.94
Klf9_1					**Znf592_1**				
Homo sapiens	ggacaaactgttcc	45287	−5481	0.88	Homo sapiens	gaagataatgttct	218121	92619	0.92
Bos taurus	ggacaaactgttcc	45287	−5884	0.88	Bos taurus	gaggaggatgttct	218121	83347	0.86
Rattus norvegicus	*ggacaaactgttcc*	*45287*	*−6345*	*0.88*	*Rattus norvegicus*	*gaagatactgttct*	*218121*	*92248*	*0.92*
Mus musculus	ggacaaactgttcc	45287	−6133	0.88	Mus musculus	gaagatactgttct	218121	85402	0.92
Klf9_2					**Znf592_2**				
Homo sapiens	gagcttgatgttcc	46231	−4616	0.81	Homo sapiens	ggacagtatggcct	216299	90890	0.84
Bos taurus	gagcttgatgttcc	46231	−4991	0.81	Bos taurus	gaacagcgtggcct	216299	81672	0.87
Rattus norvegicus	*gagcttgatgttcc*	*46231*	*−5522*	*0.81*	*Rattus norvegicus*	*ggacagcatgacct*	*216299*	*90506*	*0.82*
Mus musculus	gagcttgatgttcc	46231	−5265	0.81	Mus musculus	ggacagcatgacct	216299	83680	0.82

Chapter Three

A genome-wide signature of glucocorticoid receptor binding in neuronal PC12 cells

J.A.E. Polman[1], J.E. Welten[1], D.S. Bosch[1], R.T. de Jonge[1], J. Balog[2], S.M. van der Maarel[2], E.R. de Kloet[1], N.A. Datson[1,2]

[1] Division of Medical Pharmacology, Leiden/Amsterdam Center for Drug Research & Leiden University Medical Center, Leiden, the Netherlands
[2] Department of Human Genetics, Leiden University Medical Center, Leiden, the Netherlands

GLUCOCORTICOIDS, secreted by the adrenals in response to stress, profoundly affect structure and plasticity of neurons. Glucocorticoid action in neurons is mediated by glucocorticoid receptors (GR) that operate as transcription factors in the regulation of gene expression and either bind directly to genomic glucocorticoid response elements (GREs) or indirectly to the genome via interactions with bound transcription factors. These two modes of action, respectively called transactivation and transrepression, result in the regulation of a wide variety of genes important for neuronal function. The objective of the present study was to identify genome-wide glucocorticoid receptor binding sites in neuronal PC12 cells using Chromatin ImmunoPrecipitation combined with next generation sequencing (ChIP-Seq). In total we identified $1,183$ genomic binding sites of GR, the majority of which were novel and not identified in other ChIP-Seq studies on GR binding. More than half (58%) of the binding sites contained a GRE. The remaining 42% of the GBS did not harbour a GRE and therefore likely bind GR via an intermediate transcription factor tethering GR to the DNA. While the GRE-containing binding sites were more often located nearby genes involved in general cell functions and processes such as apoptosis, cell motion, protein dimerization activity and vasculature development, the binding sites without a GRE were located nearby genes with a clear role in neuronal processes such as neuron projection morphogenesis, neuron projection regeneration, synaptic transmission and catecholamine biosynthetic process. A closer look at the sequence of the GR binding sites revealed the presence of several motifs for transcription factors that are highly divergent from those previously linked to GR-signaling, including Gabpa, Prrx2, Zfp281, Gata1 and Zbtb3. These transcription factors may represent novel crosstalk partners of GR in a neuronal context. Here we present the first genome-wide inventory of GR-binding sites in a neuronal context. These results provide an exciting first global view into neuronal GR targets and the neuron-specific modes of GR action and potentially contributes to our understanding of glucocorticoid action in the brain.

3.1   Introduction

The brain is a major target of glucocorticoids (GCs) that are secreted by the hypothalamus-pituitary-adrenal axis in response to stress. In the brain there are two receptors for glucocorticoids, the mineralocorticoid receptor (MR) and the glucocorticoid receptor (GR), that differ in their expression pattern and affinity for GCs. GR is abundantly expressed throughout the brain both in neurons and non-neuronal cells such as microglia and astrocytes (Chao et al., 1989; Morimoto et al., 1996; Sierra et al., 2008; Vielkind et al., 1990). GR has a relatively low affinity for its ligand, cortisol in humans and corticosterone in rodents (both abbreviated as CORT), and is activated when CORT levels rise, for example during stress. Upon CORT binding, GR migrates from the cytoplasm to the nucleus where it is involved in the regulation of gene transcription.

Transcriptional regulation by GR is complex and several molecular mechanisms have been described involving both homodimers and monomers of GR. Direct binding of GR dimers to Glucocorticoid Response Elements (GREs) in the vicinity of target genes, a process known as transactivation, is the classical mode of action which generally results in a potentiation of transcription (Schoneveld et al., 2004). However, GR also exhibits extensive crosstalk with other transcription factors (TFs), and besides simple GREs composite sites exist that contain a binding site for another TF in close proximity to the GRE, resulting in either a synergistic activation or a repression of transcription (Biola et al., 2000; Kassel and Herrlich, 2007). Furthermore, GR monomers can also exert effects on gene transcription by indirectly binding to the DNA via an intermediate DNA-bound TF in so called tethering response elements (Yamamoto et al., 1998), mostly resulting in a repression of transcription of the associated gene, a process referred to as transrepression. This extensive crosstalk of GR with other TFs not only vastly expands the range of GR-control on physiological processes compared to the classical GRE-driven transcriptional control in simple GREs, but it also underlies the highly context-dependent action of GCs.

Several TFs have been described that participate in this crosstalk with GR, including Oct1, Ets1, AP-1 and CREB at composite GREs and NF-κB, AP-1, CREB, Oct-1/2, STAT6, SMAD3,4 and PU.1/Spi-1 at tethering sites (Biola et al., 2000; De Bosscher K. et al., 2006; Gauthier et al., 1993; Imai et al., 1993; Jonat et al., 1990; Kassel and Herrlich, 2007; Schule et al., 1990; Song et al., 1999; Stocklin et al., 1996; Wieland et al., 1991). However, most of these crosstalk partners of GR have been identified in studies on the immunosuppressive and the tumor suppressor properties of GR (Chebotaev et al., 2007; De Bosscher K. et al., 2008; Glass and Saijo, 2010), while very little is known about crosstalk partners in a neuronal context.

In neuronal cells GR regulates the expression of a wide diversity of genes involved in general cellular processes such as energy metabolism, cell cycle and re-

Chapter 3

sponse to oxidative stress, but also clearly is involved in regulating a wide variety of genes important for neuronal structure and plasticity (Datson et al., 2008). Despite the fact that many neuronal GC-responsive genes have been identified (Datson et al., 2001b; Datson et al., 2001a; Datson et al., 2004), it remains unclear whether these genes are primary or downstream targets of GR. The onset of high-throughput sequencing combined with chromatin immunoprecipitation (ChIP-Seq) has made it possible to characterize genome-wide binding sites of TFs and today several studies have used this approach to identify global primary GR-targets in a variety of cell types, including human lung carcinoma cells (A549), mouse adipocytes (3T3-L1), premalignant breast epithelial cells (MCF10A-Myc), murine mammary epithelial cells (3134) and pituitary (AtT-20) cells (John et al., 2011; Pan et al., 2011; Reddy et al., 2009; Yu et al., 2010). These studies have yielded an unprecedented insight into genome wide GR targets as well as molecular mechanisms of GR-signaling, but perhaps one of the most striking findings is the low degree of overlap in GR binding sites when comparing different cell types, indicating that GR occupancy is highly cell type specific (John et al., 2011). Therefore, in order to gain insight into global GR primary target in neurons, it is essential to characterize GR binding in a neuronal context. So far no studies have taken a ChiP-Seq approach to characterize GR-binding in a neuronal context.

The aim of the current study was to analyze genome-wide GR-binding sites (GBS) in rat neuronal PC12 cells using ChIP-Seq. The PC12 cell line is derived from a pheochromocytoma of the rat adrenal medulla and can be differentiated into a neuronal phenotype by stimulation with nerve growth factor (Greene and Tischler, 1976). NGF- treated PC12 cells stop dividing, develop neurites, display electrical activity and develop many other properties similar to those of sympathetic neurons (Allen et al., 1987; Greene and Tischler, 1976). They are considered a useful model system for neurosecretion and neuronal differentiation (Taupenot, 2007) and have been extensively used to study neuronal function in relation to GCs (Morsink et al., 2006a; Sotiropoulos et al., 2008; Yang et al., 2007). In this study, besides identifying the binding sites of GR in neuronal PC12 cells, we analysed which genes were located in the vicinity of the binding sites, which gene ontology classes were overrepresented, whether GR-binding resulted in regulation of gene expression of nearby genes and the motif composition of the binding sites.

3.2   Materials & Methods

Cell culture and harvest

Rat pheochromocytoma PC12 cells were cultured and differentiated for ten days with NGF as described before in collagen-coated culture flasks ($75\,\mathrm{cm}^2$ and $175\,\mathrm{cm}^2$ for mRNA-analysis and chromatin immunoprecipitation (ChIP) respectively; Becton Dickinson) (Morsink et al., 2006a). On the last day of differentiation, the cells

were stimulated continuously for 90 minutes or 180 minutes with either 100 nM Dexamethasone (DEX) or ethanol (0.1 %) in corticosteroid-depleted medium for ChIP or mRNA analysis respectively. For ChIP, after 90 minutes incubation the protein-DNA interactions were fixed by crosslinking for 10 minutes with 1 % formaldehyde (Calbiochem, Darmstadt, Germany), after which they were incubated for 10 minutes with 0.125 M glycine. After discarding the medium, the cells were washed twice with phosphate buffered saline (PBS) containing Phenylmethanesulfonyl fluoride solution (PMSF; Fluka, Steinheim, Switserland). Finally, the cells were collected in PBS containing Protease Inhibitors (PI, Roche, Mannheim Germany). The centrifuged cell pellet was stored at $-80\,°C$ until sonication. For sonication, the defrosted cell pellets were dissolved in 0.6 ml PI-containing RIPA (0.1 % SDS, 1 % NaDOC, 150 mM NaCL, 10 mM Tris pH 8.0, 2 mM EDTA, 1 mM $NaVO_3$, 1 % NP-40, β-glycerolphophate and Na-butyrate) and incubated on ice for 30 minutes. Subsequently, the chromatin was sheared (Bioruptor, Diagenode; 25 pulses of 30 sec., 200 W), resulting in chromatin fragments of 100–500 bp. The sheared chromatin-containing supernatants were stored at $-80\,°C$ until use in the ChIP-procedure. For the mRNA-analysis ($n = 6$), the cells were harvested after 180 minutes incubation with 100 nM DEX and total RNA was isolated using Trizol reagent (Invitrogen Life Technologies, Carlsbad, USA) according to manufacturer's protocol.

ChIP-Seq

For ChIP Sepharose A beads (GE Health care, Uppsala Sweden) were blocked with 1 mg/ml BSA (Biolabs, Ipswich, UK) and 0.2 mg/ml fish sperm (Roche) for 1 hr at $4\,°C$. Three independent ChIPs each were performed on chromatin (60–120 μg per treatment) of the same batch of differentiated cells. Per ChIP the chromatin was precleared by incubation with blocked beads for 1 hr. After preclearing, an input sample was taken to control for the amount of DNA that was used as input for the ChIP procedure. The remaining sample was divided into two samples, each incubated O/N at $4\,°C$ under continuous rotation with either 6 μg of ChIP-grade GR-specific H300 or normal rabbit IgG antibody (Santa Cruz Biotechnology, California, USA). Subsequently, the antibody-bound DNA-fragments were isolated by incubating the samples with blocked protein A beads for 1 hr at $4\,°C$. The beads were washed 5 times in 1 ml washing buffer ($1\times$ low salt; $1\times$ high salt; $1\times$ LiCl; $2\times$ TE according to Nelson et al. (Nelson et al., 2006) after which they were incubated with 0.25 ml elution buffer (0.1 M $NaHCO_3$; 1 % SDS) for 15 min (RT, continuous rotation) to isolate the DNA-protein complexes. To reverse crosslink the DNA-protein interactions, the samples were incubated O/N at $65\,°C$ with 0.37 M NaCl. RNAse treatment (0.5 μg/250 μl; Roche, Mannheim, Germany was performed for 1 hr at $37\,°C$ followed by purification of DNA fragments on Nucleospin columns (Macherey-Nagel, Düren Germany). The immunoprecipitated samples were eluted in 50 μl elution buffer (Nelson et al., 2006). Half of one ChIP-sample was used for sequencing.

For sequencing, DNA was prepared according to the protocol supplied with the Illumina Genome Analyser GA1. In brief, the DNA fragments were blunted and ligated to sequencing adapters after which the DNA was amplified for 18 rounds of PCR. The DNA was electrophoresed on a 2 % Agarose gel, of which a region containing DNA fragments 100–500 bp in length was excised. Subsequently, DNA was isolated from this gel-slice with the Qiagen Gel Extraction Kit. DNA quality was checked on the Agilent Bioanalyser (Waldbronn, Germany). Single end sequencing of the first 36 bp of the resulting DNA library was performed on the Illumina Genome Analyser (Leiden Genome Technology Center, Leiden University Medical Center).

Peak calling and mapping

The single-end read sequences were aligned to the reference rat genome (RGSC v3.4) using the CLC genomics workbench 3.6.5 (Aarhus, Denmark), according to the default settings which allowed up to 1 mismatch per read or 2 unaligned nucleotides at the ends. Subsequently, DEX-induced peaks were detected using the CLC workbench peak finding algorithm in which the null distribution of background sequencing signal was set for both treatments at 1,200 bp and the maximum false discovery rate at 5 %. Further settings were left at default. Using Galaxy (`http://main.g2.bx.psu.edu/`) (Blankenberg et al., 2010; Goecks et al., 2010; Nelson et al., 2006), Refseq genes in the vicinity of the GBS were determined. As a reference genome Rattus Norvegicus 4 (rn4) was used. Data was visualized by uploading wiggle-files containing the raw ChIP-Seq data on the UCSC genome browser (`http://genome.ucsc.edu`).

Motif search

The regions containing the GBS were trimmed to 200 bp-width sequences and screened for de novo motifs using MEME (Bailey and Elkan, 1994; Nelson et al., 2006). The 500 most significant GBS were screened for motifs consisting of 8 to 40 nucleotides. The 15 most significant motifs were given as output. Using TOM-TOM (Gupta et al., 2007), the identified motifs were compared against databases of known motifs.

Comparison of PC12 GBS with other datasets

The genomic regions identified in the PC12 cells were compared to two published datasets consisting of GR-bound genomic regions in human A549 cells (Reddy et al., 2009) and in mouse adipocytes (Yu et al., 2010). For this purpose, the significant regions of the published datasets were converted to rat equivalents using the Galaxy website (`http://main.g2.bx.psu.edu/`) under default conditions. Subsequently, these rat regions were compared to the PC12 GR-bound regions and overlap was calculated using Galaxy (Blankenberg et al., 2010; Goecks et al., 2010).

Gene ontology analysis

The nearest genes surrounding the significant GBS were analysed with The Database for Annotation, Visualization and Integrated Discovery (DAVID) v6.7 (http://david.abcc.ncifcrf.gov/home.jsp). As a cutoff, the biological processes (BP) that had a Benjamini-Hochberg p-value < 0.05 were considered to be significant. Clustering all the identified GO-terms according to their functional annotation was performed under medium classification stringency (standard setting at DAVID).

RT-qPCR

RT-qPCR was performed to validate GR-binding to identified GBS using the immunoprecipitated chromatin as input. PCR was conducted using the capillary-based LightCycler® thermocycler and LightCycler® FastStart DNA MasterPLUS SYBR Green I kit (Roche, Mannheim, Germany) according to manufacturer's instructions. The primers were designed in NCBI/Primerblast according to the following criteria: (a) PCR product size between 80 and $150\,\mathrm{bp}$; (b) an optimal primer size of $20\,\mathrm{bp}$; (c) an optimal Tm of $60\,^{\circ}\mathrm{C}$; (d) amplicon aimed at the centre of the GBS.

The ChIP PCR signal was normalized by subtracting the amount of nonspecific binding of the IgG antibody in the same sample. This was then calculated as a percentage of the amount of input DNA which was originally included into the ChIP procedure. Known GBS upstream of DNA damaged induced transcript 4 (Ddit4) (Datson et al., 2011) and Metallothionein 2A (MT2a), served as positive controls for the ChIP. As a negative control, exon 2 of Myoglobin 2 (MB) was amplified. MB is involved in oxygen storage in muscle cells and does not contain a GRE to our knowledge. All selected GBS were measured in three independently performed ChIPs, resulting in 3 measurements per validated genomic location. Normalized data were analysed with GraphPad Prism 5 (trial version 5.00; GraphPad Software, Inc.). An unpaired two-tailed T-test was used to assess significant GR-binding. All primer sequences for mRNA and ChIP validation are listed in Table 3.7 and Table 3.8 respectively.

For mRNA analysis, cDNA was synthesized using the iScript cDNA synthesis kit (Bio-Rad, California, USA), according to manufacturer's instructions. PCR was conducted as described above. All PCR reactions on cDNA were performed in duplo. The standard curve method was used to quantify the expression differences (Livak and Schmittgen, 2001). cDNA values were normalized against Tubb2a expression levels. Normalized data was analysed with GraphPad Prism 5. The non-parametric Wilcoxon Signed Ranks Test was used to assess significant differential expression of GC-responsive genes. Significance was accepted at a p-value < 0.05.

Acknowledgements

3.3   Results

Identification and genomic distribution of GR binding sites in PC12 cells

ChIP-Seq resulted in the identification of 2,252 genomic regions that were bound by GR after 90 minutes of continuous DEX-stimulation of neuronal PC12 cells. Of this list, 1,183 regions had a p-value < 0.05 and were considered to be significant and were used for further analysis. An example of the ChIP-Seq data showing GR-binding upstream of the tyrosine hydroxylase gene (Th) is shown in Figure 3.1. To get insight into the genomic distribution of GR binding, the shortest distance of the center of each significant GBS to the nearest gene was determined within a 100 kb region. Approximately one third (31 %) of all significant GBS was located within a gene, while 47 % did not overlap with a gene but were located within a 100 kb distance upstream or downstream of a gene (Figure 3.2A). The remaining 22 % of
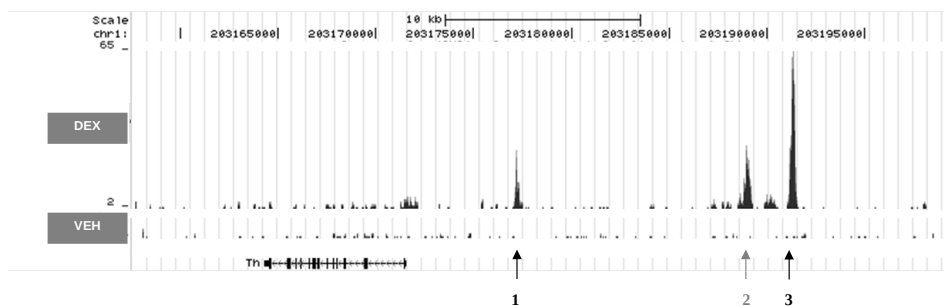
Figure 3.1: Genomic distribution of Glucocorticoid Receptor binding sites (GBS) upstream of the Tyrosine Hydroxylase gene (TH).
Two significant peaks representing GR-binding are observed at approximately 5.7 kb (peak 1) and 19.7 kb (peak 3) upstream of the transcription start site (TSS) as indicated by arrows. The 5.7 kb GBS was previously described in PC12 cells transfected with the TH promoter (Rani et al., 2009). A third peak (peak 2) upstream of the TH gene was apparent, but was not significantly above background (IgG signal) at this position, so was not further analysed. Data was visualized with the UCSC genome browser (Kent et al., 2002).

GBS were located further than $100\,\text{kb}$ upstream or downstream from the closest gene. In total there were more GBS located upstream to genes than downstream: $38\,\%$ vs $31\,\%$ respectively.

Based on their genetic location, the intragenic GBS were subdivided into the following groups: 5′UTR and 3′UTR (including introns and exons that are located there), introns, exons and GBS overlapping an exon/intron junction (Figure 3.2B). The majority ($79\,\%$) of intragenically located GBS were confined to intronic regions. Only $16\,\%$ of the intragenic GBS were located within the 5′UTR, upstream of the coding sequence of the gene, a region classically considered to be involved in regulation of gene expression (Kapranov, 2009). A list of the 50 most significant regions containing GBS and the most nearby gene is shown in Table 3.1. The full list of $1,183$ GBS is available in the additional material (Table 3.4).

Chapter 3

A

| 11% | | 18% | | 9% | | | 6% | | 14% | | 11% |
| 136 | | 212 | | 102 | Gene X | | 72 | | 162 | | 131 |

31%

B
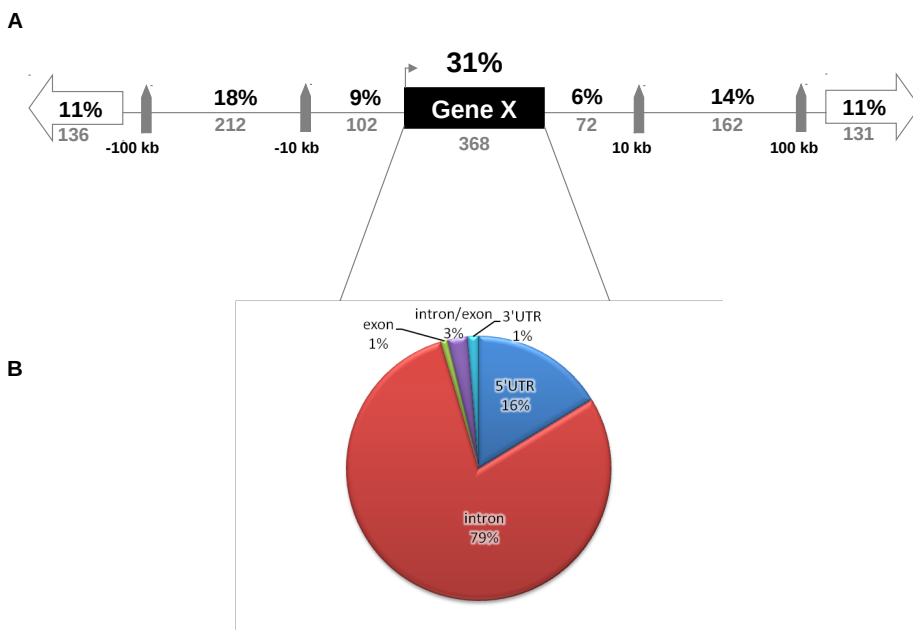
Figure 3.2: Genomic distribution of GBS relative to nearby genes.
A The percentage of GBS that are present intragenically or within a certain range from the nearest gene are indicated, showing that the number of GBS located within a gene is highest. **B** Intragenic GBS can be further subdivided into subregions: 5′UTR (exon or intron), intron, exon, intron/exon overlap and 3′UTR regions.

	chr	region start	end	p-value	nearest TSS (bp)	Gene symbol	Gene description
1	chr14	92730207	92730300	0	58382	ddc	dopa decarboxylase
2	chr12	4225730	4225800	0	41349	N4BP2L2	NEDD4 binding protein 2-like 2
3	chr8	84942839	84942945	6.66E−16	−40027	FILIP1	filamin A interacting protein 1
4	chr3	159002303	159002377	3.44E−15	−68132	ptpm	protein tyrosine phosphatase, non-receptor type 1
5	**chr1**	**170271212**	**170271308**	**1.07E−14**	**38820**	**PARVA**	**parvin, alpha**
6	chr20	44499841	44499940	1.25E−14	−27572	CDC2L6	cell division cycle 2-like 6 (CDK8-like)
7	chr1	208485510	208485587	2.67E−14	24399	FRMD8	FERM domain containing 8
8	chr10	55856373	55856471	1.24E−13	−3428	Per1	period homolog 1
9	chr10	95336367	95336493	1.82E−13	−1827	CYB561	cytochrome b-561
10	chr9	82139844	82139973	2.12E−13	−22571	AGFG1	ArfGAP with FG repeats 1
11	chr2	214126583	214126707	5.58E−13	119898	snx7	sorting nexin 7
12	**chr7**	**71292501**	**71292588**	**1.31E−12**	**452930**	**Cohh**	**Cohen syndrome homolog 1**
13	**chr10**	**108442435**	**108442545**	**1.13E−11**	**10507**	**C1qtnf1**	**C1q and tumor necrosis factor related protein 1**
14	**chr1**	**14981944**	**14982032**	**2.76E−11**	**16334**	**il2ora**	**interleukin 20 receptor, alpha**
15	**chr10**	**69940043**	**69940119**	**1.77E−10**	**250224**	**ACCN1**	**amiloride-sensitive cation channel 1, neuronal**
16	chr4	26732111	26732175	1.87E−10	−20533	cyp51	cytochrome P450, subfamily 51
17	chr1	203191165	203191336	2.39E−10	−19745	TH	tyrosine hydroxylase
18	chr3	159218917	159219016	2.51E−10	−11706	Pard6b	par-6 (partitioning defective 6) homolog beta
19	**chr3**	**11220641**	**11220714**	**2.76E−10**	**11081**	**PPAPDC3**	**phosphatidic acid phosphatase type 2 domain containing 3**
20	chr13	98085339	98085424	8.73E−10	−40128	srp9	signal recognition particle 9
21	chr10	16132564	16132677	1.10E−09	−105921	LOC685957	cytoplasmic polyadenylation element binding protein 4
22	chr1	128794365	128794456	2.01E−09	−74086	CHD2	chromodomain helicase DNA binding protein 2
23	**chr1**	**148370534**	**148370610**	**2.72E−09**	**483095**	**Dlg2**	**discs, large homolog 2**
24	chr14	99179170	99179253	3.03E−09	−356843	etaa1	Ewing tumor-associated antigen 1; similar to ETAA16 protein
25	chr3	120538726	120538946	4.16E−09	−32899	CHGB	chromogranin B
26	chr16	36611065	36611165	5.78E−09	−285078	HAND2	heart and neural crest derivatives expressed 2
27	chr13	100632670	100632774	6.77E−09	58936	hlx	H2.0-like homeobox
28	chr1	83486283	83486376	8.07E−09	2794	ZFP36	zinc finger protein 36
29	chr2	242852558	242852668	1.23E−08	50854	sh3glb1	SH3-domain GRB2-like endophilin B1

	chr	region start	end	p-value	nearest TSS (bp)	Gene symbol	Gene description
30	chr19	36308488	36308565	1.45E−08	36674	Zfp90	zinc finger protein 90
31	chr2	218383549	218383633	1.75E−08	12542	F3	coagulation factor III (thromboplastin, tissue factor)
32	chr7	72391772	72391896	2.24E−08	−85708	YWHAZ	tyrosine 3-monooxygenase/tryptophan 5-monooxygenase activation protein, zeta polypeptide
33	chr10	63291887	63291961	2.45E−08	−26356	rph3al	rabphilin 3A-like (without C2 domains)
34	chr1	203177190	203177316	3.19E−08	−5747	TH	tyrosine hydroxylase
35	chr8	121454771	121454890	4.05E−08	−35296	Snrk	SNF related kinase
36	**chr7**	**7534539**	**7534637**	**4.25E−08**	**90348**	**Npepo**	**aminopeptidase O**
37	chr7	45295426	45295501	4.78E−08	155311	PPFIA2	protein tyrosine phosphatase, receptor type, f polypeptide (PTPRF), interacting protein (liprin), alpha 2
38	chr10	19716893	19717068	6.83E−08	−7100	ccdc99	coiled-coil domain containing 99
39	**chr1**	**179785291**	**179785400**	**7.20E−08**	**17710**	**Polr3e**	**polymerase (RNA) III (DNA directed) polypeptide E (80kD)**
40	**chr3**	**85831724**	**85831796**	**7.86E−08**	**14876**	**DDR2**	**discoidin domain receptor tyrosine kinase 2**
41	chr2	240315238	240315326	8.89E−08	−18368	PDLIM5	PDZ and LIM domain 5
42	chr3	155445628	155445734	1.01E−07	−503522	Sdc4	syndecan 4
43	chr6	22356139	22356299	1.05E−07	19144	SLC8A1	solute carrier family 8 (vesicular monoamine), member 1
44	chr10	75271499	75271582	1.65E−07	−112174	LOC688105	hypothetical protein LOC688105; LOC360590
45	**chr6**	**6562495**	**6562603**	**1.71E−07**	**2931**	**NT5DC2**	**5′-nucleotidase domain containing 2**
46	**chr6**	**22377983**	**22378135**	**1.74E−07**	**21756**	**SLC8A1**	**solute carrier family 8 (vesicular monoamine), member 1**
47	**chr6**	**75731811**	**75731965**	**1.97E−07**	**587**	**NFKBIA**	**nuclear factor of kappa light polypeptide gene enhancer in B-cells inhibitor, alpha**
48	chr8	68790635	68790830	2.10E−07	−84	Rab1a	RAB1a, member RAS oncogene family
49	chr8	44864109	44864180	3.27E−07	188782	SORL1	sortilin-related receptor, LDLR class A repeats-containing
50	chr8	124992930	124993041	4.02E−07	237699	Cx3cr1	chemokine (C-X3-C motif) receptor 1

Table 3.1: Top 50 of significant GR-binding sites.
The 50 most significant GR-binding sites (GBS) as determined by CLCbio workbench software. Per GBS, the p-value is indicated as well as the nearest gene and the distance relative to the Transcription Start Site (TSS) of this gene. Negative numbers indicate a location upstream of the TSS, positive numbers downstream of the TSS. GBS that are located intragenically are indicated in bold print.

Reliability of ChIP-Seq data

To assess the reliability of the ChIP-seq data and the stringency of the applied statistical threshold, ChIP-qPCR experiments were performed in a new isolate of GR-bound DNA on a total of 17 GBS which covered a wide range of p-values (from $1E-6$ to 0.03). The selection included five significant regions previously identified in other studies, in the vicinity of Ddit4, Per1, Tle3, FRMD8 and Ddc, which were also identified in the current study and served as positive controls (Reddy et al., 2009; Yu et al., 2010) Figure 3.3A, B: grey bars). In addition, 12 novel GBS identified in this study in neuronal PC12 cells were selected for validation (Figure 3.3A: black bars). All but one GBS (Ccdc99) were successfully validated, showing that the selected cut-off of significant GBS (p-value < 0.05) was appropriate. Several of the novel GBS identified and validated in neuronal PC12 cells were associated with genes that have a known neuronal function, such as dopamine decarboxylase (Ddc) and tyrosine hydroxylase (TH), both important enzymes in the biosynthesis of catecholamines. Other examples are voltage-gated potassium channel subunit beta-1 (Kcnab1), NMDA receptor-regulated gene 2 (Narg2), Period circadian protein homolog 1 (Per1) and neurofascin (Nfasc).

GR-binding sites and regulation of nearby genes

RNA was isolated from neuronal PC12-cells to establish whether GR activation by DEX-treatment induced expression of the genes closest to the validated GBS. Six out of 14 genes (Per1, Ddc, Kcnab1, Pik3r5, Il20ra, Th) showed a significant upregulation upon GR activation and another 2 genes (Frmd8 and Tle3) a clear trend towards significance with p-values of 0.055 and 0.051 respectively (Figure 3.3C). One gene, Ddit4, was downregulated by GR activation rather than upregulated. Five out of the 14 genes tested did not show a change in expression at the time point measured, i.e. 3 hours after GR activation. Eight out of 14 tested genes contained a GRE, including the GBS near Ddit4.

Overlap with GR-binding sites in other tissues is limited

We next compared the GR binding regions in rat neuronal PC12 cells to two previously published GR ChIP-Seq studies performed in human lung carcinoma (A549) (Reddy et al., 2009) and mouse adipocytes (3T3-L1) (Yu et al., 2010). This resulted in a list of GBS unique to neuronal PC12 cells and lists of GBS shared with either or both of the other cell types. The majority of GBS identified in PC12, 1,031 in total, appeared unique to neuronal PC12 cells. Only 79 (7 %) of the GBS identified in PC12 cells were shared with A549 cells and 127 (11 %) with 3T3-L1 cells (Figure 3.4). A similar degree of overlap was observed comparing GBS of A549 and 3T3-L1 cells
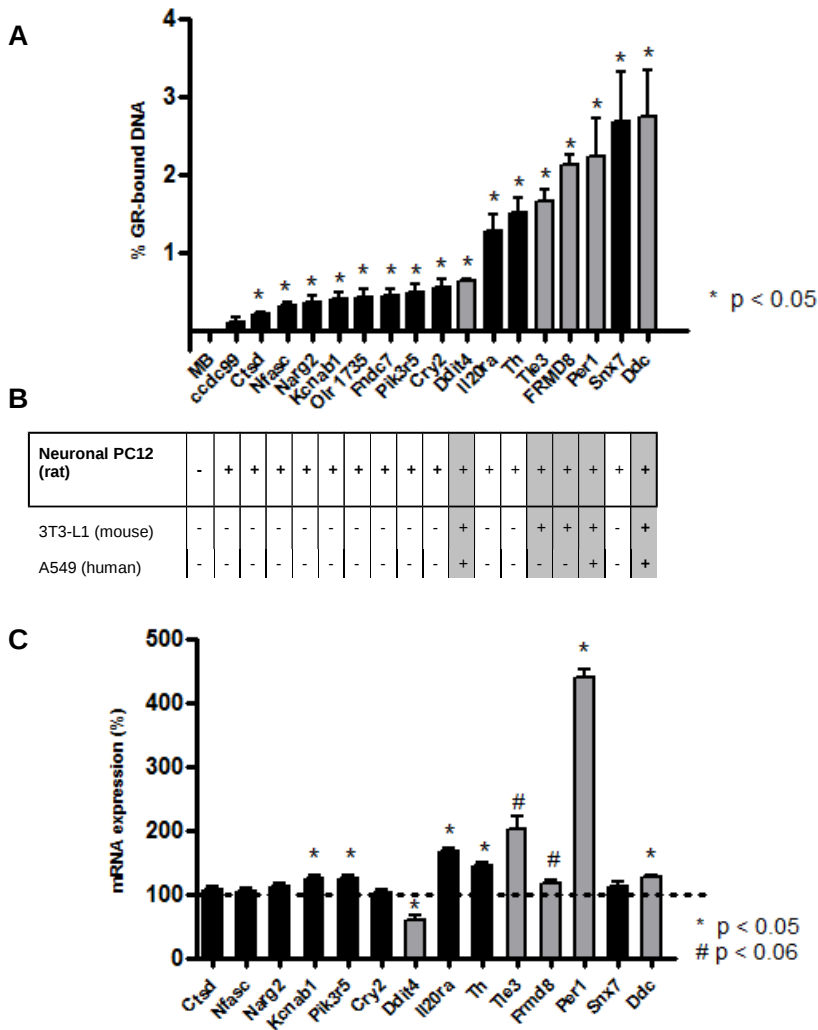
Figure 3.3: Validation of GR binding sites and effects on mRNA expression.
A ChIP-PCR validation of identified GBS, previously shown to be GR-targets in literature (grey bars) or representing newly identified GBS (black bars). The genes that are associated with the GBS are listed on the x-axis. The y-axis represents the % of input DNA that was bound by the GR after subtracting the aspecific IgG-bound fraction and the amount of GR bound after vehicle (VEH) treatment. The error bars represent the standard error of the mean (SEM) when comparing the DEX-induced GBS versus the VEH-induced GBS. An unpaired two-tailed T-test was used for statistics. **B** Diagram indicating whether the known GR-binding regions were previously detected in other published GR-ChIPseq studies based on BlastZ-based interspecies conservation (http://main.g2.bx.psu.edu/) (Goecks et al., 2010). The genomic locations corresponding to the GBS are listed in Table 3.5 as region numbers 1 (Ddc), 7 (FRMD8), 8 (Per1), 11 (Snx7), 14 (Il20ra), 17 (Th), 75 (TLE3), 94 (Ddit4), 345 (Olr1735), 352 (Fndc7), 366 (Pik3r5), 526 (Cry2), 704 (Nfasc), 842 (Narg2), 976 (Kcnab1), 1020 (Ctsd). **C** mRNA expression of the genes associated with the validated GBS after DEX-treatment relative to VEH-treatment (100 %). Expression was normalized against tubulin 2a mRNA expression. The non-parametric Wilcoxon Signed Ranks Test was used for statistics.

65

Neuronal PC12 cells
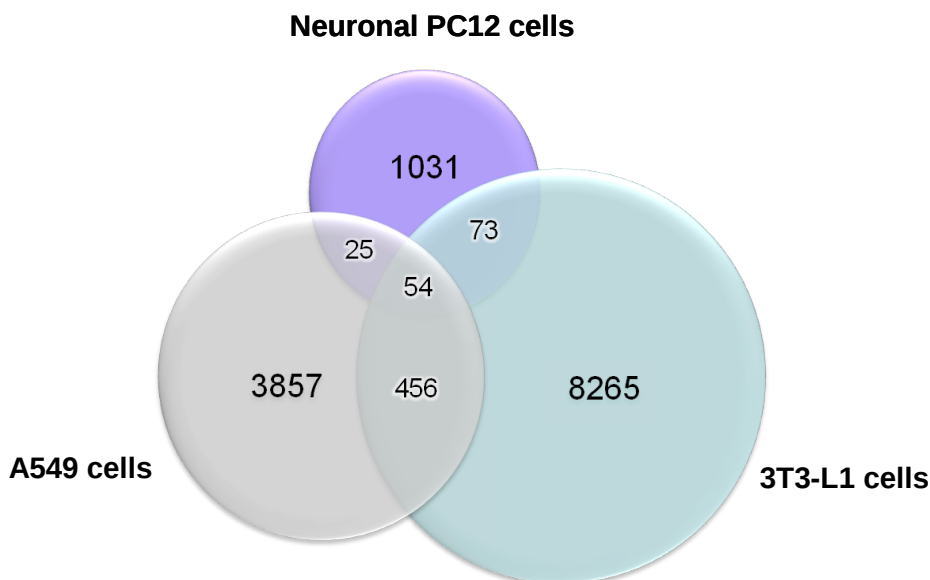
Figure 3.4: Venn diagram representing overlap between GR-targets in different ChIP-Seq studies.
The overlap of GBS identified in PC12 cells is compared to those genomic regions bound by GR in two other ChIP-Seq studies in human lung carcinoma cells (A549) (Reddy et al., 2009) and mouse adipocytes (3T3-L1) (Yu et al., 2010).

that shared a total of 510 GBS being 12% and 6% respectively. Only 54 GBS (4%) of all PC12 GBS were common to all 3 cell types.

PC12-specific GBS are located nearby genes with a neuronal function

To analyse which biological processes are likely to be affected by GR-binding in neuronal PC12 cells, the genes nearest to the GBS were analysed for overrepresentation of specific gene ontology classes using DAVID (Huang et al., 2009b; Huang et al., 2009a). Genes closest to $1{,}031$ sites uniquely identified in PC12 cells were used as input in the analysis. The genes near PC12-unique GBS had a high representation of GO-terms linked to neuronal function and clustering of all identified GO-terms revealed that the most enriched cluster in this group was "neuron development", with other neuron-related clusters being "neuron projection", "synapse" and "biogenic amine biosynthetic process" (Table 3.2).

These results indicate that in neuronal PC12 cells the majority of GR binding is to genomic regions that are nearby or within genes with a known neuronal function. The full list of GO terms of the genes associated with the PC12-unique GBS are available in the additional material (Table 3.5).

neuronal PC12 unique GBS

GO Term	Category	Enrichment score
1 neuron development	BP	4.4
2 cytoplasmic vesicle	CC	3.4
3 neuron projection	CC	3.1
4 metal ion binding	MF	3.0
5 blood vessel development	BP	3.0
6 cell motion	BP	2.8
7 identical protein binding	MF	2.6
8 biogenic amine biosynthetic process	BP	2.6
9 synapse	CC	2.2
10 protein tyrosine kinase activity	MF	2.0

Table 3.2: Top 10 enriched functional GO clusters in neuronal PC12-specific GR binding regions (GBS).
Gene ontology analysis of genes associated with GBS identified in neuronal PC12 cells. The 10 most enriched functional GO clusters in GBS that are uniquely found in neuronal PC12 cells. Analysis was performed with the Database for Annotation, Visualization and Integrated Discovery (DAVID). Per cluster, the first GO-term is shown. In addition, the category to which the GO term belongs to is indicated, i.e. Biological Processes (BP), Molecular Function (MF) or Cellular Compartment (CC). The enrichment score indicates the geometric mean (in -log scale) of p-value of the GO cluster.

GR binding sites represent both transactivation and transrepression modes of action

Screening the significant GBS with MEME and TOMTOM for presence of known DNA-motifs revealed that 683 (58 %) regions contained a Glucocorticoid Response Element (GRE). The identified GRE-motif was similar to the motif identified by others and also had a comparable prevalence (John et al., 2011; Reddy et al., 2009). This indicates that more than half of the GBS are most likely involved in transactivational effects of GR on gene transcription. We subsequently subdivided the list of GBS into a group of GBS with GREs, in which GR presumably exerts its actions via transactivation and the remainder without GREs, in which GR in all probability operates via transrepression of other transcription factors. Strikingly, the most significant GBS were enriched for GREs, while non-GRE containing GBS tended to have a lower p-value in the ChIP-Seq data (Figure 3.5). More than 80 % of the top 100 most significant GBS contained a GRE, dropping to approximately 50 % for GBS ranking lower in the list from position 400 downwards.

Not only the significance of the GBS differed between GRE and non-GRE containing binding sites, but also their composition in terms of motifs for transcription factor binding differed considerably. Both groups were subjected to de novo motif discovery to investigate the prevalence and identity of other motifs representing transcription factor binding sites within the binding regions. A total of 225 (33 %) of the 683 GRE-containing GBS represented simple GREs, only harbouring a GRE-like sequence but no other motifs (Figure 3.6). However, the majority of the GRE-containing GBS represented so called composite sites and also contained one
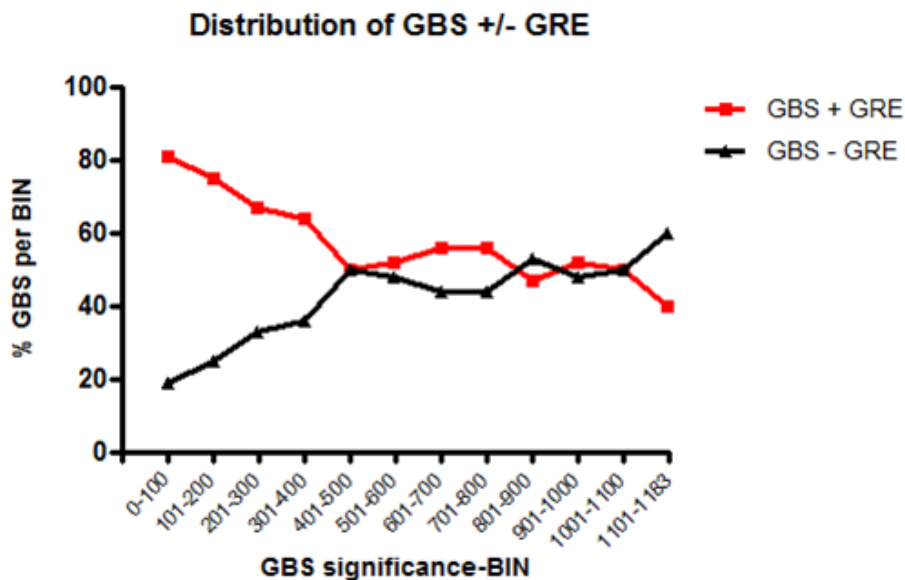
Figure 3.5: Significance of GR-binding sites with and without a GRE.
GR binding sites containing a GRE-like sequence have smaller p-values in the ChIP-Seq data compared to those regions without a GRE. On the x-axis the 1183 GBS are ranked into BINs consisting of 100 binding regions ranked according to significance. For example, the 100 most significant GBS are represented in BIN 1 (1–100), while the 83 least significant GBS are represented in the last BIN (1101–1183). On the y-axis the percentage of GRE and non-GRE containing GBS per BIN is indicated.

or more other motifs besides the GRE. In the group of GRE-containing genomic regions a motif for binding of Activator Protein-1 (AP-1) was most frequently observed, followed by motifs for binding of GA binding protein transcription factor, alpha subunit (Gabpa), Zinc Finger Protein 281 (Zfp281) and paired related homeobox 2 (Prrx2) (Figure 3.6). An entirely different distribution of motifs was observed in the genomic regions that did not contain a GRE. Interestingly, two motifs were identified that were unique for the regions without a GRE: a motif for binding of zinc finger and BTB (bric-a-bric, tramtrack, broad complex)-domain- containing 3 (ZBTB3) gene, present in over 80 % of the regions, and a motif for binding of GATA binding protein 1 (GATA1), present in 15 % of the genomic regions (Figure 3.6). Besides differences there were also some motifs found in both groups, regardless of whether the regions contained a GRE or not. For example, in both groups motifs corresponding to AP-1, Prrx2 and Zfp281 were identified, albeit at different frequencies.

Next, the co-occurrence of the various motifs was investigated. In the GRE-containing group, 26 % of the GBS contained an AP-1 site besides a GRE, making it the most prevalent combination of transcription factor binding sites. Other frequently observed combinations of motifs were a GRE in conjunction with motifs

683 GRE-containing GBS (58%)   **500 NON GRE-containing GBS** (42%)
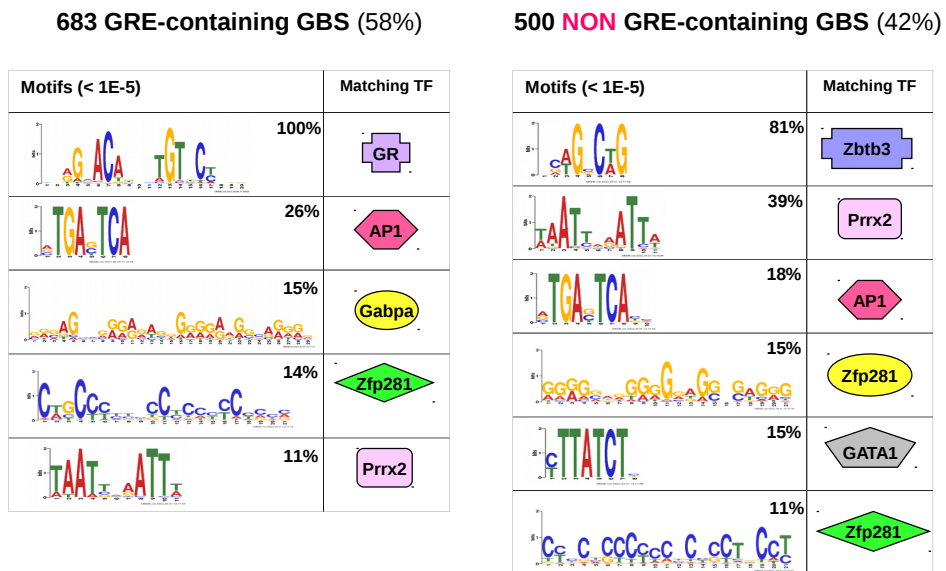
Figure 3.6: MEME de novo motif discovery within GBS.
A. Motifs for transcription factor binding in the 683 GBS that contain a GRE-like sequence. **B.** Motifs for transcription factor binding in the 500 GBS without a GRE. Analysis was performed within a 200 bp-frame containing the GBS-centre in the middle. The frequency of identified motifs in the PC12-dataset is indicated as well as transcription factors of which the known binding motif most significantly matches the identified motif. Only motifs with an E-value $< 1\mathrm{E}-5$ are depicted.

for binding of Gabpa, Zfp281 and Prrx2 (Figure 3.7). In the group without a GRE, all frequently observed combinations of motifs included Zbtb3. The most frequently observed combination was Zbtb3 in conjunction with Prrx2 (in 30 % of the regions), followed by combinations of Zbtb3 with AP-1, GATA1 and Zfp281.

Different biological processes are regulated via transactivation and transrepressive modes of action

We subsequently investigated whether GBS that contain a GRE regulated different biological processes than those without a GRE, representing transactivation or transrepression modes of action respectively. Genes near GRE-containing GBS showed an involvement in general cell functions and processes such as apoptosis, cell motion, protein dimerization activity and vasculature development (Table 3.3). In contrast, genes near regions without a GRE had a clear role in neuronal processes such as neuron projection morphogenesis, neuron projection regeneration, synaptic transmission and catecholamine biosynthetic process. The full list of GO terms of the genes associated with GBS with and without GREs are available in the additional material (Table 3.5).

	GBS with GRE			GBS without GRE		
	GO Term	Category	Enrichment score	GO Term	Category	Enrichment score
1	cell motion	BP	4.2	neuron projection morphogenesis	BP	3.8
2	protein kinase binding	MF	3.5	cytoplasmic vesicle	CC	2.5
3	vasculature development	BP	3.3	metal ion binding	MF	2.4
4	protein dimerization activity	MF	2.9	phospholipid binding	MF	2.3
5	metal ion binding	MF	2.8	catecholamine biosynthetic process	BP	2.2
6	regulation of apoptosis	BP	2.3	protein complex assembly	BP	2.0
7	apoptosis	BP	2.2	muscle cell development	BP	1.9
8	regulation of myeloid cell differentiation	BP	2.1	neuron projection regeneration	BP	1.6
9	cell adhesion	BP	1.9	actin filament binding	MF	1.6
10	cytoplasmic vesicle	CC	1.8	synaptic transmission	BP	1.6

Table 3.3: Top 10 enriched functional GO clusters in GR binding regions (GBS) with and without a GRE.
The 10 most enriched functional GO clusters in GBS that do or do not contain a GRE according to the Database for Annotation, Visualization and Integrated Discovery (DAVID). In both cases the GO-term that best represents the annotation cluster is shown. In addition, the category to which the GO term belongs to is indicated, i.e. Biological Processes (BP), Molecular Function (MF) or Cellular Compartment (CC). The enrichment score indicates the geometric mean (in -log scale) of p-value of the GO cluster.

3.4 Discussion

GR is widely expressed throughout body and brain and is an important transcriptional regulator of a diversity of biological processes, ranging from glucose and lipid homeostasis to immune suppression and cell proliferation and differentiation. Today several ChIP-Seq studies have been published focusing on genome-wide discovery of GR binding in different cell types (John et al., 2011; Pan et al., 2011; Reddy et al., 2009; Yu et al., 2010), and these studies have contributed immensely to our understanding of GR-signalling. What has become apparent, is that GR-binding is highly cell type-specific with minimal overlap in GBS between different cell types. Therefore, in order to gain insight into cell type-specific GR targets or mechanisms it is essential to investigate GR-signalling in a specific cell system or tissue of interest.

Here we present the first genome-wide discovery of GR-binding sites in a neuronal context. GR is an important transcription factor in neurons and is known to exert effects on neuronal structure and plasticity. So far the focus on GR-mediated action of glucocorticoids in a neuronal context has remained largely in the dark and most of the knowledge on GR modes of action, GR responsive genes and pathways and crosstalk partners of GR has come from studies on peripheral tissues including the immune system, the respiratory tract, skeletal muscle and adipose tissue as well as various types of cancer cells (Kinyamu et al., 2008; Masuno et al., 2011; Viguerie et al., 2012). Approximately 1,100 genomic binding sites of GR were identified in neuronal PC12 cells, the majority of which are novel and display only very limited
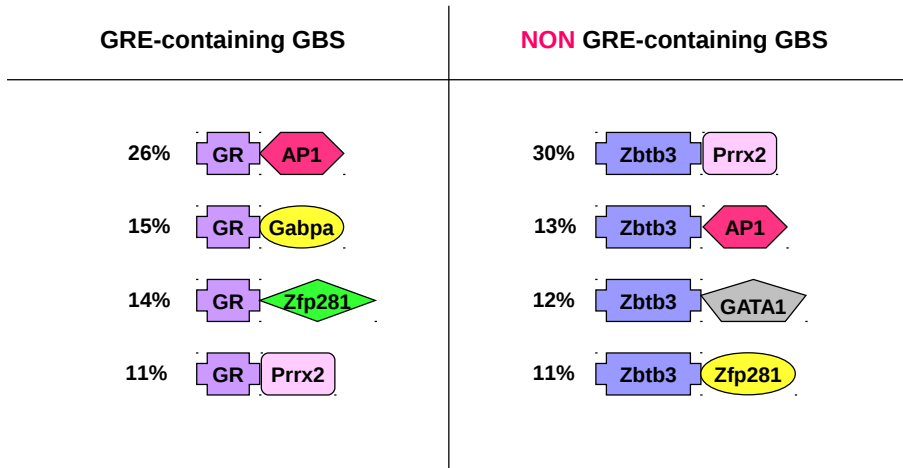
Figure 3.7: The most frequent motif-combinations within the GBS.
Specific combinations of motifs for transcription factor binding were observed, with differences in occurrence and frequency between the GBS with and without a GRE. TF: transcription factor.

overlap with GR binding sites in other non-neuronal cell types. Moreover, most of the identified GR-binding sites were located in the vicinity of genes with a neuronal function. Finally, we identified several motifs for transcription factor binding that may represent novel crosstalk partners of GR in neurons.

Reliability of ChIP-Seq data

We assessed whether our ChIP-Seq data met different reliability criteria. First, a very high proportion (16 out of 17 = 94 %) of ChIP-Seq peaks covering a wide range of p-values could be validated using ChIP RT-qPCR in chromatin derived from an independent experiment. Second, several GBS were located in the vicinity of known GR-target genes. Third, 13 % of the identified GBS overlapped with previously identified GBS in other tissues (mouse adipocytes and human lung carcinoma cells). Finally, highly significant motifs resembling GREs were detected in almost 60 % of the peaks. Together these criteria underscore the high quality of our ChIP-Seq dataset of 1,183 GBS.

Genomic binding sites of GR by far exceed GR-responsive genes

The number of GBS identified in PC12 cells (1,183) was relatively low compared to other studies, i.e. 4,392 GBS in human lung carcinoma (A549) and 8,848 GBS in mouse adipocytes (3T3-L1) (John et al., 2011; Reddy et al., 2009; Yu et al., 2010). However, this could be the consequence of the high stringency we applied, supported by the high validation rate of GR-binding to 16 out of 17 selected GBS. We cannot exclude that the actual number of genomic regions exhibiting GR-binding in PC12 cells may be considerably higher. Comparison of GBS between different tissues is

hampered by the different thresholds used in different studies without a standard accepted cut-off for reliability of ChIP-Seq data. Nonetheless, the identified GBS still considerably outnumbered by more than 10-fold the differentially expressed genes observed after a single 100 nM corticosterone pulse in neuronally differentiated PC12 cells (Morsink et al., 2006a). In fact, this is a more general observation that applies to several of the ChIP-Seq studies on GR so far (John et al., 2011; Reddy et al., 2009; Yu et al., 2010). In A549 cells, for example, 1 hour of DEX-stimulation resulted in the identification of 4,392 GBS, whereas only 234 genes were differentially expressed at this time-point. Similarly in 3T3-L1 cells, 8,848 GBS were identified and 620 genes were found to be DEX-responsive after 6 hours. It therefore seems likely that GR-binding to genomic sites is a measure of the potential of GR to mediate effects on gene expression of nearby genes rather than a direct predictor of whether a gene is differentially expressed. Whether this potential is converted to an actual effect on transcription most likely depends to a large extent on the availability and binding of other TFs.

To further examine the relationship between GR-binding and regulation of gene expression of nearby genes, we tested whether GR activation by DEX regulated expression levels of the genes closest to the validated GBS. In approximately half of the cases we could validate differential mRNA expression of the associated genes, illustrating the functionality of GR-binding. This percentage is quite high, considering that for the tested genes the GBS were often located at large distances from the genes we tested and not necessarily in classical promoter regions. In a recent ChIP-Seq study on PAX8 binding sites the overlap with responsive genes as identified by DNA microarray was only 6.5 %, despite the fact that only binding sites for PAX8 located within 1 kb of a TSS were taken into account (Ruiz-Llorente et al., 2012).

However, this also means that in the other half of the cases we were not able to confirm an effect of GR-binding on expression of the closest gene. There are several possible explanations for this. First, maybe the nearest gene is not necessarily the most relevant gene for studying functional effects of GR-binding. Another explanation is that we measured gene expression at the wrong moment. Since GR binding precedes effects on gene expression, we chose to measure mRNA expression after 3 hours of DEX-exposure. We therefore cannot exclude that the genes that were not GC-responsive at this moment might still be regulated by GR, albeit at different time-points or under different conditions. Temporal dynamics of individual genes are known to differ (Conway-Campbell et al., 2010; Jilg et al., 2010; Morsink et al., 2006a), which may explain why not all genes with a nearby GBS are responsive to DEX at one given time-point. Investigating gene expression at other time-points would be necessary to determine this. In addition, measuring mRNA may not be sensitive enough to pick up the effects of GR-binding on gene expression in all cases. Conway-Campbell et al. showed that administration of pulses of corticosterone to adrenalectomised rats resulted in pulsatile GR-binding to the Per1 promoter region followed by a burst of transcription, which was measurable by qPCR of nascent heterogeneous nuclear RNA but was not obvious from measuring mRNA

levels (Conway-Campbell et al., 2010), despite the fact the Per1 is a well-established GR target gene. This may therefore also be the case for the genes in this study that showed no or a small change in expression 3 hrs after DEX administration. Finally, we can not exclude that some of the GBS are derived from unspecific binding at spurious genomic locations, due to the applied continuous dosing regime with the synthetic GC DEX, rather than pulsatile exposure to the endogenous ligand, explaining why differential expression of the nearest gene was not observed.

Genomic location of GBS

What is becoming increasingly clear is that the majority of GBS are not located in promoter regions upstream of the transcription start site of genes or in the 5′UTR. In fact, only 9 % of the significant GBS identified in the current study were located within 10 kb upstream of the TSS and an additional 5 % were located within the 5′UTR. In contrast, a higher number of GBS (11 %) were located at a distance >100 kb upstream the TSS. These distant regions might be functional, since it is known that transcription factor binding sites are able to exert effects on gene expression through chromosome folding and therefore can be effective at large genomic distances (Biddie et al., 2010).

A much higher percentage of GBS occurred in intragenic regions, almost exclusively in introns, representing 31 % of the total list of significant GBS. A similar phenomenon was observed in 3T3-L1 adipocytes, where 48 % of the GBS were found in intragenic regions, either in exons or introns (Yu et al., 2010). Why intragenic regions show so much GR binding is at the least intriguing. Studies using artificial constructs in luciferase reporter assays have suggested that intronic GBS contain GREs with functional properties (Yu et al., 2010).

The 1,183 GBS identified in this study were associated with considerably fewer than 1,183 different genes, given that there were many examples of multiple GBS being located in each others vicinity nearby the same gene. An example is Disks large homolog 2 (Dlg2), that had 7 different GBS located nearby or Tolloid-like protein 1 (TLL1) with 5 GBS nearby. A question that still needs answering is whether the most nearby gene to a GBS is in fact the most likely candidate to be transcriptionally regulated by GR binding, or whether multiple genes could be affected. Several GBS had multiple genes in their vicinity. To solve this point linking ChIP-Seq studies on TF-binding with expression studies remains important, as well as performing studies in which GBS are mutated in their natural chromatin environment to investigate the effect on transcription of nearby genes.

Tissue-specificity of GR-binding reveals a neural signature

The majority of the GBS identified in this study were novel and unique to neuronal PC12 cells and were located nearby genes with a high representation of GO-terms linked to neuronal function. For example, one of the enriched GO clusters among

the genes near PC12-unique GBS was "biogenic amine biosynthetic process", which refers to the biosynthesis of biologically active amines, such as norepinephrine, histamine, and serotonin, many of which act as neurotransmitters. Indeed, we identified GBS in the vicinity of a number of genes involved in the synthesis of catecholamines, such as dopamine decarboxylase (Ddc) (Table 3.4: regions nr. 17 and 34) and tyrosine hydroxylase (TH) (Table 3.4: region 1). "Neuron projection" was another of the enriched GO clusters and accordingly several GBS were located in the vicinity of genes that play a role in outgrowth of axons, such as the semaphorins SEMA3E and SEMA5A (Table 3.4: regions 529, 663, 774 and 891 respectively), proteins that act as axonal growth cone guidance molecules (Goshima et al., 2002). Four other GBS were located nearby SLIT2 (Table 3.4: region 455) and SLIT3 (Table 3.4: regions 53, 750 and 1134), molecules that act as guidance cues in cellular migration (Brose et al., 1999). In addition, several GBS near genes involved in neurotransmission were observed, such as the serotonin receptors HTR1A, HTR1D, HTR1F and HTR2A (Table 3.4: regions nr. 660, 284, 1070 and 807 respectively) and 18 GBS located near a wide variety of voltage-gated potassium channel subunits, including KCNA3, KCNA4, KCNAB1, KCNC1, KCNH1, KCNH2, KCNH6, KCNK9 and KCNMA1, which play a role in neuronal excitability and neurotransmitter release (Kim and Hoffman, 2008). Finally, several GBS were located nearby the synaptotagmins SYT1 (Table 3.4: region 752, 1011, 1159), SYT13 (Table 3.4: region 1032) and SYT17 (Table 3.4: region 280, 879, 1019) which are integral membrane proteins of synaptic vesicles thought to participates in triggering neurotransmitter release at the synapse (Fernandez-Chacon et al., 2001). These are just a few of the many examples of GBS located in the vicinity of genes with neuronal function. Tissue-specific co-factors or transcription factors likely mediate binding of GR to the DNA or alter chromatin accessibility, resulting in these distinct tissue-specific patterns of GR-binding.

The overlap in GBS with other tissues was low, with only 7 % and 11 % of the GBS overlapping with A549 cells 3T3-L1 cells respectively and is very much in line with what has been observed in expression studies and other GR ChIP-Seq studies. For example, comparison of mouse mammary and mouse pituitary cells revealed an overlap of 4.5 % and 11.4 % respectively of the total number of GBS identified in either of the cell types (John et al., 2011). A similar high degree of tissue-specificity has also been observed for other TFs, such as STAT3, where an overlap of only 34 of 1352 (2.5 %) identified STAT3 binding sites was observed when comparing ChIP-Seq data derived from 3 different tissues (mouse peritoneal macrophages. mouse embryonic stem cells and CD4+ T cells (Hutchins et al., 2012).

Potential crosstalk partners of GR of relevance for neuronal function

GR operates in conjunction with an extensive network of other TFs. Previous studies in a non-neuronal setting, *e.g.* involving the immune system, muscle and adipose tissue, have generated extensive knowledge on GR-binding to the genome, the motifs that are recognized by GR and the transrepression partners that it can inhibit

by protein-protein interaction (Glass and Saijo, 2010; Kinyamu et al., 2008; Masuno et al., 2011; Viguerie et al., 2012). However, confirmation of this knowledge in a neuronal context is lacking.

The importance of other TFs for GR-function is evident from the high percentage of GBS consisting of composite GREs or binding sites for multiple TFs we observed in this study. Only twenty percent of the identified GBS consisted of simple GREs, harbouring a GRE-like sequence but no other motifs. The vast majority of the GBS were composite sites containing binding motifs for multiple TFs. This included composite GREs that contained a GRE in addition to one or more other motifs, as well as tethering GBS that did not contain a direct binding site for GR but most often a combination of motifs for TF-binding. Motifs for binding of AP-1, were frequently observed in the GBS in PC12 cells, both in combination with a GRE as well as in tethering sites. AP-1 is a well-known crosstalk partner of GR (Yang-Yen et al., 1990) and AP-1 binding sites overlap extensively with GR binding sites (Biddie et al., 2011). Interestingly, however, we also observed a number of motifs for TFs within the GBS that may represent novel crosstalk partners of GR that are relevant in a neuronal context.

In composite GREs, besides AP-1, three different motifs were abundantly observed, corresponding to binding sites for Gapba, Zfp281 and Prrx2. In tethering sites, the most frequently observed motif was a binding motif for Zbtb3, occurring in more than 80% of the GBS and by far outnumbering AP-1 motifs which had a frequency of only 18%. Other abundant motifs represented binding sites for GATA1, Zfp281 and Prrx2. For many of these TFs information in literature is sparse. Moreover, a link to neuronal function and/or GR has not been reported.

Zfp281 is a GC-box binding transcription factor and is involved in the regulation of genes implicated in pluripotency of murine embryonic stem cells (Wang et al., 2006b; Wang et al., 2008). Recently, we identified GC-box associated motifs in flanking regions surrounding GREs of hippocampal CORT-responsive genes. The presence of a GC-box motif in close proximity to the GRE correlated with GR-binding in the hippocampus, but not in other non-neuronal cell types (Datson et al., 2011). We hypothesized that GC-boxes may play a role in determining tissue specificity of GR binding to a defined group of GREs. The GC-box motif we identified in hippocampus resembled the binding motif of the MAZ TF which is in fact very similar to the Zfp281 motif identified in neuronal PC12 cells (Figure 3.6). According to Allen Brain Atlas (Lein et al., 2007), both MAZ and Zfp281 are very highly expressed in the mouse brain, especially in the hippocampus. Either one might be a novel crosstalk partner of GR in a neuronal context.

Gabpa, also known as nuclear respiratory factor 2 alpha (NRF2a), is a DNA-binding unit of the GA binding protein transcription factor which is involved in the nuclear control of mitochondrial function in neurons (Bruni et al., 2010; Ongwijitwat and Wong-Riley, 2005). Gabpa responds to an altered energy demand within primary neurons by altering the expression of mitochondrial genes (Ongwijitwat et

al., 2006) and has been implicated in neuronal viability after brain injury (Gutsaeva et al., 2006). Prrx2 is a member of the paired family of homeobox proteins, and is mainly known for its essential role in orofacial development (Balic et al., 2009). It was recently discovered to be a novel pituitary transcription factor (Susa et al., 2009). Otherwise very little is known on this TF and it has not been linked to GR-signalling before.

The transcription factor GATA1 is known to play an essential role in hematopoiesis (Ferreira et al., 2005). GR was reported to interfere with GATA-1 function and inhibits the expression of erythroid structural genes (Chang et al., 1993). Zbtb3 was observed in over 80% of the GBS that did not contain a GRE and was encountered in all frequently observed combinations of TFs binding sites in tethering GBS. Zbtb3 belongs to a family of transcription factors, many of which are important for B and T cell differentiation. A recent modeling study indicated that Zbtb3 may be a remote homologue of the Drosophila GAGA factor which is involved in both gene activation and gene repression and plays a role in the modulation of chromatin structure (Kumar, 2011). Zbtb3 contains a BTB domain, which plays a role in protein dimerization and transcriptional repression and interacts with histone deacetylase corepressor complexes such as NCoR (nuclear receptor corepressor) and SMRT (silencing mediator of retinoic acid and thyroid hormone receptor) (Bardwell and Treisman, 1994; Deweindt et al., 1995; Huynh and Bardwell, 1998). Relevance for the brain has not been indicated yet.

It must be noted that linking the de novo motifs to binding sites of known proteins is difficult and since in many cases more proteins can bind to a given motif, additional ChIP-experiments would need to be performed to address experimentally whether the TFs described above and predicted by TOMTOM actually bind to the DNA at the identified genomic regions.

Non-GRE containing tethering GBS are associated with genes involved in aspects of neuronal function

More than half of the GBS (58%) contained a GRE. Interestingly, the GRE-containing GBS were located near other types of genes than those without a GRE, as revealed by GO-analysis of the most nearby genes. While the GRE-containing GBS associated with more general cell functions such as apoptosis, cell motion, protein dimerization activity and vasculature development, the GBS without a GRE were more often located near genes involved in neuronal function. Motif analysis of the 54 sites in common between PC12, A549 and 3T3-L1 cells revealed that 91% contained a GRE (data not shown). This suggests that there is a core set of ubiquitous GBS that regulate key cellular processes in multiple tissues by the transactivation mode of action. On the other hand, tissue-specific TFs appear to play a role in tethering GR to genomic regions in a cell type-specific manner, regulating particular biological processes relevant for the tissue of interest. Of course many of the GRE-containing GBS were also unique to neuronal PC12 cells. In these cases it seems

likely that tissue-specific TFs facilitate binding of GR to the chromatin, guiding it to GREs that are relevant for that particular tissue. It has been shown by John et al. that this cell type-specificity is predetermined by differences in chromatin landscapes which affect the accessibility of GR to bind to its targets (John et al., 2011).

Conclusions

In this study we identified over 1,100 GBS in neuronal PC12 cells, the majority of which were unique and exhibited very little overlap with GBS in other cell types. The PC12 unique GBS were located in the vicinity of genes involved in neuronal functions such as axonogenesis, neuron differentiation and neuron development. Moreover, we confirmed that in more than half of tested GBS the most closely located gene was indeed GC-responsive, suggesting that these GBS play a role in GC-dependent transcriptional control. Intriguingly, we found striking differences in the identity of genes near GBS with or without a GRE. GBS containing a GRE were more often located nearby genes involved in general cellular functions such as regulation of cell proliferation and intracellular signaling, while tethering GBS, in which GR is indirectly bound to the DNA via another TF, were more often located near genes involved in neuronal function. Finally, we characterized the motif content of the GBS and identified a number of binding sites for TFs that may represent novel crosstalk partners of GR in neurons, and would vastly expand the repertoire of TFs in the GR interactome. Future studies should focus on confirming the binding of these predicted TFs within the identified GBS and on establishing their role as neuronal crosstalk partners of GR and their relevance in other neuronal cell types.

We conclude that the current ChIP-Seq study in neuronal PC12 cells has provided insight into some exciting new aspects of GR-mediated action of glucocorticoids in a neuronal context, an area which has so far remained in the dark. Understanding GR-signalling in a neuronal context is important given the profound effects of glucocorticoids on neuronal plasticity and consequently on brain function.

Competing interests

The authors declare that they have no competing interests.

Table 3.4: Total list of significant GR-binding sites.
online available at `http://www.biomedcentral.com/1471-2202/13/118`
Significant GR-binding sites (GBS) as determined by CLCbio workbench software. Per GBS, additional information about the nearest gene and the shortest distance of the GBS to the gene is shown as well as p-values. Intergenic GBS that are nearest to a Transcription Start Site (TSS) contain a $-$ distance, representing the upstream distance of the GBS to the gene. The other intergenic GBS have a positive distance that illustrates their distance to the nearest Transcription End Site (TSE). GBS that are located intragenically are indicated with bold print and in these cases, the indicated distance of the GBS to the gene is relative to the Transcription Start Site (TSS). The column named NB gives provides more detail about the intragenic location of the GBS.

Enriched GO terms in neuronal PC12-unique GBS

Category	Term	PValue	Benjamini
CC	GO:0005886~plasma membrane	2.98E$-$8	1.18E$-$5
MF	GO:0046872~metal ion binding	1.07E$-$6	8.33E$-$4
MF	GO:0043169~cation binding	1.59E$-$6	6.18E$-$4
MF	GO:0043167~ion binding	2.94E$-$6	7.62E$-$4
BP	GO:0048666~neuron development	7.65E$-$6	0.021
BP	GO:0048858~cell projection morphogenesis	1.39E$-$5	0.019
BP	GO:0042401~biogenic amine biosynthetic process	1.69E$-$5	0.015
BP	GO:0032989~cellular component morphogenesis	1.72E$-$5	0.011
BP	GO:0007409~axonogenesis	1.85E$-$5	0.010
BP	GO:0000904~cell morphogenesis involved in differentiation	1.87E$-$5	0.008
BP	GO:0048812~neuron projection morphogenesis	2.07E$-$5	0.008
BP	GO:0032990~cell part morphogenesis	2.86E$-$5	0.010
BP	GO:0000902~cell morphogenesis	3.17E$-$5	0.010
BP	GO:0048667~cell morphogenesis involved in neuron differentiation	3.31E$-$5	0.009
BP	GO:0030030~cell projection organization	4.29E$-$5	0.011
BP	GO:0031175~neuron projection development	5.65E$-$5	0.013
BP	GO:0006928~cell motion	6.29E$-$5	0.013
CC	GO:0031410~cytoplasmic vesicle	7.16E$-$5	0.014
BP	GO:0030182~neuron differentiation	9.08E$-$5	0.018
CC	GO:0044459~plasma membrane part	1.11E$-$4	0.014
CC	GO:0030427~site of polarized growth	1.19E$-$4	0.011
CC	GO:0030426~growth cone	1.19E$-$4	0.012
CC	GO:0043005~neuron projection	1.27E$-$4	0.010
CC	GO:0031982~vesicle	1.48E$-$4	0.010
BP	GO:0042423~catecholamine biosynthetic process	2.19E$-$4	0.040
CC	GO:0016023~cytoplasmic membrane-bounded vesicle	2.39E$-$4	0.013
BP	GO:0007243~protein kinase cascade	2.49E$-$4	0.042
BP	GO:0009309~amine biosynthetic process	2.88E$-$4	0.046
CC	GO:0045202~synapse	4.36E$-$4	0.021
CC	GO:0031226~intrinsic to plasma membrane	5.01E$-$4	0.022
CC	GO:0031988~membrane-bounded vesicle	5.77E$-$4	0.023

Table 3.5: Gene Ontology (GO) analysis of neuronal PC12-unique GBS.
The most enriched GO-terms in GBS that were uniquely identified in neuronal PC12 cells. GO-analysis was performed with the Database for Annotation, Visualization and Integrated Discovery (DAVID). Listed are the category to which the GO term belongs: Biological Processes (BP), Molecular Function (MF) or Cellular Compartment (CC). Finally, per GO-term the p-value before and after Benjamini-Hochberg correction is shown. Cutoff: All GO-terms with a Benjamini < 0.05 are listed.

Enriched GO terms in GBS containing a GRE

Category	Term	PValue	Benjamini
BP	GO:0007242~intracellular signaling cascade	2.08E−7	5.39E−4
BP	GO:0008284~positive regulation of cell proliferation	8.20E−7	0.001
BP	GO:0007243~protein kinase cascade	1.03E−6	8.88E−4
MF	GO:0046872~metal ion binding	2.20E−6	0.001
MF	GO:0043169~cation binding	4.64E−6	0.002
MF	GO:0043167~ion binding	6.99E−6	0.002
CC	GO:0005886~plasma membrane	7.38E−6	0.003
BP	GO:0042127~regulation of cell proliferation	2.49E−5	0.016
BP	GO:0006928~cell motion	2.62E−5	0.013
BP	GO:0016477~cell migration	5.88E−5	0.025
BP	GO:0048870~cell motility	1.05E−4	0.038
BP	GO:0051674~localization of cell	1.05E−4	0.038
BP	GO:0001944~vasculature development	1.39E−4	0.044
MF	GO:0019901~protein kinase binding	1.54E−4	0.025
MF	GO:0019899~enzyme binding	2.49E−4	0.032
MF	GO:0005267~channel activity	5.43E−4	0.050
MF	GO:0022803~passive transmembrane transporter activity	5.43E−4	0.050
MF	GO:0005080~protein kinase C binding	5.50E−4	0.044
MF	GO:0042802~identical protein binding	6.14E−4	0.044
MF	GO:0019900~kinase binding	6.72E−4	0.043
MF	GO:0022838~substrate specific channel activity	7.63E−4	0.044
MF	GO:0032403~protein complex binding	7.88E−4	0.042
MF	GO:0046983~protein dimerization activity	8.13E−4	0.040
MF	GO:0022836~gated channel activity	0.001	0.049
MF	GO:0005261~cation channel activity	0.001	0.047
MF	GO:0022832~voltage-gated channel activity	0.001	0.048
MF	GO:0005244~voltage-gated ion channel activity	0.001	0.048

Enriched GO terms in GBS *without* a GRE

Category	Term	PValue	Benjamini
BP	GO:0030182~neuron differentiation	4.10E−06	0.008
BP	GO:0048666~neuron development	4.24E−06	0.004
BP	GO:0048667~cell morphogenesis involved in neuron differentiation	3.26E−05	0.021
BP	GO:0007409~axonogenesis	3.94E−05	0.019
BP	GO:0048812~neuron projection morphogenesis	5.06E−05	0.020
BP	GO:0000904~cell morphogenesis involved in differentiation	5.45E−05	0.018
BP	GO:0031175~neuron projection development	6.76E−05	0.019
MF	GO:0043169~cation binding	8.77E−05	0.044
MF	GO:0046872~metal ion binding	9.31E−05	0.024
BP	GO:0048858~cell projection morphogenesis	1.58E−04	0.038
MF	GO:0043167~ion binding	1.64E−04	0.028
BP	GO:0030030~cell projection organization	2.34E−04	0.050
BP	GO:0032990~cell part morphogenesis	2.49E−04	0.048

The most enriched GO-terms associated with GBS identified in neuronal PC12 with and without a GRE- like sequence. GO-analysis was performed with the Database for Annotation, Visualization and Integrated Discovery (DAVID). The category to which the GO term belongs is indicated: Biological Processes (BP), Molecular Function (MF) or Cellular Compartment (CC). Finally, per GO-term the p-value before and after Benjamini-Hochberg correction is shown. Cutoff: All GO-terms with a Benjamini < 0.05 are listed.

Table 3.6: Gene Ontology (GO) analysis of GBS that do or do not contain a GRE.

Chapter 3

mRNA	Forward primer (5′–3′)	Reverse primer (3′–5′)
myo	AGCAGAGAACAGAAGAGGGGAGCA	AAGCAGAGGCCACTTTGCACCT
Ctsd	TGGTAGCTGCCGGGATGGATTGT	TTGCCTGCTTCAGAGTGCTGCC
Nfasc	TGGTCCCGCCCTCAACTATGGT	ATGGGGGCAGCATGGAGACACA
Narg2	AGGTGCGCTGTGTACCAGTGA	TGCAGTGGCTGTTTCGTTGGG
Kcnab1	CCACACACTACACCGTATGCATGA	AGATTCTGAGTGCAAAGCTAAGCCC
Pik3r5	AGTGGTGCTCTGCCCTAGTGCA	TGCAACCCGGGGGCAATTTGG
Cry2	TGGAATCAGTGCGAACGCTCCTG	CACAGTGCGAGTCAGAGCAGCT
Ddit4	TCTGAAAGGACCGAGCTTGT	ATAGCTGCCTCGAACAGGTC
Il2ora	GCTCTGAGCTTTGTCGTAGACAGAG	ACAGGGACCATGGTGAGTTCTTCT
Th	TCCCATGTGTGTGGCTGGGC	GACCACCCTGGAGTGCATGCA
Tle3	TGTCGACATGCCTGTCTGGAGT	ACCCTAACCCTCCCTTCTGGCT
Frmd8	TCGGCCACCTTCTGGTCATTTTGA	CCTAGAGGGTTAAGGCACAAGTGGA
Per1	AGGCCCTCGATGTAACGGCTTG	TCTGAGAAGAGAGGGTCGTCCGA
Snx7	GGCCGAGGAGAACATCCGCT	TCGGGATCTTCTTCCAACGGGA
Ddc	AGCTTCTGTTCTTTGTGTGGCCG	AAGCCTTTTCTACCACCTACGGCT
Tubulin 2a	TGAGCAGGGCGAGTTCGAGGA	GACCATGCTGGAGGACAACAGAAGT

Table 3.7: mRNA primer sequences.

ChIP	Forward primer (5′–3′)	Reverse primer (3′–5′)
myo	TAGTGTGCATCCAGCAGAGG	ACACTGTGGCCTTTTTGTCC
ccdc99	CAGATGTTCCTCGGTCAGAACACTG	GAGGCATTGCAGGTGTGGCT
Ctsd	TGCCTGGACAAGCCTATCACCTG	TCCCTTCACAACCAGAGCTGATGA
Nfasc	GTTAGCTGGGCTCAGGCGCAG	TGGGGACGACAGTCAGCCAGG
Narg2	TGTCTTGACATTCCTACTCGGGCA	TCCTCCTGGCACAAACTGGCA
Kcnab1	TGCAGGAATTAAATGAAGCCCGAGG	CCTGGGTTCTCATGGCAGCTTT
Olr1735	TGAGCTGCAGTGATGTGAGGCT	TCATGCTGTGCAGAGACTGGCT
Fndc7	AGAGCGTGCTGGAACACAGAACA	TGTCAGCCCAGGCATCTCACC
Pik3r5	GCGGTGATGGTGATGGGGTGA	GCTCCAGCCCACAGAACAGAAGAC
Cry2	TTGGCACCACTCTCTGACTACAGA	GTGGGCTGGGGCATGTGATTT
Ddit4	CTGTGGGTGAGCTGAGAACA	GGCCTGTAGGTCCAGCACTA
Il2ora	CTGGTCAGCGTCCACCTCTAGA	GATCAGAGCGCATTAAGCCATGCT
Th	TGGGCACGGCGTAGTCTAGTG	CAGGCAGGAGGCTGAGCACG
Tle3	ATGTCTCAGGGCCCAAGCTACA	ACGTAATGTGCCCTCTGTGCAGG
Frmd8	AGTGCATGTTTTTGCGCAGGGT	GTCAGCACTTCCGGCCCAGC
Per1	GGGTTGGGGGAGGCGCCAA	GGCGGCCAGCGCACTAGG
Snx7	TGCGGAACAGAACATCTCACAGCA	AGGGACAGGACACCATGCAACCT
Ddc	GCCCTGGGGAATGACATCAGC	AGCTCAGCCAAGCAAGTCGAAG

Table 3.8: ChIP primer sequences.

Chapter Four

Two populations of glucocorticoid receptor-binding sites in the male rat hippocampal genome

J.A.E. Polman[1], E.R. de Kloet[1], N.A. Datson[1],

Chapter 4

[1] Division of Medical Pharmacology, Leiden/Amsterdam Center for Drug Research & Leiden University Medical Center, Leiden, the Netherlands.

Iɴ the present study, genomic binding sites of glucocorticoid receptors (GR) were identified in vivo in the rat hippocampus by applying chromatin immunoprecipitation followed by next-generation sequencing. We identified 2,470 significant GR-binding sites (GBS) and were able to confirm GR binding to a random selection of these GBS covering a wide range of P values. Analysis of the genomic distribution of the significant GBS revealed a high prevalence of intragenic GBS. Gene ontology clusters involved in neuronal plasticity and other essential neuronal processes were overrepresented among the genes harboring a GBS or located in the vicinity of a GBS. Male adrenalectomized rats were challenged with increasing doses of the GR agonist corticosterone (CORT) ranging from 3 to 3,000 µg/kg, resulting in clear differences in the GR-binding profile to individual GBS. Two groups of GBS could be distinguished: a low-CORT group that displayed GR binding across the full range of CORT concentrations, and a second high-CORT group that displayed significant GR binding only after administering the highest concentration of CORT. All validated GBS, in both the low-CORT and high-CORT groups, displayed mineralocorticoid receptor binding, which remained relatively constant from 30 µg/kg CORT upward. Motif analysis revealed that almost all GBS contained a glucocorticoid response element resembling the consensus motif in literature. In addition, motifs corresponding with new potential GR-interacting proteins were identified, such as zinc finger and BTB domain containing 3 (Zbtb3) and CUP (CG11181 gene product from transcript CG11181-RB), which may be involved in GR-dependent transactivation and transrepression, respectively. In conclusion, our results highlight the existence of 2 populations of GBS in the rat hippocampal genome.

4.1 Introduction

Stress, an actual or perceived threat to homeostasis, activates a neuroendocrine cascade leading to the release of glucocorticoid (GC) stress hormones (cortisol in humans and corticosterone in rodents (both abbreviated as CORT) by the adrenal. In the brain, GC bind to mineralocorticoid receptors (MR) and GC receptors (GR). GR are abundantly expressed throughout the brain (Chao et al., 1989; Morimoto et al., 1996), whereas MR have a much more restricted expression in predominantly limbic brain structures. GR have a relatively low affinity for their ligand ($K_d = 2.5$–5 nM), and are therefore activated when circulating GC levels increase, eg, during stress or at the circadian peak, whereas brain MR are already activated under basal nonstress conditions ($K_d = 0.5$ nM) (Reul and de Kloet, 1985). GR and MR mediate complementary and different, sometimes opposing, actions of CORT. Although MR are involved in maintenance of neuronal excitability and basal activity of the stress system and onset of the stress reaction, GR activation results in suppression of excitability transiently raised by excitatory stimuli, recovery from stress, and behavioral adaptation. Their balanced activation is an important determinant of neuronal excitability, neuronal health, and stress responsiveness (de Kloet et al., 1998; de Kloet et al., 2005).

MR and GR belong to the superfamily of ligand-activated nuclear receptors and are involved in the regulation of gene transcription. GR dimers interact directly with 15-nucleotide glucocorticoid-responsive elements (GRE) that are present in the DNA, to mostly stimulate transcription, a mechanism called transactivation (Chandler et al., 1983). In addition, GR can bind other transcription factors such as activation protein-1, c-Jun N-terminal kinase, and nuclear factor-κB (Bruna et al., 2003; Herrlich and Ponta, 1994; Scheinman et al., 1995), thereby inhibiting their action, a mechanism known as transrepression.

The hippocampus, a brain structure important for learning, memory, mood, and regulation of the stress system, is a major target for GC and has high expression levels of both GR and MR (de Kloet et al., 2005; Reul and de Kloet, 1985; van Steensel B. et al., 1996). The balance of activated GR and MR influences not only cell birth and death but also other forms of neuroplasticity (de Kloet et al., 1998). Hippocampal neurons are particularly sensitive to GC and display a high degree of adaptive plasticity upon chronic GC exposure. Besides chronic exposure to GC, acute GC exposure can also affect structural plasticity in the brain. In the hippocampus, a few hours of intense stress reduced spine density on dendrites of CA3 neurons (Chen et al., 2008), whereas exposure to an acute restraint stress increased the density of spines on neurons in area CA1 of male rats (Shors et al., 2001). Besides structural changes, GC affect electrical properties of hippocampal neurons. Chronic stress or chronic CORT exposure suppresses hippocampal long-term potentiation (LTP), a

lasting synaptic strengthening that likely underlies learning and memory formation (Alfarez et al., 2003; Bodnoff et al., 1995; Krugers et al., 2006). Consistent with these GR-mediated effects on structure and function, hippocampal GR regulate a wide variety of genes involved in diverse aspects of neuroplasticity (Datson et al., 2008).

Although studies into GC- and stress-responsive genes in the hippocampus have been insightful (Andrus et al., 2012; Datson et al., 2008; Datson et al., 2012; Lisowski et al., 2011; Morsink et al., 2006b), the identified genes are notoriously a mixture of primary and more downstream transcriptional responses, and it remains unclear whether GR actually bind to regulatory elements controlling expression of these genes. Technological advances in high-throughput sequencing combined with chromatin immunoprecipitation (ChIP-Seq) have made it possible to characterize genome-wide binding sites of GR in a variety of cell types (John et al., 2011; Polman et al., 2012b; Reddy et al., 2009; Yu et al., 2010), providing an unprecedented view on the motifs and genomic locations to which GR bind in different cellular contexts. However, so far today, the genome-wide binding sites of GR in vivo in the brain have not been characterized.

The aim of the current study was to identify genome-wide primary targets of GR in vivo in the hippocampus using ChIP-Seq and study whether activated GR bind to their primary targets in a dose-dependent way. In addition, we wanted to gain more knowledge on the genes that are located near genomic binding sites for GR and search for cross-talk partners of GR in the brain that might explain the cell type-specific targets of GR that are often observed (John et al., 2011; Polman et al., 2012b; Reddy et al., 2009; Yu et al., 2010). Finally, we set out to investigate whether MR also bind to genomic binding sites of GR.

4.2   Materials and Methods

Experimental groups and tissue handling

For ChIP analysis, 8-week-old male Sprague Dawley rats (Harlan, Venray, The Netherlands) were housed in groups of 4 with food and water available ad libitum in a temperature ($21\,°C$) and humidity ($55\,\%$) controlled room with a 12-hour light, 12-hour dark cycle (lights on at 7:30am). All experiments were conducted during the light phase. The rats were adrenalectomized as described before to completely deplete endogenous CORT levels and ensure there were no GR bound to the DNA (Sarabdjitsingh et al., 2010a). Three days after adrenalectomy (ADX), 4 groups of animals received an ip injection with 3, 30, 300, or $3,000\,\mu g/kg$ CORT-hydroxypropyl-cyclodextrin complex while 1 group was left undisturbed ($n = 6$ per group). All animals were decapitated after 1 hour for ChIP, and their hippocampi were isolated and processed for ChIP (see below). CORT levels in the blood 2 days after ADX and at the moment of decapitation were measured by RIA, showing that both the ADX

Peptide/Antigen Sequence Protein Target		Name of Antibody	Manufacturer, Catalog No., or Name of Source	Species Raised in Monoclonal or Polyclonal	Dilution Used
MR	Amino acids 1–300 at N terminus of human MR	MR antibody (MR H-300) X	Santa Cruz Biotechnology sc-11412X (ChIP application)	Rabbit polyclonal IgG	6 μg/600 μl
GR	Amino acids 121–420 within an internal region of human GRα	GR antibody (H-300) X	Santa Cruz Biotechnology sc-8992X (ChIP application)	Rabbit polyclonal IgG	6 μg/600 μl

Table 4.1: Antibodies Used for the ChIP Study.

operation was successful as well as a significant increase in CORT 1 or 3 hours after injection (Supplemental Figure 1, published on The Endocrine Society's Journals Online web site at `http://endo.endojournals.org`). Experiments were approved by the Local Committee for Animal Health, Ethics, and Research of the University of Leiden (DEC 06055 and 10044). Animal care was conducted in accordance with the European Commission Council Directive of November 1986 (86/609/EEC).

Antibodies

Details on the antibodies used for ChIP are listed in Table 4.1. The antibodies used for GR and MR are commonly used in literature to study GR and MR in Western blot and immunohistochemical as well as immunoprecipitation studies in a wide variety of cells and tissues (`www.scbt.com`). We have successfully used the GR (H-300) antibody in the hippocampus for immunohistochemistry (Sarabdjitsingh et al., 2010b) and Western blot (Champagne et al., 2008) and have obtained specific signals. Furthermore, we have used this antibody for ChIP and a ChIP-Seq study in undifferentiated and neuronally differentiated PC12 cells, respectively (Polman et al., 2012b; van der Laan et al., 2008). The MR H-300 antibody has been used for Western blot analysis in the guinea pig and rat hippocampus (Chan et al., 2005; Owen and Matthews, 2003).

ChIP-Seq procedure

Because in vivo ChIP-Seq on brain tissue requires a minimum amount of chromatin as input, more than could be obtained from a single animal, 6 hippocampal hemispheres of 1 experimental group were pooled after shearing by sonication and divided in 2 equal portions, so that 2 ChIP procedures on identical samples (technical replicates) could be performed. This was done for both hemispheres, resulting in 4 ChIP samples that were stored at −80 °C until further processing.

The ChIP procedure was performed as described before (Polman et al., 2012a). A detailed description of the ChIP procedure is available in Supplemental Document 1. Briefly, the samples were separately precleared by incubating them with Sepharose A beads. After preclearing, an input aliquot was taken of each sample to control for the amount of DNA used as input for the ChIP procedure. To reduce

Chapter 4

87

technical and biological variation, each sample was divided in 3 portions and incubated overnight at $4\,^{\circ}\mathrm{C}$ under continuous rotation with $6\,\mu g$ of either a GR, MR, or normal rabbit IgG antibody (Santa Cruz Biotechnology, Santa Cruz, California). Subsequently, the antibody-bound DNA fragments were isolated by incubating the samples with blocked protein A beads, after which the beads were washed and incubated with elution buffer to isolate the DNA-protein complexes. Finally, the DNA fragments were isolated by reverse cross-linking the samples, followed by ribonuclease treatment and purification on Nucleospin columns (Macherey-Nagel, Düren, Germany) (Polman et al., 2012a). The immunoprecipitated samples were eluted in $50\,\mu l$ elution buffer.

For sequencing, IgG and GR ChIP samples of rats that received $3,000\,\mu g/kg$ CORT were prepared according to the protocol supplied with the Illumina Genome Analyzer GA1 (Illumina, San Diego, California). In brief, the DNA fragments were blunted and ligated to sequencing adapters after which the DNA was amplified for 18 rounds of PCR. The DNA was electrophoresed on a 2% agarose gel, of which a region containing DNA fragments 100 to 500 base pairs (bp) in length was excised and the DNA extracted with the QIAGEN Gel Extraction Kit (QIAGEN, Hilden, Germany). DNA quality was checked on the Agilent Bioanalyzer (Waldbronn, Germany). Single end sequencing of the first $35\,bp$ of the resulting DNA library was performed on the Illumina Genome Analyzer (Leiden Genome Technology Center, Leiden University Medical Center, Leiden University).

Read alignment, peak calling, and mapping

We used the Burrows-Wheeler Aligner (Li and Durbin, 2009) to align $35\,bp$ reads to the rat genome (rn4), controlling for unique tags, mismatch, and DNA gaps. Using BEDtools (Quinlan and Hall, 2010), we generated BED files that were used for model-based analysis of ChIP-Seq (MACS) (Zhang et al., 2008) and wiggle files which could be used to visualize the reads on the UCSC genome browser (`http://genome.ucsc.edu`).

GR-binding sites (GBS) in the DNA relative to the nonspecific binding of the corresponding IgG ChIP-Seq sample were identified with the MACS peak caller (Zhang et al., 2008). For peak calling, a P value cutoff of 1.00×10^{-5}, a model fold of 30 and a λ set of 1,000/5,000/10,000 were used to determine significant bound DNA regions. Per peak, a false discovery rate (FDR) was calculated by MACS.

Using Galaxy (`http://main.g2.bx.psu.edu/`) (Blankenberg et al., 2010; Goecks et al., 2010), Refseq genes near the GBS were determined. As a reference genome, *Rattus norvegicus* 4 (rn4) was used. Data were visualized by uploading wiggle files containing the raw ChIP-Seq data on the UCSC genome browser.

Real-time quantitative PCR

For ChIP-Seq validation, a selection of GBS was validated by applying real-time quantitative PCR on immunoprecipitated chromatin. All cycle threshold values ranged from 25 to 32. The ChIP PCR signal was normalized by subtracting the amount of nonspecific binding of the IgG antibody in the same sample. Metallothionein 2A (MT2a), which has 2 well-documented GREs (Kelly et al., 1997), served as a positive control for the ChIP. As a negative control, we analyzed GR binding to a nonbound GR region (exon 2 of the myoglobin gene). Normalized data were analyzed with GraphPad Prism version 5.

One-way ANOVA with a Tukey's multiple-comparison test was used to assess significant binding of GR and/or MR. Significance was accepted at $P \leq .05$.

The primer sequences for ChIP validation are listed in Table 4.4.

Motif search

The regions containing the GBS were trimmed to $200\,\mathrm{bp}$ sequences and screened for de novo motifs consisting of 8 to 40 nucleotides using MEME (multiple expectation maximization for motif elicitation) (Bailey and Elkan, 1994). The 15 most significant motifs were given as output and compared against databases of known motifs using TOMTOM Motif Comparison Tool (Gupta et al., 2007).

Gene ontology analysis

The genes nearest to the significant GBS were clustered with the Database for Annotation, Visualization, and Integrated Discovery (DAVID) version 6.7 (`http://david.abcc.ncifcrf.gov/home.jsp`) according to their functional annotation.

4.3 Results

ChIP-Seq results

Sequencing of the DNA fragments acquired by ChIP resulted in the generation of 1.9×10^7 and 1.5×10^7 reads that were bound by GR and IgG, respectively. Approximately 1.1×10^6 and 0.47×10^6 reads could be uniquely mapped to the rat genome (rn4) for GR and IgG, respectively. MACS peak calling resulted in the identification of 16,614 peaks that were bound by GR (GBS) with FDR percentages that ranged from 0 to 58 (Table 4.5). Plotting the distribution of FDR values for all GBS revealed that the FDRs were not distributed as a continuum but that there were some gaps in which a range of FDR values were not represented. Based on this, an FDR cutoff of $13\,\%$ was chosen, which coincided with the point in the FDR distribution curve just before the first major gap (Figure 4.1). This cutoff resulted in a total of 2,460 GBS with P values ranging from 3.3×10^{-116} to 1.13×10^{-12} (Table 4.6).

Chapter 4

89
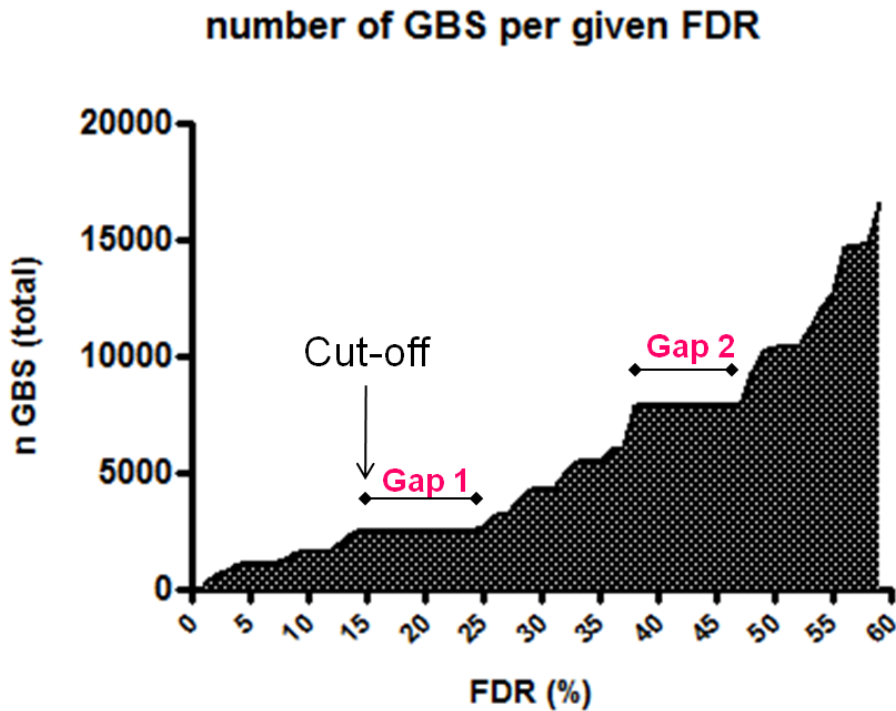
Figure 4.1: The number of GBSs (y-axis) are plotted against the corresponding FDR (x-axis). Two FDR gaps are evident: 1) from 12.98 % to 24.08 % and 2) from 37.16 % to 47.28 %, in which a rise in FDR does not yield an increase in GBS. FDRs are shown in percentages.

Genomic distribution of GBS in rat hippocampus

The 2,460 significant GBS were associated with 1,823 unique gene IDs. Examination of the location of the 2,460 GBS relative to nearby genes revealed that 965 GBS (39 %) were located within genes (Figure 4.2). Interestingly, the intragenic GBS were mainly located within intronic regions (78 %), followed by 5′-untranslated region (UTR) (15 %), intron/exon junctions (4 %), and 3′-UTR (3 %). Only 1 % of the intragenic GBS were located within exons. Considering GBS that were located outside annotated RefSeq genes, 12 % of GBS were located within 10 kilobases (kb) upstream or downstream from the nearest gene and another 27 % between 10 and 100 kb. The remaining 22 % were located further than 100 kb upstream or downstream of the nearest genes, of which 111 GBS (5 %) were at more than 500 kb.

Validation of GBS confirms ChIP-Seq results

To validate the results obtained from ChIP-Seq, a selection of 13 GBS covering a wide spectrum of P values was measured in ChIP samples obtained from an inde-

A

B
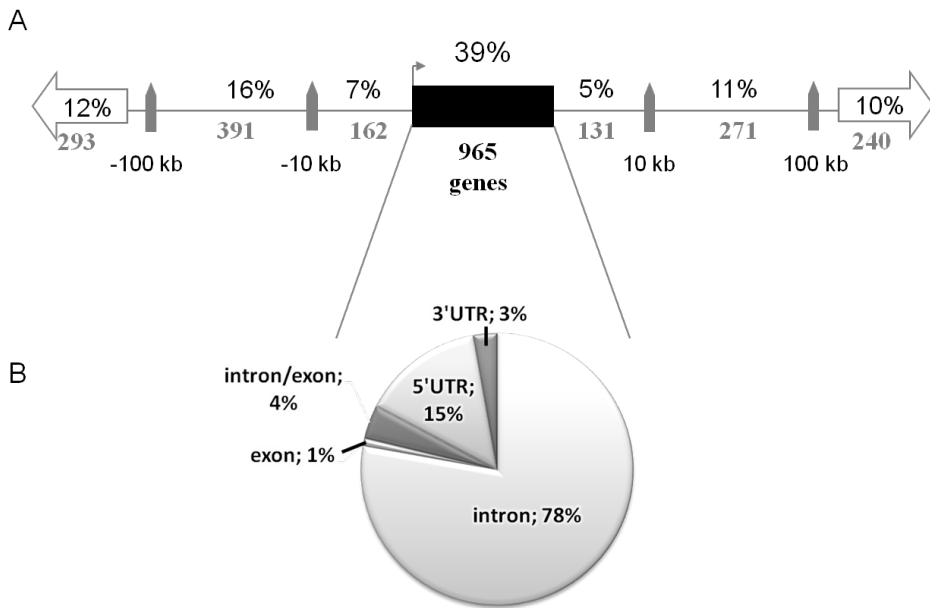
Figure 4.2: Distribution of GBS relative to the nearest gene, resulting in regions that lie within or outside genes.
The black bar represents a gene, showing that $39\,\%$ of the GBS are located within genes. The GBS that are located up or downstream from the nearest gene are divided into 3 bins: within $10\,\text{kb}$, between 10 and $100\,\text{kb}$, and more than $100\,\text{kb}$ from a gene. B, Pie chart showing the location of intragenic GBS within annotated RefSeq genes, devided into $5'$-UTR (exon or intron), intron, exon, intron/exon overlap, and $3'$-UTR (exon or intron) regions.

pendent set of hippocampi. In all cases, significant GR binding relative to untreated ADX animals was confirmed (Figure 4.3). Interestingly, there was a large variation in degree of GR binding to the GBS, ranging from $0.06\,\%$ to $3.5\,\%$ of the DNA that was bound by GR in the selected genomic regions. In general, the GBS with the highest degree of GR binding were the most significant, with lower FDR and P values in comparison with GBS with lower levels of GR binding (Figure 4.3).

GRs bind to their genomic targets in a ligand concentration-dependent manner

To investigate whether GR binding to its genomic targets was dependent on the concentration of available ligand, we analyzed GR binding within the hippocampi of 4 groups of animals that received different doses of CORT, namely 3, 30, 300, or $3{,}000\,\mu\text{g}/\text{kg}$. We performed ChIP-PCR on the same selection of GBS described above (Figure 4.3). In all cases, significant GR binding was observed in a dose-dependent manner. A more detailed analysis allowed the GBS to be divided into
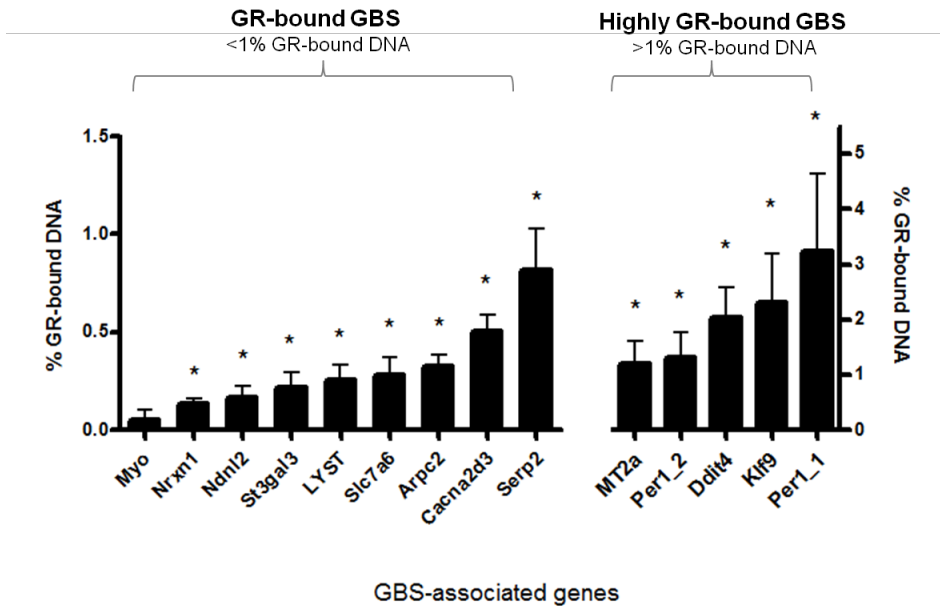
Figure 4.3: Graph showing ChIP-PCR validation of a selection of GBS that were identified by ChIP-Seq.
Because the intensity of GR binding varies enormously, the graph was split in two, showing the GBS with lower GR binding on the left (percent GR-bound DNA < 1.0) and GBS with higher GR-binding (percent GR-bound DNA > 1.0) on the right with different y-axes. The gene nearest to the GBS is listed on the x-axis and the percentage of GR-bound DNA (corrected for IgG) is indicated on the y-axis. Statistical analysis was performed using 1-way ANOVA with Tukey's multiple-comparison test to identify GBS that show significant GR binding compared with noninjected animals. *, Significance was accepted at $P <$ .05. GR binding in myoglobin exon2 was measured as a negative control. Details of all the validated GBS are present in Table 4.6 (GBS number): *Nrxn1*(1826), *Ndnl2* (1529), *St3gal3* (529), *Lyst* (535), *Slc7a6* (640), *Arpc2* (759), *Cacna2d3* (1540), *Serp2* (61), *MT2a* (63), *Per1_2* (1362), *Ddit4* (211), *Klf9*(25), *Per1_1* (12).

2 distinct groups based on their differential binding at lower CORT concentrations (Figure 4.4). The first group, the high-CORT GBS, showed no binding after injecting 3 or 30 µg/kg CORT, in some cases minimal binding at 300 µg/kg CORT, but a sharp increase in binding at 3,000 µg/kg CORT (Figure 4.4A). The second group, the low-CORT GBS, displayed GR binding starting at 30 µg/kg CORT, which increased thereafter and reached relatively high levels of GR binding at the highest CORT concentration of 3,000 µg/kg (Figure 4.4C). Interestingly, the low-CORT group coincided with the most intensely bound GBS and the high-CORT group with the less intensely bound GBS (Figure 4.3).

MRs and GRs bind to the same GBSs, but at different ratios depending on the ligand concentration

Although the binding sites reported here were identified using a GR-specific antibody, we were interested in whether they might also be bound by MR, because
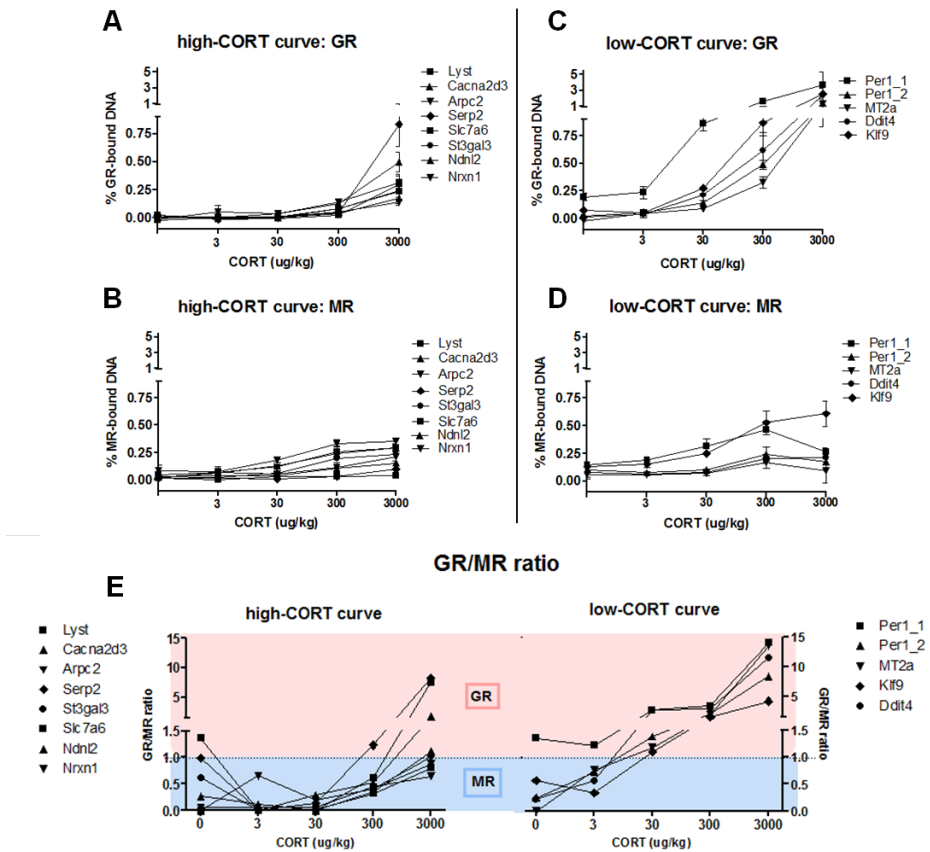
Figure 4.4: Graphs visualizing the concentration-dependent binding of GR and MR to its targets.
The CORT concentration is indicated on the x-axis. Point 0 of the x-axis represents undisturbed animals that did not receive a CORT injection. The GBS were assigned into 2 different groups: the high-CORT and the low-CORT groups. A, GR binding to the high-CORT group is shown, in which GR binding to the GBS is evident after injecting 3,000 µg/kg but not at lower concentrations. B, MR binding to these high-CORT GBS is apparent at 30 µg/kg as well but in most cases stabilizes thereafter. C, GR binding to low-CORT GBS, where GR binding is present at 30 µg/kg CORT and increases with higher CORT concentrations. D, MR binding to low-CORT GBS that resembles the pattern observed in the high-CORT GBS. E, Graph in which the GR to MR ratio for the high-CORT and low-CORT groups are visualized. All GBS were significantly bound by GR according to 1-way ANOVA analysis with Tukey's multiple-comparison test relative to noninjected animals. Significance was accepted at $P < .05$.

MR and GR have DNA-binding domains that are 94 % identical and may form heterodimers. Because MR and GR have different affinities for CORT, we performed ChIP for MR and GR under varying amounts of available ligand, ranging from 3 to 3,000 µg/kg. The lowest dose of 3 µg/kg was chosen, because we expected both poor activation of GR and MR and hence very little DNA binding to be observed at this CORT concentration. The next dose of 30 µg/kg was chosen because we expected predominant MR activation and very little GR activation, whereas 300 and

3,000 µg/kg are in the CORT range of additional significant GR activation. Significant MR binding was observed at all GBS except at *Per1_2, MT2a*, and *Slc7a6*. Analysis of MR binding to the low-CORT and high-CORT GBS described above showed a different binding pattern than GR binding (Figure 4.4, B and D), with MR binding starting at either 30 or 300 µg/kg CORT but not increasing at higher CORT doses. This is in contrast to GR binding, where a sharp increase at 3,000 µg/kg CORT was observed. Calculating the ratio of MR and GR binding to the validated GBS showed that the low-CORT GBS have a GR to MR ratio above 1, indicating that they display relatively more GR binding over the full range of CORT concentrations ranging from 30 to 3,000 µg/kg. In contrast, the high-CORT GBS mostly have a GR to MR binding ratio below 1, in particular in the CORT concentration range of 3 to 300 µg/kg.
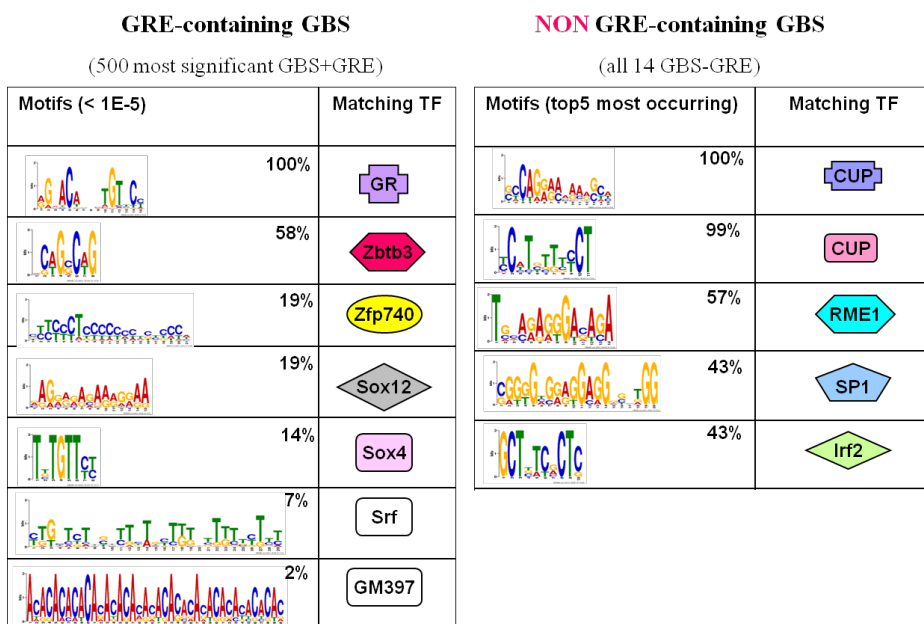
Figure 4.5: Motifs identified in GBS that do or do not contain a GRE.
For GBS that do contain a GRE, the motifs with an e-value < 0.05 were considered. Because only 14 GBS did not contain a GRE, all e-values are higher than 0.05 and therefore the 5 most frequent occurring motifs are depicted. The e-value indicates the statistical significance of the motif and is calculated by MEME. The e-value is an estimate of the expected number of motifs with the given log likelihood ratio (or higher), and with the same width and site count, that one would find in a similarly sized set of random sequences.

Motif analysis reveals Zbtb3 to be an important possible transactivation partner

A remarkably high proportion of GBS contained a GRE. The GRE sequence itself was identical to the consensus sequence that was identified in other ChIP-Seq studies on GR (Figure 4.5) (John et al., 2011; Reddy et al., 2009; Yu et al., 2010).

Only 14 of the 2460 GBS lacked a GRE, indicating that the remaining 2446 GBS likely regulate target gene expression through direct GR-GRE interaction, also known as transactivation. Continuing the motif screening within the 500 GRE-containing GBS with the lowest FDR revealed that 288 GBS (58 %), in addition to a GRE motif, also contained a motif that significantly resembled the binding motif of the transcription factor zinc finger and BTB domain containing 3 (Zbtb3) (Figure 4.5). Other identified motifs involved sequences similar to binding sites for zinc finger protein 740 (Zfp740), SRY-box containing gene 12 (Sox12), Sox4, serum response factor (Srf), and zinc finger and SCAN domain containing 4C (GM397 or Zscan4c). Analysis of the top 5 co-occurring motifs within 1 GBS revealed that the combination of GR and Zbtb3 binding motifs within the GBS without the presence of any of the other motifs was most prevalent (37 %) (Figure 4.6). This was followed by the combination of GR, Zbtb3, and zinc finger protein 740 or Sox12 binding motifs, both combinations occurring in 10 % of this selection of GRE-containing GBS. Co-occurrence of GR with Sox12 or Sox4 binding motifs was observed in 7 % of these GBS.

Of the 14 GBS that did not contain a GRE, all contained 2 motifs significantly resembling the motif recognized by the protein CG11181 gene product from transcript CG11181-RB (CUP) (Figure 4.5). Eight of these GBS (57 %) additionally contained a binding motif significant for the zinc-coordinating protein zf-C2H2 Zinc finger, C2H2 type (RME1). Binding motifs resembling the transcription factor specificity protein 1 and interferon regulatory factor 2 (Irf2) binding sites occurred in 6 GBS (43 %) (Figure 4.6).

GBS-associated genes are involved in neuronal functioning and cell survival

To investigate the biological relevance of the identified GBS, we analyzed the functional annotations of the 2,460 associated genes and sorted them into clusters using DAVID (Table 4.2). Within the top 10 clusters, we found neuronal-associated clusters, namely, cell and neurite projection (cluster 1) and neuron differentiation (cluster 9) as well as cell-survival clusters like apoptosis (cluster 5) and regulation of programmed cell death (cluster 7). The remaining clusters involved enzyme binding (cluster 3), response to organic substance (cluster 4), phosphate metabolic process (cluster 8), and positive regulation of transcription (cluster 10).

As described above, a motif resembling Zbtb3-binding sequences was identified in 58 % of the 500 GRE-containing GBS that have the lowest FDR. We next

	GO Term	Category	ES
1	cell and neurite projection	CC	6.8
2	blood vessel development	BP	6.3
3	enzyme binding	MF	5.5
4	response to organic substance	BP	5.4
5	apoptosis	BP	5.2
6	cell and membrane fraction	CC	5.0
7	regulation of programmed cell death	BP	4.3
8	phosphate metabolic process	BP	4.0
9	neuron differentiation	BP	4.0
10	positive regulation of transcription	BP	3.9

Table 4.2: Top 10 Enriched Functional GO Clusters of GBS-Associated Genes Identified in Rat Hippocampus.

investigated whether the genes associated with these Zbtb3-containing GBS were involved in different biological processes and functions from the GBS without a Zbtb3-binding sequence. Clustering of the acquired gene ontology (GO) revealed differences between GBS that do or do not contain a Zbtb3-binding sequence with regard to the types of clusters and the degree of enrichment (Table 4.3). GBS harboring a Zbtb3 motif generally had clusters with higher enrichment scores compared with GBS without Zbtb3 motifs. For example, 7 clusters showed an enrichment of more than 2 versus only 2 clusters with this degree of enrichment in the group lack-
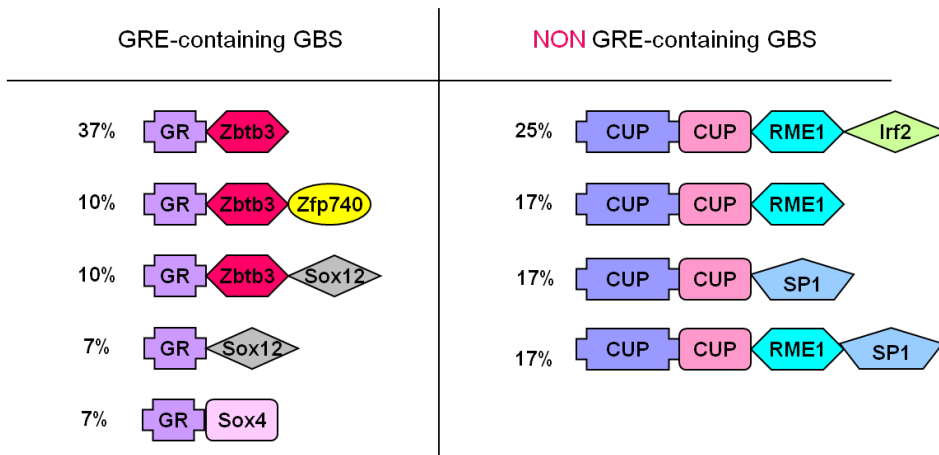
Figure 4.6: Most frequently observed combinations of motifs identified within GBS with or without a GRE.
For GBS that did contain a GRE, the top 5 co-occurring motifs are depicted. For GBS without a GRE, all observed combinations are shown.

	with Zbtb3			without Zbtb3		
	GO Term	Category	ES	GO Term	Category	ES
1	negative regulation of cell communication	BP	3.9	protein kinase binding	MF	3.7
2	insoluble fraction	CC	3.0	ion binding	MF	2.3
3	negative regulation of transcription	BP	2.7	biological adhesion	BP	1.9
4	regulation of apoptosis	BP	2.7	protein amino acid dephosphorylation	BP	1.3
5	positive regulation of anti-apoptosis	BP	2.5	eye morphogenesis	BP	1.3
6	positive regulation of macromolecule metabolic process	BP	2.4	protein kinase cascade	BP	1.3
7	negative regulation of insulin receptor signaling pathway	BP	2.3	in utero embryonic development	BP	1.2
8	blood vessel development	BP	1.7	regulation of nucleotide biosynthetic process	BP	1.1
9	regulation of cell-substrate adhesion	BP	1.7	mitochondrial part	CC	1.0
10	response to inorganic substance	BP	1.6	rhythmic process	BP	1.0

Table 4.3: Top 10 Enriched Functional GO Clusters in Rat Hippocampus in the 500 Most Significant GBS-Associated Genes With and Without Zbtb3 Motifs.

ing a Zbtb3 motif. Furthermore, the Zbtb3-containing group was enriched for clusters involved in regulation of apoptosis (clusters 4 and 5), regulation of transcription (cluster 3), and regulation of macromolecule metabolic process and insulin receptor signaling pathway (cluster 6 and 7). The non-Zbtb3-containing group, in contrast, was mainly involved in protein kinase binding (cluster 1, 3.7 enrichment), followed by ion binding and biological adhesion.

4.4 Discussion

Because neuronal plasticity within the hippocampus is known to be very sensitive to GR activation, resulting in functional as well as structural changes (Datson et al., 2012; McLaughlin et al., 2007; Sousa et al., 2000), we were interested in the composition of the GR-binding repertoire within hippocampal tissue. In the current study in rat hippocampus, we identified 2,460 significant GBS using ChIP-Seq. Analysis of a selection of these GBS in animals that received different doses of CORT showed that the GR-binding potential differs depending on the GBS that is analyzed and the concentration of ligand that has been administered. We showed MR binding to several validated GBS, but to a lower extent than GR binding, in particular at the higher CORT concentrations. Finally, motif analysis revealed a high prevalence of sequences within the GBS that significantly resemble binding sites for Zbtb3 and CUP, which might be potential new cross-talk partners involved in GR-mediated transactivation and transrepression, respectively.

Chapter 4

Reliability of ChIP-Seq data

To validate the reliability of our GBS, we randomly selected 13 GBS with FDRs ranging from 0 % to 13 % for validation by ChIP-PCR. In all cases, we were able to successfully validate GR binding to the GBS, supporting that the statistical threshold we applied was stringent enough to detect bona fide GBS. The fact that 99 % of the GBS that we considered to be significant contain a GRE, in our opinion, strengthens the hypothesis that these are real GBS. In a previous ChIP-Seq study on genome-wide GR binding in neuronal PC12 cells, we observed that more than 80 % of the 100 most significant GBS contained a GRE, with this percentage slowly decreasing as GBS significance descended (Polman et al., 2012b), suggesting that our cutoff detecting 2,460 GBS may even have been too stringent. GRE-dependent processes are important in the brain, as shown in $GR^{dim/dim}$ mutant mice, in which the mutation prevented GR homodimerization and therefore binding to most GREs. These mice showed an impairment of modulation of hippocampal excitability and spatial memory (Karst et al., 2000; Oitzl et al., 2001).

Additional support for the reliability of the ChIP-Seq data presented here comes from the observation of hippocampal GR binding near several known GR targets such as Per1, Ddit4 (Datson et al., 2011; Polman et al., 2012b; So et al., 2007), Mt2a, and Klf9 (Datson et al., 2011; Polman et al., 2012b; So et al., 2007) as well as near many genes previously reported to be differentially regulated upon a psychological or physiological stressor, such as, microtubule-associated protein 2 (*MAP2*) (Cereseto et al., 2006), microtubule-associated protein 1b (*MAP1b*) (Antonow-Schlorke et al., 2003), neuroligin 1 (*nlgn1*) (Dai et al., 2009), growth-associated protein 43 (*GAP43*) (Pascale et al., 2011), calcium/calmodulin-dependent protein kinase IIα (*Camk2a*) (Orsetti et al., 2008), FK506 binding protein (*Fkbp5*) (Lee et al., 2010), glutamate receptor, ionotropic, *N*-methyl d-aspartate 2B (*Grin2b*) (Ayalew et al., 2012), glutamate receptor, ionotropic, AMPA 2 (*Gria2*) (Teyssier et al., 2011), and N-myc downregulated gene 2 (*NDRG2*) (Araya-Callis et al., 2012). Interestingly, *NDRG2* is a target of MR and is activated by the MR ligand aldosterone in the kidney and distal colon (Boulkroun et al., 2002).

The GR-binding data were obtained in ADX rats replaced with a specific dose of CORT, which creates an artificial context due to the depletion of endogenous CORT. However, the fact that we detected several known GR targets and almost all binding sites contained a highly significant GRE sequence does give us confidence in the data.

A high percentage of GBSs are located within introns or far away from genes

A relatively high percentage (39 %) of the 2,460 significant GBS was located within genes, in particular within introns, which is a finding that we previously observed in neuronal PC12 cells and that has also been observed by others (Polman et al., 2012b;

Reddy et al., 2009; Yu et al., 2010). It is becoming increasingly clear that many intronic regions have a regulatory function and harbor *cis*-acting regulatory elements such as tissue-specific enhancers (Hoo et al., 2010; Meyer et al., 2010; Ott et al., 2009; Vazquez et al., 2012) and noncoding RNAs, which play an important role in autoregulation and gene regulation processes (Bosia et al., 2012; Gromak, 2012). Approximately 22 % of the GBS were located at distances of at least 100 kb from the nearest gene and 5 % at even 500 kb or more. It has been shown that these gene deserts that are devoid of coding sequence may contain regulatory sequences that act at large distances to control gene expression (Ovcharenko et al., 2005).

GR binding to genomic targets is dependent on ligand availability

A few studies have shown dose-response effects of CORT on the expression of target genes (Bagamasbad et al., 2012; Ma et al., 2012). We studied the dose-response relationship of GR binding to a selection of the GBS identified after administration of a high dose of CORT (3,000 µg/kg). Our results indicated that in a subset of GBS, the high-CORT GBS, GR binding to the GBS became evident only after injecting 3,000 µg/kg CORT, but not at lower CORT concentrations. In contrast, another subset had a more step-wise GR-binding profile, starting at 30 µg/kg CORT and slowly increasing thereafter, which we called the low-CORT GBS. Interestingly, the low-CORT GBS had the lowest FDRs and the highest relative GR binding (Figure 4.4). Hence, these low-CORT GBS represent the binding sites that become occupied upon replacement of the ADX animal with CORT toward physiological levels, whereas the high-CORT group is identified in a dose range common for pharmacotherapy of inflammatory processes, a distinction that has been indicated by Sapolsky et al (Sapolsky et al., 2000) as indicative for permissive and regulatory (eg, stimulatory, suppressive, and preparative) actions of GCs.

What could the differences in GR-binding potential to the various targets implicate? First, it appears that the GC concentration affects the repertoire of genomic targets to which GRs bind. The GBS near the low-CORT genes are bound at relatively low levels of CORT as well as at higher levels of CORT. This indicates that these genes are likely to be activated during daily variations of CORT. The high-CORT GBS, conversely, appear to be less sensitive to changing CORT levels. Only when the organism is exposed to a higher concentration of CORT, which may occur at the circadian peak or in response to more severe stressors, and the concentration of the hormone is sufficiently high for the activation of GR will binding of GR to these high-CORT GBS occur, resulting in the activation of the corresponding genes near these GBS. The question can therefore be raised, whether the distinction in low-CORT and high-CORT genes may relate to the enormous diversity in permissive and regulatory actions of GCs that have been suggested to be complementary in coordination of daily activities and sleep-related events as well as organization of the response to stress, respectively (Sapolsky et al., 2000).

99

Interestingly, classical known GR targets such as *Per1*, *Ddit4*, *Mt2a*, and *Klf9*, ubiquitously bound by GRs in multiple cell types and tissues, were all present within the low-CORT group and perhaps may therefore be important for any kind of daily variation in actions of a permissive nature. Our findings imply that, depending on the amount of secreted CORT, different sets of GR-target genes are recruited in the hippocampus. Because the level of CORT secretion is directly related to duration and severity of the stressor, this may explain how the high-CORT GBS affect the profound functional and structural changes in plasticity of hippocampal neurons caused by chronic GC overexposure.

MRs bind to GBS, but at lower CORT concentrations

Knowledge of MR targets is sparse, in particular in the brain. Because MR have a near identical DNA-binding domain to GR, we were curious whether MR also displayed binding to GBS. Both receptors are activated by the ligand CORT, with the only difference that MR have a much higher affinity for CORT and, consequently, are activated at lower CORT levels in comparison with GR. In particular in the high-CORT GBS, MR binding at the lower CORT concentrations might disable GR binding and allow GR binding only when CORT levels become so high that MR are fully occupied. Indeed, we observed relatively higher MR binding to the high-CORT GBS than to the low-CORT GBS. At an absolute level, the difference in MR binding was not apparent, indicating a saturation of MR in both situations, further supporting the importance of the balance in MR- and GR-mediated actions in maintaining homeostasis (de Kloet et al., 1998).

It is unlikely that the differences in MR and GR binding can be linked to differences in relative concentrations of MR and GR protein levels in the hippocampal preparations we used, although we did not measure this in the current study. However, it is known from our original radioligand binding and Western blot studies over the years that MR and GR concentrations in hippocampus are in the same range but that the values may change depending on strain, age, and stress history. Reul and de Kloet (Reul and de Kloet, 1985) reported an MR concentration of $250\,\mathrm{fmol/mg}$ protein in the hippocampus cytosol of ADX Wistar rats, whereas the GR concentration was $310\,\mathrm{fmol/mg}$ protein.

GR monomers may also form dimers via heterodimerization with MR, potentially increasing the level of functional diversity (Trapp et al., 1994). A recent study using green fluorescent protein-based fluorescence resonance energy transfer in living cultured hippocampal neurons provided evidence that MR and GR directly interact with each other in the nucleus (Nishi et al., 2004). The results from this study suggested that MR may predominantly form homodimers at lower CORT concentrations, whereas at higher concentrations mimicking stressful conditions when GR activation becomes more abundant, the incidence of heterodimerization with GR increased (Nishi et al., 2004).

We have previously reported that MR and GR have distinct yet overlapping target genes in the hippocampus (Datson et al., 2001b). Strikingly, MR bound to almost all the GBS we tested here. However, because the study was designed to identify GBS and not MR-binding sites, we cannot exclude the existence of MR-specific binding sites that might be detected in a genome-wide screen using an MR-specific antibody.

GBS near CORT-regulated genes are involved in neuronal plasticity

Recent insights from ChIP-Seq studies have revealed that GR bind to the genome in a cell-type-specific manner. Therefore we expect GR to target genomic sites in the hippocampus that are different from those in other nonneuronal cell types (John et al., 2011; Polman et al., 2012b; Reddy et al., 2009; Yu et al., 2010). Because GR play an important role in hippocampal neuronal plasticity, we hypothesized that GBS in the hippocampus would be located nearby or within genes associated with neuronal plasticity. Indeed, we observed GR binding near several genes involved in neuronal plasticity, such as neurochondrin (*NCDN*), ionotropic N-methyl-D aspartate (NMDA) receptor-2 (*GRIN2A* and *GRIN2B*), metabotropic 5 (*GRM5*), and signal-induced proliferation-associated 1 like 1 glutamate receptor (*SIPA1L1*). Furthermore, GO analysis showed that GR bind to genomic sites that are located near genes involved in neuron projection and neuron differentiation, which were over-represented GO terms.

An important pathway that is known to be involved in cell survival and neuronal plasticity is the mammalian target of rapamycin (mTOR) pathway. We have recently shown that a number of regulators of the mTOR pathway, such as *Ddit4* and *Fkbp51* are primary targets of GR and are differentially expressed within the rat hippocampus after a CORT challenge (Polman et al., 2012a). In the current study, we confirmed these primary binding sites and in addition observed GR binding near other mTOR pathway members, such as phosphatidylinositol 3-kinase, catalytic subunit type 3 (*Pik3c3*) and regulatory subunit 1 [alpha] (*Pik3r1*) as well as Pi3k-regulator insulin receptor substrate 2 (*Irs2*). Interestingly, phosphatidylinositol 3-kinase signaling is indicated to play a key role in mediating the stress-induced modification of hippocampal synaptic plasticity (Yang et al., 2008). Strikingly, brain-specific deletion of the *Irs2* gene is associated with disrupted hippocampal synaptic plasticity (Costello et al., 2012). These findings support our previous proposal that direct regulation of the mTOR pathway by CORT represents an important mechanism regulating neuronal plasticity in the rat hippocampus (Polman et al., 2012a).

Hippocampal GBS provide new insight into cross-talk partners of GR in the brain

The extremely high proportion of GRE-containing GBS (99 %) is considerably higher than observed in other GR ChIP-Seq studies, where GRE percentages ranged from

60 % to 80 % (John et al., 2011; Polman et al., 2012b; Reddy et al., 2009; Yu et al., 2010). However, the present study differs in several aspects from previous ChIP-Seq studies, which were all performed in vitro in cell lines and also used the synthetic ligand dexamethasone instead of the natural GR ligand CORT. Different GR ligands are known to differentially affect the conformation state of GR, with consequences for the availability of the ligand-binding domain of GR, dissociation rate from the DNA, and its affinity to interact with the genome (Schaaf et al., 2005).

GR regulate gene transcription in conjunction with an extensive network of other transcription factors. Almost 60 % of the GBS consisted of composite sites containing a motif for Zbtb3 besides a GRE. Zbtb3 was identified as a potential interaction partner of GR (Ravasi et al., 2010). Interestingly, we previously identified a motif for Zbtb3 to be present in 81 % of the GBS that lacked a GRE in neuronal PC12 cells (Polman et al., 2012b). Together these findings suggest that Zbtb3 may play a role in directing GR to their binding sites within the hippocampus. Unfortunately, not much is known about this protein, and its precise role in GR signaling requires further exploration.

The 14 GBS that did not contain a GRE all contained motifs for the DNA-binding sequence of CUP, a protein that has been studied extensively in *Drosophila* but not at all in mammals yet (Igreja and Izaurralde, 2011). CUP is an eukaryotic translation initiation factor 4E (EIF4E)-binding protein that represses the expression of specific maternal mRNAs. Interestingly, eukaryotic translation initiation factor 4E (EIF4E)-binding protein is an upstream[1] component of the mTOR pathway, which we have previously identified to be regulated by GR within the brain. CUP may therefore be an interesting potential novel cross-talk partner of GR in the hippocampus.

A striking observation in this study is the complete lack of binding sites for classical GR cross-talk partners like activation protein-1 (Jonat et al., 1990) and nuclear factor-κB (De Bosscher K. et al., 2008), which are known to occur both in composite sites together with a GRE as well as in sites lacking a GRE. Similar to our previous study on GR binding in neuronal PC12 cells, we identified motifs for transcription factors that had not previously been associated with GR function within the GBS (Polman et al., 2012b). A likely explanation for this is that most of the cross-talk partners of GR were identified in studies on the immunosuppressive and tumor-suppressive properties of GR (Chebotaev et al., 2007; De Bosscher K. et al., 2008; Glass and Saijo, 2010), whereas until now, very little effort has been put into identifying cross-talk partners in a neuronal context.

In conclusion, the current study has provided new insight into GR functioning in the brain. Besides having identified thousands of genomic GBS within the hippocampus, we have shown that under varying GC concentrations, different binding sites are recruited. Our results highlight the existence of 2 distinct populations of GBS in the rat hippocampal genome that can be discriminated by the extent of CORT binding. Furthermore, within the GBS, we have identified several motifs for

---

[1] Correction: upstream should be downstream

proteins that may be potential cross-talk partners of GR within the hippocampal interactome.

Chapter 4

Supplemental Document 1: Detailed description of the ChIP procedure with Supplemental Figure 1
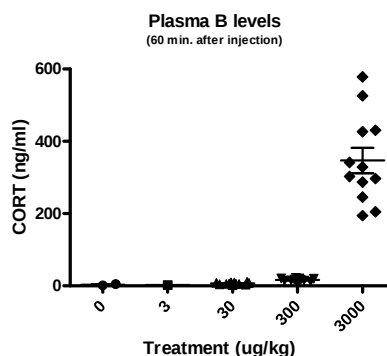
Tissue fixation and sonication

Hippocampal tissue was chopped into pieces of approximately 1 mm within 10 minutes after decapitation. Consequently, the tissue was fixated with 1% formaldehyde for 15 minutes under continuous rotation. The crosslinking was stopped by adding 0.125 M glycine for 5 minutes after which the tissue was washed 3 times with PBS and once with PBS containing protease inhibitors (PI). Finally, the pellets were snap frozen and stored at $-80\,°C$ until homogenization.

The defrosted brain tissue pellets were homogenized for 2×10 sec in 0.5 ml mild lysis buffer (10 mM Tris-HCl pH 7.5; 10 mM NaCl; 0.2% NP-40) supplemented with PI using the Bio-Gen PRO200 homogenizer.

Plasma B levels
(60 min. after injection)

CORT (ng/ml) — Treatment (ug/kg)

Supplemental Figure 1
Plasma CORT levels measured by Radio Immune Assay in trunk blood at decapitation, 60 minutes after injection of 3, 30, 300 or 3,000 µg/kg CORT.

After centrifugation, the pellets were dissolved in 0.6 ml PI-containing RIPA (0.1% SDS, 1% DOC, 150 mM NaCL, 10 mM Tris pH 8.0, 2 mM EDTA, 1 mM $NaVO_3$, 1% NP-40, β-glycerolphophate and Na-butyrate) and incubated on ice for 30 minutes. Subsequently, the chromatin was sheared (Bioruptor, Diagenode; 20 pulses of 30 sec., 200 W), resulting in chromatin fragments of 100–500 bp. After shearing by sonication, 6 hippocampal hemispheres of one experimental group were pooled and divided in two equal portions, so that two ChIP procedures on equal samples could be performed. This was done for both hemispheres, resulting in 4 ChIP samples, that were stored at $-80\,°C$ until further processing for ChIP.

ChIP-seq

Sepharose A beads (GE Health care) were blocked with 1 mg/ml BSA (Westburg) and 0.2 mg/ml fish sperm (Roche Applied Science, Basel, Switzerland)) for 1 hr at 4 °C. Per ChIP, the chromatin was precleared by incubation with blocked beads for 1 hr. After preclearing, an input sample was taken to control for the amount of DNA that used as input for the ChIP procedure. The remaining sample was divided into three samples, each incubated O/N at 4 °C under continuous rotation with either 6 µg of GR or MR- specific antibody or normal rabbit IgG (sc-8992, sc-11412, sc-2027; Santa Cruz Biotechnology). Subsequently, the antibody-bound DNA-fragments were isolated by incubating the samples with blocked protein A beads for 1 hr at 4 °C. The beads were washed 5 times in 1 ml washing buffer ($1\times$ low salt; $1\times$ high salt; $1\times$ LiCl; $2\times$ TE) after which they were incubated with 0.25 ml elution buffer (0.1 M $NaHCO_3$; 1% SDS) for 15 min (RT, continuous rotation) to isolate the DNA-protein complexes. To reverse crosslink the DNA-protein interactions, the samples were incubated O/N at 65 °C with 0.37 M NaCl. RNAse treatment (0.5 µg/250 µl) was performed for 1 hr at 37 °C

followed by purification of DNA fragments on Nucleospin columns (Macherey-Nagel). The immunoprecipitated samples were eluted in 50 μl elution buffer.

For sequencing, ChIP-samples treated with either IgG- or GR-antibody of rats that received 3,000 μg/kg CORT were prepared according to the protocol supplied with the Illumina Genome Analyser GA1. In brief, the DNA fragments were blunted and ligated to sequencing adapters after which the DNA was amplified for 18 rounds of PCR. The DNA was electrophoresed on a 2 % Agarose gel, of which a region containing DNA fragments 100–500 bp in length was excised and the DNA extracted with the Qiagen Gel Extraction Kit (Qiagen, Germany). DNA quality was checked on the Agilent Bioanalyser (Waldbronn, Germany). Single end sequencing of the first 35 bp of the resulting DNA library was performed on the Illumina Genome Analyser (Leiden Genome Technology Center, LUMC, Leiden University).

| | **ChIP** | |
	Forward primer (5′–3′)	**Reverse primer (3′–5′)**
myo	TAGTGTGCATCCAGCAGAGG	ACACTGTGGCCTTTTTGTCC
Afaf	AGAAAGTGTGTTTGTGGCCTTTGC	TCAGCAGTAATCACAGCCCACTCT
Nrxn1	AGAAGTCACAGCTCACAACAGAACG	AACTCACAGATGGCCCAATTCAACC
Ndnl2	TCTTCCTTCTTGGCTCCAGGTGA	TGTACATTTCCTCGTTCCAGATGGC
St3gal3	GCCTCCACCCGCCACAGAGA	AGGCAACAGGTGCTAGGCAACA
Lyst	AGCTGGGCTTTGCATGGTGGT	TGAACACACACGTAGGTGGGGC
Slc7a6	ACAAGCTCTGCCTGCTGCCAC	ATCCCCTGGGATCTCCCTCGGTT
Arpc2	CCCGCACATTGCCAGTTGCC	ACCCCCACAACCGCTCCAGA
Lifr	GCAAATGCCCAGGAGAGAGCCA	AACTGCAAAACTCGGGCGGA
Cacna2d3	TGCTGAAGGGGGAGGCTTGGT	TGGCAATACAGCTGGAGTGGTTTCA
Serp2	CAGGGACACACGCTCGGCTC	GGCTTGCAAGTCACGGGCCA
MT2a	AAAGTGATGCTTGGGCTGAG	AGGCAGGAAATGTGTTACCG
Per1_2	ACCCCCTTCAGGCTTTTGCG	GGCTGACATCACGACCGGCA
Ddit4	CTGTGGGTGAGCTGAGAACA	GGCCTGTAGGTCCAGCACTA
Klf9	ATCTAGGGCAGTTTGTTCAA	GGCAGGTTCATCTGAGGACA
Per1_1	GGAGGCGCCAAGGCTGAGTG	CGGCCAGCGCACTAGGGAAC

Table 4.4: ChIP primer sequences.

Table 4.5: MACS peak calling results.
online available at `https://goo.gl/OOOENR`

Table 4.6: Total list of significant GR-binding sites with associated genes.
online available at `https://goo.gl/OOOENR`

Chapter Five

Glucocorticoids modulate the mTOR pathway in the hippocampus: differential effects depending on stress history

J.A.E. Polman[1], R.G. Hunter[2], N. Speksnijder[1], J.M.E. van den Oever[1], O.B. Korobko[1], B.S. McEwen[2], E.R. de Kloet[1], N.A. Datson[1]

Chapter 5

*J.A.E.P. and R.G.H. contributed equally to this work.

[1] Division of Medical Pharmacology, Leiden/Amsterdam Center for Drug Research & Leiden University Medical Center, Leiden, the Netherlands
[2] Laboratory of Neuroendocrinology, The Rockefeller University, New York, USA

Gʟᴜᴄᴏᴄᴏʀᴛɪᴄᴏɪᴅ (GC) hormones, released by the adrenals in response to stress, are key regulators of neuronal plasticity. In the brain, the hippocampus is a major target of GC, with abundant expression of the GC receptor. GC differentially affect the hippocampal transcriptome and consequently neuronal plasticity in a subregion-specific manner, with consequences for hippocampal information flow and memory formation. Here, we show that GC directly affect the mammalian target of rapamycin (mTOR) signaling pathway, which plays a central role in translational control and has long-lasting effects on the plasticity of specific brain circuits. We demonstrate that regulators of the mTOR pathway, DNA damage-induced transcript (DDIT)4 and FK506-binding protein 51 are transcriptionally up-regulated by an acute GC challenge in the dentate gyrus (DG) subregion of the rat hippocampus, most likely via a GC-response element-driven mechanism. Furthermore, two other mTOR pathway members, the mTOR regulator DDIT4-like and the mTOR target DDIT3, are down-regulated by GC in the rat DG. Interestingly, the GC responsiveness of DDIT4 and DDIT3 was lost in animals with a recent history of chronic stress. Basal hippocampal mTOR protein levels were higher in animals exposed to chronic stress than in controls. Moreover, an acute GC challenge significantly reduced mTOR protein levels in the hippocampus of animals with a chronic stress history but not in unstressed controls. Based on these findings, we propose that direct regulation of the mTOR pathway by GC represents an important mechanism regulating neuronal plasticity in the rat DG, which changes after exposure to chronic stress.

5.1 Introduction

The hippocampus is a brain structure involved in cognitive processes and is a major target of glucocorticoid (GC) hormones, which are released by the adrenals in response to stress. Upon release, GC readily pass the blood-brain-barrier and target the GC receptor (GR), which is abundantly expressed throughout the brain and in particular in the hippocampus. GR is a ligand-inducible transcription factor and a member of the nuclear receptor family of transcription factors (Pratt, 1990). Due to its relatively low ligand affinity, most GR activation occurs at the circadian peak or during the stress response (Reul and de Kloet, 1985). Although nongenomic effects of GR exist (Johnson et al., 2005), GC effects on function and morphology of hippocampal neurons are to a large extent caused by transcriptional regulation of a wide repertoire of genes that play a central role in plasticity, energy metabolism, response to oxidative stress, and survival of hippocampal neurons (Magarinos et al., 1996; Tsolakidou et al., 2008).

GC are key regulators of neuronal plasticity and have profound effects on hippocampal function and viability. Hippocampal synaptic plasticity, a process fundamental to hippocampus-dependent learning and memory, is clearly affected by acute stress and concomitant GR activation and persists for hours after stress exposure (Howland and Wang, 2008; Kim et al., 2006). Acute stress and high concentrations of GC increase calcium current amplitude and impair long-term potentiation (LTP) in both hippocampal cornu ammonis (CA)1 and CA3 cell fields (Joels et al., 2003). Although the dentate gyrus (DG) region seems less sensitive to the effects of acute stress with respect to functional properties such as calcium current amplitude and α-amino-3-hydroxy-5-methyl-4-isoxazolepropionic acid (AMPA) receptor-mediated synaptic responses (Gemert Van et al., 2009; Joels et al., 2003), acute stress decreases new cell proliferation rate and increases apoptosis in the rat DG (Heine et al., 2004).

Like acute stress, chronic stress also affects hippocampal structure and function. Repeated stress causes remodeling of dendrites in the CA3 region (Magarinos et al., 1996; Sousa et al., 2000; Vyas et al., 2002; Watanabe et al., 1992). In the DG, chronic stress has effects on cell turnover of DG neurons and progenitor cells in the subgranular zone, where chronic stress suppresses both apoptosis and neurogenesis (Gould et al., 1997; Heine et al., 2004; Magarinos et al., 1996). After chronic stress exposure, synaptic excitation of DG cells may be enhanced when GC levels rise. This enhanced synaptic flow could contribute to enhanced excitation of projection areas of the DG, most notably the CA3 hippocampal region (Karst and Joels, 2003).

An important signaling pathway in the hippocampus is the mammalian target of rapamycin (mTOR) pathway, which plays a central role in translational control and long-lasting synaptic plasticity (Hoeffer and Klann, 2010). The mTOR pathway

integrates signals from nutrients, growth factors, and information on energy status to regulate many processes, including cell growth, cell proliferation, cell motility, and cell survival (Swiech et al., 2008; Wu et al., 2009). In neurons, the mTOR pathway modulates local translation of proteins at the synapse and therefore is critical for different forms of synaptic plasticity, including LTP and long-term depression (LTD) (Bekinschtein et al., 2007; Tang et al., 2002). Dysregulation of this pathway is a common hallmark in a wide variety of brain disorders, including autism, brain tumors, tuberous sclerosis, and neurodegenerative disorders, such as Parkinson's, Alzheimer's, and Huntington's disease (Akhavan et al., 2010; Bourgeron, 2009; Malagelada et al., 2008; Mozaffari et al., 2009; Pei and Hugon, 2008; Williams et al., 2008).

Although it is known that the mTOR pathway is subject to regulation by GC in the periphery (Shah et al., 2000c; Shah et al., 2000b; Wang et al., 2006a), so far little is known whether this also is the case in the brain. Two recent studies showed an inhibitory effect of GC on mTOR signaling in rat hypothalamic organotypic cultures and mouse cortical primary cultures (Howell et al., 2011; Shimizu et al., 2010), but to our knowledge, this has not been shown *in vivo* in the brain. In this study, we used an integrated genomics approach consisting of *in silico* predictions of GR binding sites, DNA microarrays, and chromatin immunoprecipitation (ChIP), to investigate whether the mTOR pathway is regulated by GC *in vivo* in the hippocampus. Here, we present data demonstrating that key regulators of the mTOR pathway, DNA damage-induced transcript (DDIT)4 [also known as regulated in development and DNA damage responses (REDD)1], FK506-binding protein 51 (FKBP51), DDIT4-like (DDIT4L) [also known as REDD2], and mTOR target DDIT3 (also known as CCAAT-enhancer-binding proteins homologous protein 3 or CHOP are regulated by GC in the DG subregion of the hippocampus. Interestingly, the GC regulation of DDIT4 and DDIT3 transcription as well as hippocampal mTOR protein levels after an acute GC challenge are differentially affected in animals previously exposed to chronic stress compared with controls. Based on these findings, we propose that direct regulation of the mTOR pathway by GC represents an important mechanism underlying GC effects on neuroplasticity in the brain, with different outcomes depending on previous stress history.

5.2   Materials and Methods

Experimental groups and collection of tissue

Animal experiments were performed to measure effects on the mTOR pathway at multiple levels, including DNA binding and effects on mRNA and protein levels. Because in the temporal sequence of events DNA binding precedes effects on transcription, which ultimately translate into effects at the protein level, different time

points were chosen depending on the parameter of interest. DNA binding was quantified at $t = 1$ h, mRNA changes at $t = 3$ h, and protein levels at $t = 5$ h.

For microarray analysis, male Sprague Dawley rats of 70 d of age (Charles River, Kingston, NY) were either handled for 21 d (control) or subjected to chronic restraint stress (CRS) for 6 h a d during 21 d (Hunter et al., 2009). On d 22, half of the rats received a challenge, which consisted of an injection with corticosterone (CORT) (sc 5 mg/kg, in propylene glycol), and were killed 3 h later. The other half of the rats (control and CRS) were not challenged. Therefore, these rats were left undisturbed and did not receive a vehicle injection to avoid eliciting a stress response. The unchallenged rats were killed at the same time point as the injected rats. This resulted in four experimental groups (all $n = 6$) for the microarray analysis: 1) control, 2) control + CORT, 3) CRS, and 4) CRS + CORT. After decapitation, brains were rapidly dissected and snap frozen in isopentane (cooled in ethanol placed on pulverized dry ice) and stored at -80 °C for later use.

The experiment was repeated as described above ($n = 8$ per group) to determine effects of CRS and CORT challenge on mTOR protein levels using Western blot analysis, with the difference that the rats were killed 5 h after the CORT challenge on d 22. Hippocampi were immediately removed from the brain and processed for Western blot analysis (see below).

In a separate experiment, body weight and relative thymus weight were determined in control and CRS animals as a bioassay reflecting CORT exposure over the 21 d period. A clear decrease in body weight gain and relative thymus weight was observed upon CRS (Figure 5.6). Animal care was conducted in accordance with the Rockefeller University Animal Care Committee.

For ChIP analysis, male Sprague Dawley rats of 70 d of age (Harlan, Horst, The Netherlands) were adrenalectomized (ADX) as described before to completely deplete endogenous CORT levels and ensure that there was no GR bound to the DNA (Sarabdjitsingh et al., 2010a). Three days after ADX, one group of animals received an ip injection with 3 mg/kg CORT-hydroxypropyl-cyclodextrin complex, whereas the other group was left undisturbed ($n = 6$ per group). All animals were decapitated after 1 h for ChIP. Immediately after decapitation, the hippocampi were isolated and further processed for ChIP (see below). CORT levels in the blood 2 d after ADX and at the moment of decapitation were measured by RIA, showing that both the ADX operation was successful as well as a significant increase in CORT 3 h after injection (data not shown). Experiments were approved by the Local Committee for Animal Health, Ethics, and Research of the University of Leiden (Dier Experimenten Commissie nos. 06055 and 10044). Animal care was conducted in accordance with the European Commission Council Directive of November 1986 (86/609/EEC).

Microarray analysis

CA3 and DG subregions were isolated by laser microdissection from coronal brain sections (8 µm) containing the rostral rat hippocampus as previously described

Chapter 5

(Datson et al., 2004). RNA was isolated using TRIzol (Invitrogen, Carlsbad, CA), linearly amplified for two rounds, and hybridized to Rat Genome 230 2.0 Arrays (Affymetrix, Santa Clara, CA) containing 31,099 probe sets representing over 28,000 well-substantiated rat genes. Hybridizations were conducted at the Leiden Genome Technology Center (Leiden University), according to the manufacturer's recommendations (Affymetrix). MAS 5.0 normalization of microarray data was performed in BRB-Array Tools version 3.7.0, an integrated package for the visualization and statistical analysis of DNA microarray gene expression data that operates as an add-in to Microsoft Excel (Simon et al., 2007). Normalized data were subsequently subjected to statistical analysis using Linear Models for Microarray Data (Smyth, 2005), a package for the R computing environment that allows multiple comparison of experimental groups. Differences in gene expression between groups were evaluated using two-way ANOVA with group and treatment as factors, followed by pairwise *post hoc* comparisons. Genes with $P \leq 0.05$ were considered significant. An extensive list of mTOR pathway members was assembled based on literature and checked for representation on the Affymetrix Rat Genome 230 2.0 Array.

Chromatin immunoprecipitation

Immediately after decapitation, the hippocampal tissue was chopped into pieces of approximately $1\,\mathrm{mm}$ and fixed in $1\,\%$ formaldehyde for $15\,\mathrm{min}$ under continuous rotation. Cross-linking was stopped by adding $0.125\,\mathrm{M}$ glycine for $5\,\mathrm{min}$. Subsequently, the tissue was washed three times with PBS and once with PBS containing protease inhibitors (PI). Pellets were snap frozen and stored at $-80\,°\mathrm{C}$.

Defrosted pellets were homogenized for 2×10 sec in $0.5\,\mathrm{ml}$ of mild lysis buffer [$10\,\mathrm{mm}$ Tris-HCl (pH 7.5), $10\,\mathrm{mm}$ NaCl, and $0.2\,\%$ Nonidet P-40] supplemented with PI using the Bio-Gen PRO200 homogenizer. After centrifugation, the pellets were dissolved in $0.6\,\mathrm{ml}$ of PI-containing radioimmunoprecipitation assay buffer [$0.1\,\%$ sodium dodecyl sulfate, $1\,\%$ deoxycholate, $150\,\mathrm{mm}$ NaCL, $10\,\mathrm{mm}$ Tris (pH 8.0), $2\,\mathrm{mm}$ EDTA, $1\,\mathrm{mm}$ NaVO$_3$, $1\,\%$ Nonidet P-40, β-glycerolphophate, and Na-butyrate] and incubated on ice for 30 min. Subsequently, the chromatin was sheared (20 pulses of 30 sec., 200 W; Bioruptor, Diagenode, Liège, Belgium), resulting in chromatin fragments of $100–500\,\mathrm{bp}$, and stored at $-80\,°\mathrm{C}$.

Sepharose A beads (GE Healthcare, Princeton, NJ) were blocked with $1\,\mathrm{mg/ml}$ bovine serum albumin (Westburg, Leusden, The Netherlands) and $0.2\,\mathrm{mg/ml}$ fish sperm (Roche Applied Science, Basel, Switzerland) for $1\,\mathrm{h}$ at $4\,°\mathrm{C}$. Two ChIPs each were performed on the same batch of hippocampal chromatin derived from three different animals. Per ChIP, the chromatin was precleared by incubation with blocked beads for $1\,\mathrm{h}$. After preclearing, an input sample was taken to control for the amount of DNA used as input for the ChIP procedure. The remaining sample was divided into two samples, each incubated overnight (O/N) at $4\,°\mathrm{C}$ under continuous rotation with either $6\,\mu\mathrm{g}$ of GR-specific H300 or normal rabbit IgG (Santa Cruz Biotechnology, Inc., Santa Cruz, CA). Subsequently, the antibody-bound DNA

fragments were isolated by incubating the samples with blocked protein A beads for 1 h at 4 °C. The beads were washed five times in 1 ml of washing buffer (1× low salt, 1× high salt, 1× LiCl, and 2× Tris-EDTA), followed by incubation with 0.25 ml of elution buffer (0.1 M NaHCO$_3$ and 1 % sodium dodecyl sulfate) for 15 min (room temperature, continuous rotation) to isolate the DNA-protein complexes. To reverse cross-link the DNA-protein interactions, the samples were incubated O/N at 65 °C with 0.37 M NaCl. RNAse treatment (0.5 µg/250 µl) was performed for 1 h at 37 °C followed by purification of DNA fragments on Nucleospin columns (Macherey-Nagel, Düren, Germany). The immunoprecipitated samples were eluted in 50 µl of elution buffer.

Western blot analysis

Hippocampal tissue was homogenized in radioimmunoprecipitation assay buffer with PI (04693124001; Roche Applied Science). Total protein concentration was measured by bicinchoninic acid assay according to the manufacturer's protocol (no. 23225, BCA Assay kit; Thermo Scientific, Rockford, IL). Electrophoresis of 20 µg of protein per sample was performed on a precast 4–20 % gradient gel (no. 456–1096; Bio-Rad Laboratories, Inc., Hercules, CA) and transferred O/N at 4 °C to Immobilon-P Transfer membrane (Millipore Corp., Billerica, MA). Primary antibody for mTOR (no. 2972; Cell Signaling Technology, Beverly, MA) was diluted 1:5000 and incubated O/N at 4 °C. Secondary antibody (goat antirabbit IgG horseradish peroxidase, no. 2054; Santa Cruz Biotechnology, Inc.) was incubated for 1 h at room temperature. Blots were exposed to ECL Hyperfilm (Amersham Biosciences, Buckinghamshire, UK) for 30 sec and scanned using an Epson V350 photo scanner (Epson, Long Beach, CA). Protein levels were quantified using ImageJ version 1.42. Signals were normalized against α-tubulin. Two-way ANOVA with group and treatment as factors was used to determine whether there were any significant differences, followed by pairwise *post hoc* comparisons. Significance was accepted at $P \leq 0.05$.

In silico GC response element (GRE) prediction

GenSig, an *in silico* screening method that uses a position weight matrix based on 44 published GREs, was used to identify evolutionary conserved GREs in the coding regions and a region 50 kb up- and downstream of the DDIT3 and DDIT4L genes (Simon et al., 2007; Datson et al., 2011). For DDIT4 and FKBP51, we had previously identified GREs and shown that GR binds to these sequences *in vivo* in the hippocampus (Simon et al., 2007; Datson et al., 2011).

Real-time quantitative PCR (RT-qPCR)

RT-qPCR was performed to validate the microarray results for the selected mTOR signaling genes. For mRNA analysis, cDNA was synthesized from the same experi-

Probe Set ID	Gene Symbol	Gene Title	ANOVA P-value	Control + CORT FC	Control + CORT P-value	Stress + CORT FC	Stress + CORT P-value
1369590_a_at	*Ddit3*	DNA damage-inducible transcript 3	5.5E−03	0.6	2.2E−03	NS	NS
1368025_at	*Ddit4*	DNA damage-inducible transcript 4	NS	1.9	3.0E−02	NS	NS
1368013_at	*Ddit4l*	DNA damage-inducible transcript 4 like	1.9E−08	0.3	1.8E−07	0.4	8.4E−06
1380611_at	*Fkbp5*	FK506-binding protein 5	8.6E−06	2.0	1.3E−04	2.0	1.7E−04
1388901_at	*Fkbp5*	FK506-binding protein 5	8.0E−11	2.0	5.0E−09	2.0	1.4E−08

Table 5.1: CORT regulation of the mTOR-associated transcripts.
CORT regulation of the mTOR-associated transcripts DDIT4, FKBP51, DDIT4L, and DDIT3 is indicated in control animals (*left*) and in animals with a recent history of CRS (*right*). The fold change (FC) is shown, in which *numbers* above 1 indicate an up-regulation and below 1 a down-regulation by acute CORT. $P > 0.05$ is considered not to be significant (NS).

mental RNA samples that were used for microarray analysis, using the iScript cDNA synthesis kit (Bio-Rad Laboratories, Inc.), according to manufacturer's instructions. PCR was conducted using the capillary-based LightCycler thermocycler and Light-Cycler FastStart DNA MasterPLUS SYBR Green I kit (Roche Applied Science) according to manufacturer's instructions. All PCR reactions on cDNA were performed in duplo, and obtained threshold cycle values were all between 12 (Tubulin beta-2A chain) and 19–25 (mTOR signaling genes). The standard curve method was used to quantify the expression differences (Smyth, 2005). cDNA values were normalized against Tubb2a expression levels and analyzed with GraphPad Prism 5 (GraphPad Software, Inc., San Diego, CA). Two-way ANOVA with group and treatment as factors was used in combination with *post hoc* testing to assess significant differential expression of GC-responsive genes. Significance was accepted at $P < 0.05$.

GR binding to predicted evolutionary conserved GREs in the vicinity of DDIT3, DDIT4, DDIT4L, and FKBP51 was validated using RT-qPCR on immunoprecipitated chromatin. All threshold cycle values ranged from 25 to 32. The ChIP PCR signal was normalized by subtracting the amount of nonspecific binding of the IgG antibody in the same sample. A further normalization for background noise was performed by subtracting the signal obtained at a nonbound GR region (exon 2 of the myoglobin gene). Metallothionein 2A, which has two well-documented GREs (Kelly et al., 1997), served as a positive control for the ChIP. Control genes metallothionein 2A and myoglobin were measured twice by RT-qPCR in both ChIPs. The hypothesized GREs were measured once per ChIP. Normalized data were analyzed with GraphPad Prism 5. An unpaired two-tailed t test was used to assess significant GR binding. Significance was accepted at a $P < 0.05$.

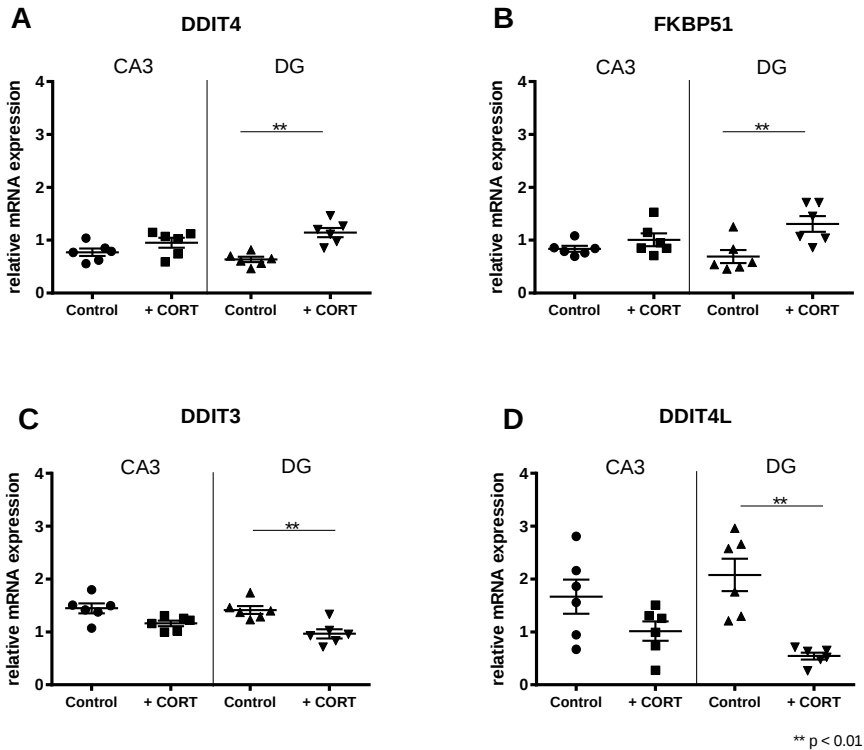The primer sequences for microarray and ChIP validation are listed in Table 5.2.

Figure 5.1: RT-qPCR validation of expression levels in control animals before and after GC challenge for DDIT4 (A), FKBP51 (B), DDIT3 (C), and DDIT4L (D).
RT-qPCR expression values were normalized against TUBB2a. *Each point in the graph* represents the expression of one animal. *Asterisks* indicate statistical significance: *, $P < 0.05$; **, $P < 0.01$.

5.3   Results

GC affect the expression of mTOR regulators in the hippocampus

Microarray analysis of mRNA expression in the rat hippocampal DG revealed differential expression of several mTOR regulators (FKBP51, DDIT4, and DDIT4L) and the mTOR target DDIT3 3 h after a CORT injection (Table 5.1). Both DDIT4 and FKBP51 were significantly up-regulated in the DG, whereas DDIT3 and DDIT4L were down-regulated. RT-qPCR confirmed the subregional differences in GC responsiveness of three out of four mTOR-associated transcripts (Figure 5.1).

According to the microarray analysis, none of these mTOR regulators were significantly affected by CORT in the CA3 region of the hippocampus at the applied

threshold of significance. However, according to RT-qPCR, DDIT3 was also GC responsive in CA3 ($P = 0.026$), albeit to a lesser extent than in the DG.

mRNA expression of mTOR itself and of other mTOR regulators such as v-akt thymoma viral proto-oncogene 1, tuberous sclerosis protein 1 and 2, regulatory associated protein of mTOR, rapamycin-insensitive companion of mTOR, and phosphatidylinositol 3 kinase were not differentially expressed in either the DG or the CA3 subregion of the hippocampus according to microarray analysis. A total of four other mTOR pathway members were expressed at significantly different levels between the groups according to ANOVA, of which two were differentially expressed in response to GC challenge both in control and in CRS animals: ribosomal protein S6 kinase polypeptide 2 and insulin receptor (Table 5.3).

FKBP51 and DDIT4 are primary targets of the GR in rat hippocampus

Using a position weight matrix based on 44 published GREs, we previously identified and confirmed GR binding to three evolutionary conserved GREs in the FKBP51 gene and a GRE 20 kb upstream of DDIT4 (Table 5.4) (Simon et al., 2007; Datson et al., 2011). Here, we replicated this finding in an independent experiment and confirmed GR binding to FKBP51_1 (one of the three GREs for FKBP51 that we selected) and the GRE near DDIT4 (Figure 5.2). Based on the GR binding to the GREs and their CORT-induced up-regulation, we conclude that FKBP51 and DDIT4 are primary targets of GR*in vivo* in the rat hippocampus and are most likely regulated by the transactivation mode of action of GR induced by GR-GRE interaction (Datson et al., 2011; Simon et al., 2007).

We used the same approach to screen for GREs in the vicinity of DDIT3 and DDIT4L, resulting in the identification of evolutionary conserved GRE-like sequences at 2,586 bp (DDIT3) and 2,199 bp (DDIT4L) downstream of the transcription start site of both genes (Table 5.4). However, we did not find GR binding to these predicted GREs associated with DDIT3 and DDIT4L under the given conditions.

GC effects on the mTOR pathway are modulated by previous chronic stress exposure

Because chronic stress is known to affect hippocampal synaptic plasticity, we were interested whether having experienced chronic stress shortly before receiving a CORT challenge would affect the pattern of GC regulation of the mTOR regulators and target. Interestingly, in animals with a previous history of CRS, the GC regulation of DDIT4 and DDIT3 in the DG was lost, whereas that of FKBP51 and DDIT4L was maintained (Table 5.1 and Figure 5.3). According to the microarray data, no GC regulation of any of the mTOR-associated genes was observed in the CA3 region in the CRS rats (data not shown).
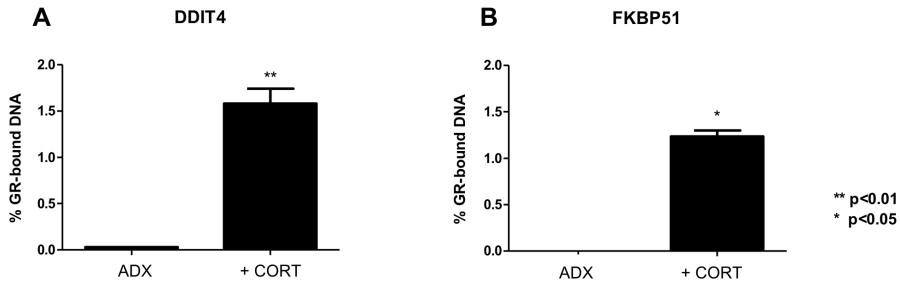
Figure 5.2: GR binding to the *in silico* predicted GREs in total hippocampus at 60 min after an ip injection of 3 mg/kg CORT.
GR binding is shown to the GRE associated with (A) DDIT4 and (B) FKBP51. The y-axis shows the percentage of input DNA that was bound by the GR. *Columns* represent average binding of two independent ChIP experiments each containing brain tissue of three different animals. The *error bars* equal sem. *Asterisks*indicate statistical significance: *, $P < 0.05$; **, $P < 0.01$.
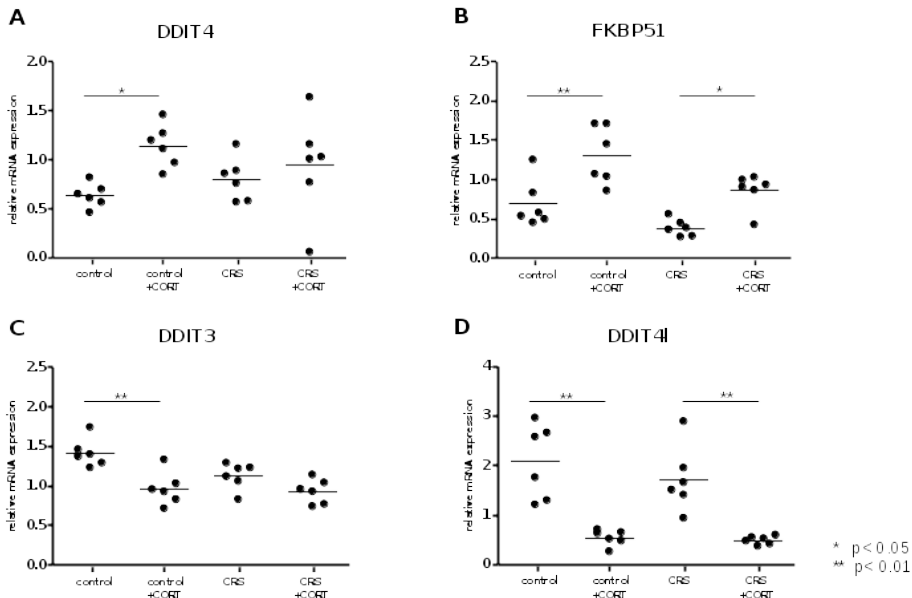

Figure 5.3: RT-qPCR indicating expression levels of DDIT4 (A), FKBP51 (B), DDIT3 (C), and DDIT4L (D) with and without an acute GC challenge in control animals and animals with a previous history of stress.
The GC responsiveness of DDIT3 and DDIT4 is lost in animals previously exposed to chronic stress. RT-qPCR expression values were normalized against TUBB2a. *Each point in the graph* represents the expression of one animal. *Asterisks*indicate statistical significance: *, $P < 0.05$; **, $P < 0.01$.

Chapter 5

117
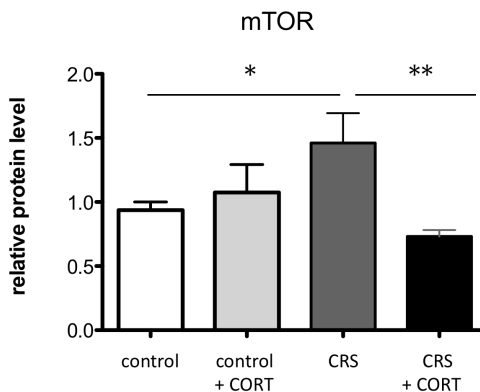
Figure 5.4: mTOR protein levels in the hippocampus measured by Western blotting.
mTOR protein levels were normalized against α-tubulin expression levels. Two-way ANOVA indicated that CORT had a significant effect on mTOR $F(1, 28)$ 4.200; $P = 0.050$. In addition, there was a strong group-treatment interaction [$F(1, 28)$ 11.667; $P = 0.002$], indicating that CORT has significantly different effects on hippocampal mTOR protein levels in control and stress animals. *Asterisks* indicate statistical significance: *, $P < 0.05$; **, $P < 0.01$.

Hippocampal mTOR protein levels are differentially affected by acute GR activation depending on previous stress history

Based on the observation that in CRS animals, the GC regulation of DDIT4 and DDIT3 in the DG was lost, we were curious to determine the overall effect this would have on mTOR protein levels. Therefore, we quantified basal mTOR protein levels and levels 5 h after GR activation by an acute GC injection in control and CRS rats (Figure 5.4). Data were subjected to a two-way ANOVA with the factors group: control and CRS treatment, no treatment, and CORT. In addition, a *post hoc* test was applied to identify statistical significance between the four conditions. CORT had a significant effect on hippocampal mTOR protein levels [main effect of treatment, $F(1, 28)$ 4.200; $P = 0.050$]. In addition, there was a significant group-treatment interaction [$F(1, 28)$ 11.667; $P = 0.002$], indicating that the CORT challenge had significantly different effects on hippocampal mTOR protein levels in control and CRS groups. In other words, giving an acute GC challenge had no effect on mTOR protein levels in the hippocampus of control animals ($P = 0.559$). However, in animals with a previous history of stress, an acute GC challenge resulted in a significant reduction in hippocampal mTOR protein ($P = 0.004$) (Figure 5.4). Without treatment, the stress group had significantly higher mTOR levels than the control group ($P = 0.032$).

5.4 Discussion

Here, we show that regulators of the mTOR pathway are targets of GC stress hormones in the hippocampal DG and to a lesser extent in CA3 pyramidal neurons. Furthermore, we demonstrate that the action of GC on the expression of mTOR pathway members as well as on hippocampal mTOR protein levels is context dependent and is highly sensitive to chronic stress.

GC as regulators of mTOR signaling in the brain

The mTOR pathway is a dynamically regulated system and has many upstream regulators that confer information from the extracellular environment to the cell. So far, not much is known on the extracellular signals that lead to mTOR activation in the brain. Several neuronal surface receptors, including N-methyl-D-aspartate receptors, dopaminergic, and metabotropic glutamate receptors as well as brain-derived neurotrophic factor, implicated in induction and maintenance of LTP and LTD, are known to influence mTOR function upon activation (Hoeffer and Klann, 2010). Although GC have been shown to repress mTOR signaling in several cell types, including lymphoid cells, skeletal muscle, hypothalamic organotypic cultures, and primary cortical neurons, to our knowledge, this has not been shown before *in vivo* in the brain (Howell et al., 2011; Shimizu et al., 2010; Wang et al., 2006a; Yan et al., 2006).

One of the proteins that is regulated by GC in the hippocampus is DDIT4 (or REDD1), which is known to inhibit mTOR activity, resulting in an increase in apoptosis in mouse embryonic fibroblasts (Corradetti et al., 2005; Ellisen et al., 2002). DDIT4L (or REDD2), which is approximately 50% homologous to DDIT4, has also been found to inhibit mTOR signaling after GC stimulation in human embryonic kidney 293 and Chinese hamster ovary cells (Corradetti et al., 2005). This indicates that DDIT4 and DDIT4L are able to reduce cell proliferation and plasticity by inhibiting mTOR-mediated synthesis of proteins.

FKBP51 acts as a scaffolding protein decreasing v-akt thymoma viral proto-oncogene 1 functioning, resulting in decreased mTOR signaling and increased cell death (Pei et al., 2009; Pei et al., 2010). Interestingly, FKBP51 is one of the cochaperones involved in the nuclear signaling of GR and plays a role in GR sensitivity and regulation of the hypothalamic-pituitary-adrenal axis. Polymorphisms in FKBP51 have been associated with differences in GR sensitivity and GC stress response (Binder, 2009; Schiene-Fischer and Yu, 2001; Vermeer et al., 2003). Variations in the gene have been associated with increased recurrence of depression and with rapid response to antidepressant treatment (Binder et al., 2004). In particular, alleles associated with enhanced expression of FKBP51 after GR activation may represent a risk factor for stress-related psychiatric disorders (Binder, 2009).

DDIT3 (or CCAAT-enhancer-binding proteins homologous protein 3 or CHOP3) is a proapoptotic transcription factor that responds to availability of key nutrients,

such as amino acids, glucose, and lipids, and to endoplasmatic reticulum stress. DDIT3 is regulated by the mTOR pathway as well as by the activating transcription factor family and affects the expression of cell survival and death pathways (Chen et al., 2010; Di Nardo A. et al., 2009; Oyadomari and Mori, 2004).

Here, we present data that imply a fundamental and essential role of GC in regulating the mTOR pathway in the hippocampus, by transcriptionally regulating several mTOR pathway members. The GC regulation of mTOR pathway members was more robust in the DG than in the CA3. The relative lack of GR expression in CA3 (Van Eekelen et al., 1987) may explain the difference in degree of GC regulation of the mTOR pathway between both subregions. However, differences in GR expression are only one of the many fundamental differences in molecular architecture between the different subregions of the hippocampus, as we and others have previously shown (Datson et al., 2004; Datson et al., 2008; Greene et al., 2009; Lein et al., 2004).

GC responsiveness of FKBP51 and DDIT4 occurs via GR binding to GRE

In line with our findings, DDIT4 and FKBP51 were previously reported to be GC responsive and to contain potential GREs in their vicinity (Paakinaho et al., 2010; So et al., 2007). DDIT4 was originally identified to be responsive to dexamethasone treatment in T-cell lymphoma cell lines and thymocytes (Wang et al., 2003). Because treatment of these cells with the GR antagonist RU486 inhibited the induction of DDIT4, regulation via GR seemed likely. Indeed, in a ChIP-sequencing study, in which A549 cells (human lung adenocarcinoma epithelial cell line) were screened for GR-binding sites after dexamethasone stimulation, DDIT4 was found to be a primary GR target (So et al., 2007). Analysis of the GR-binding region revealed a GRE-like sequence, which is identical to the region that we have previously identified (Simon et al., 2007; Datson et al., 2011). Here, we demonstrate that DDIT4 is a primary target of the GR in the rat hippocampus.

In case of FKBP51, GREs surrounding the gene have also been studied extensively in A549 cells (Paakinaho et al., 2010). We recently predicted three evolutionary conserved GREs surrounding FKBP51 and showed that all three are bound by GR in the hippocampus (Simon et al., 2007; Datson et al., 2011). One of these (FKBP51_3) is a previously undescribed GRE and might be a specific GR target *in vivo* in the brain. This is of particular interest, given that polymorphisms in FKBP51 have been implicated as risk factors for several stress-related brain disorders, such as depression and posttraumatic stress disorder (Binder, 2009; Gillespie et al., 2009; Yehuda et al., 2009).

DDIT3 and DDIT4L are GC responsive but not GRE driven

DDIT3 and DDIT4L do not appear to be primary targets of GR in the rat brain, based on the fact that we did not find evidence of GR binding to the predicted GREs in the brain regions under the applied conditions. Consequently, we cannot fully exclude that these GREs might be bound by GR in a different time frame or in other tissues. However, given that both genes are down-regulated by GC in the DG, it seems more likely that they are regulated via the transrepression mode of action of GR, inhibiting the action of key transcription factors controlling DDIT3 and DDIT4L expression. Alternatively, they may be downstream secondary targets of GR, regulated by an intermediate GC-responsive transcription factor (Morsink et al., 2006a). DDIT3 is known to be a target of mTOR, but can also be regulated by the activating transcription factor family (Lein et al., 2004). Finally, a remote possibility is that the history of ADX has resulted in chromatin remodeling, shielding the GREs from GR binding. Chromatin remodeling has been postulated to occur as a consequence of GC pulsatility (Conway-Campbell et al., 2012) and aberrant GC exposure (Zhang et al., 2011).

What is the consequence of mTOR regulation by GC for the hippocampus?

In this study, we found opposing effects of GC injections on expression levels of mTOR regulators in control animals, *i.e.* up-regulation of DDIT4 and FKBP51 but down-regulation of DDIT4L, making it hard to predict *a priori* what the overall effect on mTOR protein levels would be. The opposing effects on mTOR regulators identified in the current study may represent a mechanism by which GC can fine-tune the overall outcome on mTOR signaling (Figure 5.5). A careful balance between mTOR inhibition and activation is essential to maintain neuronal health and function and prevent brain disease. For example, aberrant mTOR activation is a hallmark of brain tissue from rats with chronic seizures (Huang et al., 2010), but at the same time, mTOR is activated in the rat hippocampus during spatial learning (Qi et al., 2010) and is required for memory consolidation by controlling the increase of synaptic glutamate receptor 1 (Slipczuk et al., 2009).

Despite the GC-induced changes in expression of mTOR regulators in the DG after an acute challenge with GC, no change in mTOR protein was observed in the hippocampus of control animals, suggesting that a change in expression of mTOR regulators may be necessary to maintain the mTOR balance in the hippocampus.

Stress history changes GC responsiveness of the mTOR pathway

An interesting observation in this study is that chronic stress exposure had profound effects on the mTOR pathway. Chronic stress not only increased basal mTOR protein levels in the hippocampus but also abolished the GC responsiveness of
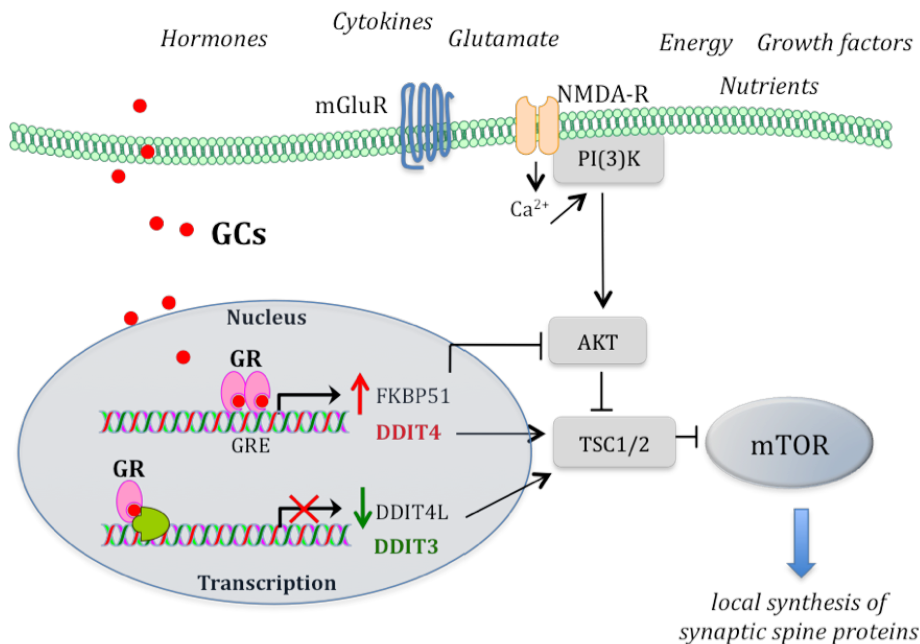
Chapter 5

Figure 5.5: Schematic overview of key components of the mTOR pathway and a number of its physiological and molecular regulators in the brain, indicating a role for GC.
After GC binding to GR, FKBP51 and DDIT4 are up-regulated by a GRE-driven mechanism, whereas DDIT4L and DDIT3 are down-regulated via a non-GRE-driven mechanism. These mTOR regulators will influence the overall levels of mTOR, with consequences for local synthesis of synaptic spine proteins and thus for synaptic plasticity. PI3K, Phosphatidylinositol 3 kinase; AKT, v-akt thymoma viral protooncogene 1; NMDA-R, N-methyl-D-aspartate receptor; GluR, glutamate receptor; TSC1/2, tuberous sclerosis protein 1/2.

DDIT4 and DDIT3 in the DG. Moreover, an acute GC challenge was associated with a significant reduction in hippocampal mTOR protein levels.

Chronic stress has well-described effects on hippocampal structure and function, *i.e.* dendritic remodeling in CA3 (Magarinos et al., 1996; Sousa et al., 2000; Vyas et al., 2002; Watanabe et al., 1992) and suppression of apoptosis and neurogenesis in the DG (Gould et al., 1997; Heine et al., 2004; Magarinos et al., 1996). However, some of the changes in hippocampal function after chronic stress are not obvious under baseline conditions and only become apparent when GR is subsequently activated, such as the enhanced synaptic excitation of DG cells with respect to α-amino-3-hydroxy-5-methyl-4-isoxazolepropionic acid (AMPA) receptor-mediated synaptic responses in the DG (Karst and Joels, 2003). Local chromatin remodeling differentially affecting the transcriptional potential of individual genes and consequently the altered response to a subsequent GR activation may underlie both the enhanced synaptic excitability as well as the changes in GC regulation of mTOR pathway members in the DG after chronic stress. Indeed, CRS was recently shown to affect histone methylation patterns, resulting in changes in chromatin structure and conse-

quently changes in transcriptional potential (Hunter et al., 2009). These findings may explain why the GC responsiveness of DDIT4, a primary GR target driven by a classical GRE, is lost after CRS. For DDIT3, the mechanism is less clear, because we do not know whether it is a primary GR target via transrepression, a secondary target via an intermediate GC-responsive transcription factor, or a target gene of the mTOR pathway that is indirectly affected by GC. Future studies are required to elucidate the precise mechanism.

We hypothesize a model in which acute and chronic stress have differential effects on mTOR signaling, with consequences for LTP, LTD, and other neuroplastic processes as well as for survival/resilience pathways. In our model, control animals have a healthy mTOR balance, leading to efficient LTP and neuroprotection, which is not compromised by exposure to an acute GC challenge. Our data show that in animals exposed to chronic stress, hippocampal mTOR levels are increased, whereas if these animals are subjected to an additional stressor in the form of an acute GC challenge, mTOR levels are decreased. We therefore speculate that exposure to chronic stress results in a more dynamic mTOR balance, making it difficult to maintain a healthy equilibrium upon subsequent challenge and tipping the mTOR signaling balance toward a decrease in LTP and an increase in cell death pathways. Whether the effects of chronic stress on the mTOR balance signify greater vulnerability to damage or better adaptation is unclear. Future studies are required to test this model.

Interestingly, activation of the mTOR signaling pathway in the prefrontal cortex was recently shown to underlie the antidepressant action of ketamine, a nonselective N-methyl-D-aspartate receptor antagonist (Li et al., 2010). Fast activation of mTOR signaling by ketamine resulted in a rapid increase of synapse-associated proteins and spine number in the prefrontal cortex. Conversely, mTOR inhibition has been reported to have neuroprotective properties and to delay neurodegeneration (Choi et al., 2010; Spilman et al., 2010). GC may be important regulators of this delicate balance between mTOR activation and inhibition in the brain, with different effects depending on the context, timing, and exposure of neurons (Du et al., 2009). An optimal balance of the mTOR pathway would promote LTP and memory formation, while at the same time promoting cell survival and resilience. Indeed, chronic stress exposure suppresses LTP in the DG (Alfarez et al., 2003; Bodnoff et al., 1995; Krugers et al., 2006) and enhances vulnerability of DG granule cells to cell death (Gemert van et al., 2006).

Chapter 5

5.5   Conclusion

The data presented here indicate that mTOR activity and the resulting translational processes it is involved in are regulated by GC in the rat brain. We show that GC regulate upstream mTOR regulators and that DDIT4 and FKBP51 are primary targets of GR in the hippocampus. Moreover, we demonstrate that the GC regulation of upstream mTOR regulators and downstream target DDIT3 differs between hippocampal subregions CA3 and DG, suggesting a key role of the mTOR pathway in the differential plasticity of these hippocampal subregions in response to acute GC exposure. Considering the fact that both GC and mTOR play an important role in neuroplasticity and neuronal survival (Bekinschtein et al., 2007; Swiech et al., 2008; Tang et al., 2002), we propose that GC play an important role in regulating the mTOR balance in the brain. Because GC regulation of mTOR regulators and mTOR protein levels is affected by a history of chronic stress, it would be of interest to further examine how these regulators are implicated in the pathogenesis of stress-related mental disorders.

Gene	mRNA Forward primer (5′–3′)	mRNA Reverse primer (3′–5′)	ChIP Forward primer (5′–3′)	ChIP Reverse primer (3′–5′)
Ddit3	CATGAACTGTTGGCATCACC	TGGAGATTACATGCTTGGCA	CCCCTTTCTCCACAGTGTTCCAGAA	AGCTGACTGGGAGGGTGGCTAA
Ddit4	TCTGAAAGGACCGAGCTTGT	ATAGCTGCCTCGAACAGGTC	CTGTGGGTGAGCTGAGAACA	GGCCTGTAGGTCAGCGACTA
Ddit4L	CACCCTGGGAGTCTGCTAAG	TTCAAACACCCTCGTTGA	GGTGTTTGAAGAGACAACATGCCAGA	TGAGACCCGCAGGACATCTTGG
FKBP5_1	AAGTGGCAAAGTGCCAG	TCCAGGCTCAGGGTGTGAAGA	TCAGCACCACGAGTTCATGT	CTGGTCACTGCAAAACATCATT
MT2	AAGCTGCTGTTCCTGCTGCC	TTGTGAGGACGCGCCCCACTTCA	AAAGTGATGCTTGGGCTGAG	AGGCAGGAAATGTGTTACCG
Myoglobin	AGCAGAGAACAGAGAGGGGAGCA	AAGCAGAGGCCACTTTGCACCT	TAGTGTGCATCCAGCAGAGG	ACACTGTGGCCTTTTGTCC

Table 5.2: Primer sequences for microarray and ChIP validation.

Probe Set ID	Gene Symbol	Gene Title	ANOVA P-value	Control + CORT		Stress + CORT	
				FC	P-value	FC	P-value
1368862_at	Akt1	v-akt murine thymoma viral oncogene homolog 1	NS	NS	NS	NS	NS
1375178_at	Akt1	V-akt murine thymoma viral oncogene homolog 1	NS	NS	NS	NS	NS
1383126_at	Akt1	V-akt murine thymoma viral oncogene homolog 1	NS	NS	NS	NS	NS
1372879_at	Akt1s1	AKT1 substrate 1 (proline-rich)	NS	NS	NS	NS	NS
1375117_at	Akt1s1	AKT1 substrate 1 (proline-rich)	NS	NS	NS	NS	NS
1375766_at	Akt1s1	AKT1 substrate 1 (proline-rich)	NS	NS	NS	NS	NS
1368832_at	Akt2	v-akt murine thymoma viral oncogene homolog 2	NS	NS	NS	NS	NS
1378425_at	Akt2	v-akt murine thymoma viral oncogene homolog 2	NS	NS	NS	NS	NS
1387353_at	Akt2	V-akt murine thymoma viral oncogene homolog 2	NS	NS	NS	NS	NS
1388765_at	Akt2	V-akt murine thymoma viral oncogene homolog 2	NS	NS	NS	NS	NS
1372874_at	Akt3	v-akt murine thymoma viral oncogene homolog 3	NS	NS	NS	NS	NS
1387592_at	Akt3	v-akt murine thymoma viral oncogene homolog 3	NS	NS	NS	NS	NS
1373837_at	Aktip	AKT interacting protein	NS	NS	NS	NS	NS
1385103_at	Aktip	AKT interacting protein	NS	NS	NS	NS	NS
1372243_at	Cab39	calcium binding protein 39	NS	NS	NS	NS	NS
1372244_at	Cab39	calcium binding protein 39	NS	NS	NS	NS	NS
1383341_at	Cab39l	calcium binding protein 39-like	NS	NS	NS	NS	NS
1369590_a_at	Ddit3	DNA-damage inducible transcript 3	5.5E−03	0.6	2.2E−03	NS	NS
1368025_at	Ddit4	DNA-damage-inducible transcript 4	9.1E−02	1.9	3.0E−02	NS	NS
1368013_at	Ddit4l	DNA-damage-inducible transcript 4-like	1.9E−08	0.3	1.8E−07	0.4	8.4E−06

Chapter 5

Probe Set ID	Symbol	Gene Title	ANOVA	Control + CORT		Stress + CORT	
1369621_s_at	Fkbp1a	FK506 binding protein 1a	NS	NS	NS	NS	NS
1398828_at	Fkbp1a	FK506 binding protein 1a	NS	NS	NS	NS	NS
1398829_at	Fkbp1a	FK506 binding protein 1a	NS	NS	NS	NS	NS
138061_at	Fkbp51	FK506 binding protein 5	8.6E−06	2.0	1.3E−04	2.0	1.7E−04
138901_at	Fkbp51	FK506 binding protein 5	8.0E−11	2.0	5.0E−09	2.0	1.4E−08
1371528_at	Fkbp8	FK506 binding protein 8	NS	NS	NS	NS	NS
1376070_at	Fkbp8	FK506 binding protein 8	NS	NS	NS	NS	NS
1371255_at	Hras	Harvey rat sarcoma virus oncogene	NS	NS	NS	NS	NS
1370333_a_at	Igf1	insulin-like growth factor 1	NS	NS	NS	NS	NS
1367652_at	Igfbp3	insulin-like growth factor binding protein 3	NS	NS	NS	NS	NS
1368681_at	Igfbp3	insulin-like growth factor binding protein 3	NS	NS	NS	NS	NS
1368424_at	Ikbkb	inhibitor of kappa light polypeptide gene enhancer in B-cells, kinase beta	NS	NS	NS	NS	NS
1397547_at	Ikbkb	Inhibitor of kappa light polypeptide gene enhancer in B-cells, kinase beta	NS	NS	NS	NS	NS
1369051_at	Insr	insulin receptor	NS	NS	NS	NS	NS
1392043_at	Insr	insulin receptor	4.5E−03	0.8	2.4E−02	0.7	9.4E−03
1369771_at	Irs1	insulin receptor substrate 1	NS	NS	NS	NS	NS
1369078_at	Mapk1	mitogen activated protein kinase 1	NS	NS	NS	NS	NS
1373426_at	Mapk1	mitogen activated protein kinase 1	NS	NS	NS	NS	NS
1398346_at	Mapk1	mitogen activated protein kinase 1	NS	NS	NS	NS	NS
1387771_a_at	Mapk3	mitogen activated protein kinase 3	NS	NS	NS	NS	NS
1389167_at	Mapkap1	mitogen-activated protein kinase associated protein 1	NS	NS	NS	NS	NS
1367963_at	Mlst8	MTOR associated protein, LST8 homolog (S. cerevisiae)	NS	NS	NS	NS	NS
1368019_at	Mtor	mechanistic target of rapamycin (serine/threonine kinase)	NS	NS	NS	NS	NS
1368079_at	Pdk1	pyruvate dehydrogenase kinase, isozyme 1	NS	NS	NS	NS	NS
1370052_at	Pdpk1	3-phosphoinositide dependent protein kinase-1	NS	NS	NS	NS	NS
1377895_at	Pik3ap1	phosphoinositide-3-kinase adaptor protein 1	NS	NS	NS	NS	NS
1378506_at	Pik3c2a	phosphoinositide-3-kinase, class 2, alpha polypeptide	NS	NS	NS	NS	NS
1379433_at	Pik3c2a	phosphoinositide-3-kinase, class 2, alpha polypeptide	NS	NS	NS	NS	NS
1385576_at	Pik3c2b	phosphoinositide-3-kinase, class 2, beta polypeptide	NS	NS	NS	NS	NS
1394770_at	Pik3c2b	phosphoinositide-3-kinase, class 2, beta polypeptide	NS	NS	NS	NS	NS
1369050_at	Pik3c2g	phosphoinositide-3-kinase, class 2, gamma polypeptide	NS	NS	NS	NS	NS
1369655_at	Pik3c3	phosphoinositide-3-kinase, class 3	NS	NS	NS	NS	NS

Probe Set ID	Symbol	Gene Title	ANOVA	Control + CORT	Stress + CORT
1374232_at	Pik3ca	phosphoinositide-3-kinase, catalytic, alpha polypeptide	NS	NS	NS
1379041_at	Pik3ca	phosphoinositide-3-kinase, catalytic, alpha polypeptide	NS	NS	NS
1382366_at	Pik3ca	phosphoinositide-3-kinase, catalytic, alpha polypeptide	NS	NS	NS
1389143_at	Pik3ca	phosphoinositide-3-kinase, catalytic, alpha polypeptide	NS	NS	NS
1393499_at	Pik3ca	phosphoinositide-3-kinase, catalytic, alpha polypeptide	NS	NS	NS
1396411_at	Pik3ca	phosphoinositide-3-kinase, catalytic, alpha polypeptide	NS	NS	NS
1373528_at	Pik3cd	phosphoinositide-3-kinase, catalytic, delta polypeptide	NS	NS	NS
1393755_at	Pik3cd	phosphoinositide-3-kinase, catalytic, delta polypeptide	NS	NS	NS
1370114_a_at	Pik3r1	phosphoinositide-3-kinase, regulatory subunit 1 (alpha)	NS	NS	NS
1370100_at	Pik3r2	phosphoinositide-3-kinase, regulatory subunit 2 (beta)	NS	NS	NS
1376190_at	Pik3r2	phosphoinositide-3-kinase, regulatory subunit 2 (beta)	NS	NS	NS
1369518_at	Pik3r3	phosphoinositide-3-kinase, regulatory subunit 3 (gamma)	NS	NS	NS
1389723_at	Pik3r4	phosphoinositide-3-kinase, regulatory subunit 4	NS	NS	NS
1374317_at	Pik3r6	Phosphoinositide-3-kinase, regulatory subunit 6	3.9E−02	NS	2.0E−02
1370529_a_at	Pld1	phospholipase D1	NS	NS	NS
1370530_a_at	Pld1	phospholipase D1	NS	NS	NS
1370531_a_at	Pld1	phospholipase D1	NS	NS	NS
1370532_at	Pld1	phospholipase D1	NS	NS	NS
1370679_at	Pld1	phospholipase D1	NS	NS	NS
1368954_at	Pld2	phospholipase D2	NS	NS	NS
1387384_at	Pld2	phospholipase D2	NS	NS	NS
1369104_at	Prkaa1	protein kinase, AMP-activated, alpha 1 catalytic subunit	NS	NS	NS
1394921_at	Prkaa1	protein kinase, AMP-activated, alpha 1 catalytic subunit	NS	NS	NS
1369654_at	Prkaa2	protein kinase, AMP-activated, alpha 2 catalytic subunit	NS	NS	NS
1386945_a_at	Prkab1	protein kinase, AMP-activated, beta 1 non-catalytic subunit	NS	NS	NS
1366271_at	Prkab2	protein kinase, AMP-activated, beta 2 non-catalytic subunit	NS	NS	NS
1378845_at	Prkab2	Protein kinase, AMP-activated, beta 2 non-catalytic subunit	NS	NS	NS
1367947_at	Prkag1	protein kinase, AMP-activated, gamma 1 non-catalytic subunit	NS	NS	NS
1373952_at	Prkag2	protein kinase, AMP-activated, gamma 2 non-catalytic subunit	NS	NS	NS
1375835_at	Prkag2	Protein kinase, AMP-activated, gamma 2 non-catalytic subunit	NS	NS	NS
1383122_at	Prkag2	protein kinase, AMP-activated, gamma 2 non-catalytic subunit	NS	NS	NS
1392263_at	Prkag2	protein kinase, AMP-activated, gamma 2 non-catalytic subunit	NS	NS	NS

Chapter 5

Probe Set ID	Symbol	Gene Title	ANOVA	Control + CORT	Stress + CORT
1394711_at	Prkag3	protein kinase, AMP-activated, gamma 3 non-catalytic subunit	NS	NS	NS
1370112_at	Pten	phosphatase and tensin homolog	4.2E−02	NS	NS
1375360_at	Rheb	Ras homolog enriched in brain	NS	NS	NS
1398787_at	Rheb	Ras homolog enriched in brain	NS	NS	NS
1397877_at	Rictor	RPTOR independent companion of MTOR, complex 2	NS	NS	NS
1370261_at	Rps6ka1	ribosomal protein S6 kinase polypeptide 1	NS	NS	NS
1374811_at	Rps6ka2	ribosomal protein S6 kinase polypeptide 2	3.4E−07	1.9 3.1E−06	1.7 5.2E−05
1382271_at	Rps6ka5	ribosomal protein S6 kinase, polypeptide 5	NS	NS	NS
1398582_at	Rps6ka5	ribosomal protein S6 kinase, polypeptide 5	NS	NS	NS
1388646_at	Rptor	regulatory associated protein of MTOR, complex 1	NS	NS	NS
1367736_at	Rraga	Ras-related GTP binding A	NS	NS	NS
1369696_at	RragB	Ras-related GTP binding B	NS	NS	NS
1382719_at	RragB	Ras-related GTP binding B	NS	NS	NS
1371723_at	Rragc	Ras-related GTP binding C	NS	NS	NS
1382537_at	Rragc	Ras-related GTP binding C	NS	NS	NS
1373427_at	Rragd	Ras-related GTP binding D	NS	NS	NS
1375238_at	Stk11	Serine/threonine kinase 11	NS	NS	NS
1375364_at	Stk11	serine/threonine kinase 11	NS	NS	NS
1381830_x_at	Stk11	Serine/threonine kinase 11	NS	NS	NS
1375896_at	Stradb	STE20-related kinase adaptor beta	NS	NS	NS
1376476_at	Telo2	TEL2, telomere maintenance 2, homolog (S. cerevisiae)	NS	NS	NS
1394982_at	Telo2	TEL2, telomere maintenance 2, homolog (S. cerevisiae)	NS	NS	NS
1367830_a_at	Tp53	tumor protein p53	NS	NS	NS
1367831_at	Tp53	tumor protein p53	NS	NS	NS
1370752_a_at	Tp53	tumor protein p53	NS	NS	NS
1369362_at	Tsc1	tuberous sclerosis 1	NS	NS	NS
1368056_at	Tsc2	tuberous sclerosis 2	NS	NS	NS
1370168_at	Ywhaq	tyrosine 3-monooxygenase/tryptophan 5-monooxygenase activation protein, theta polypeptide	NS	NS	NS
1387862_at	Ywhaq	tyrosine 3-monooxygenase/tryptophan 5-monooxygenase activation protein, theta polypeptide	NS	NS	NS

Table 5.3: Microarray analysis of mRNA expression in the rat hippocampal DG in control animals (left) and in animals with a recent history of CRS (right). The fold change (FC) is shown, in which *numbers* above 1 indicate an up-regulation and below 1 a down-regulation by acute CORT. $P > 0.05$ is considered not to be significant (NS). NS: not significant ($p > 0.05$), FC: fold change

	Gene	GRE sequence	Distance from TSS
Ddit4	*Rattus Norvegicus*	*gaacattgtgttct*	$-20{,}879$
	Homo sapiens	gaacattgtgttct	$-24{,}936$
	Mus Musculus	gaacattgtgttct	$-22{,}516$
	Bos Taurus	gaacattgtgttct	$-15{,}283$
Ddit4L	*Rattus Norvegicus*	*gaactgtctgtcca*	$2{,}199$
	Homo sapiens	gaactgtctgtcca	$2{,}382$
	Mus Musculus	gaactgtctgtcca	$2{,}324$
	Bos Taurus	gaactgtctgtcca	$2{,}557$
Ddit3	*Rattus Norvegicus*	*ctccacagtgttcc*	$2{,}586$
	Homo sapiens	gcccacagtgttca	$2{,}755$
	Mus Musculus	ctccacagtgttcc	$2{,}894$
	Bos Taurus	ccccacagtgttcc	$2{,}613$
Fkbp51_1	*Rattus Norvegicus*	*gaacagggtgttct*	$62{,}946$
	Homo sapiens	gaacagggtgttct	$86{,}842$
	Mus Musculus	gaacagggtgttct	$20{,}724$
	Bos Taurus	gaacagggtgttct	$99{,}485$

Table 5.4: The in silico predicted GRE-sequences and their location relative to the transcription startsites in four different species. In case of DDIT4, DDIT4L and FKBP51_1, the sequence is 100 % conserved in all species.
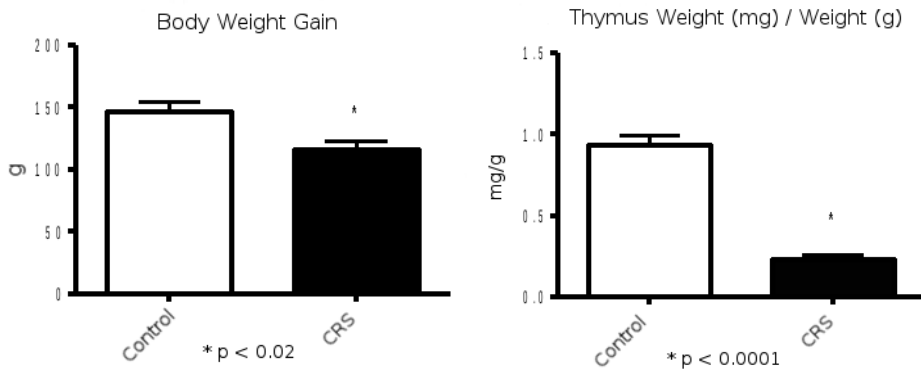
Figure 5.6: Body weight gain and relative thymus weight in control and CRS animals.
Students test shows significant differences on both measures ($n = 8$ for both groups).

Chapter Six

General Discussion

6.1 Summary of main conclusions

In this thesis, we have reported studies in which the primary response to glucocorticoids was examined in a neuronal context by analyzing the DNA-targets bound to and genes regulated by the activated glucocorticoid receptor (GR). The neuronal context was either the widely used PC12 neuronal pheochromocytoma cell line or the hippocampus of the rat brain. DNA sequences with GR binding motifs were identified either with an *in silico* approach or with next generation sequencing of DNA samples obtained by chromatin immunoprecipitation (ChIP-seq). In addition, DNA microarray analysis of discrete hippocampal subregions isolated with laser microdissection was performed to identify genes regulated by the endogenous glucocorticoid hormone in the rat, corticosterone (CORT). The thesis is concluded with the study of the effect of chronic stress on one of the identified CORT-responsive gene networks, the mammalian target of rapamycin (mTOR) pathway.

Our results showed that we were able to successfully validate *in silico* predicted GRE-containing GR-binding sites (GBS). In the rat hippocampus these GBS were located near genes previously found to be regulated by stress and CORT (*Chapter 2*). This suggests functionality of these evolutionary conserved GREs. We subsequently applied ChIP-seq to identify genomic binding sites of GR in two different neuronal substrates: neuronal-like PC-12 and rat hippocampal tissue (*Chapter 3 and 4*). At the time of publication, these studies were the first to demonstrate the application of the ChIP-seq technique in a neuronal context.

Using ChIP-seq we identified thousands of GBS of which the majority is novel. In order to validate these findings we analyzed the extent and pattern of GR binding for a selection of the identified GBS in rat hippocampus after administration of different amounts of CORT (*Chapter 4*). Our findings imply that, depending on the amount of CORT, different sets of GR-target genes are activated in the hippocampus. In addition, we were able to measure binding of MR to a majority of this GBS selection. In almost all cases, MR binding was already apparent at lower CORT concentrations than GR binding (*Chapter 4*), which is in line with the ten-fold higher affinity to CORT displayed by MR as compared to GR (Reul and de Kloet, 1985).

We subsequently screened the GBS that were identified in the ChIP-seq studies for motifs that resemble known binding sites of GR and other transcription factors. As expected, a motif strongly resembling the canonical GRE consensus sequence was the most prevalent motif identified. In neuronal PC12 cells 58 % of GBS contained a canonical GRE sequence (*Chapter 3*) and this figure nearly approached 100 % in hippocampus (*Chapter 4*). In addition to the GRE, other motifs were identified that resemble sequences of possible transactivation and transrepression partners of GR. These include Maz1, SP1, Zbtb3, Gabpa, Prrx2, Zfp281, Gata1, Zfp740,

Sox12, Sox4, Srf and GM397 or Zscan4c, several of which had not yet been linked to GR function and may be important factors for GR signaling in a neuronal context

6.2 Methodology

The main method used in this thesis was ChIP-seq, which was a relatively new method still subject to technological improvements. *In vivo* studies performed in brain tissue were scarce and we therefore choose to first apply the technique *in vitro* in neuronal PC12 cells. This allowed us to get more acquainted with the technique and to obtain the first ChIP-seq data in a neuronal setting. Subsequently, we were able to develop our own methods and to apply the ChIP-seq technique successfully in rat hippocampus. In neuronal PC12 cells as well as in the rat hippocampal tissue we identified thousands of new GBS. Since a consensus in ChIP-seq analysis is lacking in literature, we considered validation of our methods using RT-qPCR to be essential. The validation provided the evidence that our methods and the cut-offs we applied in both Chapter 3 and 4 were appropriate. It is clear that ChIP-seq has contributed tremendously to a better understanding of the interaction of transcription factors with the genome (Mundade et al., 2014). Recently, special guidelines and practices of the ENCODE consortium have been published allowing standardization of ChIP experiments (Landt et al., 2012; Mundade et al., 2014).

The *in silico* approach GenSig, that we have developed (*Chapter 2*), proved to be a suitable method to screen known CORT-responsive genes for GRE-like sequences. We were able to show GR-binding to 47% of the predicted and selected GREs, which is a high success rate. We believe that this high percentage is due to the fact that GenSig takes evolutionary conservation into account. For Estrogen Receptor binding sites, it was recently confirmed that the higher affinity estrogen response elements display a higher degree of evolutionary conservation in comparison to their flanking sites (Gertz et al., 2013), which supports our *in silico* GenSig approach. Other factors contributing to the predictive success rate of GenSig are the fact that the GRE consensus motif was based on validated GREs and only genes known to be responsive to CORT were included in the analysis. In conclusion, the methods used in this thesis were suitable to investigate our aim which was to identify primary GR targets in neuronal-like cells and hippocampal tissue.

6.3 Chapter 3: discussion

Findings

In *Chapter 3*, a genome-wide analysis of GR-binding sites in neuronal PC12 cells was presented. Where previously knowledge regarding GR-mediated action of glucocorticoids had come from studies on peripheral tissues, we were now able to show

Chapter 6

data in a neuronal context. This is important, since it was already apparent that GR-binding is highly cell type-specific with minimal overlap in GBS between different cell types (John et al., 2011; Pan et al., 2011; Reddy et al., 2009; Yu et al., 2010).

The raw ChIP-seq data was analyzed using the software of CLC genomics workbench, resulting in 1,183 GBS that we considered to be significant (FDR cut off 5 %). When these GBS were compared with other non-neuronal studies, it turned out that 87 percent of these sites were unique to the neuronal PC12 cells (Figure 6.1). Interestingly, the majority of these PC12-unique GBS were located nearby genes with a known neuronal function, such as axonogenesis, neuronal differentiation and neuronal development. In terms of genomic location, almost one third of the GBS were located within genes and mostly within intronic regions, which is consistent with other GR ChIP-seq studies (Reddy et al., 2009; Yu et al., 2010). The functionality of GR-binding to an intron was demonstrated in an *in vitro* study investigating the effect of DEX stimulation of cultured Beas-2B airway epithelial cells on the expression of, amongst others, the anti-inflammatory target tumor necrosis factor, alpha-induced protein 3 (TNFAIP3) (Altonsy et al., 2014). It became evident that GR-binding to an intronic GBS in the TNFAIP3gene was required to enhance its transcription. At the time we did our experiments, an *in vivo* study demonstrating the functional relevance of intronic GR binding was lacking.

The GBS were screened for DNA-motifs which are known to bind certain proteins. This resulted in the identification of motifs for GR (the canonical GRE motif), Gabpa, Prrx2, Zfp281, Gata1 and *Zbtb3*. The GRE motif was similar to the motif identified by others and also had a comparable prevalence. The GRE was the most prevalent motif identified in our study, indicating that direct GR binding to specific sites in the DNA via transactivation is an important mechanism GR uses to regulate gene expression in a neuronal context. Zbtb3 was exclusively found in non-GRE containing GBS and was the most frequently observed non-GRE motif with a frequency of 80 % within this group. This suggested that Zbtb3 might be a new transrepression partner of GR.

In neuronal PC12 cells the genes that were associated with a GRE-GBS were involved in general cell functions and processes, i.e. cell motility, vascular processes and protein dimerization activity. In contrast, genes near a non-GRE GBS had a clear role in neuronal processes such as neurogenesis, plasticity and growth, synap-
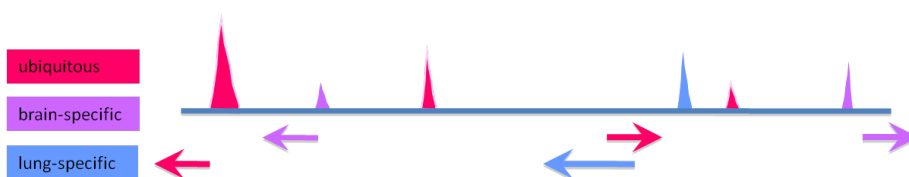
Figure 6.1: GBS are cell-type specific. Whereas the GBS that are shared between different experimental models seem to be more ubiquitous expressed, the cell-specific genes are located nearby genes with a known neuronal function.

tic transmission and neurotransmitter biosynthetic processes. This suggests that the Zbtb3 transcription factor is a novel crosstalk partner of GR that tethers GR to DNA sites in a transrepressive mode of action in order to regulate neuronal gene expression in neuronal PC12 cells upon GR activation.

Update of Chapter 3: findings since publication

Since our publication appeared, other ChIP-seq studies have been published on GR-binding *in vitro* in cell lines *(Gertz et al., 2013; He et al., 2013; Paakinaho et al., 2014)*. The cell type specificity of GBS has also been found *in vitro* in A549 cells, a lung carcinoma cell line, and ECC-1 cells, an endometrial cancer cell line, where only 7.7 % shared GBS were identified between those two cell types (Gertz et al., 2013). In addition, it was found that these shared GBS were significantly enriched for GRE's, suggesting that cell-specific and shared GBS have distinct underlying DNA sequence patterns. Interestingly, 75 % of the GRE-GBS only became accessible after DEX-treatment which is in contrast with nonGRE-GBS where 67 % was found in open chromatin prior to treatment. This would imply that DEX activation of GR facilitates chromatin accessibility of GRE-regions, enabling modulation of gene transcription. This has previously been found by others as well who in addition had found that the GRE-composition could be linked to the degree of chromatin accessibility prior to hormone treatment (John et al., 2011). Zbtb3 is essential for the growth of cancer cells involved in human melanoma, lung carcinoma and breast carcinoma (Lim, 2014). Since the PC12 cells originate from tumor cells, we cannot exclude that our finding is not neuronal but rather carcinoma-specific. However, in Chapter 4 binding motifs of Zbtb3 were also frequently observed in hippocampal tissue. In contrast to the neuronal PC12 cells where all identified Zbtb3 motifs occurred in non-GRE containing GBS, Zbtb3 was found in the hippocampal GBS that did contain a GRE, suggesting they may function as GR tethering sites. Interestingly, in a study focusing on combinatorial interactions among transcription factors, it was found *in vitro* that GR and Zbtb3 proteins are able to interact (Ravasi et al., 2010). Since this was only one of more than 700 interactions that were studied, no additional information was provided regarding the GR-Zbtb3 interaction. It is clear that the combination of GR and Zbtb3 in a neuronal setting requires further investigation. Regarding the other proteins Gabpa, Prrx2, Zfp281 and Gata1, no new information in relation to glucocorticoids in a neuronal setting has been found since publication of Chapter 3.

To conclude, the study in Chapter 3 has provided insight into new aspects of GR-mediated action of glucocorticoids in the neuronal PC12 cells. Even though we have not been able to validate all the discovered GBS and the newly hypothesized transactivation and transrepression partners, they provide a valuable inventory for new investigations into GR action in a neuronal context.

Chapter 6

6.4   Chapter 4: discussion

Findings

Similar to Chapter 3, the aim of this chapter was to identify GBS within a neuronal context. Instead of a cell line, rat hippocampal tissue was used for ChIP-seq, resulting in an inventory of 2,460 significant GBS. The analysis was designed to compare the GR binding profile at different doses of CORT (ranging from 3–3,000 µg/kg) at 1 hour after administration to ADX rats. In addition to GR also MR-binding to a selection of GBS was examined. It appeared that the binding pattern of GR to its genomic targets is dependent on the concentration of CORT. Whereas some of the DNA-targets are more sensitive and did bind GR at the lower CORT dose (30 µg/kg and higher), others required higher CORT (300–3,000 µg/kg) doses. Our results showed the existence of 2 populations of GBS in the rat hippocampal genome that can be distinguished by their binding at different CORT concentrations.

The population of GBS identified under low dose conditions suggests that GR is already active during basal levels of circulating CORT. The genes activated by low CORT levels may therefore be involved in the permissive actions of CORT that operate during synchronization and coordination of daily and sleep-related events. The other population of GBS that becomes occupied during the higher CORT concentrations as present during stress, likely is involved in stress adaptation, learning and memory processes and recovery. The current inventory provides an important source of information to dissect the function of these GBS in different contexts.

We were interested in whether the GBS are also bound by MR, because MR and GR have DNA-binding domains that are 94 % identical and may form heterodimers. Both receptors are activated by CORT, with the only difference that MR has a much higher affinity for CORT and, consequently, is activated at lower CORT levels in comparison with GR. We were able to show significant MR-binding to 10 out of 13 GBS. However, in contrast to GR, a plateau of MR binding capacity was reached at 300 µg/kg CORT, while for GR a sharp increase in binding was observed at 3,000 µg/kg CORT. A hypothesis that would need further investigation is that at lower CORT concentrations MR may predominantly form homodimers, whereas at higher concentrations mimicking stressful conditions when GR activation becomes more abundant, the incidence of heterodimerization with GR and ultimately GR homodimerization increases, with differential consequences for the repertoire of bound GBS.

Similar to in neuronal PC-12 cells, intragenic GBS were highly represented (39 %) in rat hippocampus, the majority of which was located within introns. It was striking that except for 14 GBS, all the other GBS contained a GRE-like motif. In addition to the GRE, the 500 most significant GBS contained motifs resembling binding sites of transcription factor Zbtb3, Zfp740, Sox12, Sox4, Srf and Zscan4c. Zbtb3, of which the motif is present in 58 % of the GRE-GBS, is of particular interest, since these results in rat hippocampus contradict our observations in PC12 cells, where motifs for

Zbtb3 binding were exclusively observed in non-GRE containing GBS. Within the rat hippocampus, a combination of GRE and Zbtb3 motifs were present in GBS associated with genes involved in regulation of apoptosis, regulation of transcription, regulation of macromolecule metabolic processes and the insulin receptor signaling pathway. Interestingly, these processes are connected to the mTOR pathway (Figure 1.7, Chapter 1). The 14 GBS that did not contain a GRE, all contained 2 motifs resembling the binding motif of the protein CUP. In Drosophila, CUP is an eukaryotic translation initiation factor 4E (EIF4E)-binding protein that represses the expression of specific maternal mRNAs. Since EIF4E is a downstream target of the mTOR pathway this might imply that GR operates at several levels affecting regulators as well as targets of the mTOR pathway.

Update of Chapter 4: findings since publication

The fact that we were able to perform a ChIP experiment with MR *in vivo* was at that time very new and exciting. Since then ChIP-seq for MR has been performed by others *in vitro* in a murine distal convoluted tubular epithelial cell-line (mDCT) that was stimulated with 10^{-7} M aldosterone (Ueda et al., 2014). Sgk1, Fkbp5, Rasl12, Tns1 and Tsc22d3 (Gilz) were identified by ChIP-seq and validated as direct target genes of MR by quantitative RT-qPCR and ChIP-qPCR. MR binding regions adjacent to Ctgf and Serpine1 were also validated. Interestingly, with the exception of Rasl12, we have found GBS near all the above mentioned genes. To what extent these regions overlap with the GBS identified in rat hippocampus is unknown and beyond the scope of the current thesis. It would be of interest for a future study to investigate this further.

Dose-dependent GR-binding has also been described by others, *e.g.* in A549 cells where a distinction was made between hypersensitive (bound at 0.5 nM DEX after 60 min), medium sensitive (bound at 5 nM DEX after 60 min) and low sensitive GBS (bound at 50 nM DEX after 60 min). The hypersensitive GBS had overall stronger binding signals which is similar to our observations in the rat hippocampus in the low-CORT group. In addition it was found that dose-dependency of GR binding is not driven by a specific version of the GRE (Reddy et al., 2012). Instead chromatin accessibility appeared to be a determinant of GR binding, predominantly to the hypersensitive sites. The sequences that surround the GBS may affect chromatin accessibility by recruiting proteins that increase or decrease this accessibility or that aid in stabilization of GR-DNA interactions. This may be one of the molecular causes for differences in affinity of GR to its GBS within one tissue-or cell-type as well as potentially underlying the cell-specificity of GBS.

Interestingly PER1, of which one of its GBS's is the most sensitive in our selection of validated GBS, was found by others to be uniquely sensitive to low doses of glucocorticoids. In this in vitro study in A549 cells, 50% of the PER1 expression response occurred at 0.47 nM DEX which was accompanied by GR-binding at an upstream GBS at the same DEX-concentration and time-point. This is in contrast

Chapter 6

to the other GBS and genes investigated where GR-binding and differential gene expression were not measured until approximately 8 nM of DEX was used for stimulation with (Reddy et al., 2012). .

Another source of diminished chromatin accessibility can be methylation signatures present within the GBS which prevent GR binding to the GBS in one cell type in comparison to another. DNA methylation predominanty occurs at CpG dinucleotides in the human genome, but recently evidence has been found showing that adult human brain tissue is among the tissues with the highest number of methylated non-CpG cytosines (Varley et al., 2013). Methylated non-CpG cytosines might explain why GBS that have been identified in other non-neuronal studies were not identified in our hippocampal dataset. The presence of methylated non-CpG cytosines in the brain was confirmed in mouse frontal cortex (Xie et al., 2012).

In our analysis we have found motifs resembling the binding site of Zbtb3, Sox4 and Srf. New findings regarding Zbtb3 have been described in the previous section regarding Chapter 3. Since publication of this data, it has been found that Sox4, a neurogenesis-related transcription factor, has a crucial role in regulating hippocampal neurogenesis in mice (Miller et al., 2013). Srf, an important regulator of cell growth and differentiation, appears to be involved in an alternative cellular mechanism for the regulation of cell death in hippocampal CA1 neurons. Since five of the ten most enriched functional GO clusters in Chapter 4 are "Apoptosis" and "regulation of programmed cell death", "neurite projection" and "neuron differentiation" and "positive regulation of transcription", Srf and Sox4 transcription factors appear to be good candidates to further explore as a transactivation or tethering partner of GR, in addition to Zbtb3 (Chang and Chao, 2013).

As a reference genome Rattus Norvegicus 4 (rn4) was used to align the isolated DNA tags (7). However, since then two new versions have been published and Rn6 contains a new, partially assembled Y chromosome as well as improvements to other regions of the genome. If one would continue with the outcome of the experiments of this chapter, aligning the reads against the newest version of the rat genome should be performed.

6.5   Chapter 5: Discussion

Findings

In this study we showed that in the rat hippocampus CORT directly regulates the mTOR signalling pathway, which plays a central role in translational control and has long-lasting effects on the plasticity of specific brain circuits. We demonstrated that rats with a history of chronic stress have higher basal hippocampal mTOR protein levels in comparison to control animals. Interestingly, mTOR protein was decreased when chronically stressed animals received an acute CORT challenge. This

is in contrast with the non-stressed controls which did not show an effect on mTOR protein.

Using microarray expression analysis, we identified three regulators of the mTOR protein (DDIT4, FKBP51 and DDIT4L) as well as a downstream target (DDIT3), to be differentially expressed in response to a CORT-injection. Interestingly, this expression differed between the hippocampal subregions CA3 and DG, suggesting a key role of the mTOR pathway in the differential plasticity of these subregions in response to acute CORT exposure. If the animals had experienced CRS, DDIT4 and DDIT3 were no longer differentially expressed in the rat DG, which was accompanied by higher mTOR protein levels in whole hippocampus. Interestingly, using ChIP-seq in a separate experiment, GREs were found near the mTOR regulators DDIT4, DDIT4L, FKBP51 as well as near DDIT3, which were validated in the case of DDIT4 and FKBP51.

Update of Chapter 5: findings since publication

In chapter 5, we demonstrated that the action of glucocorticoids on the expression of mTOR pathway members as well as on hippocampal mTOR protein levels is context-dependent and is highly sensitive to chronic stress. In addition, we proposed that direct regulation of the mTOR pathway by CORT represents an important mechanism underlying CORT-effects on neuroplasticity in the brain, with different outcomes depending on prior stress history. The sensitivity of mTOR for environmental stressors has been demonstrated recently by others as well, showing that chronic restraint stress in rats (10-days, plastic restrainer, 6 h daily) leads to increased mTOR mRNA expression, which is in line with the increased protein levels that we have found (Orlovsky et al., 2014).

Several studies have demonstrated that extracellular signal-regulated kinase (ERK) levels are decreased in the hippocampus in animal models of chronic stress and chronic CORT exposure (First et al., 2011; Gourley et al., 2008). ERK1/2 plays a crucial role in synaptic and structural plasticity and operates upstream of the mTOR pathway. There are indications that the decreased ERK level in the aforementioned animal models is specifically present within the dentate gyrus (First et al., 2011; Gourley et al., 2008). Since a decrease in ERK 1/2 leads to a reduced inhibitory action on the mTOR pathway, it is to be expected that mTOR expression would be increased, which is consistent with our findings.

The fact that CRS affects gene transcription has been observed in another study as well where 21 days of chronic restraint stress resulted in an increased basal gene expression level when measured one day later in the hippocampus of Male C57/bl6 mice (Gray et al., 2014). Even though expression of most genes recovered after a r period of 3 weeks upon cessation of the chronic stressor, many other genes remained altered and did not return to baseline including glutamate transporter EAAT2 (Slc1a2), Histone deacetylase 8 (Hdac8) and Period circadian clock 2 (Per2). Interestingly it has been found that different stress paradigms induce distinct tran-

scriptional profiles (Gray et al., 2014; Orlovsky et al., 2014). This might explain some of the conflicting results obtained in different studies. Whereas CRS rats (10-days, plastic restrainer, 6 h daily) showed an increase in GR and a decrease in MR mRNA levels in the hippocampus, GR mRNA was decreased in another study performed in Male C57/bl6 that experienced CRS (21-days, conical tubes, 2 h daily), of which GR was elevated again after a recovery period of 22 days. Even though the results are not consistent, collectively these studies support our finding that GR-mediated gene transcription is affected by CRS.

Similar to our results, it was found in other studies that some of the hippocampal changes induced by chronic stress can only be observed if GR is activated acutely by stress-induced or injected CORT (Datson et al., 2013; Gray et al., 2014). Naturally, immediate early genes always were induced after 1 hour by the forced swim exposure, independent of the CRS background, and this group included besides c-fos, also Per1 and Sgk1. However, the study by Gray et al (Gray et al., 2014) also showed that CRS + forced swim resulted after one hour in an enormous increase in the amount of differential expressed genes, which increased from 1,298 to 3,999 genes. Many of these responsive genes are involved in chromatin modification, epigenetics and the cytokine/NFκB pathways. Interestingly, similar cytokine/NFκB genomic changes were observed after repeated social defeat (Feldker et al., 2006). The responsive network showed overlap with the genomic response to CORT applied to rats with a similar stress history (*e.g.* the Ddit4 pathway), in this case restricted to the dentate gyrus only (Datson et al., 2013). Allowing the animal to recover brought the number of differentially expressed genes back to the level observed in naïve FST exposed animals, being 1,251 genes. However, the overlap of this gene pattern between the recovery and the naïve groep exposed to forced swim was low. The stress-induced change in some of the genes of the CRS group, such as GR and BDNF, persisted for several weeks.

The findings illustrate that chronic stress creates a profoundly altered state of transcriptional reactivity to a novel stressor. The altered gene expression response is likely to be the result of local chromatin remodeling induced by CRS resulting in altered chromatin accessibility for transcription factors such as GR. Within the rodent DG, genes that are involved in chromatin structure and epigenetic processes have been found to be differentially expressed after CRS, which supports this hypothesis (Datson et al., 2013). This new information is in line with our finding that a history of CRS affects chromatin accessibility and consequently the ability of GR to bind to its genetic targets.

To summarize, it is evident that chronic stress affects the genomic response within rodent hippocampus. This becomes evident when the animal is subsequently exposed to an acute CORT-injection or novel stressor, the response to which is shaped by the chromatin accessibility caused by CRS. It has been suggested that the altered transcriptional response at least partially underlies the enhanced vulnerability to stress-related disorders like depression that can be caused by chronic stress
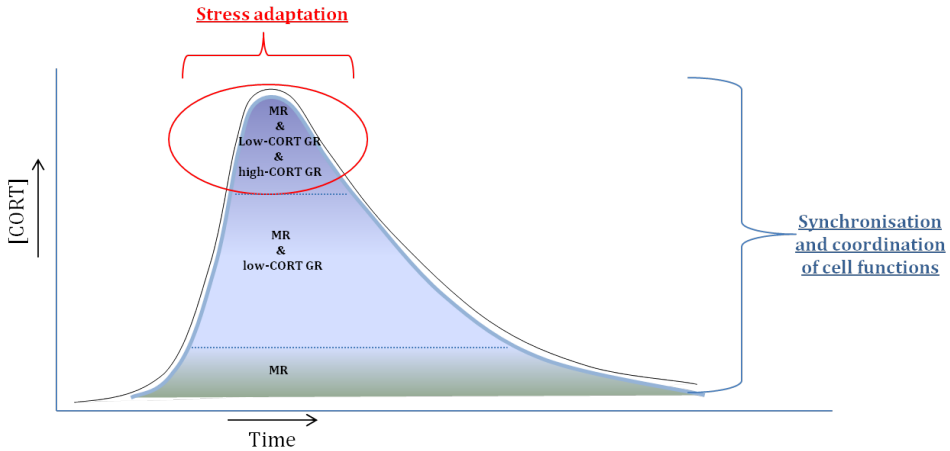
Figure 6.2: A model that illustrates the stress-response which is divided into three parts based on the CORT-receptors that are active.

(Datson et al., 2013). One of the molecular pathways affected is mTOR for which evidence has been found in our experiments and is supported by others (Orlovsky et al., 2014). While in our study we did not focus on GR and MR expression, neither mRNA nor protein based on new findings in literature this would be a very relevant topic to add. In addition, it would be of added value if mTOR protein would be measured in the DG separately.

6.6   Proposed Models

The results obtained in Chapters 2–5 and the studied literature has led to the formulation of two hypothetical models described below. Model 1 focuses on the functional implication of targeted GBS-groups that are subjected to various CORT-concentrations, following the stress response. Model 2 elaborates on the hypothe-sized regulatory role that CORT has in maintaining an optimal balance of the mTOR pathway and how this balance is impaired by CRS.

Model 1: stress adaptation involves the activation of a distinct GBS population

In our hippocampus model, GR binds to its genomic targets in accessible chromatin. There are two distinct populations of GBS, namely the Low-CORT and High-CORT populations. In the High-CORT group, MR predominantly binds the GBS and it is not until the CORT concentration becomes very high that GR-binding takes over this dominant role (Chapter 4). We propose a model in which a stress-response is divided into three parts based on the CORT-receptors that are active (see also (de

141

Kloet et al., 2005; de Kloet, 2014) (Figure 6.2)). The MR-group is activated at low levels of CORT (between 3 and 30 μg/kg) and remains to be active at higher CORT as well. The high-CORT GR group is only activated at high CORT concentrations (3,000 μg/kg) and the low-CORT group is activated somewhere in between depending on the GBS investigated. The group of genes that are associated with GBS can be divided into two groups. The genes that are targeted by MR as well as GR during lower and higher [CORT] are involved in general cell processes such as coordination of daily and sleep-related events involving genes like Per1, MT2a, Ddit4, Klf9. The genes that are bound by GR only during high [CORT] are involved in the cell specific processes required for stress adaptation such as energy metabolism, neuronal plasticity and recovery ultimately leading to memory formation, recovery and in preparation for coping with a new stressor. In the hippocampus, we have identified the following genes for this group: Lyst, Cacna2d3, Arpc2, Serp2, Slc7a6, St3gal3, Ndnl2, Nrxn1.

Model 2: History of chronic stress modulates mTOR regulation: possible implications

We have observed that GR binding to its targets after an acute CORT challenge is affected by the stress history of the rats. When rats are challenged with CORT and do not have a history of chronic stress, GR binds to thousands of GBS in the hippocampus, which in almost all cases contain a GRE-like sequence (Chapter 4). This list of GBS includes several mTOR pathway-members, which are differentially expressed in the rat Dentate Gyrus, being either up (FKBP51 and DDIT4) or down-regulated (DDIT4L and downstream target DDIT3) (Chapter 5). Both DDIT4 and FKBP51 contain a GRE-like sequence to which GR binds which implies that these mTOR regulators are upregulated after an acute CORT challenge via direct interaction of GR with a GRE. At the level of mTOR protein expression, acute CORT does cause a minor increase but this is not significant.

Animals that have experienced a history of CRS have significantly higher mTOR protein levels in the hippocampus during basal conditions, which is dramatically decreased when the animals experience a subsequent CORT challenge. DDIT4 and mTOR downstream target DDIT3 are not differentially expressed in these animals. Apparently, the accessibility of the GRE of DDIT4 for GR-binding is compromised, thus inhibiting the regulatory function of DDIT4 in the mTOR pathway. These findings demonstrate that the hippocampal mTOR protein is sensitive to a history of chronic restraint stress in rats.

It has become clear that mTOR activity is very sensitive to stimulation by CORT in changing environments. Whether a low or high mTOR activity is better for neuronal functioning, is unclear and depends on the context and timing of such stressful stimuli. As suggested in Chapter 5, an optimal balance of the mTOR pathway would promote LTP and memory formation, while at the same time promoting
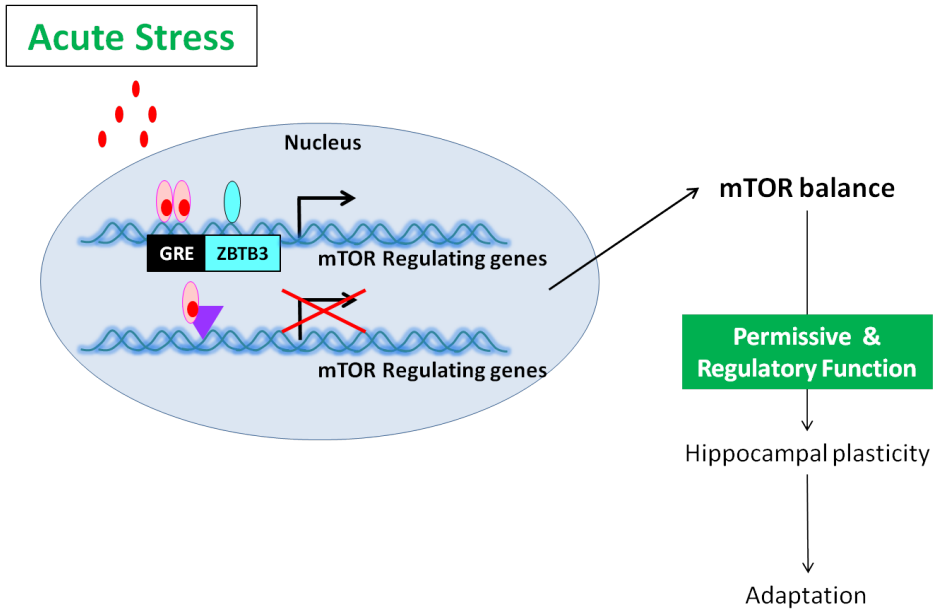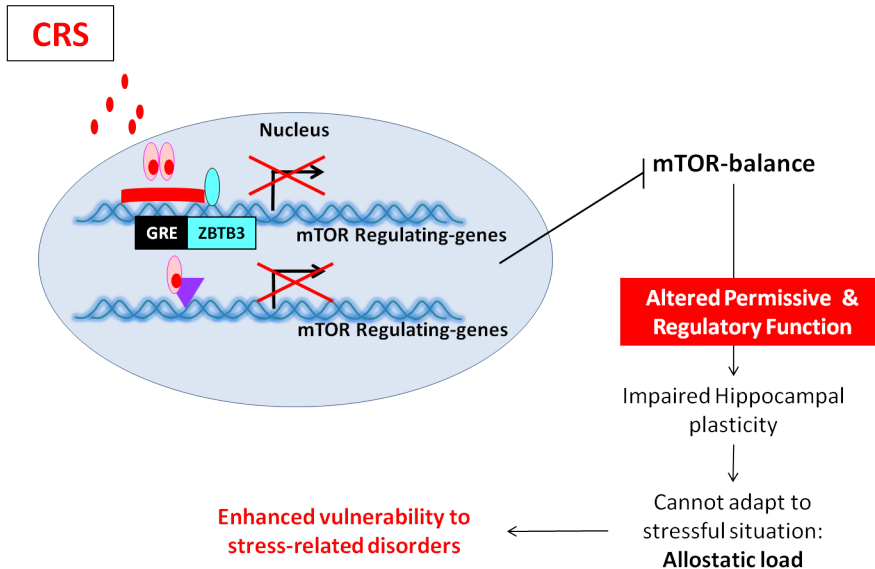
Figure 6.3: A model that illustrates the regulatory role that CORT has in maintaining an optimal balance of the mTOR pathway, allowing the organism to adapt to the situation.

cell survival and resilience. CORT is proposed to be a regulatory component of the mTOR balance in the hippocampus (Figure 6.3).

Chronic stress affects the chromatin accessibility and poses an extra regulatory level to CORT action. Ultimately this is reflected in an impaired hippocampal synaptic plasticity and enhanced vulnerability to stress-related disorders (Figure 6.4). CORT functioning is regulated in the context of chronic stress as well by chromatin remodeling that affects the capability of CORT-receptor GR to bind to its genetic targets, including mTOR regulators. This illustrates the complexity of regulation of the mTOR pathway by external and internal factors. If mTOR regulation is not well balanced, than this might result in affected LTP/LTD and resilience/survival pathways ultimately leading to enhanced vulnerability and to the development of stress-related neuropsychiatric disorders such as major depressive disorder or post traumatic stress syndrome.

Putting our findings into a translational perspective it would be of interest to examine in future studies to what extent the stress-CORT-mTOR interplay plays a role in the proliferation, migration and positioning of newborn neurons in the hippocampal circuitry. Such studies would help to understand to what extent the mTOR pathway is implicated in regulating neuronal plasticity, a process which underlies hippocampal-dependent learning and memory.

Chapter 6

143

Figure 6.4: A model that illustrates the inhibiting effect of CRS on the mTOR balance that can result in impaired hippocampal plasticity which might contribute to an enhanced vulnerability to stress-related disorders.

6.7   General Conclusion

In this thesis the primary genomic targets of GR have been analysed within a neuronal context. Using ChIP-sequencing thousands of GBS were identified in neuronal PC12 cells and in the rat hippocampus. New transactivation and transrespression partners that enable GR potentially to generate neuronal-specific gene transcription were proposed. Two populations of GR were observed that have different sensitivities to their genetic targets depending on the concentration of CORT. Furthermore, MR was found to be capable of binding to identified GBS. Finally, a direct suppression of the mTOR pathway by CORT within the rat hippocampus was revealed if the animals previously had experienced chronic stress. Taken together, these findings contribute to a better insight into the interaction of GR with the genome in a neuronal setting and point to the pathways that are under control of GR during stress exposure and recovery. The mTOR regulation within the rat hippocampus which is clearly affected by the stress history calls for further research.

Chapter 6

Chapter Seven

Summary

In daily life, the human body is faced with internal and external stimuli (also referred to as stressors) that challenge homeostasis. The body responds to these stimuli by turning on a stress response, which consists of activation of the sympathetic nervous system and the hypothamus-pituitary-adrenal (HPA) axis and their end products adrenaline and corticosteroid hormone respectively, that are released from the adrenal gland. CORT readily penetrates the brain and gives feedback to precisely on those structures that have initially produced the stress response. One important target is the hippocampus, a limbic brain structure which assigns a context, time and place to the experience of a stressor. In the hippocampus CORT promotes learning and memory processes. This effect exerted by CORT is mediated by the Glucocorticoid Receptor (GR) and the Mineralocorticoid Receptor (MR), after which the receptors migrate into the nucleus, affecting the transcription of CORT-responsive genes. While MR is involved in maintenance of basal activity of the stress system, the regulation of appraisal processes and the onset of the stress reaction, GR activation results in recovery from stress and behavioral adaptation. Ultimately, their balanced activation is an important determinant of neuronal excitability, neuronal health and stress responsiveness.

Since GR has an important role in the normalization of the homeostasis after the occurrence of a stressor, this protein has received a lot of attention in research in relation to the hippocampus. This has led to an impressive amount of information that has been gathered throughout the years regarding CORT-responsive genes. However, these inventories are a mix of primary GR-targets as well as downstream targets and a differentiation between these groups was not possible. Due to innovative technologies, resulting in the first ChIP-seq studies, it became possible to perform genome-wide identification of transcription factor binding sites. Aim of this thesis was to investigate the genome-wide targets of GR within a neuronal context and the possible functional implications that these binding sites might have on a pathway involved in neuronal plasticity, the mTOR pathway. For this purpose four aims were specified which are addressed in **Chapters 2** till **5**.

AIM I: "To use an *in silico* approach with the goal to predict neuronal-specific GREs in the genome followed by their experimental validation. For this purpose we have developed the Position Specific Scoring Matrix (PSSM) GenSig."

GR is able to dimerize and as such can recognize and bind glucocorticoid response elements (GREs) in the DNA by which it can regulate the expression of target genes. GRE-dependent processes are important in the brain, because mice in which GR is not able to bind to GREs, due to a mutation that inhibits GR homodimerization, hippocampal excitability and spatial memory were impaired. The GREs responsible for the action of GR *in vivo* in the brain are largely unknown which makes it

very difficult to predict them. Furthermore, GR-binding to a GRE-like sequence may not always lead to a functional effect. In **Chapter 2** the application is reported of a position-specific scoring matrix from 44 GREs described in literature that is used to predict evolutionary-conserved GREs. Using this matrix, large genomic regions were scanned surrounding CORT-responsive genes that have been identified in a neuronal context. Fifteen out of 32 predicted GREs were identified that are bound by GR in the rat hippocampus of which at least 10 are novel. Furthermore GC-box associated motifs were discovered that are present in the GRE-flanking sequences. This characteristic of binding was found to be absent in another dataset with GR-binding and GR-nonbinding sites, suggesting a mechanism for tissue-specific CORT signaling that may determine GRE usage in the hippocampus. In conclusion, our current finding can be considered a first step towards understanding the direct downstream pathways of GR signaling in the brain.

AIM II: "To identify genome-wide GR-binding sites (GBS) in vitro in neuronal PC12 cells and in vivo in rat hippocampus using ChIP-seq and to identify genes located in the vicinity of these GBS that are activated/repressed by GR in a neuronal-specific context."

GR is able to bind directly to genomic glucocorticoid response elements (GREs) or indirectly to the genome via interactions with bound transcription factors. These two modes of action, respectively called transactivation and transrepression, result in the regulation of a wide variety of genes important for neuronal function. Despite the fact that a lot of knowledge was already available regarding differential expressed genes after the activation of GR, its primary targets were not investigated yet in a genome-wide neuronal context. In **Chapter 3**, a genome-wide analysis is presented of GR-binding sites (GBS) in neuronal PC12 cells. At the time of publication, this was the first genome-wide discovery of GR-binding sites in a neuronal context. Interestingly, the majority of the PC12 GBS that were uniquely identified in this model system were located nearby genes with a known neuronal function. In **Chapter 4**, a genome-wide analysis of GBS in rat hippocampus is reported after administration of an acute CORT pulse to the rats. Both chapters revealed a high prevalence of intragenic GBS of which the majority was located within introns. In both **Chapter 3** and **4** motif screening revealed that the GRE was the most prevalent motif, indicating that direct GR binding to specific sites in the DNA via transactivation is an important mechanism GR uses to regulate gene expression in a neuronal context. In addition, in both **Chapter 3** and **4** a Zbtb3-binding motif in the GBS was discovered. In neuronal PC12 cells, Zbtb3 is reported to be exclusively found in non-GRE containing GBS (Chapter 3), suggesting that it might be a new transrepression partner of GR in the neuronal context of this cell line. In contrast, in the rat Zbtb3 was only identified in GRE-containing GBS (**Chapter 4**), implying it may be a new transactivation partner of GR. Within the rat hippocampus, a combina-

Chapter 7

tion of GRE and Zbtb3 motifs was found to be present in GBS that are associated with genes involved in regulation of apoptosis, regulation of transcription, and regulation of macromolecular metabolic processes and the insulin receptor signaling pathway. Interestingly, these processes are all connected to the mTOR pathway. To conclude, the studies in **Chapters 3** and **4** have provided insight into new aspects of GR-mediated action of glucocorticoids in a neuronal context. Even though we have not been able to validate all the discovered GBS and the newly hypothesized transactivation and transrepression partners, they provide a valuable inventory for new investigations into GR action in a neuronal context. Understanding GR-signalling in a neuronal context is important given the profound effects of glucocorticoids on neuronal plasticity and consequently on brain function.

AIM III: "To investigate whether MR binds to the same GBS as GR in the hippocampus and to measure binding of both receptors to these DNA sites in response to different concentrations of ligand."

In the brain, CORT binds to MR and GR. Whereas GR is abundantly expressed throughout the brain, MR has a much more restricted expression in predominantly limbic brain structures. Both receptors differ in their affinity for CORT, where GR has a relatively low affinity for CORT and MR a relatively high affinity. As a consequence, GR is activated when circulating CORT increases, during stress, and MR is already activated under basal nonstress conditions. Their balanced activation is an important determinant of neuronal excitability, neuronal integrity, and stress responsiveness. For GR it is known that it can bind as a dimer to GREs that are present in the DNA and consequently induces transactivation. Furthermore, GR is able to bind via other Transcription Factors indirectly to the genome resulting in transrepression of these stress-induced pathways.

Knowledge on interaction of MR and GR with the genome is sparse, in particular in the brain. In **Chapter 4**, we investigated GR-binding to hippocampal GBS identified in male adrenalectomized rats that were challenged with increasing doses of the GR agonist CORT ranging from 3 to 3,000 μg/kg. Furthermore, we analyzed the potential of MR to bind to these GBS under the same conditions. We have shown that under varying CORT concentrations, 2 groups of different binding sites are recruited. The low-CORT group shows GR binding to GBS at 30 μg/kg CORT which increases with higher CORT concentrations. In the high-CORT group GR binding to the GBS is evident after injecting 3,000 μg/kg but not at lower concentrations. MR-binding at both groups is apparent at 30 μg/kg and in most cases stabilizes thereafter, indicating a saturation of MR in both situations.

In conclusion, our results highlight the existence of 2 distinct populations of GBS in the rat hippocampal genome that can be discriminated by the extent of CORT binding. Furthermore, we have shown that MR is able to bind to a selection of GBS which contributes to the knowledge on the primary genomic targets of MR.

The simultaneous binding of GR and MR to the same GRE-containing GBS might imply heterodimerization of GR and MR.

AIM IV: "To translate the genome-wide knowledge regarding GBS into a functional application by investigating how chronic stress affects GR-mediated action of acute glucocorticoid exposure to the mTOR pathway as a novel mechanism involved in the regulation of brain plasticity."

The mTOR pathway plays a central role in translational control and has long-lasting effects on the plasticity of specific brain circuits. Whether low or high mTOR activity is better for neuronal functioning, is unclear and depends on the context and timing of stressful stimulation this pathway operates. An optimal balance of the mTOR pathway would promote LTP and memory formation, while at the same time promoting cell survival and resilience. The mTOR pathway is known to be activated by a wide variety of extracellular stimuli and also by hormones such as CORT. However, this knowledge is based mainly on peripheral tissues and has been studied less well in the brain.

In **Chapter 5**, we showed that CORT directly regulates the mTOR signalling pathway in the dentate gyrus of the rat hippocampus. Furthermore, we demonstrated that rats with a history of chronic stress have higher basal hippocampal mTOR protein levels in comparison to control animals. Interestingly, mTOR protein was decreased when chronically stressed animals received an acute CORT challenge. This is in contrast to the non-stressed controls where CORT did not show an effect on mTOR protein. We have observed that regulators of the mTOR pathway are differentially expressed after an acute CORT pulse, which was affected by a history of chronic stress. Interestingly, direct GR-binding has been validated in the case of mTOR regulators DDIT4 and FKBP51. In conclusion, we propose that direct regulation of the mTOR pathway by CORT represents an important mechanism regulating neuronal plasticity in the rat hippocampal dentate gyrus, which changes after exposure to chronic stress.

Conclusion

In this thesis the primary genomic targets of GR have been analysed within a neuronal context. Using ChIP-sequencing thousands of GBS were identified in neuronal PC12 cells and in the rat hippocampus. New transactivation and transrepression partners that enable GR potentially to generate neuronal-specific gene transcription were proposed. Two populations of GR were observed that have different sensitivities to their genetic targets depending on the concentration of CORT. Furthermore, MR was found to be capable of binding to identified GBS. Finally, a direct suppression of the mTOR pathway by CORT within the rat hippocampus was revealed if the

Chapter 7

animals previously had experienced chronic stress. Taken together, these findings contribute to a better insight into the interaction of GR with the genome in a neuronal setting and point to the pathways that are under control of GR during stress exposure and recovery. The mTOR regulation within the rat hippocampus which is clearly affected by the stress history calls for further research.

Chapter Eight

Samenvatting

Tijdens het dagelijkse leven wordt het lichaam geconfronteerd met interne en externe stimuli (ook wel stressoren genoemd) die de homeostase dreigen te verstoren. Het lichaam reageert op deze stimuli door een stressrespons te initiëren, die tot stand komt door activatie van het sympatisch zenuwstelsel en de hypothalamus-hypofyse-bijnier (HHB) as resulterend in de afgifte van respectievelijk adrenaline en corticosteroïde hormoon (CORT) uit de bijnier. CORT dringt gemakkelijk door in de hersenen en koppelt terug op die hersenstructuren die betrokken zijn bij de ontwikkeling van de stressrespons. Dit betreft o.a. de hippocampus, een limbische hersenstruktuur die van belang is voor de context waarin de stress respons ervaren is. In de hippocampus bevordert CORT leer- en geheugenprocessen. Voor dit doel bindt CORT aan twee nauw verwante receptortypen, de glucocorticoïd receptor (GR) en de mineralocorticoïd receptor (MR), waarna de receptoren migreren naar de celkern waar ze de transcriptie van CORT-responsieve genen kunnen regelen. Terwijl MR betrokken is bij het onderhouden van de basale activiteit van het stress-systeem, de inschatting van de betekenis van de stressor en het starten van de stressreactie, zorgt GR voor het herstel na de stress respons en de gedragsadaptatie. Uiteindelijk is de gebalanceerde activatie van de receptoren een belangrijke factor in neuronale exciteerbaarheid en stressresponsiviteit.

De laatste jaren is veel kennis verzameld betreffende de CORT-responsieve genen. Echter, deze inventarisaties zijn een mix van primaire CORT-responsieve genen en van genen die indirekt door MR en GR gereguleerd worden, waarbij het niet mogelijk was deze twee groepen te onderscheiden. Dankzij innovatieve technologieën, die resulteerden in de eerste ChIP-seq studies, werd het mogelijk om bindingsplaatsen van transcriptiefactoren te identificeren in het gehele genoom. Het doel van deze thesis was om de bindingsplaatsen van GR en ook MR in het genoom in een neuronale context te onderzoeken. Tevens zijn de functionele implicaties van met name de GR binding aan deze genomische locaties onderzocht. Hiervoor zijn 4 specifieke doelen geformuleerd die behandeld worden in Hoofdstukken 2 t/m 5.

Doel I: "Een *in silico* benadering gebruiken om neuronaal-specifieke GREs in het genoom te voorspellen en experimenteel te valideren".

GR kan dimerizeren en als zodanig kan het glucocorticoïd-responsieve elementen (GREs) in het DNA herkennen en binden waardoor de expressie van genen kan worden gereguleerd. GRE-afhankelijke processen zijn belangrijk in de hersenen, omdat bij muizen waar GR niet kan dimerizeren en als zodanig niet kan binden aan GREs, hippocampale exciteerbaarheid en ruimtelijk geheugen aangetast zijn. De GREs die verantwoordelijk zijn voor de GR-werking *in vivo* in de hersenen zijn grotendeels onbekend. Daarbij hoeft GR-binding aan een GRE niet altijd te leiden tot een functioneel effect. In **hoofdstuk 2** is de ontwikkeling van een Positie Specifiek Score Matrix (PSSM) beschreven van 44 GREs die toegepast is om de aanwezigheid van

evolutionair-geconserveerde GREs te voorspellen. Met deze matrix zijn grote geno-mische regio's gescand die zich rond neuronale CORT-responsieve genen bevinden. In de rat hippocampus zijn 15 van de 32 voorspelde GREs geïdentificeerd waarvan tenminste 10 GREs nieuw zijn. Verder zijn in sequenties rondom de GREs, GR-box geassocieerde motieven geïdentificeerd. Dit karakteristieke bindingsprofiel was af-wezig in een andere dataset afkomstig van een ander weefsel. Deze vondst is een aanwijzing dat GREs gebruikt kunnen worden voor het vaststellen van een weefsel-specifieke CORT werking. Concludeerd, zien we onze huidige bevindingen als een eerste stap naar een beter begrip van CORT werking in de hippocampus.

Doel II: "Het identificeren van genoomwijde GR-bindingsplaatsen (GBS) *in vitro* in neuronale PC12 cellen en *in vivo* in rat hippocampus door het toepassen van ChIP-seq en het identificeren van responsieve genen die zich in de buurt van deze GBS bevinden".

GR kan direct binden aan GREs of indirect aan het genoom via interacties met transcriptiefactoren. Deze twee mogelijkheden, die respectievelijk transactivatie en transrepressie worden genoemd, resulteren in de regulatie van een grote hoeveel-heid genen die belangrijk zijn voor neuronaal functioneren. Ondanks het feit dat veel kennis al beschikbaar was aangaande genen die differentieel tot expressie ko-men na activatie van GR, waren de primaire genomische bindingsplaatsen van GR nog niet onderzocht in een neuronale context. In **hoofdstuk 3**, is een genoombrede analyse van GBS in neuronale PC12 cellen beschreven. Op het moment van publi-catie was dit de eerste inventarisatie van GBS in een neuronale context. De meer-derheid van de PC12 GBS die uniek waren voor dit celmodel bleken gelokaliseerd te zijn bij genen met een bekende neuronale functie. **Hoofdstuk 4** betreft een ana-lyse van genomische GBS in de rat hippocampus na een acute CORT puls. In bei-de hoofdstukken is een hoge prevalentie van intragene GBS aangetoond waarvan de meerderheid gelocaliseerd is in intronen. In **hoofdstuk 3** en **4** laat een motief-analyse zien dat de GRE het meest voorkomende motief is. Dit is een aanwijzing dat GR-binding aan specifieke locaties in het DNA via transactivatie een belangrijk mechanisme is van GR om genexpressie te regelen.

In **hoofdstuk 3** en **4** is de ontdekking gerapporteerd van een motief voor Zbtb3 in de GBS, die in PC12 cellen alleen voorkwam in de niet-GRE bevattende GBS, wat aangeeft dat het een nieuwe transrepressie partner van GR in een neuronale context zou kunnen zijn (**hoofdstuk 3**). Echter bij de rat hippocampus werd Zbtb3 alleen geïdentificeerd in de GRE-bevattende GBS, wat een nieuwe transactivatie partner van GR impliceert (**hoofdstuk 4**). In de rat hippocampus waren de GBS die een combinatie van GRE and Zbtb3 bevatten geassocieerd met genen die betrokken zijn bij regulatie van apoptose, regulatie van transcriptie, regulatie van macromoleculai-re metabole processen en het insuline receptor werkingsmechanisme. Interessant genoeg zijn deze processen allemaal gekoppeld aan de mTOR signaalcascade. Con-

cluderend kan gesteld worden dat het onderzoek beschreven in **hoofdstuk 3** en **4** inzicht heeft verschaft in nieuwe aspecten van glucocorticoïdwerking via GR in een neuronale context. Ook al is het niet mogelijk gebleken alle geïdentificeerde GBS en de nieuw veronderstelde transactivatie en transrepressie partners te valideren, deze inventarisatie is van belang voor verder onderzoek naar glucocorticoïdwerking in een neuronale context. Het begrijpen hoe GR de werking van glucocorticoïden in een neuronale context tot stand brengt is belangrijk gezien de grote effecten van glucocortioïden op neuronale plasticiteit en uiteindelijk op hersenfunctie.

Doel III: "Onderzoek naar het bindingsprofiel van MR en GR aan GBS van het hippocampus genoom als functie van de CORT concentratie".

In de hersenen bindt CORT aan MR en GR. Terwijl GR tot expressie komt in iedere hersencel, is de expressie van MR beperkt tot met name de limbische hersenstructuren. Beide receptoren verschillen in hun affiniteit voor CORT; MR heeft een tien maal hogere affiniteit voor CORT dan GR. Hierdoor zal GR geactiveerd worden bij een hogere concentratie circulerend CORT, zoals tijdens stress, en zal MR al reeds geactiveerd zijn onder basale niet-stressvolle condities. De activatie van beide receptoren is een belangrijke determinant voor neuronal exciteerbaarheid en stress responsiviteit. De GR kan als dimeer binden aan GREs die aanwezig zijn in het DNA en transactivatie induceren. Verder is bekend dat GR via binding aan andere transcriptiefactoren transrepressie van door stress-geïnduceerde signaalcascades kan bewerkstelligen.

Kennis over de MR-interactie met het genoom is schaars, met name in de hersenen. In **hoofdstuk 4** hebben we gekeken naar hippocampale GR-gebonden GBS die geïdentificeerd zijn in mannelijke bijnierloze ratten die verschillende doseringen van de GR-agonist CORT, variërend van 3 tot 3,000 μg/kg intraperitoneaal toegediend hebben gekregen. Verder hebben we het vermogen van MR om te binden aan deze GBS geanalyseerd. Het blijkt dat afhankelijk van de CORT concentratie, 2 verschillende groepen GBS worden gerecruteerd. De lage-CORT groep laat GR-binding zien aan GBS bij 30 μg/kg, die verder toeneemt bij hogere CORT concentraties. In de hoge-CORT groep is GR-binding aanwezig na het injecteren van 3,000 μg/kg maar niet bij lagere concentraties CORT. MR-binding is in beide groepen al verzadigd bij 30 μg/kg.

Concluderend wijzen de resultaten op het bestaan van 2 verschillende populaties van GBS in het rat hippocampale genoom die onderscheiden kunnen worden op basis van de mate van CORT binding. Verder bindt de MR aan een selectie van GBS. De gelijktijdige binding van GR en MR aan dezelfde GRE-bevattende GBS kan heterodimerizatie van GR en MR impliceren.

Doel IV: "Onderzoek naar het effect van acute CORT toediening op de mTOR signaalcascade in ratten die blootgesteld zijn aan chronische stress."

De mTOR signaalcascade speelt een centrale rol in de controle van translatie en heeft langdurige effecten op de plasticiteit van specifieke hersengebieden. Of een lage of hoge mTOR activiteit beter is voor het neuronaal functioneren is onduidelijk en hangt af van de context en de timing van de stressvolle stimulatie die de signaalcascade beïnvloedt. mTOR is van belang voor langetermijnpotentiëring (LTP) en geheugenvorming, terwijl het ook met de handhaving van cellulaire homeostase in verband is gebracht. Het is bekend dat de mTOR signaalcascade door een groot aantal extracellulaire stimuli geactiveerd wordt. Echter, deze kennis is met name gebaseerd op het perifere systeem en is minder goed bestudeerd in de hersenen.

In **hoofdstuk 5** is beschreven dat de mTOR signaalcascade direct door CORT gereguleerd wordt in de gyrus dentatus van de rat hippocampus. Verder wordt aangetoond dat ratten die blootgesteld zijn aan chronische stress, een hoger basaal mTOR eiwitniveau hebben in de hippocampus in vergelijking met controle dieren. Echter, mTOR eiwit was drie uur na een acute CORT injectie verlaagd in de chronisch gestresste dieren. Onder deze condities komen de regulatoren van de mTOR cascade differentieel tot expressie. Voorts is de GR-binding gevalideerd bij de mTOR regulatoren DDIT4 en FKBP51. Concluderend, het blijkt dat de mTOR cascade in de rat hippocampale gyrus na chronischestress in aanzienlijke mate onderdrukt wordt door een acute toediening van CORT.

Conclusie

In deze thesis zijn de primaire genomische bindingsplaatsen van MR en GR geanalyseerd binnen een neuronale context. Door ChIP-sequencing te gebruiken zijn er duizenden GBS geïdentificeerd in neuronale PC12 cellen en in de rat hippocampus. Nieuwe transactivatie en transrepressie partners zijn geïdentificeerd waarmee GR potentieel in staat is om neuronaal-specifiek gentranscriptie te regelen. Twee GBS-populaties zijn aangetoond, die afhankelijk van de CORT concentratie door GR gebonden worden. Verder is vastgesteld dat MR bindt aan een selectie van GBS. Tenslotte is aangetoond dat in de rat hippocampus met name na chronische stress de mTOR cascade sterk onderdrukt wordt na een CORT toediening.

Tesamen dragen deze bevindingen bij aan een beter inzicht in de interactie van de GR en MR met het genoom in een neuronale context.

Chapter 8

References

Adams,M., Meijer,O.C., Wang,J., Bhargava,A., and Pearce,D. (2003). Homodimerization of the glucocorticoid receptor is not essential for response element binding: activation of the phenylethanolamine N-methyltransferase gene by dimerization-defective mutants. Mol. Endocrinol. *17*, 2583–2592.

Akhavan,D., Cloughesy,T.F., and Mischel,P.S. (2010). mTOR signaling in glioblastoma: lessons learned from bench to bedside. Neuro. Oncol. *12*, 882–889.

Alboni,S., Tascedda,F., Corsini,D., Benatti,C., Caggia,F., Capone,G., Barden,N., Blom,J.M., and Brunello,N. (2011). Stress induces altered CRE/CREB pathway activity and BDNF expression in the hippocampus of glucocorticoid receptor-impaired mice. Neuropharmacology *60*, 1337–1346.

Alfarez,D.N., Joels,M., and Krugers,H.J. (2003). Chronic unpredictable stress impairs long-term potentiation in rat hippocampal CA1 area and dentate gyrus in vitro. Eur. J. Neurosci. *17*, 1928–1934.

Allen,J.M., Martin,J.B., and Heinrich,G. (1987). Neuropeptide Y gene expression in PC12 cells and its regulation by nerve growth factor: a model for developmental regulation. Brain Res. *427*, 39–43.

Altonsy,M.O., Sasse,S.K., Phang,T.L., and Gerber,A.N. (2014). Context-dependent cooperation between nuclear factor kappaB (NF-kappaB) and the glucocorticoid receptor at a TN-FAIP3 intronic enhancer: a mechanism to maintain negative feedback control of inflammation. J. Biol. Chem. *289*, 8231–8239.

Andrus,B.M., Blizinsky,K., Vedell,P.T., Dennis,K., Shukla,P.K., Schaffer,D.J., Radulovic,J., Churchill,G.A., and Redei,E.E. (2012). Gene expression patterns in the hippocampus and amygdala of endogenous depression and chronic stress models. Mol. Psychiatry *17*, 49–61.

Antonow-Schlorke,I., Schwab,M., Li,C., and Nathanielsz,P.W. (2003). Glucocorticoid exposure at the dose used clinically alters cytoskeletal proteins and presynaptic terminals in the fetal baboon brain. J. Physiol *547*, 117–123.

Araya-Callis,C., Hiemke,C., Abumaria,N., and Flugge,G. (2012). Chronic psychosocial stress and citalopram modulate the expression of the glial proteins GFAP and NDRG2 in the hippocampus. Psychopharmacology (Berl) *224*, 209–222.

Ayalew,M., Le-Niculescu,H., Levey,D.F., Jain,N., Changala,B., Patel,S.D., Winiger,E., Breier,A., Shekhar,A., Amdur,R., Koller,D., Nurnberger,J.I., Corvin,A., Geyer,M., Tsuang,M.T., Salomon,D., Schork,N.J., Fanous,A.H., O'Donovan,M.C., and Niculescu,A.B. (2012). Convergent functional genomics of schizophrenia: from comprehensive understanding to genetic risk prediction. Mol. Psychiatry *17*, 887–905.

Bagamasbad,P., Ziera,T., Borden,S.A., Bonett,R.M., Rozeboom,A.M., Seasholtz,A., and Denver,R.J. (2012). Molecular basis for glucocorticoid induction of the Kruppel-like factor 9 gene in hippocampal neurons. Endocrinology *153*, 5334–5345.

Bailey,T.L. and Elkan,C. (1994). Fitting a mixture model by expectation maximization to discover motifs in biopolymers. Proc. Int. Conf. Intell. Syst. Mol. Biol. *2*, 28–36.

Bailey,T.L., Williams,N., Misleh,C., and Li,W.W. (2006). MEME: discovering and analyzing DNA and protein sequence motifs. Nucleic Acids Res. *34*, W369–W373.

Balic,A., Adams,D., and Mina,M. (2009). Prx1 and Prx2 cooperatively regulate the morphogenesis of the medial region of the mandibular process. Dev. Dyn. *238*, 2599–2613.

Bardwell,V.J. and Treisman,R. (1994). The POZ domain: a conserved protein-protein interaction motif. Genes Dev. *8*, 1664–1677.

Barsegyan,A., Mackenzie,S.M., Kurose,B.D., McGaugh,J.L., and Roozendaal,B. (2010). Glucocorticoids in the prefrontal cortex enhance memory consolidation and impair working memory by a common neural mechanism. Proc. Natl. Acad. Sci. U. S. A *107*, 16655–16660.

Barski,A., Cuddapah,S., Cui,K., Roh,T.Y., Schones,D.E., Wang,Z., Wei,G., Chepelev,I., and Zhao,K. (2007). High-resolution profiling of histone methylations in the human genome. Cell *129*, 823–837.

Beato,M., Chalepakis,G., Schauer,M., and Slater,E.P. (1989). DNA regulatory elements for steroid hormones. J. Steroid Biochem. *32*, 737–747.

Bekinschtein,P., Katche,C., Slipczuk,L.N., Igaz,L.M., Cammarota,M., Izquierdo,I., and Medina,J.H. (2007). mTOR signaling in the hippocampus is necessary for memory formation. Neurobiol. Learn. Mem. *87*, 303–307.

Biddie,S.C., John,S., and Hager,G.L. (2010). Genome-wide mechanisms of nuclear receptor action. Trends Endocrinol. Metab *21*, 3–9.

Biddie,S.C., John,S., Sabo,P.J., Thurman,R.E., Johnson,T.A., Schiltz,R.L., Miranda,T.B., Sung,M.H., Trump,S., Lightman,S.L., Vinson,C., Stamatoyannopoulos,J.A., and Hager,G.L. (2011). Transcription factor AP1 potentiates chromatin accessibility and glucocorticoid receptor binding. Mol. Cell *43*, 145–155.

Binder,E.B. (2009). The role of FKBP5, a co-chaperone of the glucocorticoid receptor in the pathogenesis and therapy of affective and anxiety disorders. Psychoneuroendocrinology *34 Suppl 1*, S186-S195.

Binder,E.B., Salyakina,D., Lichtner,P., Wochnik,G.M., Ising,M., Putz,B., Papiol,S., Seaman,S., Lucae,S., Kohli,M.A., Nickel,T., Kunzel,H.E., Fuchs,B., Majer,M., Pfennig,A., Kern,N., Brunner,J., Modell,S., Baghai,T., Deiml,T., Zill,P., Bondy,B., Rupprecht,R., Messer,T., Kohnlein,O., Dabitz,H., Bruckl,T., Muller,N., Pfister,H., Lieb,R., Mueller,J.C., Lohmussaar,E., Strom,T.M., Bettecken,T., Meitinger,T., Uhr,M., Rein,T., Holsboer,F., and Muller-Myhsok,B. (2004). Polymorphisms in FKBP5 are associated with increased recurrence of depressive episodes and rapid response to antidepressant treatment. Nat. Genet. *36*, 1319–1325.

Biola,A., Andreau,K., David,M., Sturm,M., Haake,M., Bertoglio,J., and Pallardy,M. (2000). The glucocorticoid receptor and STAT6 physically and functionally interact in T-lymphocytes. FEBS Lett. *487*, 229–233.

Blankenberg,D., Von,K.G., Coraor,N., Ananda,G., Lazarus,R., Mangan,M., Nekrutenko,A., and Taylor,J. (2010). Galaxy: a web-based genome analysis tool for experimentalists. Curr. Protoc. Mol. Biol. *Chapter 19*, Unit-21.

Bledsoe,R.K., Montana,V.G., Stanley,T.B., Delves,C.J., Apolito,C.J., McKee,D.D., Consler,T.G., Parks,D.J., Stewart,E.L., Willson,T.M., Lambert,M.H., Moore,J.T., Pearce,K.H., and Xu,H.E. (2002). Crystal structure of the glucocorticoid receptor ligand binding domain reveals a novel mode of receptor dimerization and coactivator recognition. Cell *110*, 93–105.

Bodnoff,S.R., Humphreys,A.G., Lehman,J.C., Diamond,D.M., Rose,G.M., and Meaney,M.J. (1995). Enduring effects of chronic corticosterone treatment on spatial learning, synaptic plasticity, and hippocampal neuropathology in young and mid-aged rats. J. Neurosci. *15*, 61–69.

Bosia,C., Osella,M., Baroudi,M.E., Cora,D., and Caselle,M. (2012). Gene autoregulation via intronic microRNAs and its functions. BMC. Syst. Biol. *6*, 131.

Boulkroun,S., Fay,M., Zennaro,M.C., Escoubet,B., Jaisser,F., Blot-Chabaud,M., Farman,N., and Courtois-Coutry,N. (2002). Characterization of rat NDRG2 (N-Myc downstream regulated gene 2), a novel early mineralocorticoid-specific induced gene. J. Biol. Chem. *277*, 31506–31515.

Bourgeron,T. (2009). A synaptic trek to autism. Curr. Opin. Neurobiol. *19*, 231–234.

Bourtchuladze,R., Frenguelli,B., Blendy,J., Cioffi,D., Schutz,G., and Silva,A.J. (1994). Deficient long-term memory in mice with a targeted mutation of the cAMP-responsive element-binding protein. Cell *79*, 59–68.

Brose,K., Bland,K.S., Wang,K.H., Arnott,D., Henzel,W., Goodman,C.S., Tessier-Lavigne,M., and Kidd,T. (1999). Slit proteins bind Robo receptors and have an evolutionarily conserved role in repulsive axon guidance. Cell *96*, 795–806.

Brudno,M., Do,C.B., Cooper,G.M., Kim,M.F., Davydov,E., Green,E.D., Sidow,A., and Batzoglou,S. (2003). LAGAN and Multi-LAGAN: efficient tools for large-scale multiple alignment of genomic DNA. Genome Res. *13*, 721–731.

Bruna,A., Nicolas,M., Munoz,A., Kyriakis,J.M., and Caelles,C. (2003). Glucocorticoid receptor-JNK interaction mediates inhibition of the JNK pathway by glucocorticoids. EMBO J. *22*, 6035–6044.

Bruni,F., Polosa,P.L., Gadaleta,M.N., Cantatore,P., and Roberti,M. (2010). Nuclear respiratory factor 2 induces the expression of many but not all human proteins acting in mitochondrial DNA transcription and replication. J. Biol. Chem. *285*, 3939–3948.

Cannarile,L., Zollo,O., D'Adamio,F., Ayroldi,E., Marchetti,C., Tabilio,A., Bruscoli,S., and Riccardi,C. (2001). Cloning, chromosomal assignment and tissue distribution of human GILZ, a glucocorticoid hormone-induced gene. Cell Death. Differ. *8*, 201–203.

Carroll,J.S., Meyer,C.A., Song,J., Li,W., Geistlinger,T.R., Eeckhoute,J., Brodsky,A.S., Keeton,E.K., Fertuck,K.C., Hall,G.F., Wang,Q., Bekiranov,S., Sementchenko,V., Fox,E.A., Silver,P.A., Gingeras,T.R., Liu,X.S., and Brown,M. (2006). Genome-wide analysis of estrogen receptor binding sites. Nat. Genet. *38*, 1289–1297.

Cereseto,M., Reines,A., Ferrero,A., Sifonios,L., Rubio,M., and Wikinski,S. (2006). Chronic treatment with high doses of corticosterone decreases cytoskeletal proteins in the rat hippocampus. Eur. J. Neurosci. *24*, 3354–3364.

Champagne,D.L., Bagot,R.C., van,H.F., Ramakers,G., Meaney,M.J., de Kloet,E.R., Joels,M., and Krugers,H. (2008). Maternal care and hippocampal plasticity: evidence for experience-dependent structural plasticity, altered synaptic functioning, and differential responsiveness to glucocorticoids and stress. J. Neurosci. *28*, 6037–6045.

Chan,O., Inouye,K., Akirav,E.M., Park,E., Riddell,M.C., Matthews,S.G., and Vranic,M. (2005). Hyperglycemia does not increase basal hypothalamo-pituitary-adrenal activity in diabetes but it does impair the HPA response to insulin-induced hypoglycemia. Am. J. Physiol Regul. Integr. Comp Physiol *289*, R235-R246.

Chandler,V.L., Maler,B.A., and Yamamoto,K.R. (1983). DNA sequences bound specifically by glucocorticoid receptor in vitro render a heterologous promoter hormone responsive in vivo. Cell *33*, 489–499.

Chang,C.M. and Chao,C.C. (2013). Protein kinase CK2 enhances Mcl-1 gene expression through the serum response factor-mediated pathway in the rat hippocampus. J. Neurosci. Res. *91*, 808–817.

Chang,T.J., Scher,B.M., Waxman,S., and Scher,W. (1993). Inhibition of mouse GATA-1 function by the glucocorticoid receptor: possible mechanism of steroid inhibition of erythroleukemia cell differentiation. Mol. Endocrinol. *7*, 528–542.

Chao,H.M., Choo,P.H., and McEwen,B.S. (1989). Glucocorticoid and mineralocorticoid receptor mRNA expression in rat brain. Neuroendocrinology *50*, 365–371.

Charmandari,E., Chrousos,G.P., Ichijo,T., Bhattacharyya,N., Vottero,A., Souvatzoglou,E., and Kino,T. (2005). The human glucocorticoid receptor (hGR) beta isoform suppresses the transcriptional activity of hGRalpha by interfering with formation of active coactivator complexes. Mol. Endocrinol. *19*, 52–64.

Chebotaev,D., Yemelyanov,A., and Budunova,I. (2007). The mechanisms of tumor suppressor effect of glucocorticoid receptor in skin. Mol. Carcinog. *46*, 732–740.

Chen,Y., Dube,C.M., Rice,C.J., and Baram,T.Z. (2008). Rapid loss of dendritic spines after stress involves derangement of spine dynamics by corticotropin-releasing hormone. J. Neurosci. *28*, 2903–2911.

Chen,Y.J., Tan,B.C., Cheng,Y.Y., Chen,J.S., and Lee,S.C. (2010). Differential regulation of CHOP translation by phosphorylated eIF4E under stress conditions. Nucleic Acids Res. *38*, 764–777.

Chinenov,Y., Gupte,R., Dobrovolna,J., Flammer,J.R., Liu,B., Michelassi,F.E., and Rogatsky,I. (2012). Role of transcriptional coregulator GRIP1 in the anti-inflammatory actions of glucocorticoids. Proc. Natl. Acad. Sci. U. S. A *109*, 11776–11781.

Choi,K.C., Kim,S.H., Ha,J.Y., Kim,S.T., and Son,J.H. (2010). A novel mTOR activating protein protects dopamine neurons against oxidative stress by repressing autophagy related cell death. J. Neurochem. *112*, 366–376.

Chong,Z.Z., Shang,Y.C., Wang,S., and Maiese,K. (2012). Shedding new light on neurodegenerative diseases through the mammalian target of rapamycin. Prog. Neurobiol. *99*, 128–148.

Chrousos,G.P. and Kino,T. (2009). Glucocorticoid signaling in the cell. Expanding clinical implications to complex human behavioral and somatic disorders. Ann. N. Y. Acad. Sci. *1179*, 153–166.

Cole,T.J., Blendy,J.A., Monaghan,A.P., Krieglstein,K., Schmid,W., Aguzzi,A., Fantuzzi,G., Hummler,E., Unsicker,K., and Schutz,G. (1995). Targeted disruption of the glucocorticoid receptor gene blocks adrenergic chromaffin cell development and severely retards lung maturation. Genes Dev. *9*, 1608–1621.

Conway-Campbell,B.L., Pooley,J.R., Hager,G.L., and Lightman,S.L. (2012). Molecular dynamics of ultradian glucocorticoid receptor action. Mol. Cell Endocrinol. *348*, 383–393.

Conway-Campbell,B.L., Sarabdjitsingh,R.A., McKenna,M.A., Pooley,J.R., Kershaw,Y.M., Meijer,O.C., de Kloet,E.R., and Lightman,S.L. (2010). Glucocorticoid ultradian rhythmicity directs cyclical gene pulsing of the clock gene period 1 in rat hippocampus. J. Neuroendocrinol. *22*, 1093–1100.

Corradetti,M.N., Inoki,K., and Guan,K.L. (2005). The stress-inducted proteins RTP801 and RTP801L are negative regulators of the mammalian target of rapamycin pathway. J. Biol. Chem. *280*, 9769–9772.

Costeas,P.A. and Chinsky,J.M. (2000). Glucocorticoid regulation of branched-chain alpha-ketoacid dehydrogenase E2 subunit gene expression. Biochem. J. *347*, 449–457.

Costello,D.A., Claret,M., Al-Qassab,H., Plattner,F., Irvine,E.E., Choudhury,A.I., Giese,K.P., Withers,D.J., and Pedarzani,P. (2012). Brain deletion of insulin receptor substrate 2 disrupts hippocampal synaptic plasticity and metaplasticity. PLoS. One. *7*, e31124.

Dai,J., Wang,X., Chen,Y., Wang,X., Zhu,J., and Lu,L. (2009). Expression quantitative trait loci and genetic regulatory network analysis reveals that Gabra2 is involved in stress responses in the mouse. Stress. *12*, 499–506.

Datson,N.A., Meijer,L., Steenbergen,P.J., Morsink,M.C., van der Laan,S., Meijer,O.C., and de Kloet,E.R. (2004). Expression profiling in laser-microdissected hippocampal subregions in rat brain reveals large subregion-specific differences in expression. Eur. J. Neurosci. *20*, 2541–2554.

Datson,N.A., Morsink,M.C., Meijer,O.C., and de Kloet,E.R. (2008). Central corticosteroid actions: Search for gene targets. Eur. J. Pharmacol. *583*, 272–289.

Datson,N.A., Polman,J.A., de Jonge,R.T., van Boheemen,P.T., van Maanen,E.M., Welten,J., McEwen,B.S., Meiland,H.C., and Meijer,O.C. (2011). Specific regulatory motifs predict glucocorticoid responsiveness of hippocampal gene expression. Endocrinology *152*, 3749–3757.

Datson,N.A., Speksnijder,N., Mayer,J.L., Steenbergen,P.J., Korobko,O., Goeman,J., de Kloet,E.R., Joels,M., and Lucassen,P.J. (2012). The transcriptional response to chronic stress and glucocorticoid receptor blockade in the hippocampal dentate gyrus. Hippocampus *22*, 359–371.

Datson,N.A., van den Oever,J.M., Korobko,O.B., Magarinos,A.M., de Kloet,E.R., and McEwen,B.S. (2013). Previous history of chronic stress changes the transcriptional response to glucocorticoid challenge in the dentate gyrus region of the male rat hippocampus. Endocrinology *154*, 3261–3272.

Datson,N.A., van der Perk,J., de Kloet,E.R., and Vreugdenhil,E. (2001a). Expression profile of 30.000 genes in rat hippocampus using SAGE. Hippocampus *11*, 430–444.

Datson,N.A., van der Perk,J., de Kloet,E.R., and Vreugdenhil,E. (2001b). Identification of corticosteroid-responsive genes in rat hippocampus using serial analysis of gene expression. Eur. J. Neurosci. *14*, 675–689.

De Bosscher K., Van,C.K., Meijer,O.C., and Haegeman,G. (2008). Selective transrepression versus transactivation mechanisms by glucocorticoid receptor modulators in stress and immune systems. Eur. J. Pharmacol. *583*, 290–302.

De Bosscher K., Vanden Berghe,W., and Haegeman,G. (2006). Cross-talk between nuclear receptors and nuclear factor kappaB. Oncogene 25, 6868–6886.

de Kloet,E.R. (2014). From receptor balance to rational glucocorticoid therapy. Endocrinology *155*, 2754–2769.

de Kloet,E.R., Joels,M., and Holsboer,F. (2005). Stress and the brain: from adaptation to disease. Nat. Rev. Neurosci. *6*, 463–475.

de Kloet,E.R., Vreugdenhil,E., Oitzl,M.S., and Joels,M. (1998). Brain corticosteroid receptor balance in health and disease. Endocr. Rev. *19*, 269–301.

de Lange,P., Segeren,C.M., Koper,J.W., Wiemer,E., Sonneveld,P., Brinkmann,A.O., White,A., Brogan,I.J., de Jong,F.H., and Lamberts,S.W. (2001). Expression in hematological malignancies of a glucocorticoid receptor splice variant that augments glucocorticoid receptor-mediated effects in transfected cells. Cancer Res. *61*, 3937–3941.

De Rijk,R.H., Schaaf,M., Stam,F.J., de Jong,I.E., Swaab,D.F., Ravid,R., Vreugdenhil,E., Cidlowski,J.A., de Kloet,E.R., and Lucassen,P.J. (2003). Very low levels of the glucocorticoid receptor beta isoform in the human hippocampus as shown by Taqman RT-PCR and immunocytochemistry. Brain Res. Mol. Brain Res. *116*, 17–26.

Deweindt,C., Albagli,O., Bernardin,F., Dhordain,P., Quief,S., Lantoine,D., Kerckaert,J.P., and Leprince,D. (1995). The LAZ3/BCL6 oncogene encodes a sequence-specific transcriptional inhibitor: a novel function for the BTB/POZ domain as an autonomous repressing domain. Cell Growth Differ. *6*, 1495–1503.

Di Nardo A., Kramvis,I., Cho,N., Sadowski,A., Meikle,L., Kwiatkowski,D.J., and Sahin,M. (2009). Tuberous sclerosis complex activity is required to control neuronal stress responses in an mTOR-dependent manner. J. Neurosci. *29*, 5926–5937.

Djordjevic,J., Djordjevic,A., Adzic,M., Mitic,M., Lukic,I., and Radojcic,M.B. (2015). Alterations in the Nrf2-Keap1 signaling pathway and its downstream target genes in rat brain under stress. Brain Res. *1602*, 20–31.

Drouin,J., Sun,Y.L., Chamberland,M., Gauthier,Y., De,L.A., Nemer,M., and Schmidt,T.J. (1993). Novel glucocorticoid receptor complex with DNA element of the hormone-repressed POMC gene. EMBO J. *12*, 145–156.

Du,J., Wang,Y., Hunter,R., Wei,Y., Blumenthal,R., Falke,C., Khairova,R., Zhou,R., Yuan,P., Machado-Vieira,R., McEwen,B.S., and Manji,H.K. (2009). Dynamic regulation of mitochondrial function by glucocorticoids. Proc. Natl. Acad. Sci. U. S. A *106*, 3543–3548.

Dwyer,J.M., Lepack,A.E., and Duman,R.S. (2012). mTOR activation is required for the antidepressant effects of mGluR(2)/(3) blockade. Int. J. Neuropsychopharmacol. *15*, 429–434.

Ellisen,L.W., Ramsayer,K.D., Johannessen,C.M., Yang,A., Beppu,H., Minda,K., Oliner,J.D., McKeon,F., and Haber,D.A. (2002). REDD1, a developmentally regulated transcriptional target of p63 and p53, links p63 to regulation of reactive oxygen species. Mol. Cell *10*, 995–1005.

Euskirchen,G.M., Rozowsky,J.S., Wei,C.L., Lee,W.H., Zhang,Z.D., Hartman,S., Emanuelsson,O., Stolc,V., Weissman,S., Gerstein,M.B., Ruan,Y., and Snyder,M. (2007). Mapping of transcription factor binding regions in mammalian cells by ChIP: comparison of array- and sequencing-based technologies. Genome Res. *17*, 898–909.

Fang,Z.H., Lee,C.H., Seo,M.K., Cho,H., Lee,J.G., Lee,B.J., Park,S.W., and Kim,Y.H. (2013). Effect of treadmill exercise on the BDNF-mediated pathway in the hippocampus of stressed rats. Neurosci. Res. *76*, 187–194.

Feldker,D.E., Morsink,M.C., Veenema,A.H., Datson,N.A., Proutski,V., Lathouwers,D., de Kloet,E.R., and Vreugdenhil,E. (2006). The effect of chronic exposure to highly aggressive mice on hippocampal gene expression of non-aggressive subordinates. Brain Res. *1089*, 10–20.

Fernandez-Chacon,R., Konigstorfer,A., Gerber,S.H., Garcia,J., Matos,M.F., Stevens,C.F., Brose,N., Rizo,J., Rosenmund,C., and Sudhof,T.C. (2001). Synaptotagmin I functions as a calcium regulator of release probability. Nature *410*, 41–49.

Ferreira,R., Ohneda,K., Yamamoto,M., and Philipsen,S. (2005). GATA1 function, a paradigm for transcription factors in hematopoiesis. Mol. Cell Biol. *25*, 1215–1227.

First,M., Gil-Ad,I., Taler,M., Tarasenko,I., Novak,N., and Weizman,A. (2011). The effects of fluoxetine treatment in a chronic mild stress rat model on depression-related behavior, brain neurotrophins and ERK expression. J. Mol. Neurosci. *45*, 246–255.

Galliher-Beckley,A.J. and Cidlowski,J.A. (2009). Emerging roles of glucocorticoid receptor phosphorylation in modulating glucocorticoid hormone action in health and disease. IUBMB. Life *61*, 979–986.

References

Gauthier,J.M., Bourachot,B., Doucas,V., Yaniv,M., and Moreau-Gachelin,F. (1993). Functional interference between the Spi-1/PU.1 oncoprotein and steroid hormone or vitamin receptors. EMBO J. *12*, 5089–5096.

Gemert Van, arvalho,D.M., arst,H., an der Laan,S., hang,M., eijer,O.C., ell,J.W., and oels,M. (2009). Dissociation between rat hippocampal CA1 and dentate gyrus cells in their response to corticosterone: effects on calcium channel protein and current. Endocrinology *150*, 4615–4624.

Gemert van,N.G., Meijer,O.C., Morsink,M.C., and Joels,M. (2006). Effect of brief corticosterone administration on SGK1 and RGS4 mRNA expression in rat hippocampus. Stress. *9*, 165–170.

Gertz,J., Savic,D., Varley,K.E., Partridge,E.C., Safi,A., Jain,P., Cooper,G.M., Reddy,T.E., Crawford,G.E., and Myers,R.M. (2013). Distinct properties of cell-type-specific and shared transcription factor binding sites. Mol. Cell *52*, 25–36.

Gillespie,C.F., Phifer,J., Bradley,B., and Ressler,K.J. (2009). Risk and resilience: genetic and environmental influences on development of the stress response. Depress. Anxiety. *26*, 984–992.

Glass,C.K. and Saijo,K. (2010). Nuclear receptor transrepression pathways that regulate inflammation in macrophages and T cells. Nat. Rev. Immunol. *10*, 365–376.

Goecks,J., Nekrutenko,A., and Taylor,J. (2010). Galaxy: a comprehensive approach for supporting accessible, reproducible, and transparent computational research in the life sciences. Genome Biol. *11*, R86.

Goshima,Y., Ito,T., Sasaki,Y., and Nakamura,F. (2002). Semaphorins as signals for cell repulsion and invasion. J. Clin. Invest *109*, 993–998.

Gould,E., McEwen,B.S., Tanapat,P., Galea,L.A., and Fuchs,E. (1997). Neurogenesis in the dentate gyrus of the adult tree shrew is regulated by psychosocial stress and NMDA receptor activation. J. Neurosci. *17*, 2492–2498.

Gourley,S.L., Wu,F.J., Kiraly,D.D., Ploski,J.E., Kedves,A.T., Duman,R.S., and Taylor,J.R. (2008). Regionally specific regulation of ERK MAP kinase in a model of antidepressant-sensitive chronic depression. Biol. Psychiatry *63*, 353–359.

Gray,J.D., Rubin,T.G., Hunter,R.G., and McEwen,B.S. (2014). Hippocampal gene expression changes underlying stress sensitization and recovery. Mol. Psychiatry *19*, 1171–1178.

Greene,J.G., Borges,K., and Dingledine,R. (2009). Quantitative transcriptional neuroanatomy of the rat hippocampus: evidence for wide-ranging, pathway-specific heterogeneity among three principal cell layers. Hippocampus *19*, 253–264.

Greene,L.A. and Tischler,A.S. (1976). Establishment of a noradrenergic clonal line of rat adrenal pheochromocytoma cells which respond to nerve growth factor. Proc. Natl. Acad. Sci. U. S. A *73*, 2424–2428.

Gromak,N. (2012). Intronic microRNAs: a crossroad in gene regulation. Biochem. Soc. Trans. *40*, 759–761.

Gupta,S., Stamatoyannopoulos,J.A., Bailey,T.L., and Noble,W.S. (2007). Quantifying similarity between motifs. Genome Biol. *8*, R24.

Gutsaeva,D.R., Suliman,H.B., Carraway,M.S., Demchenko,I.T., and Piantadosi,C.A. (2006). Oxygen-induced mitochondrial biogenesis in the rat hippocampus. Neuroscience *137*, 493–504.

Harris,A.P., Holmes,M.C., de Kloet,E.R., Chapman,K.E., and Seckl,J.R. (2012). Mineralocorticoid and glucocorticoid receptor balance in control of HPA axis and behaviour. Psychoneuroendocrinology.

He,X., Chatterjee,R., John,S., Bravo,H., Sathyanarayana,B.K., Biddie,S.C., FitzGerald,P.C., Stamatoyannopoulos,J.A., Hager,G.L., and Vinson,C. (2013). Contribution of nucleosome binding preferences and co-occurring DNA sequences to transcription factor binding. BMC. Genomics *14*, 428.

Heine,V.M., Maslam,S., Zareno,J., Joels,M., and Lucassen,P.J. (2004). Suppressed proliferation and apoptotic changes in the rat dentate gyrus after acute and chronic stress are reversible. Eur. J. Neurosci. *19*, 131–144.

Hellman,L.M. and Fried,M.G. (2007). Electrophoretic mobility shift assay (EMSA) for detecting protein-nucleic acid interactions. Nat. Protoc. 2, 1849–1861.

Her,S., Claycomb,R., Tai,T.C., and Wong,D.L. (2003). Regulation of the rat phenylethanolamine N-methyltransferase gene by transcription factors Sp1 and MAZ. Mol. Pharmacol. *64*, 1180–1188.

Herman,J.P. (2013). Neural control of chronic stress adaptation. Front Behav. Neurosci. 7, 61.

Herrlich,P. and Ponta,H. (1994). Mutual cross-modulation of steroid/retinoic acid receptor and AP-1 transcription factor activities: a novel property with practical implications. Trends Endocrinol. Metab 5, 341–346.

Hoeffer,C.A. and Klann,E. (2010). mTOR signaling: at the crossroads of plasticity, memory and disease. Trends Neurosci. 33, 67–75.

Hoo,R.L., Chu,J.Y., Yuan,Y., Yeung,C.M., Chan,K.Y., and Chow,B.K. (2010). Functional identification of an intronic promoter of the human glucose-dependent insulinotropic polypeptide gene. Gene *463*, 29–40.

Horie-Inoue,K., Takayama,K., Bono,H.U., Ouchi,Y., Okazaki,Y., and Inoue,S. (2006). Identification of novel steroid target genes through the combination of bioinformatics and functional analysis of hormone response elements. Biochem. Biophys. Res. Commun. *339*, 99–106.

Hou,L. and Klann,E. (2004). Activation of the phosphoinositide 3-kinase-Akt-mammalian target of rapamycin signaling pathway is required for metabotropic glutamate receptor-dependent long-term depression. J. Neurosci. *24*, 6352–6361.

Howell,J.J. and Manning,B.D. (2011). mTOR couples cellular nutrient sensing to organismal metabolic homeostasis. Trends Endocrinol. Metab *22*, 94–102.

Howell,K.R., Kutiyanawalla,A., and Pillai,A. (2011). Long-term continuous corticosterone treatment decreases VEGF receptor-2 expression in frontal cortex. PLoS. One. *6*, e20198.

Howland,J.G. and Wang,Y.T. (2008). Synaptic plasticity in learning and memory: stress effects in the hippocampus. Prog. Brain Res. *169*, 145–158.

Huang,d.W., Sherman,B.T., and Lempicki,R.A. (2009a). Bioinformatics enrichment tools: paths toward the comprehensive functional analysis of large gene lists. Nucleic Acids Res. *37*, 1–13.

Huang,d.W., Sherman,B.T., and Lempicki,R.A. (2009b). Systematic and integrative analysis of large gene lists using DAVID bioinformatics resources. Nat. Protoc. *4*, 44–57.

Huang,X., Zhang,H., Yang,J., Wu,J., McMahon,J., Lin,Y., Cao,Z., Gruenthal,M., and Huang,Y. (2010). Pharmacological inhibition of the mammalian target of rapamycin pathway suppresses acquired epilepsy. Neurobiol. Dis. *40*, 193–199.

Hudson,W.H., Youn,C., and Ortlund,E.A. (2013). The structural basis of direct glucocorticoid-mediated transrepression. Nat. Struct. Mol. Biol. *20*, 53–58.

Hunter,R.G., McCarthy,K.J., Milne,T.A., Pfaff,D.W., and McEwen,B.S. (2009). Regulation of hippocampal H3 histone methylation by acute and chronic stress. Proc. Natl. Acad. Sci. U. S. A *106*, 20912–20917.

Hutchins,A.P., Poulain,S., and Miranda-Saavedra,D. (2012). Genome-wide analysis of STAT3 binding in vivo predicts effectors of the anti-inflammatory response in macrophages. Blood *119*, e110-e119.

Huynh,K.D. and Bardwell,V.J. (1998). The BCL-6 POZ domain and other POZ domains interact with the co-repressors N-CoR and SMRT. Oncogene *17*, 2473–2484.

Igreja,C. and Izaurralde,E. (2011). CUP promotes deadenylation and inhibits decapping of mRNA targets. Genes Dev. *25*, 1955–1967.

Imai,E., Miner,J.N., Mitchell,J.A., Yamamoto,K.R., and Granner,D.K. (1993). Glucocorticoid receptor-cAMP response element-binding protein interaction and the response of the phosphoenolpyruvate carboxykinase gene to glucocorticoids. J. Biol. Chem. *268*, 5353–5356.

Jernigan,C.S., Goswami,D.B., Austin,M.C., Iyo,A.H., Chandran,A., Stockmeier,C.A., and Karolewicz,B. (2011). The mTOR signaling pathway in the prefrontal cortex is compromised in major depressive disorder. Prog. Neuropsychopharmacol. Biol. Psychiatry *35*, 1774–1779.

Ji,H., Jiang,H., Ma,W., Johnson,D.S., Myers,R.M., and Wong,W.H. (2008). An integrated software system for analyzing ChIP-chip and ChIP-seq data. Nat. Biotechnol. *26*, 1293–1300.

Jilg,A., Lesny,S., Peruzki,N., Schwegler,H., Selbach,O., Dehghani,F., and Stehle,J.H. (2010). Temporal dynamics of mouse hippocampal clock gene expression support memory processing. Hippocampus *20*, 377–388.

Joels,M., Velzing,E., Nair,S., Verkuyl,J.M., and Karst,H. (2003). Acute stress increases calcium current amplitude in rat hippocampus: temporal changes in physiology and gene expression. Eur. J. Neurosci. *18*, 1315–1324.

John,S., Johnson,T.A., Sung,M.H., Biddie,S.C., Trump,S., Koch-Paiz,C.A., Davis,S.R., Walker,R., Meltzer,P.S., and Hager,G.L. (2009). Kinetic complexity of the global response to glucocorticoid receptor action. Endocrinology *150*, 1766–1774.

John,S., Sabo,P.J., Thurman,R.E., Sung,M.H., Biddie,S.C., Johnson,T.A., Hager,G.L., and Stamatoyannopoulos,J.A. (2011). Chromatin accessibility pre-determines glucocorticoid receptor binding patterns. Nat. Genet. *43*, 264–268.

Johnson,D.S., Mortazavi,A., Myers,R.M., and Wold,B. (2007). Genome-wide mapping of in vivo protein-DNA interactions. Science *316*, 1497–1502.

Johnson,L.R., Farb,C., Morrison,J.H., McEwen,B.S., and LeDoux,J.E. (2005). Localization of glucocorticoid receptors at postsynaptic membranes in the lateral amygdala. Neuroscience *136*, 289–299.

Jonat,C., Rahmsdorf,H.J., Park,K.K., Cato,A.C., Gebel,S., Ponta,H., and Herrlich,P. (1990). Antitumor promotion and antiinflammation: down-modulation of AP-1 (Fos/Jun) activity by glucocorticoid hormone. Cell *62*, 1189–1204.

Kapranov,P. (2009). From transcription start site to cell biology. Genome Biol. *10*, 217.

Karatsoreos,I.N. and McEwen,B.S. (2013). Resilience and vulnerability: a neurobiological perspective. F1000Prime. Rep. *5*, 13.

Karst,H. and Joels,M. (2003). Effect of chronic stress on synaptic currents in rat hippocampal dentate gyrus neurons. J. Neurophysiol. *89*, 625–633.

Karst,H., Karten,Y.J., Reichardt,H.M., de Kloet,E.R., Schutz,G., and Joels,M. (2000). Corticosteroid actions in hippocampus require DNA binding of glucocorticoid receptor homodimers. Nat. Neurosci. *3*, 977–978.

Kassel,O. and Herrlich,P. (2007). Crosstalk between the glucocorticoid receptor and other transcription factors: molecular aspects. Mol. Cell Endocrinol. *275*, 13–29.

Kel,A.E., Gossling,E., Reuter,I., Cheremushkin,E., Kel-Margoulis,O.V., and Wingender,E. (2003). MATCH: A tool for searching transcription factor binding sites in DNA sequences. Nucleic Acids Res. *31*, 3576–3579.

Kelly,E.J., Sandgren,E.P., Brinster,R.L., and Palmiter,R.D. (1997). A pair of adjacent glucocorticoid response elements regulate expression of two mouse metallothionein genes. Proc. Natl. Acad. Sci. U. S. A *94*, 10045–10050.

Kent,W.J., Sugnet,C.W., Furey,T.S., Roskin,K.M., Pringle,T.H., Zahler,A.M., and Haussler,D. (2002). The human genome browser at UCSC. Genome Res. *12*, 996–1006.

Kim,J. and Hoffman,D.A. (2008). Potassium channels: newly found players in synaptic plasticity. Neuroscientist. *14*, 276–286.

Kim,J.J., Song,E.Y., and Kosten,T.A. (2006). Stress effects in the hippocampus: synaptic plasticity and memory. Stress. *9*, 1–11.

Kinyamu,H.K., Collins,J.B., Grissom,S.F., Hebbar,P.B., and Archer,T.K. (2008). Genome wide transcriptional profiling in breast cancer cells reveals distinct changes in hormone receptor target genes and chromatin modifying enzymes after proteasome inhibition. Mol. Carcinog. *47*, 845–885.

Komatsuzaki,Y., Hatanaka,Y., Murakami,G., Mukai,H., Hojo,Y., Saito,M., Kimoto,T., and Kawato,S. (2012). Corticosterone induces rapid spinogenesis via synaptic glucocorticoid receptors and kinase networks in hippocampus. PLoS. One. *7*, e34124.

Kooi van der, Onuma,H., Oeser,J.K., Svitek,C.A., Allen,S.R., Vander Kooi,C.W., Chazin,W.J., and O'Brien,R.M. (2005). The glucose-6-phosphatase catalytic subunit gene promoter contains both positive and negative glucocorticoid response elements. Mol. Endocrinol. *19*, 3001–3022.

Krugers,H.J., Goltstein,P.M., van der Linden,S., and Joels,M. (2006). Blockade of glucocorticoid receptors rapidly restores hippocampal CA1 synaptic plasticity after exposure to chronic stress. Eur. J. Neurosci. *23*, 3051–3055.

Krum,S.A., Miranda-Carboni,G.A., Lupien,M., Eeckhoute,J., Carroll,J.S., and Brown,M. (2008). Unique ERalpha cistromes control cell type-specific gene regulation. Mol. Endocrinol. *22*, 2393–2406.

Kumar,S. (2011). Remote homologue identification of Drosophila GAGA factor in mouse. Bioinformation. *7*, 29–32.

Kunarso,G., Chia,N.Y., Jeyakani,J., Hwang,C., Lu,X., Chan,Y.S., Ng,H.H., and Bourque,G. (2010). Transposable elements have rewired the core regulatory network of human embryonic stem cells. Nat. Genet. *42*, 631–634.

Landt,S.G., Marinov,G.K., Kundaje,A., Kheradpour,P., Pauli,F., Batzoglou,S., Bernstein,B.E., Bickel,P., Brown,J.B., Cayting,P., Chen,Y., DeSalvo,G., Epstein,C., Fisher-Aylor,K.I., Euskirchen,G., Gerstein,M., Gertz,J., Hartemink,A.J., Hoffman,M.M., Iyer,V.R., Jung,Y.L., Karmakar,S., Kellis,M., Kharchenko,P.V., Li,Q., Liu,T., Liu,X.S., Ma,L., Milosavljevic,A., Myers,R.M., Park,P.J., Pazin,M.J., Perry,M.D., Raha,D., Reddy,T.E., Rozowsky,J., Shoresh,N.,

Sidow,A., Slattery,M., Stamatoyannopoulos,J.A., Tolstorukov,M.Y., White,K.P., Xi,S., Farnham,P.J., Lieb,J.D., Wold,B.J., and Snyder,M. (2012). ChIP-seq guidelines and practices of the ENCODE and modENCODE consortia. Genome Res. 22, 1813–1831.

Langlais,D., Couture,C., Balsalobre,A., and Drouin,J. (2012). The Stat3/GR interaction code: predictive value of direct/indirect DNA recruitment for transcription outcome. Mol. Cell 47, 38–49.

Leal,G., Comprido,D., and Duarte,C.B. (2014). BDNF-induced local protein synthesis and synaptic plasticity. Neuropharmacology 76 Pt C, 639–656.

Lee,P.R., Brady,D., and Koenig,J.I. (2003). Corticosterone alters N-methyl-D-aspartate receptor subunit mRNA expression before puberty. Brain Res. Mol. Brain Res. 115, 55–62.

Lee,R.S., Tamashiro,K.L., Yang,X., Purcell,R.H., Harvey,A., Willour,V.L., Huo,Y., Rongione,M., Wand,G.S., and Potash,J.B. (2010). Chronic corticosterone exposure increases expression and decreases deoxyribonucleic acid methylation of Fkbp5 in mice. Endocrinology 151, 4332–4343.

Lein,E.S., Hawrylycz,M.J., Ao,N., Ayres,M., Bensinger,A., Bernard,A., Boe,A.F., Boguski,M.S., Brockway,K.S., Byrnes,E.J., Chen,L., Chen,L., Chen,T.M., Chin,M.C., Chong,J., Crook,B.E., Czaplinska,A., Dang,C.N., Datta,S., Dee,N.R., Desaki,A.L., Desta,T., Diep,E., Dolbeare,T.A., Donelan,M.J., Dong,H.W., Dougherty,J.G., Duncan,B.J., Ebbert,A.J., Eichele,G., Estin,L.K., Faber,C., Facer,B.A., Fields,R., Fischer,S.R., Fliss,T.P., Frensley,C., Gates,S.N., Glattfelder,K.J., Halverson,K.R., Hart,M.R., Hohmann,J.G., Howell,M.P., Jeung,D.P., Johnson,R.A., Karr,P.T., Kawal,R., Kidney,J.M., Knapik,R.H., Kuan,C.L., Lake,J.H., Laramee,A.R., Larsen,K.D., Lau,C., Lemon,T.A., Liang,A.J., Liu,Y., Luong,L.T., Michaels,J., Morgan,J.J., Morgan,R.J., Mortrud,M.T., Mosqueda,N.F., Ng,L.L., Ng,R., Orta,G.J., Overly,C.C., Pak,T.H., Parry,S.E., Pathak,S.D., Pearson,O.C., Puchalski,R.B., Riley,Z.L., Rockett,H.R., Rowland,S.A., Royall,J.J., Ruiz,M.J., Sarno,N.R., Schaffnit,K., Shapovalova,N.V., Sivisay,T., Slaughterbeck,C.R., Smith,S.C., Smith,K.A., Smith,B.I., Sodt,A.J., Stewart,N.N., Stumpf,K.R., Sunkin,S.M., Sutram,M., Tam,A., Teemer,C.D., Thaller,C., Thompson,C.L., Varnam,L.R., Visel,A., Whitlock,R.M., Wohnoutka,P.E., Wolkey,C.K., Wong,V.Y., Wood,M., Yaylaoglu,M.B., Young,R.C., Youngstrom,B.L., Yuan,X.F., Zhang,B., Zwingman,T.A., and Jones,A.R. (2007). Genome-wide atlas of gene expression in the adult mouse brain. Nature 445, 168–176.

Lein,E.S., Zhao,X., and Gage,F.H. (2004). Defining a molecular atlas of the hippocampus using DNA microarrays and high-throughput in situ hybridization. J. Neurosci. 24, 3879–3889.

Lemetre,C. and Zhang,Z.D. (2013). A brief introduction to tiling microarrays: principles, concepts, and applications. Methods Mol. Biol. 1067, 3–19.

Li,H. and Durbin,R. (2009). Fast and accurate short read alignment with Burrows-Wheeler transform. Bioinformatics. 25, 1754–1760.

Li,N., Lee,B., Liu,R.J., Banasr,M., Dwyer,J.M., Iwata,M., Li,X.Y., Aghajanian,G., and Duman,R.S. (2010). mTOR-dependent synapse formation underlies the rapid antidepressant effects of NMDA antagonists. Science 329, 959–964.

Lim,J.H. (2014). Zinc finger and BTB domain-containing protein 3 is essential for the growth of cancer cells. BMB. Rep. 47, 405–410.

Lipton,J.O. and Sahin,M. (2014). The neurology of mTOR. Neuron 84, 275–291.

Lisowski,P., Juszczak,G.R., Goscik,J., Wieczorek,M., Zwierzchowski,L., and Swiergiel,A.H. (2011). Effect of chronic mild stress on hippocampal transcriptome in mice selected for high and low stress-induced analgesia and displaying different emotional behaviors. Eur. Neuropsychopharmacol. *21*, 45–62.

Liu,Q., Qiu,J., Liang,M., Golinski,J., van,L.K., Jung,J.E., You,Z., Lo,E.H., Degterev,A., and Whalen,M.J. (2014). Akt and mTOR mediate programmed necrosis in neurons. Cell Death. Dis. 5, e1084.

Liu,Y., Wei,L., Batzoglou,S., Brutlag,D.L., Liu,J.S., and Liu,X.S. (2004). A suite of web-based programs to search for transcriptional regulatory motifs. Nucleic Acids Res. 32, W204-W207.

Livak,K.J. and Schmittgen,T.D. (2001). Analysis of relative gene expression data using real-time quantitative PCR and the 2(-Delta Delta C(T)) Method. Methods 25, 402–408.

Lu,N.Z. and Cidlowski,J.A. (2005). Translational regulatory mechanisms generate N-terminal glucocorticoid receptor isoforms with unique transcriptional target genes. Mol. Cell *18*, 331–342.

Lu,Y., Wang,C., Xue,Z., Li,C., Zhang,J., Zhao,X., Liu,A., Wang,Q., and Zhou,W. (2015). PI3K/AKT/mTOR signaling-mediated neuropeptide VGF in the hippocampus of mice is involved in the rapid onset antidepressant-like effects of GLYX-13. Int. J. Neuropsychopharmacol. *18*.

Ma,Y., Wu,X., Li,X., Fu,J., Shen,J., Li,X., and Wang,H. (2012). Corticosterone regulates the expression of neuropeptide Y and reelin in MLO-Y4 cells. Mol. Cells 33, 611–616.

Magarinos,A.M., McEwen,B.S., Flugge,G., and Fuchs,E. (1996). Chronic psychosocial stress causes apical dendritic atrophy of hippocampal CA3 pyramidal neurons in subordinate tree shrews. J. Neurosci. *16*, 3534–3540.

Malagelada,C., Jin,Z.H., and Greene,L.A. (2008). RTP801 is induced in Parkinson's disease and mediates neuron death by inhibiting Akt phosphorylation/activation. J. Neurosci. *28*, 14363–14371.

Mardis,E.R. (2007). ChIP-seq: welcome to the new frontier. Nat. Methods *4*, 613–614.

Masuno,K., Haldar,S.M., Jeyaraj,D., Mailloux,C.M., Huang,X., Panettieri,R.A., Jr., Jain,M.K., and Gerber,A.N. (2011). Expression profiling identifies Klf15 as a glucocorticoid target that regulates airway hyperresponsiveness. Am. J. Respir. Cell Mol. Biol. 45, 642–649.

McEwen, B. S. Allostasis and Allostatis Load. Encyclopedia of Stress. *1*, 145–150. 2000. Academic Press. Ref Type: Generic

McLaughlin,K.J., Gomez,J.L., Baran,S.E., and Conrad,C.D. (2007). The effects of chronic stress on hippocampal morphology and function: an evaluation of chronic restraint paradigms. Brain Res. *1161*, 56–64.

Meijsing,S.H., Pufall,M.A., So,A.Y., Bates,D.L., Chen,L., and Yamamoto,K.R. (2009). DNA binding site sequence directs glucocorticoid receptor structure and activity. Science *324*, 407–410.

Meyer,M.B., Goetsch,P.D., and Pike,J.W. (2010). Genome-wide analysis of the VDR/RXR cistrome in osteoblast cells provides new mechanistic insight into the actions of the vitamin D hormone. J. Steroid Biochem. Mol. Biol. *121*, 136–141.

Mikkelsen,T.S., Ku,M., Jaffe,D.B., Issac,B., Lieberman,E., Giannoukos,G., Alvarez,P., Brockman,W., Kim,T.K., Koche,R.P., Lee,W., Mendenhall,E., O'Donovan,A., Presser,A., Russ,C.,

Xie,X., Meissner,A., Wernig,M., Jaenisch,R., Nusbaum,C., Lander,E.S., and Bernstein,B.E. (2007). Genome-wide maps of chromatin state in pluripotent and lineage-committed cells. Nature *448*, 553–560.

Miller,J.A., Nathanson,J., Franjic,D., Shim,S., Dalley,R.A., Shapouri,S., Smith,K.A., Sunkin,S.M., Bernard,A., Bennett,J.L., Lee,C.K., Hawrylycz,M.J., Jones,A.R., Amaral,D.G., Sestan,N., Gage,F.H., and Lein,E.S. (2013). Conserved molecular signatures of neurogenesis in the hippocampal subgranular zone of rodents and primates. Development *140*, 4633–4644.

Miller,J.C., Jimenez,P., and Mathe,A.A. (2007). Restraint stress influences AP-1 and CREB DNA-binding activity induced by chronic lithium treatment in the rat frontal cortex and hippocampus. Int. J. Neuropsychopharmacol. *10*, 609–619.

Moghbelinejad,S., Nassiri-Asl,M., Farivar,T.N., Abbasi,E., Sheikhi,M., Taghiloo,M., Farsad,F., Samimi,A., and Hajiali,F. (2014). Rutin activates the MAPK pathway and BDNF gene expression on beta-amyloid induced neurotoxicity in rats. Toxicol. Lett. *224*, 108–113.

Moisan,M.P., Minni,A.M., Dominguez,G., Helbling,J.C., Foury,A., Henkous,N., Dorey,R., and Beracochea,D. (2014). Role of corticosteroid binding globulin in the fast actions of glucocorticoids on the brain. Steroids *81*, 109–115.

Morimoto,M., Morita,N., Ozawa,H., Yokoyama,K., and Kawata,M. (1996). Distribution of glucocorticoid receptor immunoreactivity and mRNA in the rat brain: an immunohistochemical and in situ hybridization study. Neurosci. Res. *26*, 235–269.

Morsink,M.C., Joels,M., Sarabdjitsingh,R.A., Meijer,O.C., de Kloet,E.R., and Datson,N.A. (2006a). The dynamic pattern of glucocorticoid receptor-mediated transcriptional responses in neuronal PC12 cells. J. Neurochem. *99*, 1282–1298.

Morsink,M.C., Steenbergen,P.J., Vos,J.B., Karst,H., Joels,M., de Kloet,E.R., and Datson,N.A. (2006b). Acute activation of hippocampal glucocorticoid receptors results in different waves of gene expression throughout time. J. Neuroendocrinol. *18*, 239–252.

Mozaffari,M., Hoogeveen-Westerveld,M., Kwiatkowski,D., Sampson,J., Ekong,R., Povey,S., den Dunnen,J.T., van den Ouweland,A., Halley,D., and Nellist,M. (2009). Identification of a region required for TSC1 stability by functional analysis of TSC1 missense mutations found in individuals with tuberous sclerosis complex. BMC. Med. Genet. *10*, 88.

Mundade,R., Ozer,H.G., Wei,H., Prabhu,L., and Lu,T. (2014). Role of ChIP-seq in the discovery of transcription factor binding sites, differential gene regulation mechanism, epigenetic marks and beyond. Cell Cycle *13*, 2847–2852.

Nelson,C.C., Hendy,S.C., Shukin,R.J., Cheng,H., Bruchovsky,N., Koop,B.F., and Rennie,P.S. (1999). Determinants of DNA sequence specificity of the androgen, progesterone, and glucocorticoid receptors: evidence for differential steroid receptor response elements. Mol. Endocrinol. *13*, 2090–2107.

Nelson,J.D., Denisenko,O., and Bomsztyk,K. (2006). Protocol for the fast chromatin immunoprecipitation (ChIP) method. Nat. Protoc. *1*, 179–185.

Nishi,M., Tanaka,M., Matsuda,K., Sunaguchi,M., and Kawata,M. (2004). Visualization of glucocorticoid receptor and mineralocorticoid receptor interactions in living cells with GFP-based fluorescence resonance energy transfer. J. Neurosci. *24*, 4918–4927.

Oakley,R.H. and Cidlowski,J.A. (2013). The biology of the glucocorticoid receptor: new signaling mechanisms in health and disease. J. Allergy Clin. Immunol. *132*, 1033–1044.

Oakley,R.H., Sar,M., and Cidlowski,J.A. (1996). The human glucocorticoid receptor beta iso-form. Expression, biochemical properties, and putative function. J. Biol. Chem. *271*, 9550–9559.

Oitzl,M.S., Reichardt,H.M., Joels,M., and de Kloet,E.R. (2001). Point mutation in the mouse glucocorticoid receptor preventing DNA binding impairs spatial memory. Proc. Natl. Acad. Sci. U. S. A *98*, 12790–12795.

Okamoto,S., Sherman,K., Bai,G., and Lipton,S.A. (2002). Effect of the ubiquitous transcription factors, SP1 and MAZ, on NMDA receptor subunit type 1 (NR1) expression during neuronal differentiation. Brain Res. Mol. Brain Res. *107*, 89–96.

Ongwijitwat,S., Liang,H.L., Graboyes,E.M., and Wong-Riley,M.T. (2006). Nuclear respiratory factor 2 senses changing cellular energy demands and its silencing down-regulates cytochrome oxidase and other target gene mRNAs. Gene *374*, 39–49.

Ongwijitwat,S. and Wong-Riley,M.T. (2005). Is nuclear respiratory factor 2 a master transcriptional coordinator for all ten nuclear-encoded cytochrome c oxidase subunits in neurons? Gene *360*, 65–77.

Orlovsky,M.A., Dosenko,V.E., Spiga,F., Skibo,G.G., and Lightman,S.L. (2014). Hippocampus remodeling by chronic stress accompanied by GR, proteasome and caspase-3 overexpression. Brain Res. *1593*, 83–94.

Orsetti,M., Di,B.F., Canonico,P.L., Genazzani,A.A., and Ghi,P. (2008). Gene regulation in the frontal cortex of rats exposed to the chronic mild stress paradigm, an animal model of human depression. Eur. J. Neurosci. *27*, 2156–2164.

Ott,C.J., Blackledge,N.P., Leir,S.H., and Harris,A. (2009). Novel regulatory mechanisms for the CFTR gene. Biochem. Soc. Trans. *37*, 843–848.

Ovcharenko,I., Loots,G.G., Nobrega,M.A., Hardison,R.C., Miller,W., and Stubbs,L. (2005). Evolution and functional classification of vertebrate gene deserts. Genome Res. *15*, 137–145.

Owen,D. and Matthews,S.G. (2003). Glucocorticoids and sex-dependent development of brain glucocorticoid and mineralocorticoid receptors. Endocrinology *144*, 2775–2784.

Oyadomari,S. and Mori,M. (2004). Roles of CHOP/GADD153 in endoplasmic reticulum stress. Cell Death. Differ. *11*, 381–389.

Paakinaho,V., Kaikkonen,S., Makkonen,H., Benes,V., and Palvimo,J.J. (2014). SUMOylation regulates the chromatin occupancy and anti-proliferative gene programs of glucocorticoid receptor. Nucleic Acids Res. *42*, 1575–1592.

Paakinaho,V., Makkonen,H., Jaaskelainen,T., and Palvimo,J.J. (2010). Glucocorticoid receptor activates poised FKBP51 locus through long-distance interactions. Mol. Endocrinol. *24*, 511–525.

Pan,D., Kocherginsky,M., and Conzen,S.D. (2011). Activation of the glucocorticoid receptor is associated with poor prognosis in estrogen receptor-negative breast cancer. Cancer Res. *71*, 6360–6370.

Pardridge,W.M. and Mietus,L.J. (1979). Transport of steroid hormones through the rat blood-brain barrier. Primary role of albumin-bound hormone. J. Clin. Invest *64*, 145–154.

Pascale,A., Amadio,M., Caffino,L., Racagni,G., Govoni,S., and Fumagalli,F. (2011). ELAV-GAP43 pathway activation following combined exposure to cocaine and stress. Psychopharmacology (Berl) *218*, 249–256.

Payvar,F., DeFranco,D., Firestone,G.L., Edgar,B., Wrange,O., Okret,S., Gustafsson,J.A., and Yamamoto,K.R. (1983). Sequence-specific binding of glucocorticoid receptor to MTV DNA at sites within and upstream of the transcribed region. Cell 35, 381–392.

Pearce,D., Matsui,W., Miner,J.N., and Yamamoto,K.R. (1998). Glucocorticoid receptor transcriptional activity determined by spacing of receptor and nonreceptor DNA sites. J. Biol. Chem. 273, 30081–30085.

Pei,H., Li,L., Fridley,B.L., Jenkins,G.D., Kalari,K.R., Lingle,W., Petersen,G., Lou,Z., and Wang,L. (2009). FKBP51 affects cancer cell response to chemotherapy by negatively regulating Akt. Cancer Cell 16, 259–266.

Pei,H., Lou,Z., and Wang,L. (2010). Emerging role of FKBP51 in AKT kinase/protein kinase B signaling. Cell Cycle 9, 6–7.

Pei,J.J. and Hugon,J. (2008). mTOR-dependent signalling in Alzheimer's disease. J. Cell Mol. Med. 12, 2525–2532.

Phuc Le P., Friedman,J.R., Schug,J., Brestelli,J.E., Parker,J.B., Bochkis,I.M., and Kaestner,K.H. (2005). Glucocorticoid receptor-dependent gene regulatory networks. PLoS. Genet. 1, e16.

Pilar-Cuellar,F., Vidal,R., Diaz,A., Castro,E., dos,A.S., Pascual-Brazo,J., Linge,R., Vargas,V., Blanco,H., Martinez-Villayandre,B., Pazos,A., and Valdizan,E.M. (2013). Neural plasticity and proliferation in the generation of antidepressant effects: hippocampal implication. Neural Plast. 2013, 537265.

Pillai,S. and Chellappan,S.P. (2009). ChIP on chip assays: genome-wide analysis of transcription factor binding and histone modifications. Methods Mol. Biol. 523, 341–366.

Polman,J.A., Hunter,R.G., Speksnijder,N., van den Oever,J.M., Korobko,O.B., McEwen,B.S., de Kloet,E.R., and Datson,N.A. (2012a). Glucocorticoids modulate the mTOR pathway in the hippocampus: differential effects depending on stress history. Endocrinology 153, 4317–4327.

Polman,J.A., Welten,J.E., Bosch,D.S., de Jonge,R.T., Balog,J., van der Maarel,S.M., de Kloet,E.R., and Datson,N.A. (2012b). A genome-wide signature of glucocorticoid receptor binding in neuronal PC12 cells. BMC. Neurosci. 13, 118.

Pratt,W.B. (1990). Glucocorticoid receptor structure and the initial events in signal transduction. Prog. Clin. Biol. Res. 322, 119–132.

Pratt,W.B. and Toft,D.O. (1997). Steroid receptor interactions with heat shock protein and immunophilin chaperones. Endocr. Rev. 18, 306–360.

Qi,S., Mizuno,M., Yonezawa,K., Nawa,H., and Takei,N. (2010). Activation of mammalian target of rapamycin signaling in spatial learning. Neurosci. Res. 68, 88–93.

Quinlan,A.R. and Hall,I.M. (2010). BEDTools: a flexible suite of utilities for comparing genomic features. Bioinformatics. 26, 841–842.

Rani,C.S., Elango,N., Wang,S.S., Kobayashi,K., and Strong,R. (2009). Identification of an activator protein-1-like sequence as the glucocorticoid response element in the rat tyrosine hydroxylase gene. Mol. Pharmacol. 75, 589–598.

Rao,N.A., McCalman,M.T., Moulos,P., Francoijs,K.J., Chatziioannou,A., Kolisis,F.N., Alexis,M.N., Mitsiou,D.J., and Stunnenberg,H.G. (2011). Coactivation of GR and NFKB alters the repertoire of their binding sites and target genes. Genome Res. 21, 1404–1416.

Ravasi,T., Suzuki,H., Cannistraci,C.V., Katayama,S., Bajic,V.B., Tan,K., Akalin,A., Schmeier,S., Kanamori-Katayama,M., Bertin,N., Carninci,P., Daub,C.O., Forrest,A.R.,

Gough,J., Grimmond,S., Han,J.H., Hashimoto,T., Hide,W., Hofmann,O., Kamburov,A., Kaur,M., Kawaji,H., Kubosaki,A., Lassmann,T., van,N.E., MacPherson,C.R., Ogawa,C., Radovanovic,A., Schwartz,A., Teasdale,R.D., Tegner,J., Lenhard,B., Teichmann,S.A., Arakawa,T., Ninomiya,N., Murakami,K., Tagami,M., Fukuda,S., Imamura,K., Kai,C., Ishihara,R., Kitazume,Y., Kawai,J., Hume,D.A., Ideker,T., and Hayashizaki,Y. (2010). An atlas of combinatorial transcriptional regulation in mouse and man. Cell *140*, 744–752.

Reddy,T.E., Gertz,J., Crawford,G.E., Garabedian,M.J., and Myers,R.M. (2012). The hypersensitive glucocorticoid response specifically regulates period 1 and expression of circadian genes. Mol. Cell Biol. *32*, 3756–3767.

Reddy,T.E., Pauli,F., Sprouse,R.O., Neff,N.F., Newberry,K.M., Garabedian,M.J., and Myers,R.M. (2009). Genomic determination of the glucocorticoid response reveals unexpected mechanisms of gene regulation. Genome Res. *19*, 2163–2171.

Reichardt,H.M., Kaestner,K.H., Tuckermann,J., Kretz,O., Wessely,O., Bock,R., Gass,P., Schmid,W., Herrlich,P., Angel,P., and Schutz,G. (1998). DNA binding of the glucocorticoid receptor is not essential for survival. Cell *93*, 531–541.

Reul,J.M. and de Kloet,E.R. (1985). Two receptor systems for corticosterone in rat brain: microdistribution and differential occupation. Endocrinology *117*, 2505–2511.

Robertson,G., Hirst,M., Bainbridge,M., Bilenky,M., Zhao,Y., Zeng,T., Euskirchen,G., Bernier,B., Varhol,R., Delaney,A., Thiessen,N., Griffith,O.L., He,A., Marra,M., Snyder,M., and Jones,S. (2007). Genome-wide profiles of STAT1 DNA association using chromatin immunoprecipitation and massively parallel sequencing. Nat. Methods *4*, 651–657.

Ru,W., Peng,Y., Zhong,L., and Tang,S.J. (2012). A role of the mammalian target of rapamycin (mTOR) in glutamate-induced down-regulation of tuberous sclerosis complex proteins 2 (TSC2). J. Mol. Neurosci. *47*, 340–345.

Ruiz-Llorente,S., Carrillo Santa de,P.E., Sastre-Perona,A., Montero-Conde,C., Gomez-Lopez,G., Fagin,J.A., Valencia,A., Pisano,D.G., and Santisteban,P. (2012). Genome-wide analysis of Pax8 binding provides new insights into thyroid functions. BMC. Genomics *13*, 147.

Sakai,D.D., Helms,S., Carlstedt-Duke,J., Gustafsson,J.A., Rottman,F.M., and Yamamoto,K.R. (1988). Hormone-mediated repression: a negative glucocorticoid response element from the bovine prolactin gene. Genes Dev. *2*, 1144–1154.

Sapolsky,R.M., Romero,L.M., and Munck,A.U. (2000). How do glucocorticoids influence stress responses? Integrating permissive, suppressive, stimulatory, and preparative actions. Endocr. Rev. *21*, 55–89.

Sarabdjitsingh,R.A., Isenia,S., Polman,A., Mijalkovic,J., Lachize,S., Datson,N., de Kloet,E.R., and Meijer,O.C. (2010a). Disrupted corticosterone pulsatile patterns attenuate responsiveness to glucocorticoid signaling in rat brain. Endocrinology *151*, 1177–1186.

Sarabdjitsingh,R.A., Meijer,O.C., and de Kloet,E.R. (2010b). Specificity of glucocorticoid receptor primary antibodies for analysis of receptor localization patterns in cultured cells and rat hippocampus. Brain Res. *1331*, 1–11.

Schaaf,M.J., de,J.J., de Kloet,E.R., and Vreugdenhil,E. (1998). Downregulation of BDNF mRNA and protein in the rat hippocampus by corticosterone. Brain Res. *813*, 112–120.

Schaaf,M.J., Lewis-Tuffin,L.J., and Cidlowski,J.A. (2005). Ligand-selective targeting of the glucocorticoid receptor to nuclear subdomains is associated with decreased receptor mobility. Mol. Endocrinol. *19*, 1501–1515.

Scheinman,R.I., Gualberto,A., Jewell,C.M., Cidlowski,J.A., and Baldwin,A.S., Jr. (1995). Characterization of mechanisms involved in transrepression of NF-kappa B by activated glucocorticoid receptors. Mol. Cell Biol. *15*, 943–953.

Schiene-Fischer,C. and Yu,C. (2001). Receptor accessory folding helper enzymes: the functional role of peptidyl prolyl cis/trans isomerases. FEBS Lett. *495*, 1–6.

Schmidt,M.V., Trumbach,D., Weber,P., Wagner,K., Scharf,S.H., Liebl,C., Datson,N., Namendorf,C., Gerlach,T., Kuhne,C., Uhr,M., Deussing,J.M., Wurst,W., Binder,E.B., Holsboer,F., and Muller,M.B. (2010). Individual stress vulnerability is predicted by short-term memory and AMPA receptor subunit ratio in the hippocampus. J. Neurosci. *30*, 16949–16958.

Schoneveld,O.J., Gaemers,I.C., and Lamers,W.H. (2004). Mechanisms of glucocorticoid signalling. Biochim. Biophys. Acta *1680*, 114–128.

Schule,R., Rangarajan,P., Kliewer,S., Ransone,L.J., Bolado,J., Yang,N., Verma,I.M., and Evans,R.M. (1990). Functional antagonism between oncoprotein c-Jun and the glucocorticoid receptor. Cell *62*, 1217–1226.

Shah,O.J., Anthony,J.C., Kimball,S.R., and Jefferson,L.S. (2000a). 4E-BP1 and S6K1: translational integration sites for nutritional and hormonal information in muscle. Am. J. Physiol Endocrinol. Metab *279*, E715-E729.

Shah,O.J., Anthony,J.C., Kimball,S.R., and Jefferson,L.S. (2000b). Glucocorticoids oppose translational control by leucine in skeletal muscle. Am. J. Physiol Endocrinol. Metab *279*, E1185-E1190.

Shah,O.J., Kimball,S.R., and Jefferson,L.S. (2000c). Acute attenuation of translation initiation and protein synthesis by glucocorticoids in skeletal muscle. Am. J. Physiol Endocrinol. Metab *278*, E76-E82.

Shimizu,H., Arima,H., Ozawa,Y., Watanabe,M., Banno,R., Sugimura,Y., Ozaki,N., Nagasaki,H., and Oiso,Y. (2010). Glucocorticoids increase NPY gene expression in the arcuate nucleus by inhibiting mTOR signaling in rat hypothalamic organotypic cultures. Peptides *31*, 145–149.

Shors,T.J., Chua,C., and Falduto,J. (2001). Sex differences and opposite effects of stress on dendritic spine density in the male versus female hippocampus. J. Neurosci. *21*, 6292–6297.

Sierra,A., Gottfried-Blackmore,A., Milner,T.A., McEwen,B.S., and Bulloch,K. (2008). Steroid hormone receptor expression and function in microglia. Glia *56*, 659–674.

Silverman,M.N. and Sternberg,E.M. (2012). Glucocorticoid regulation of inflammation and its functional correlates: from HPA axis to glucocorticoid receptor dysfunction. Ann. N. Y. Acad. Sci. *1261*, 55–63.

Simoes,D.C., Psarra,A.M., Mauad,T., Pantou,I., Roussos,C., Sekeris,C.E., and Gratziou,C. (2012). Glucocorticoid and estrogen receptors are reduced in mitochondria of lung epithelial cells in asthma. PLoS. One. 7, e39183.

Simon,R., Lam,A., Li,M.C., Ngan,M., Menenzes,S., and Zhao,Y. (2007). Analysis of gene expression data using BRB-ArrayTools. Cancer Inform. 3, 11–17.

Slipczuk,L., Bekinschtein,P., Katche,C., Cammarota,M., Izquierdo,I., and Medina,J.H. (2009). BDNF activates mTOR to regulate GluR1 expression required for memory formation. PLoS. One. 4, e6007.

Smyth,G.K.Limma: linear models for microarray data. In: Gentleman,R., Carey,V., Dudoit,S., Irizarry,R., Huber,W., eds. Bioinformatics and computational biology solutions using R and bioconductor. 397–420. 2005. New York, Springer. Ref Type: Generic

So,A.Y., Chaivorapol,C., Bolton,E.C., Li,H., and Yamamoto,K.R. (2007). Determinants of cell- and gene-specific transcriptional regulation by the glucocorticoid receptor. PLoS. Genet. 3, e94.

So,A.Y., Cooper,S.B., Feldman,B.J., Manuchehri,M., and Yamamoto,K.R. (2008). Conservation analysis predicts in vivo occupancy of glucocorticoid receptor-binding sequences at glucocorticoid-induced genes. Proc. Natl. Acad. Sci. U. S. A 105, 5745–5749.

Solomon,S.S., Majumdar,G., Martinez-Hernandez,A., and Raghow,R. (2008). A critical role of Sp1 transcription factor in regulating gene expression in response to insulin and other hormones. Life Sci. 83, 305–312.

Song,C.Z., Tian,X., and Gelehrter,T.D. (1999). Glucocorticoid receptor inhibits transforming growth factor-beta signaling by directly targeting the transcriptional activation function of Smad3. Proc. Natl. Acad. Sci. U. S. A 96, 11776–11781.

Song,J., Ugai,H., Nakata-Tsutsui,H., Kishikawa,S., Suzuki,E., Murata,T., and Yokoyama,K.K. (2003). Transcriptional regulation by zinc-finger proteins Sp1 and MAZ involves interactions with the same cis-elements. Int. J. Mol. Med. 11, 547–553.

Song,J., Ugai,H., Ogawa,K., Wang,Y., Sarai,A., Obata,Y., Kanazawa,I., Sun,K., Itakura,K., and Yokoyama,K.K. (2001). Two consecutive zinc fingers in Sp1 and in MAZ are essential for interactions with cis-elements. J. Biol. Chem. 276, 30429–30434.

Sotiropoulos,I., Catania,C., Riedemann,T., Fry,J.P., Breen,K.C., Michaelidis,T.M., and Almeida,O.F. (2008). Glucocorticoids trigger Alzheimer disease-like pathobiochemistry in rat neuronal cells expressing human tau. J. Neurochem. 107, 385–397.

Sousa,N., Lukoyanov,N.V., Madeira,M.D., Almeida,O.F., and Paula-Barbosa,M.M. (2000). Reorganization of the morphology of hippocampal neurites and synapses after stress-induced damage correlates with behavioral improvement. Neuroscience 97, 253–266.

Spiga,F. and Lightman,S.L. (2009). Dose-dependent effects of corticosterone on nuclear glucocorticoid receptors and their binding to DNA in the brain and pituitary of the rat. Brain Res. 1293, 101–107.

Spilman,P., Podlutskaya,N., Hart,M.J., Debnath,J., Gorostiza,O., Bredesen,D., Richardson,A., Strong,R., and Galvan,V. (2010). Inhibition of mTOR by rapamycin abolishes cognitive deficits and reduces amyloid-beta levels in a mouse model of Alzheimer's disease. PLoS. One. 5, e9979.

Stavreva,D.A., Wiench,M., John,S., Conway-Campbell,B.L., McKenna,M.A., Pooley,J.R., Johnson,T.A., Voss,T.C., Lightman,S.L., and Hager,G.L. (2009). Ultradian hormone stimulation induces glucocorticoid receptor-mediated pulses of gene transcription. Nat. Cell Biol. 11, 1093–1102.

Stocklin,E., Wissler,M., Gouilleux,F., and Groner,B. (1996). Functional interactions between Stat5 and the glucocorticoid receptor. Nature 383, 726–728.

Stormo,G.D. (2000). DNA binding sites: representation and discovery. Bioinformatics. 16, 16–23.

Strahle,U., Klock,G., and Schutz,G. (1987). A DNA sequence of 15 base pairs is sufficient to mediate both glucocorticoid and progesterone induction of gene expression. Proc. Natl. Acad. Sci. U. S. A 84, 7871–7875.

Surjit,M., Ganti,K.P., Mukherji,A., Ye,T., Hua,G., Metzger,D., Li,M., and Chambon,P. (2011). Widespread negative response elements mediate direct repression by agonist-liganded glucocorticoid receptor. Cell 145, 224–241.

Susa,T., Ishikawa,A., Kato,T., Nakayama,M., and Kato,Y. (2009). Molecular cloning of paired related homeobox 2 (prx2) as a novel pituitary transcription factor. J. Reprod. Dev. 55, 502–511.

Swiech,L., Perycz,M., Malik,A., and Jaworski,J. (2008). Role of mTOR in physiology and pathology of the nervous system. Biochim. Biophys. Acta 1784, 116–132.

Tang,S.J., Reis,G., Kang,H., Gingras,A.C., Sonenberg,N., and Schuman,E.M. (2002). A rapamycin-sensitive signaling pathway contributes to long-term synaptic plasticity in the hippocampus. Proc. Natl. Acad. Sci. U. S. A 99, 467–472.

Taupenot,L. (2007). Analysis of regulated secretion using PC12 cells. Curr. Protoc. Cell Biol. Chapter 15, Unit.

Teyssier,J.R., Ragot,S., Chauvet-Gelinier,J.C., Trojak,B., and Bonin,B. (2011). Activation of a DeltaFOSB dependent gene expression pattern in the dorsolateral prefrontal cortex of patients with major depressive disorder. J. Affect. Disord. 133, 174–178.

Thomas-Chollier,M., Watson,L.C., Cooper,S.B., Pufall,M.A., Liu,J.S., Borzym,K., Vingron,M., Yamamoto,K.R., and Meijsing,S.H. (2013). A naturally occurring insertion of a single amino acid rewires transcriptional regulation by glucocorticoid receptor isoforms. Proc. Natl. Acad. Sci. U. S. A 110, 17826–17831.

Trapp,T., Rupprecht,R., Castren,M., Reul,J.M., and Holsboer,F. (1994). Heterodimerization between mineralocorticoid and glucocorticoid receptor: a new principle of glucocorticoid action in the CNS. Neuron 13, 1457–1462.

Tsolakidou,A., Trumbach,D., Panhuysen,M., Putz,B., Deussing,J., Wurst,W., Sillaber,I., Holsboer,F., and Rein,T. (2008). Acute stress regulation of neuroplasticity genes in mouse hippocampus CA3 area–possible novel signalling pathways. Mol. Cell Neurosci. 38, 444–452.

Ueda,K., Fujiki,K., Shirahige,K., Gomez-Sanchez,C.E., Fujita,T., Nangaku,M., and Nagase,M. (2014). Genome-wide analysis of murine renal distal convoluted tubular cells for the target genes of mineralocorticoid receptor. Biochem. Biophys. Res. Commun. 445, 132–137.

Unlap,T. and Jope,R.S. (1995). Inhibition of NFkB DNA binding activity by glucocorticoids in rat brain. Neurosci. Lett. 198, 41–44.

van der Laan,S., Sarabdjitsingh,R.A., Van Batenburg,M.F., Lachize,S.B., Li,H., Dijkmans,T.F., Vreugdenhil,E., de Kloet,E.R., and Meijer,O.C. (2008). Chromatin immunoprecipitation scanning identifies glucocorticoid receptor binding regions in the proximal promoter of a ubiquitously expressed glucocorticoid target gene in brain. J. Neurochem. 106, 2515–2523.

Van Eekelen,J.A., Kiss,J.Z., Westphal,H.M., and de Kloet,E.R. (1987). Immunocytochemical study on the intracellular localization of the type 2 glucocorticoid receptor in the rat brain. Brain Res. 436, 120–128.

van Steensel B., van Binnendijk,E.P., Hornsby,C.D., van der Voort,H.T., Krozowski,Z.S., de Kloet,E.R., and van,D.R. (1996). Partial colocalization of glucocorticoid and mineralocorticoid receptors in discrete compartments in nuclei of rat hippocampus neurons. J. Cell Sci. 109 (Pt 4), 787–792.

Vandevyver,S., Dejager,L., and Libert,C. (2012). On the trail of the glucocorticoid receptor: into the nucleus and back. Traffic. 13, 364–374.

Varley,K.E., Gertz,J., Bowling,K.M., Parker,S.L., Reddy,T.E., Pauli-Behn,F., Cross,M.K., Williams,B.A., Stamatoyannopoulos,J.A., Crawford,G.E., Absher,D.M., Wold,B.J., and Myers,R.M. (2013). Dynamic DNA methylation across diverse human cell lines and tissues. Genome Res. 23, 555–567.

Vazquez,B.N., Laguna,T., Notario,L., and Lauzurica,P. (2012). Evidence for an intronic cis-regulatory element within CD69 gene. Genes Immun. *13*, 356–362.

Vermeer,H., Hendriks-Stegeman,B.I., van der Burg,B., van Buul-Offers,S.C., and Jansen,M. (2003). Glucocorticoid-induced increase in lymphocytic FKBP51 messenger ribonucleic acid expression: a potential marker for glucocorticoid sensitivity, potency, and bioavailability. J. Clin. Endocrinol. Metab *88*, 277–284.

Vielkind,U., Walencewicz,A., Levine,J.M., and Bohn,M.C. (1990). Type II glucocorticoid receptors are expressed in oligodendrocytes and astrocytes. J. Neurosci. Res. *27*, 360–373.

Viguerie,N., Picard,F., Hul,G., Roussel,B., Barbe,P., Iacovoni,J.S., Valle,C., Langin,D., and Saris,W.H. (2012). Multiple effects of a short-term dexamethasone treatment in human skeletal muscle and adipose tissue. Physiol Genomics *44*, 141–151.

Vinckevicius,A. and Chakravarti,D. (2012). Chromatin immunoprecipitation: advancing analysis of nuclear hormone signaling. J. Mol. Endocrinol. *49*, R113-R123.

Vyas,A., Mitra,R., Shankaranarayana Rao,B.S., and Chattarji,S. (2002). Chronic stress induces contrasting patterns of dendritic remodeling in hippocampal and amygdaloid neurons. J. Neurosci. *22*, 6810–6818.

Wang,H., Kubica,N., Ellisen,L.W., Jefferson,L.S., and Kimball,S.R. (2006a). Dexamethasone represses signaling through the mammalian target of rapamycin in muscle cells by enhancing expression of REDD1. J. Biol. Chem. *281*, 39128–39134.

Wang,J., Rao,S., Chu,J., Shen,X., Levasseur,D.N., Theunissen,T.W., and Orkin,S.H. (2006b). A protein interaction network for pluripotency of embryonic stem cells. Nature *444*, 364–368.

Wang,J.C., Derynck,M.K., Nonaka,D.F., Khodabakhsh,D.B., Haqq,C., and Yamamoto,K.R. (2004). Chromatin immunoprecipitation (ChIP) scanning identifies primary glucocorticoid receptor target genes. Proc. Natl. Acad. Sci. U. S. A *101*, 15603–15608.

Wang,Z., Malone,M.H., Thomenius,M.J., Zhong,F., Xu,F., and Distelhorst,C.W. (2003). Dexamethasone-induced gene 2 (dig2) is a novel pro-survival stress gene induced rapidly by diverse apoptotic signals. J. Biol. Chem. *278*, 27053–27058.

Wang,Z.X., Teh,C.H., Chan,C.M., Chu,C., Rossbach,M., Kunarso,G., Allapitchay,T.B., Wong,K.Y., and Stanton,L.W. (2008). The transcription factor Zfp281 controls embryonic stem cell pluripotency by direct activation and repression of target genes. Stem Cells *26*, 2791–2799.

Watanabe,Y., Gould,E., and McEwen,B.S. (1992). Stress induces atrophy of apical dendrites of hippocampal CA3 pyramidal neurons. Brain Res. *588*, 341–345.

Weinmann,A.S., Yan,P.S., Oberley,M.J., Huang,T.H., and Farnham,P.J. (2002). Isolating human transcription factor targets by coupling chromatin immunoprecipitation and CpG island microarray analysis. Genes Dev. *16*, 235–244.

Wieland,S., Dobbeling,U., and Rusconi,S. (1991). Interference and synergism of glucocorticoid receptor and octamer factors. EMBO J. *10*, 2513–2521.

Williams,A., Sarkar,S., Cuddon,P., Ttofi,E.K., Saiki,S., Siddiqi,F.H., Jahreiss,L., Fleming,A., Pask,D., Goldsmith,P., O'Kane,C.J., Floto,R.A., and Rubinsztein,D.C. (2008). Novel targets for Huntington's disease in an mTOR-independent autophagy pathway. Nat. Chem. Biol. *4*, 295–305.

Wu,P., Jiang,C., Shen,Q., and Hu,Y. (2009). Systematic gene expression profile of hypothalamus in calorie-restricted mice implicates the involvement of mTOR signaling in neuroprotective activity. Mech. Ageing Dev. *130*, 602–610.

References

Xie,W., Barr,C.L., Kim,A., Yue,F., Lee,A.Y., Eubanks,J., Dempster,E.L., and Ren,B. (2012). Base-resolution analyses of sequence and parent-of-origin dependent DNA methylation in the mouse genome. Cell *148*, 816–831.

Yamamoto,K.R., Darimont,B.D., Wagner,R.L., and Iniguez-Lluhi,J.A. (1998). Building transcriptional regulatory complexes: signals and surfaces. Cold Spring Harb. Symp. Quant. Biol. *63*, 587–598.

Yan,H., Frost,P., Shi,Y., Hoang,B., Sharma,S., Fisher,M., Gera,J., and Lichtenstein,A. (2006). Mechanism by which mammalian target of rapamycin inhibitors sensitize multiple myeloma cells to dexamethasone-induced apoptosis. Cancer Res. *66*, 2305–2313.

Yang,P.C., Yang,C.H., Huang,C.C., and Hsu,K.S. (2008). Phosphatidylinositol 3-kinase activation is required for stress protocol-induced modification of hippocampal synaptic plasticity. J. Biol. Chem. *283*, 2631–2643.

Yang,T.T., Tsao,C.W., Li,J.S., Wu,H.T., Hsu,C.T., and Cheng,J.T. (2007). Changes of dopamine content and cell proliferation by dexamethsone via pituitary adenylate cyclase-activating polypeptide in PC12 cell. Neurosci. Lett. *426*, 45–48.

Yang-Yen,H.F., Chambard,J.C., Sun,Y.L., Smeal,T., Schmidt,T.J., Drouin,J., and Karin,M. (1990). Transcriptional interference between c-Jun and the glucocorticoid receptor: mutual inhibition of DNA binding due to direct protein-protein interaction. Cell *62*, 1205–1215.

Yehuda,R., Cai,G., Golier,J.A., Sarapas,C., Galea,S., Ising,M., Rein,T., Schmeidler,J., Muller-Myhsok,B., Holsboer,F., and Buxbaum,J.D. (2009). Gene expression patterns associated with posttraumatic stress disorder following exposure to the World Trade Center attacks. Biol. Psychiatry *66*, 708–711.

Yu,C.Y., Mayba,O., Lee,J.V., Tran,J., Harris,C., Speed,T.P., and Wang,J.C. (2010). Genome-wide analysis of glucocorticoid receptor binding regions in adipocytes reveal gene network involved in triglyceride homeostasis. PLoS. One. 5, e15188.

Yudt,M.R. and Cidlowski,J.A. (2002). The glucocorticoid receptor: coding a diversity of proteins and responses through a single gene. Mol. Endocrinol. *16*, 1719–1726.

Yudt,M.R., Jewell,C.M., Bienstock,R.J., and Cidlowski,J.A. (2003). Molecular origins for the dominant negative function of human glucocorticoid receptor beta. Mol. Cell Biol. *23*, 4319–4330.

Zalachoras,I., Houtman,R., and Meijer,O.C. (2013). Understanding stress-effects in the brain via transcriptional signal transduction pathways. Neuroscience *242*, 97–109.

Zhang,L., Li,H., Hu,X., Li,X.X., Smerin,S., and Ursano,R. (2011). Glucocorticoid-induced p11 over-expression and chromatin remodeling: a novel molecular mechanism of traumatic stress? Med. Hypotheses *76*, 774–777.

Zhang,Y., Liu,T., Meyer,C.A., Eeckhoute,J., Johnson,D.S., Bernstein,B.E., Nusbaum,C., Myers,R.M., Brown,M., Li,W., and Liu,X.S. (2008). Model-based analysis of ChIP-Seq (MACS). Genome Biol. *9*, R137.

Curriculum Vitae

Japke Anne Elisabeth Polman was born on 15 Oktober 1980 in Gouda, the Netherlands. She attended secondary school at the Interconfessioneel Hofstad Lyceum, the Hague where she graduaded for both hoger algemeen voortgezet onderwijs (HAVO) in 1998 and voorbereidend wetenschappelijk onderwijs (VWO) in 2000. In 2000 Annelies started her Bachelor Biology at the University of Leiden. During this programme, she performed a 3-month internship, titled "Limbdevelopment *Gallus domesticus*" under the supervision of Prof. dr. Michael Richardson at the department Integrative Zoölogy at the University of Leiden. After graduating from her Bachelor (medical Biology) in 2004, Annelies enrolled in the Master's programme Biomedical Sciences at the Leiden University Medical Center (LUMC) in Leiden. During this programme, she performed a 5-month internship, titled "Nuchal Translucency, a comparative immunohistochemical study in human fetuses" at the department of Anatomy and Embryology at the LUMC in Leiden under the supervision of Prof. dr. A.C. Gittenberger - de Groot. She performed a second 8-month internship at the division of Medical Pharmacology, LACDR / LUMC in Leiden under the supervision of Dr. E. Vreugdenhil and drs. T. Dijkmans. This project was titled "The effect of activated GR on DCLK-short transcription in NS-1 cells". During the Master programme, Annelies participated in the Honours Class titled "Identity: the Impact of Being (Genetically) Unique" organized by Prof. dr. P. de Knijff and Prof. dr. E.C. Klasen at the LUMC. In addition, Annelies has worked as a student assistant during the biomedical bachelorcourse "hormones and the nervous system", LACDR/LUMC and as a laboratory assistant at the department of Embryology & Anatomy, LUMC Leiden.

After graduating from her Master, Annelies started working as a PhD student at the Department of Medical Pharmacology of the LACDR at Leiden University and the LUMC. She studied genome-wide binding sites of Glucocorticoid Receptors in a neuronal context under supervision of Dr. Nicole Datson and Prof. dr. Ron de Kloet. The results of her PhD research are reported in this thesis.

Since 2012, Annelies works as a Project Manager QA/RA at the company BioTop Medical in Leiden, where she provides support to medical device companies for CE-certification. Annelies is married and lives in Oegstgeest with her husband and three children.

Publication list

J.A.E. Polman, E.R. de Kloet, N.A. Datson. Two populations of glucocorticoid receptor-binding sites in the male rat hippocampal genome. Endocrinology, May 2013, 154(5): 1832–1844

J.A.E. Polman, J.E. Welten, D.S. Bosch, R.T. de Jonge, J. Balog, S.M. van der Maarel, E.R. de Kloet, N.A. Datson. A genome-wide signature of glucocorticoid receptor binding in neuronal PC12 cells. BMC Neuroscience, October 2012, 13:118

J.A.E. Polman*, R.G. Hunter*, N. Speksnijder, J.M.E. van den Oever, O.B. Korobko, B.S. McEwen, E.R. de Kloet, N.A. Datson. Glucocorticoids modulate the mTOR pathway in the hippocampus: differential effects depending on stress history. Endocrinology, September 2012, 153(9): 4317–4327.
* both authors have contributed equally to the manuscript

N.A. Datson, **J.A.E. Polman**, R.T. de Jonge, P.T.M. Van Boheemen, E.M.T. Van Maanen, Jennifer Welten, B. McEwen, H.C. Meiland, O.C. Meijer. Specific regulatory motifs predict glucorticoid responsiveness of hippocampal gene expression. Endocrinology, October 2011, 152(10): 3749–3757.

Sarabdjitsingh RA, Isenia S, **Polman A**, Mijalkovic J, Lachize S, Datson N, de Kloet ER, Meijer OC. Disrupted corticosterone pulsatile patterns attenuate responsiveness to glucocorticoid signaling in rat brain. Endocrinology. 2010 Mar;151(3):1177-86. doi: 10.1210/en.2009-1119. Epub 2010 Jan 15.

van Batenburg MF, Li H, **Polman JA**, Lachize S, Datson NA, Bussemaker HJ, Meijer OC. Paired hormone response elements predict caveolin-1 as a glucocorticoid target gene. PLoS One. 2010 Jan 21;5(1):e8839. doi:10.1371/journal.pone.0008839.

Richardson MK, Gobes SM, van Leeuwen AC, **Polman JA**, Pieau C, Sánchez-Villagra MR. Heterochrony in limb evolution: developmental mechanisms and natural selection. J Exp Zool B Mol Dev Evol. 2009 Sep 15;312(6):639–64. doi: 10.1002/jez.b.21250.

Bevan HS, van den Akker NM, Qiu Y, **Polman JA**, Foster RR, Yem J, Nishikawa A, Satchell SC, Harper SJ, Gittenberger-de Groot AC, Bates DO. The alternatively spliced anti-angiogenic family of VEGF isoforms VEGFxxxb in human kidney development. Nephron Physiol. 2008;110(4):p57–67. doi: 10.1159/000177614. Epub 2008 Nov 27.

Bekker MN, van den Akker NM, Bartelings MM, Arkesteijn JB, Fischer SG, **Polman JA**, Haak MC, Webb S, Poelmann RE, van Vugt JM, Gittenberger-de Groot AC. Nuchal edema and venous-lymphatic phenotype disturbance in human fetuses and mouse embryos with aneuploidy. J Soc Gynecol Investig. 2006 Apr;13(3):209–16.